Université de Montréal

Propriétés spatiales et temporelles des cellules des aires visuelles extrastriées (19, 21a et 21b) du chat.

par

Eric Tardif

Département de psychologie

Faculté des arts et sciences

Thèse présentée à la Faculté des études supérieures
en vue de l'obtention du grade de
Philosphiæ Doctor (Ph.D.)
en psychologie
option neuropsychologie-recherche

Octobre 1997

Université de Montréal
Faculté des études supérieures

Cette thèse intitulée:

Propriétés spatiales et temporelles des cellules
des aires visuelles extrastriées (19, 21a et 21b) du chat

présentée par:

Eric Tardif

a été évaluée par un jury composé des personnes suivantes:

Maurice Ptito, Ph.D. Dép. de psychologie, Université de Montréal	Président du jury
Franco Lepore, Ph.D. Dép. de psychologie, Université de Montréal	Directeur de recherche
Jean-Paul Guillemot, Ph.D. Dép. de kinanthropologie, Université du Québec à Montréal	Codirecteur de recherche
Martin Arguin, Ph.D. Dép. de psychologie, Université de Montréal	Membre du jury
Michael von Grünau Dép. de psychologie, Université Concordia	Examinateur externe
Stéphane Molotchnikoff Dép. de biologie, Université de Montréal	Représentant du doyen

Thèse acceptée le: 11. 12. 1997

LISTE DES AUTEURS

André Bergeron

Jean-Paul Guillemot

Franco Lepore

Louis Richer

Eric Tardif

SOMMAIRE

L'étude des bases nerveuses qui sous-tendent le fonctionnement du système visuel suscite un intérêt majeur. Parmi les nombreuses approches et techniques utilisées dans ces études, les enregistrements électrophysiologiques de l'activité unitaire ont permis d'observer la sensibilité des cellules visuelles à différents paramètres. Ceci a permis de mieux comprendre comment le cerveau traite l'information visuelle à partir de signaux acheminés par les différentes voies visuelles. Ainsi, de nombreuses aires visuelles ont été identifiées chez le chat parmi lesquelles certaines ont fait l'objet de recherches plus approfondies quant aux propriétés de leurs champs récepteurs. Cependant, plusieurs aires visuelles demeurent relativement méconnues. Dans un premier temps, nous nous sommes intéressés à l'étude des propriétés spatiales et temporelles ainsi qu'à la sensibilité au contraste des cellules situées dans trois aires visuelles chez le chat: l'aire 19, l'aire 21a et l'aire 21b. Dans un deuxième temps, nous avons effectué des enregistrements dans la zone calleuse des aires 17 et 18 ainsi que dans la zone calleuse de l'aire 19 d'animaux chiasmatomisés afin de comparer les propriétés spatiales respectives des voies thalamo-corticales et calleuses.

Tout au long de ces études, les manipulations physiologiques ont été effectuées en accord avec les règles proposées par le Conseil Canadien de la Protection des Animaux et celles du *National Institute of Health* pour ce qui est du soin et de l'entretien des animaux supérieurs durant les expériences en sciences neurologiques. De plus, les protocoles expérimentaux ont été approuvés par le comité universitaire des soins aux animaux.

Nos résultats montrent que les cellules enregistrées dans l'aire 19 ont surtout des champs récepteurs binoculaires de types complexe ou hypercomplexe. Les cellules sont

sélectives aux fréquences spatiales et temporelles et possèdent des seuils de contraste relativement bas. Les valeurs moyennes de résolution spatiale et de fréquences spatiales optimales des cellules sont inférieures aux valeurs observées dans l'aire 17 mais davantage comparables à celles des aires 18 et PMLS. D'autre part, la résolution temporelle ainsi que les fréquences temporelles optimales sont plus élevées que pour les cellules de l'aire 17. Une forte correspondance interoculaire est observée entre les propriétés des cellules binoculaires. Néanmoins, certaines différences interoculaires sont observées, principalement au niveau des cellules dont la dominance oculaire est inégale. Ces résultats suggèrent que les inputs visuels contribuent à l'activation des cellules de l'aire 19 d'une manière redondante, ce qui reflète peut-être la multiplicité des voies parallèles qui aboutissent à cette aire visuelle chez le chat.

Les cellules de l'aire 21a possèdent majoritairement des champs récepteurs binoculaires du type complexe bien qu'un nombre restreint de cellules révèlent des champs récepteurs de types simple hypercomplexe. Les courbes de syntonisation aux fréquences spatiales des cellules de cette aire peuvent être de types passe-bande ou passe-bas. La résolution spatiale et la fréquence spatiale optimale moyenne des cellules de cette aire sont inférieures à celles observées dans l'aire 17 mais comparables à celles des aires 18 et PMLS. Le seuil de contraste des cellules est généralement bas mais certaines cellules ne répondent qu'à de hauts contrastes. Les courbes de syntonisation aux fréquences temporelles des cellules sont du type passe-bande et révèlent qu'elles peuvent répondre à une vaste étendue de fréquences temporelles. Une forte correspondance interoculaire est observée au niveau des propriétés spatiales et certaines différences peuvent être expliquées par la dominance oculaire.

Les cellules de l'aire 21b possèdent de grands champs récepteurs binoculaires dont les limites sont imprécises. Plusieurs cellules sont sélectives à la direction et quelques-unes sont bidirectionnelles ou répondent à de multiples orientations. La valeur des demi-largeurs des courbes de syntonisation à la direction suggère que les cellules peuvent répondre sur une large étendue de directions. Les cellules présentent des courbes de syntonisation aux fréquences spatiales de types passe-bandes ou passe-bas et ne répondent qu'à de basses fréquences spatiales. Malgré leur faible résolution spatiale, ces cellules agissent, néanmoins, comme de bons filtres de fréquences spatiales. De plus, elles peuvent répondre à de basses, moyennes ou hautes fréquences temporelles. Bien que certaines cellules montrent une haute sensibilité au contraste, la plupart ne répondent qu'à des contrastes intermédiaires ou élevés. Nos résultats suggèrent que les cellules de cette aire pourraient encoder la vélocité et la direction d'un stimulus. De plus, ces cellules pourraient contribuer à l'analyse spatiale des objets de grandes dimensions.

Dans un deuxième temps, nous nous sommes interrogés sur la contribution de l'input calleux à l'analyse de la scène visuelle par les aires 17/18 et 19. À ce sujet, certaines études suggèrent que l'input calleux diffère de l'input thalamo-cortical et ne véhicule que des basses fréquences spatiales ayant de hauts contrastes. Toutefois, les études électrophysiologiques à la base de cette hypothèse ont été effectuées sur un nombre très restreint de cellules visuelles situées à la bordure des aires 17 et 18. Notre étude vise à vérifier si le corps calleux agit comme un filtre ne laissant passer que les stimuli de basses fréquences spatiales ayant un haut contraste. Pour ce faire, les enregistrements électrophysiologiques ont d'abord été effectués à la bordure des aires 17 et 18, dans la zone de projection et de réception calleuse. Par la suite, des

enregistrements ont été effectués dans l'aire 19 qui reçoit davantage de projections calleuses. Lors de ces deux expériences, les chats adultes ont subi une chiasmatomie, ce qui restreint les afférences thalamo-corticales aux hémisphères ipsilatéraux. L'enregistrement de cellules corticales binoculaires dans les zones calleuses permet de comparer la réponse obtenue par la voie directe (ipsilatérale) à celle obtenue par la voie calleuse (controlatérale). Nos résultats montrent qu'il existe une forte correspondance entre les propriétés spatiales des champs récepteurs de chaque oeil mais certaines différences sont observées. Celles-ci ne sont pas reliées à la nature de l'input (direct ou calleux) mais plutôt au niveau de dominance oculaire. Ces résultats infirment l'hypothèse que le corps calleux ne véhicule que des basses fréquences spatiales ayant de hauts contrastes.

L'interprétation des résultats est effectuée à la lumière des voies visuelles parallèles chez le chat. Les propriétés spatiales et temporelles observées au niveau des aires extrastriées 19, 21a et 21b suggèrent que le traitement parallèle de l'information visuelle est partiellement maintenu dans ces aires associatives. Aussi, ces aires sont sélectives à différentes étendues de fréquences spatiales, ce qui laisse croire qu'elles peuvent analyser différentes composantes spatiales de la scène visuelle. Finalement, nous tentons d'établir un parallèle entre les propriétés visuelles observées au niveau des différentes aires et la capacité à effectuer différentes tâches de discrimination visuelle. Nous proposons que les cellules visuelles des aires extrastriées peuvent contribuer à une analyse spatiale du type global qui implique surtout la perception de basses fréquences spatiales.

TABLE DES MATIÈRES

LISTE DES ABRÉVIATIONS

AC:	Area centralis
C:	Complex
CC:	Corps calleux
c/deg:	cycles/degré
CGL:	Corps genouillé latéral
Ch:	Complexe hypercomplexe
CR:	Champ récepteur
CS:	Collicule supérieur
FS:	Fréquence spatiale
FT	Fréquence temporelle
LPl:	Partie latérale du noyau latéro-postérieur
LPm:	Partie médiane du noyau latéro-postérieur
NIM:	Noyau intralaminaire médian
ODI:	Index de dominance oculaire
PLLS:	Postéro-latéro-latérale suprasylvienne
PMLS:	Postéro-médio-latérale suprasylvienne
S:	Simple
Sh:	Simple hypercomplexe
TIAD:	Transfert interhémisphérique d'apprentissage discriminatif

LISTE DES FIGURES

Article # 3

REMERCIEMENTS

Tout au long de mes études doctorales, plusieurs personnes m'ont aidé à surmonter les nombreuses épreuves auxquelles j'ai fait face. Cette aide précieuse a été un élément indispensable à la poursuite de mes études ainsi qu'au dépôt de la présente thèse. Dans cette section, je tiens à remercier les personnes qui m'ont aidé durant ce cheminement.

D'abord, je remercie mon directeur de recherche, monsieur le professeur Franco Lepore (Ph.D.) pour m'avoir accepté comme étudiant et pour m'avoir dirigé durant toutes ces années. Ses commentaires et ses conseils pertinents m'ont grandement aidé à prendre de bonnes décisions. Aussi, la sagesse et la perspicacité du professeur Lepore sont des qualités qui ont fait de lui un modèle.

Je tiens également à remercier mon codirecteur, monsieur le professeur Jean-Paul Guillemot (Ph.D.), pour son encadrement exceptionnel. En effet, le professeur Guillemot m'a aidé dans toutes les étapes de mon Ph.D., incluant plusieurs nuits d'enregistrement qui témoignent de sa passion et de son dévouement pour la Science. Une pareille attitude est remarquable et peu commune, c'est pourquoi je me considère très chanceux d'avoir bénéficié d'un tel encadrement. De plus, les multiples connaissances du professeur Guillemot ainsi que sa persistance impressionnante au travail ont apporté une contribution majeure à tous mes travaux. Je remercie également monsieur le professeur Guillemot pour m'avoir incité à entreprendre des études post-doctorales.

Je remercie vivement mes collègues de travail, avec qui j'ai partagé mon intérêt pour la recherche ainsi qu'une grande amitié. Par leur présence au laboratoire, ces

personnes ont créé une ambiance agréable et stimulante que j'ai beaucoup appréciée. Plus particulièrement, je tiens à remercier André Bergeron (M.Sc.) et Louis Richer (Ph.D.), pour leur collaboration ainsi que Benoît A. Bacon (B.Sc), Hugo Théoret (M.Sc.), Christian C. Joyal (M.Sc.), Marc Herbin (Ph.D.), Denis Boire (Ph.D.) et Stéphane Montfort (Ing.) pour leur support moral et leur aide précieuse. Merci également à Suzanne Lamothe, secrétaire au département de psychologie ainsi qu'à Eric Massicotte (B.Sc.), assistant de recherche, pour la qualité remarquable du travail qu'ils accomplissent. Enfin, je remercie tous les étudiants et professeurs en neuropsychologie avec qui j'ai travaillé de près ou de loin durant mon séjour au département.

J'aimerais aussi profiter de l'occasion pour remercier le Fond pour la Formation de Chercheurs et l'Aide à la Recherche, le Groupe de Recherche em Neuropsychologie Expérimentale ainsi que l'Université de Montréal de m'avoir octroyé des bourse de formation doctorale.

Durant mes études doctorales, j'ai eu la chance d'avoir beaucoup d'aide de la part de mes proches parents et amis. Je tiens à remercier mes parents que j'aime énormément pour m'avoir toujours écouté d'une oreille attentive ainsi que pour m'avoir supporté et enduré durant les moments difficiles. Un remerciement tout spécial va à ma mère Nicole pour la confiance qu'elle me témoigne ainsi que pour son aide lors de la rédaction de cette thèse. Je tiens à remercier mes amis Stéphan Dumais, ainsi que Sébastien et Catherine Laliberté pour la tolérance et la compréhension qu'ils ont montré à mon égard. Finalement, je remercie ma copine Caroline pour son attitude positive et réaliste que j'admire beaucoup ainsi que pour sa bonne humeur quotidienne qui fait d'elle une personne extraordinaire.

CHAPITRE 1

Hodologie et propriétés de certains champs récepteurs du système visuel du chat.

AVANT-PROPOS

De nombreuses études anatomiques, physiologiques et comportementales ont porté sur le système visuel du chat. Les résultats de ces études suggèrent que des voies parallèles existent depuis la rétine jusqu'aux multiples aires qui forment le cortex visuel. Les propriétés visuelles des cellules corticales ont été décrites au niveau des aires primaires et de certaines aires extrastriées. De façon générale, on remarque que les propriétés visuelles des cellules corticales situées dans différentes aires visuelles partagent certaines caractéristiques communes avec celles des cellules thalamiques qui projettent vers ces aires visuelles. Cependant, l'organisation hodologique du cortex visuel est complexe et chaque aire visuelle possède de nombreux liens sous-corticaux, intracorticaux (voir figure 1) et interhémisphériques. De plus, la plupart des aires visuelles extrastriées reçoivent peu d'afférences thalamiques directes et sont moins connues quant aux propriétés de leurs cellules visuelles. L'objectif général de notre étude est de décrire et de comparer les caractéristiques spatiales et temporelles des cellules des aires 19, 21a et 21b du chat afin de mieux connaître le type d'analyse visuelle qu'elles peuvent effectuer. Cette comparaison vise à déterminer si les aires extrastriées peuvent être différenciées sur la base des propriétés de leurs cellules visuelles. De plus, nous souhaitons vérifier si le traitement parallèle de l'information visuelle qui semble exister au niveau des structures sous-corticales est maintenu dans les aires visuelles extrastriées.

D'autre part, nous souhaitons comparer les propriétés visuelles des cellules binoculaires qui sont observées par la stimulation de chaque oeil. Chez l'animal normal, la correspondance interoculaire observée entre ces propriétés nous permet de vérifier si les cellules visuelles des aires extrastriées peuvent contribuer à des processus

binoculaires. Chez l'animal chiasmatomisé, cette comparaison met en évidence les contributions respectives des inputs direct et calleux au niveau des cellules corticales.

En guise d'introduction, nous exposerons l'organisation hodologique du système visuel du chat en insistant particulièrement sur les voies parallèles; puis, nous décrirons les propriétés spatiales et temporelles des cellules corticales de certaines aires visuelles. Finalement, nous aborderons les différents rôles du corps calleux (CC) dans la vision ainsi que l'hypothèse stipulant que cette structure agit tel un filtre spatio-temporel. Les résultats de nos travaux expérimentaux seront ensuite présentés sous forme d'articles scientifiques.

Classification et propriétés des cellules ganglionnaires

Plusieurs études anatomiques, physiologiques et comportementales suggèrent que l'information visuelle est traitée de façon parallèle (Enroth-Cugel et Robson, 1966; Stone, 1983, Livingstone et Hubel, 1988). De cette façon, différentes composantes de la scène visuelle telles la forme, la couleur, le mouvement et la profondeur seraient analysées par des cellules spécifiques tôt dans le système. Aussi, le fonctionnement des multiples aires visuelles corticales s'effectue à partir des différentes afférences qu'elles reçoivent. Il est donc nécessaire, pour comprendre le fonctionnement du cortex visuel, de connaître le type de traitement qui est effectué par les cellules visuelles situées à des niveaux inférieurs.

En 1893, les études anatomiques de Ramon y Cajal ont montré l'existence de différents types de cellules ganglionnaires au niveau de la rétine des vertébrés, ce qui laissait entrevoir l'existence d'un traitement parallèle effectué par des cellules

spécifiques. Boycott et Wassel (1974) ont étudié plus spécifiquement la morphologie des cellules ganglionnaires du chat et en ont identifié trois types: les cellules X (β), Y (α) et W (γ). Plusieurs autres études ont permis de constater que ces trois groupes de cellules possèdent des caractéristiques qui diffèrent à plusieurs niveaux: proportions et distribution dans la rétine, vitesse de conduction, propriétés des champs récepteurs (CR) et projections vers des structures supérieures. Les cellules X Y et W constituent respectivement 40%, 10% et 50% des cellules ganglionnaires (Cleland et Levick, 1974; Fukuda et Stone, 1974; Row et Stone, 1976). Les cellules X ont de petits CR et répondent de façon soutenue (ou tonique) à une stimulation visuelle. Elles se situent au niveau de l'*area centralis* (AC) et montrent une résolution spatiale supérieure aux autres types de cellules (Enroth Cugell et Robson, 1966; Cleland et al., 1973; Fukada et Stone, 1974; Stone, 1978), ce qui laisse croire qu'elles ont un rôle à jouer dans l'analyse de la forme et plus particulièrement des détails de la scène visuelle. Les CR des cellules Y sont plus grands et ces cellules répondent de façon phasique à une stimulation visuelle. Elles sont surtout présentes en périphérie rétinienne (Fukuda et Stone, 1974; Row et Stone, 1976) et possèdent une conduction nerveuse rapide (Bishop et al., 1969; Cleland et al., 1971; Fukada, 1971) ainsi qu'une plus grande sensibilité au contraste (Enroth-Cugell et Robson, 1966). Ceci suggère qu'elles sont importantes pour la détection des stimuli en mouvement ainsi que pour l'analyse de faibles contrastes. Même si elles montrent une résolution spatiale inférieure à celle des cellules X et qu'elles représentent une faible proportion des cellules ganglionnaires, les cellules Y pourraient quand même être impliquées dans l'analyse grossière de la forme (Stone 1983). Finalement, les cellules W sont présentes au niveau de l'AC et en périphérie rétinienne. Ces cellules ont une vitesse de conduction très lente (Bishop et al., 1969; Stone et Hoffmann, 1972; Stone et Fukuda, 1974; Cleland et Levick, 1974) et montrent une réponse instable face

aux stimuli visuels. Les cellules W demeurent les plus méconnues quant à leur rôle possible dans la vision, bien qu'elles soient vraisemblablement impliquées dans la "vision ambiante[1]" à cause de leurs riches connections avec les noyaux extragéniculés.

Les voies rétino-thalamiques et rétino-tectales

Les voies visuelles, constituées des projections des trois types de cellules ganglionnaires vers les noyaux du mésencéphale et du diencéphale, sont nombreuses et complexes. On peut toutefois distinguer deux grandes voies parallèles rétinofuges. L'une est dirigée vers le thalamus, plus précisément vers le corps genouillé latéral (CGL) dorsal et l'autre vers le collicule supérieur (CS). Le CGL dorsal est divisé en 3 couches principales: les couches A, A1 et C. La couche C peut être subdivisée en 4 sous-couches: la couche magnocellulaire C et les couches parvocellulaires C1, C2 et C3. Les couches A, C et C2 reçoivent des afférences de l'oeil controlatéral, les couches A1 et C1 reçoivent des afférences de l'oeil ipsilatéral tandis que la couche C3 ne semble pas recevoir d'afférences rétiniennes directes (Hickey et Guillery, 1974; Guillery et al., 1980). D'autres noyaux adjacents au CGL dorsal ont également été identifiés, notamment le noyau intralaminaire médian (NIM) et l'aileron du corps genouillé.

De nombreuses études anatomiques ont permis de quantifier la répartition des axones des cellules ganglionnaires selon leur site de projection: le CGL et le CS (Kelly et Gilbert; 1975; Wässle et Illing, 1980; Illing et Wässle, 1981; Sur et Sherman, 1982; Stone, 1983; Levental et al., 1985; Sherman, 1985). Les axones des cellules X projettent majoritairement vers les couches A et A1 du CGL dorsal bien qu'une faible proportion

[1] Le terme "vision ambiante" réfère aux capacités visuelles qui subsistent chez un animal lésé des aires corticales 17 et 18.

soit dirigée vers le CS. Les axones des cellules Y projettent également au CGL dorsal (couches A, A1 et C) et au NIM mais possèdent également de nombreuses collatérales qui aboutissent au CS. Les cellules W projettent massivement au CS mais possèdent aussi des projections vers le CGL dorsal (couches C) et vers l'aileron du corps genouillé.

Les différents types de neurones du CGL peuvent également être divisés en trois grandes classes (X, Y et W) selon leur morphologie (Guillery, 1966; LeVay et Ferster, 1977) et leurs propriétés physiologiques (Cleland et al., 1971; Stone et Hoffman, 1971; Hoffman et al., 1972). La distribution des différents types de cellules au niveau du CGL correspond aux différentes projections rétinogéniculées des cellules ganglionnaires. Ainsi, les cellules ganglionnaires X, Y et W projettent leurs axones vers des cellules genouillées du même type (Sherman, 1985). Les axones ou collatérales des cellules Y et W qui projettent au CS aboutissent également dans des régions distinctes. Les études électrophysiologiques de Hoffman (1973) montrent que les cellules W sont présentes à la surface du CS et que les cellules Y s'y trouvent aussi mais plus profondément. Ces travaux ont été confirmés par les études anatomiques de Itoh et al. (1981) qui ont injecté un traceur rétrograde dans différentes régions du CS. Lorsque le traceur est injecté à la surface du CS, les cellules ganglionnaires ainsi marquées montrent un petit soma, ce qui correspond aux cellules du type W. Par contre, si le traceur est injecté plus en profondeur, les cellules ganglionnaires marquées ont un soma relativement large, propre aux cellules Y. Contrairement aux cellules du CGL, les cellules du CS ne projettent pas leurs axones directement vers le cortex visuel mais plutôt vers d'autres structures sous-corticales telles le CGL dorsal (couches C1, C2 et C3), l'aileron du corps genouillé et le complexe pulvinar.

Les aires visuelles

Tel qu'illustré à la figure 1, un nombre impressionnant d'aires visuelles corticales a été identifié chez le chat (Palmer et al., 1978; Tusa et al., 1978, 1979; Tusa et Palmer, 1980). Parmi ces dernières, l'aire 17 (ou aire striée) est la plus importante quant à la superficie qu'elle occupe au niveau du cortex visuel. De plus, elle semble être la seule à comprendre une représentation totale de l'hémichamp controlatéral. Cette représentation de l'espace est organisée de façon rétinotopique, ce qui signifie que des neurones adjacents sur le cortex ont des CR adjacents dans l'espace. Les aires extrastriées 18 et 19 sont situées plus latéralement et possèdent également une représentation importante de l'espace visuel organisée de façon rétinotopique. L'aire visuelle suprasylvienne est située à l'intérieur de la fissure suprasylvienne latérale. Sur une base rétinotopique, cette aire extrastriée peut être divisée en six sous-aires: les aires antéro-médio-latérale suprasylvienne, antéro-latéro-latérale suprasylvienne, postéro-médio-latérale suprasylvienne (PMLS), postéro-latéro-latérale suprasylvienne (PLLS), ventro-latérale et dorso-latérale. Chacune de ces aires possèdent une représentation partielle de l'espace organisée de façon rétinotopique, bien que cette organisation soit plus complexe que pour les aires 17, 18 et 19 (Palmer et al., 1978). Les études électrophysiologiques de Tusa et Palmer (1980) ont permis d'identifier d'autres aires visuelles, notamment les aires 20a, 20b, 21a et 21b. Ces quatre aires visuelles représentent principalement le champ visuel supérieur et leur organisation rétinotopique est complexe. Les aires 20a et 20b ont une représentation du champ visuel qui peut s'étendre jusqu'à 50 degrés en élévation. L'aire 21a possède une représentation de l'espace visuel très limitée (20

FIGURE 1

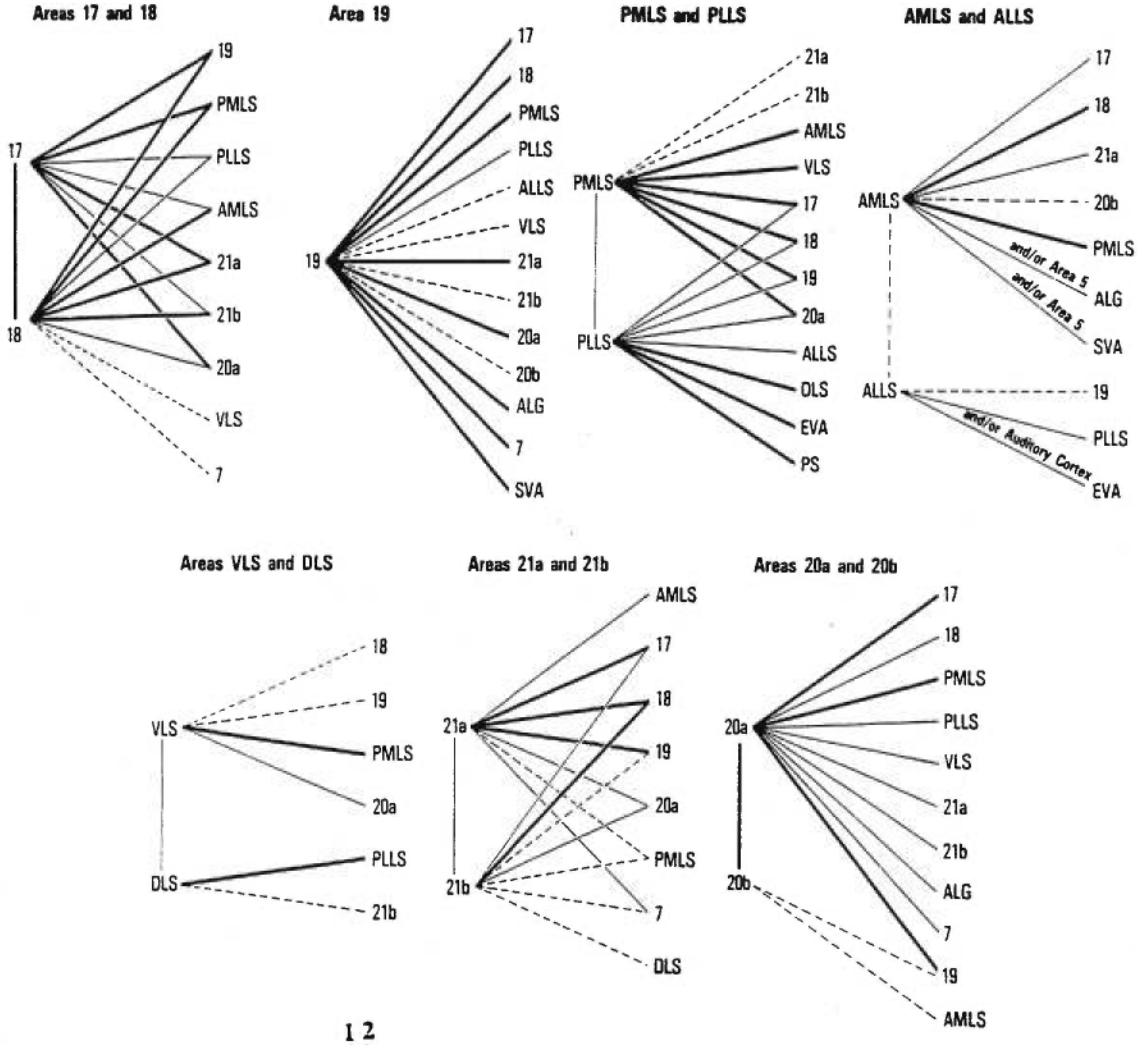

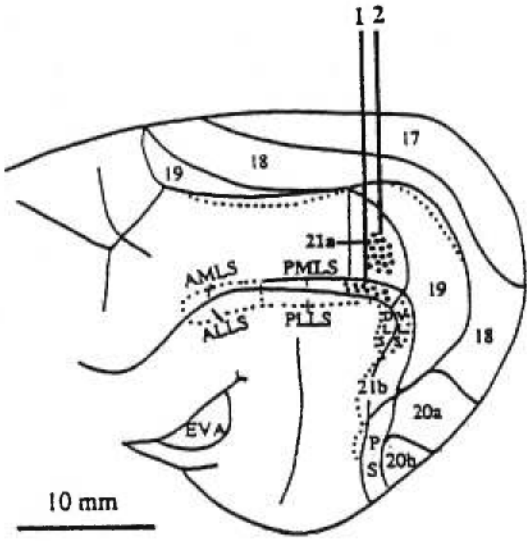

Figure 1. Ci-haut: Liens intracorticaux aux niveau des aires visuelles du chat. Les traits gras, fins et pointillés représentent respectivement des projections denses, modérées et faibles entre les aires. Modifié d'après Symonds et Rosenquist (1984).
Ci-contre: Positions relatives des aires visuelles au niveau du cortex cérébral du chat. Les lignes 1 et 2 désignent les aires 21a et PMLS, respectivement. Modifié d'après Dreher (1996).

degrés en azimuth et 20 degrés en élévation) tandis que les CR des cellules de l'aire 21b peuvent s'étendre jusqu'à 90 degrés en azimuth et 35 degrés en élévation.

Les voies géniculo-corticales

L'organisation parallèle qui existe au niveau de la rétine, du CGL et du CS est un élément déterminant pour comprendre le fonctionnement du cortex visuel. En effet, il semble que les projections corticales des cellules X, Y et W demeurent relativement séparées les unes des autres au niveau de certaines aires visuelles (Stone, 1983). D'abord, Garey et Powell (1967) ont observé que, suite à une lésion de l'aire 17, seuls les somas de petites tailles sont dégénérés au niveau du CGL alors que les larges somas ne dégénèrent que si les aires 17 et 18 sont lésées. Ainsi, ces auteurs ont conclu que les petites cellules (probablement du type X) du CGL ne projettent qu'à l'aire 17 alors que les grosses cellules (probablement du type Y) projettent à la fois à l'aire 17 et à l'aire 18. Ainsi, ces dernières survivraient à une destruction de l'aire 17 parce qu'elles possèdent une collatérale vers l'aire 18. Par la suite, Hoffmann et Stone (1971) ainsi que Stone et Dreher (1973) ont enregistré les réponses cellulaires au niveau des aires 17 et 18 suite à une stimulation électrique du chiasma optique ou des radiations optiques. Leurs résultats montrent que les cellules de l'aire 17 peuvent répondre avec une latence courte ou longue à une telle stimulation alors que dans l'aire 18, les cellules répondent davantage avec de courtes latences. Ceci suggère donc que les cellules de l'aire 17 reçoivent à la fois des projections des cellules possédant une vitesse de conduction relativement lente (cellules X) et rapide (cellules Y) alors que les cellules de l'aire 18 sont innervées principalement par les cellules à conduction rapide (cellules Y). De nombreuses études anatomiques (Gilbert et Kelly, 1975; Maciewicz, 1975; Garey et

Blakemore, 1977; Holländer et Vanegas, 1977; LeVay et Ferster, 1977; Ferster et LeVay, 1978; Leventhal, 1979; Geisert, 1980) ont utilisé le HRP comme traceur rétrograde afin de localiser et mesurer les somas des cellules genouillées qui projettent vers les aires visuelles. Les résultats de ces études suggèrent que les cellules X de la couche A du CGL dorsal projettent massivement vers l'aire 17 bien qu'un nombre minoritaire de cellules X des couches A1 et C pourrait projeter aux aires 18 et 19. Les cellules Y des couches A, A1 et C du CGL dorsal projettent aux aires 17 et 18 alors que les cellules Y du NIM projettent vers les aires 18 et 19. Les cellules W des couches C, C1 et C2 du CGL dorsal projettent aux aires 17 et 18 mais plus particulièrement à l'aire 19. Aussi, les cellules W de l'aileron du corps genouillé projettent à l'aire 19 ainsi qu'à d'autres aires extrastriées. Dreher et al. (1980) affirment en effet que l'input direct du CGL vers l'aire 19 est essentiellement formé par les cellules W. Toutefois, il est important de signaler que l'input principal de l'aire 19 ne provient pas du CGL mais plutôt du complexe formé du noyau latéro-postérieur (LP) et du pulvinar (Dreher, 1986).

En somme, on remarque que les couches A et A1 du CGL dorsal contiennent des cellules qui projettent en très grande majorité aux aires 17 et 18 et peu vers les autres aires visuelles. C'est pour cette raison que plusieurs auteurs considèrent que les aires 17 et 18 forment le cortex visuel "primaire" du chat (revue par Dreher, 1986). Toutefois, il faut souligner que dans le cas de l'aire 17, 90% des afférences thalamiques proviennent des couches A et A1 du CGL dorsal alors que pour l'aire 18, moins de 50% des afférences thalamiques proviennent de ces mêmes couches (Holländer et Vanegas, 1977). Il est également possible d'affirmer que les cellules X projettent majoritairement à l'aire 17 alors que les cellules Y projettent surtout aux aires 17 et 18. Les cellules W

projettent principalement à l'aire 19, ce qui peut constituer un élément déterminant pour comprendre les rôles éventuels de ces cellules et le type d'analyse effectuée au niveau de l'aire 19.

Les voies extragéniculées

À l'exception de l'aire 18, toutes les aires extrastriées possèdent un attribut commun: elles reçoivent la majorité de leurs afférences sous-corticales en provenance de structures situées à l'extérieur du CGL (Raczkowski et Rosenquist, 1983; Dreher, 1986). Plus précisément, ces aires visuelles reçoivent de nombreuses afférences du complexe LP-pulvinar. Ce noyau extragéniculé peut être divisé en trois grandes parties, soit le pulvinar et les parties latérale (LPl) et médiane (LPm) du noyau LP. Ces noyaux thalamiques ne reçoivent pas d'afférences rétiniennes directes mais sont plutôt innervées par d'autres zones visuelles. Le pulvinar reçoit des afférences du prétectum tandis que les noyaux LPl et LPm reçoivent des afférences du cortex visuel et du CS, respectivement (Updyke, 1977; Berson et Graybiel, 1978). Cependant, il faut noter qu'il existe un chevauchement important entre les projections corticales et tectales dirigées vers les noyaux LPl et LPm (Benedek et al., 1983).

Selon Raczkowski et Rosenquist (1983), on doit exclure les cellules X du système extragéniculé, lequel serait formé essentiellement par les cellules Y et W. Il est cependant difficile d'associer les noyaux LPl et LPm à un type de cellule en particulier parce qu'ils reçoivent des afférences chevauchées du CS et de diverses aires du cortex visuel. En retour, puisque les noyaux LPl et LPm forment les inputs thalamiques principaux pour presque toutes les aires extrastriées (Dreher, 1986), il est encore plus

difficile d'établir une relation entre ces dernières et les voies X, Y et W. De plus, les multiples aires visuelles possèdent de nombreux liens réciproques intrahémisphériques (Symonds et Rosenquist, 1984; Dreher, 1986) et interhémisphériques (Segraves et Rosenquist, 1982a, b; Dreher, 1986) qui forment un réseau complexe entre les aires visuelles. Ainsi, bien que la distinction entre les voies parallèles X, Y et W soit apparente au niveau des structures sous-corticales, elle est beaucoup plus difficile à établir en ce qui à trait aux aires visuelles corticales, plus particulièrement les aires extrastriées. Les données anatomiques à elles seules sont insuffisantes pour rendre compte du type d'information qui pourrait être traité dans les aires visuelles. Aussi est-il nécessaire d'explorer ces aires visuelles à l'aide d'autres méthodes, notamment les techniques d'enregistrements électrophysiologiques.

Les propriétés des champs récepteurs des cellules visuelles chez le chat

Les premières études électrophysiologiques chez le chat ont montré que les neurones visuels rétiniens possèdent un CR caractérisé par des régions excitatrices (ON) et inhibitrices (OFF) (Kuffler, 1953). Au niveau de la rétine et du CGL, les cellules sont monoculaires et possèdent un CR de forme plutôt circulaire caractérisé par une organisation antagoniste entre le centre et la périphérie. Les CR des cellules corticales sont plus allongés et peuvent posséder des propriétés spécifiques comme la binocularité, la sélectivité à l'orientation, à la direction ou à la disparité spatiale (Hubel et Wiesel, 1962, 1965; Barlow et al., 1967; LeVay et Voigt, 1988). Les stimuli utilisés pour l'étude des propriétés des CR visuels sont variés. De façon générale, des barres noires ou lumineuses sont utilisées pour estimer la sélectivité à l'orientation, à la disparité spatiale et à la vélocité. Un réseau de fréquences spatiales (FS) permet également d'estimer des

paramètres tels la syntonisation aux FS et aux fréquences temporelles (FT), la résolution spatiale, la résolution temporelle et la sensibilité au contraste.

L'enregistrement de cellules visuelles localisées dans différentes aires du cortex visuel (17-18 et 19) a permis d'observer que les propriétés de leurs CR deviennent plus complexes à des niveaux supérieurs comparativement aux niveaux inférieurs (Hubel et Wiesel, 1962, 1965). Les CR des cellules simples (S) possèdent des régions ON/OFF adjacentes et antagonistes. Ces cellules ont été identifiées en grande quantité dans l'aire 17. Lorsqu'elles sont stimulées à l'aide d'un réseau de FS balayé dans le champ visuel, ces cellules présentent une réponse modulée à la fréquence temporelle du balayage. Les CR des cellules complexes (C) sont plus grands et ne montrent habituellement pas de régions ON/OFF antagonistes mais plutôt un chevauchement de ces régions. Elles ont été identifiées dans l'aire 17 et dans les aires extrastriées. La réponse de ces cellules à un réseau de FS balayé ne présente généralement aucune modulation. Les CR des cellules hypercomplexes sont flanqués de régions inhibitrices qui provoquent une atténuation de la réponse cellulaire lorsque le stimulus adéquatement orienté atteint une longueur donnée. Les cellules hypercomplexes peuvent également posséder des propriétés semblables aux cellules S ou C (Henry, 1977). Les cellules hypercomplexes de types simple (Sh) ou complexe (Ch) se trouvent surtout dans les aires extrastriées, notamment dans l'aire 19 (Hubel et Wiesel, 1965). Ces observations ont mené à une conception dite hiérarchique et sérielle, laquelle suggère que l'information visuelle est initialement traitée par des aires primaires et transmise successivement à des aires associatives du cortex. Ainsi, l'image visuelle complexe serait reconstruite à des niveaux supérieurs à partir de ses éléments les plus simples précédemment analysés par les régions primaires.

D'autre part, plusieurs études suggèrent que certaines aires visuelles fonctionnent de façon parallèle. Ainsi que nous l'avons mentionné précédemment, il existe une différence importante entre les types d'afférences du CGL qui aboutissent directement aux aires 17, 18 et 19: seule l'aire 17 reçoit des afférences de types X et Y en grande quantité; l'aire 18 reçoit des afférences de types Y et W et l'aire 19 semble recevoir un nombre important d'afférences du type W. Un argument en faveur d'un traitement parallèle repose sur le fait que les propriétés des CR de ces deux aires corticales reflètent celles des cellules thalamiques qui projettent vers ces régions. En effet, les CR de l'aire 17 sont plus petits que ceux de l'aire 18, tout comme les CR des cellules X du CGL sont plus petits que ceux des cellules Y (Stone et Dreher, 1973; Stone, 1983; Dreher, 1986). Par contre, les CR des cellules de l'aire 19 sont plus petits que ceux de l'aire 18 (Hubel et Wiesel, 1965; Duysens et al., 1982a, b; Dreher, 1986; Orban, 1984), ce qui tend à confirmer l'hypothèse d'un traitement parallèle.

Les cellules de l'aire 17 montrent généralement une haute résolution spatiale (Maffei et Fiorentini, 1973; Movshon; 1978c) comparativement aux cellules de l'aire 18 (Movshon et al., 1978c; Berardi et al., 1982). Cette différence est également observée entre les cellules X et Y du CGL: les cellules X possèdent une plus haute résolution spatiale que les cellules Y (Sur et Sherman, 1984; Sherman, 1985). Cependant, les études de So et Shapley (1981) montrent que la différence entre la résolution spatiale des cellules X et Y du CGL dépend de la façon dont le stimulus est présenté. En effet, lorsque le réseau de FS est balayé dans le champ visuel, les cellules X ont une meilleure résolution spatiale mais si le réseau de FS subit un renversement de contraste, les cellules Y démontrent une résolution spatiale supérieure à celle des cellules X. La plupart des études visant à déterminer la résolution spatiale des cellules corticales ont

utilisé un réseau de FS balayé dans le champ visuel. En utilisant cette méthode, les neurones de l'aire 17 ont effectivement une résolution spatiale supérieure à ceux de l'aire 18, ce qui suggère que l'input X se manifeste davantage au niveau de l'aire 17 que de l'aire 18. En ce qui concerne la résolution spatiale des cellules de l'aire 19, elle sera étudiée au cours de notre travail.

Par ailleurs, il est également possible d'établir un lien entre les cellules X, Y et W du CGL et celles des aires 17, 18 et 19 au niveau de leurs réponses respectives à des stimuli dynamiques. Les études électrophysiologiques montrent que les cellules Y du GCL répondent généralement à de plus hautes vélocités comparativement aux cellules X (Derrington et Fuchs, 1978; Lehmkule et al., 1980; Frishman et al., 1983). Aussi, les cellules W du CGL semblent répondre à des stimuli plus lents que les cellules X et Y (Sherman, 1985). Au niveau du cortex visuel, les études de Orban et al. (1981a) montrent que les cellules des aires 17 et 18 diffèrent quant à leur réponses aux stimuli en mouvement. Les cellules de l'aire 17 répondent majoritairement à des vélocités plus basses que les cellules de l'aire 18. De plus, les neurones de l'aire 19, à l'instar de ceux qui ont été identifiés dans l'aire 17, répondent optimalement à des vélocités relativement basses. En fait, la réponse typique des cellules de l'aire 17 est atténuée quand le stimulus atteint une vélocité de quatre degrés/s. alors que la réponse des cellules de l'aire 19 est atténuée quand la vélocité du stimulus dépasse 0,3 degrés/s. (Duysens et al., 1982a). Donc, il semble que les cellules X, Y et W du CGL peuvent aussi être comparées à celles des cellules des aires 17, 18 et 19 au niveau de leur réponse face à des stimuli dynamiques. Les cellules Y ainsi que celles de l'aire 18 répondent à de hautes vélocités tandis que les cellules W du CGL et celles de l'aire 19 répondent à de très basses

vélocités. Finalement, les cellules X et celles de l'aire 17 répondraient à des vélocités intermédiaires.

Mis à part les aires 18 et 19, peu d'aires visuelles extrastriées ont été décrites en fonction des propriétés visuelles des cellules qu'elles contiennent. Néanmoins, un certain nombre d'études ont décrit ces propriétés au niveau des aires PMLS et 21a. Ainsi que nous l'avons mentionné plus haut, il demeure difficile d'associer ces aires visuelles à un type d'input particulier car elles reçoivent peu d'afférences directes en provenance du CGL. Toutefois, il est intéressant de comparer les propriétés des cellules de ces aires visuelles avec celles des cellules situées dans les régions sous-corticales qui projettent vers ces aires.

Les travaux de Hubel et Wiesel (1969) ont montré que les neurones de l'aire PMLS possèdent des CR beaucoup plus grands que ceux des aires 17, 18 et 19 et répondent mieux à des stimuli en mouvement qu'à des stimuli stationnaires. En général, l'organisation des CR de l'aire PMLS ressemble à celle des cellules du type C des aires 17 et 18. Cependant, des études montrent que certaines cellules de l'aire PMLS possèdent des CR entourés d'une région périphérique qui peut influencer la réponse cellulaire lorsqu'on y présente un stimulus en mouvement (Spear et Baumann, 1975; von Grünau et Frost, 1983). Plusieurs études démontrent également que la majorité des cellules de l'aire PMLS sont sélectives à la direction du stimulus (Hubel et Wiesel, 1969; Wright, 1969; Spear et Baumann, 1975; Turlejski, 1975; Camarda et Rizzolatti, 1976; Blakemore et Zumbroich, 1987; Rauschecker et al., 1987, von Grunau et al., 1987; Gizzi et al., 1990). Ces observations suggèrent que les cellules de l'aire PMLS

peuvent contribuer à l'analyse des stimuli en mouvement ainsi qu'à discriminer leur direction.

Certaines études ont également décrit les propriétés spatiales et temporelles des cellules des aires PMLS et PLLS (Morrone et al., 1986; Zumbroich et Blakemore, 1987). Les résultats de ces études ont montré que les cellules de l'aire PMLS et PLLS sont sélectives aux FS et aux FT. Ces cellules montrent une résolution spatiale inférieure aux cellules de l'aire 17 mais comparable à celles de l'aire 18. La FS optimale (FS à laquelle une cellule émet le plus haut taux de potentiels d'action) typique des cellules des aires PMLS et PLLS est également inférieure à celle des cellules de l'aire 17 mais comparable à ce que l'on observe dans l'aire 18. Finalement, l'étendue des FS (bande-passante) auxquelles répondent les cellules des aires PMLS et PLLS semble plus large que pour les cellules de l'aire 17 (Movshon et al., 1978c; Tolhurst et Thompson, 1981).

En général, on peut affirmer que les cellules des aires PMLS et PLLS montrent certaines propriétés semblables à celles du LPl et du LPm, lesquels sont des structures sous-corticales qui projettent massivement vers les aires extrastriées. En effet, les cellules du LPl et du LPm ont aussi de grands CR binoculaires et plusieurs d'entre elles sont sélectives à la direction (Chalupa et Abramson, 1988). De plus, les cellules du LPl montrent des propriétés spatiales et temporelles semblables à celles des aires PMLS et PLLS (Casanova et al., 1989).

Récemment, un certain nombre d'études ont porté sur les propriétés des cellules de l'aire 21a. Cette aire visuelle semble posséder des propriétés différentes des aires 19 et PMLS auxquelles elle est adjacente. En effet, les cellules de l'aire 21a montrent des

CR plus grands que ceux des aires 17, 18 et 19 mais plus petits que ceux de l'aire PMLS (Dreher, 1986; Dreher et al., 1993). De plus, les cellules de l'aire 21a répondent à des stimuli plus lents que celles de l'aire PMLS (Spear et Baumann, 1975; Dreher et al., 1986; Mizobe et al., 1988; Dreher et al., 1993) et elles ne sont généralement pas sélectives à la direction mais plutôt à l'orientation (Wimborne et Henry, 1992; Dreher, 1993). Il semble donc que différentes aires extrastriées peuvent être différenciées fonctionnellement à partir de certaines propriétés cellulaires. Par contre, les propriétés spatiales et temporelles qui ont été établies pour les cellules des aires 17, 18 et PMLS sont moins connues en ce qui concerne l'aire 19 et demeurent inexplorées au niveau de plusieurs aires extrastriées, notamment les aires 21a et 21b. Dans le but d'étendre cette comparaison entre les paramètres spatio-temporels des cellules des différentes aires visuelles, nous avons étudié la réponse aux FS des cellules des aires 19, 21a et 21b.

Au niveau de l'aire 19, une étude de Tanaka et al. (1987) a décrit certaines propriétés spatiales et temporelles des CR. Cependant, cette étude ne présente pas de données sur la résolution spatiale des cellules ni sur leur sensibilité au contraste, ce qui fera l'objet de notre étude. De plus, puisque la majorité des cellules corticales sont binoculaires, nous porterons une attention particulière à la comparaison entre les propriétés des CR obtenues par la stimulation de chaque oeil. Une étude de Skottun et Freeman (1984) entreprise dans l'aire 17 a permis de comparer les réponses de cellules binoculaires obtenues par la stimulation successive de l'oeil ipsilatéral et controlatéral. Leurs résultats montrent que pour une cellule donnée, il existe une forte correspondance entre les propriétés des CR de chaque oeil mais que des différences sont aussi observées. De plus, certaines de ces différences peuvent être expliquées par la dominance oculaire des cellules. Étant donné les différences importantes qui existent

entre les inputs respectifs au niveau des aires 17, 19 et 21a, nous vérifierons si la correspondance entre les propriétés spatiales et temporelles des cellules binoculaires des aires 19 et 21a est comparable à ce qui a été observé dans l'aire 17. De plus, les propriétés spatiales et temporelles ainsi que la sensibilité au contraste qui ont pu être observées par la stimulation de l'oeil dominant permettra de vérifier si ces aires visuelles peuvent être distinguées à partir de telles propriétés.

La distinction entre les aires 21a et 21b repose essentiellement sur la projection de l'espace visuel qu'elles sous-tendent (Tusa et al., 1980). Aussi, bien que certaines propriétés des CR des cellules de l'aire 21a sont maintenant connues, celles des cellules de l'aire 21b demeurent inexplorées. Conséquemment, il n'est pas possible d'affirmer si ces deux aires traitent le même type d'information visuelle ou s'il existe des différences à ce niveau. Nous proposons donc de comparer les propriétés visuelles des cellules présentes dans ces deux aires visuelles afin de répondre à cette question. De plus, des comparaisons additionnelles seront effectuées par rapport aux données recueillies dans d'autres aires visuelles et dans certaines régions sous-corticales. Au niveau de l'aire 21a, l'accent est mis sur les propriétés spatiales et temporelles ainsi que sur la sensibilité au contraste. En ce qui concerne les cellules de l'aire 21b, ces mêmes propriétés sont aussi étudiées en plus de leur sélectivité à l'orientation et à la direction.

Dans un deuxième temps, notre étude s'est intéressée aux propriétés de l'input calleux et des cellules visuelles des zones calleuses corticales. Étant donné l'organisation croisée du système visuel, chaque hémisphère traite l'information en provenance de l'hémichamp controlatéral et n'est informé d'un stimulus situé dans l'hémichamp ipsilatéral que par une communication avec l'hémisphère opposé. Le corps

calleux (CC) est la plus importante commissure qui relie les hémisphères cérébraux et qui assure une telle communication.

Les rôles du corps calleux dans la vision

Suite à de nombreuses études anatomiques, physiologiques et comportementales, il est aujourd'hui admis que le CC est impliqué dans certaines fonctions visuelles; il s'agit, notamment, du transfert interhémisphérique de l'information mnémonique et/ou visuelle lors d'apprentissage discriminatif, de la fusion binoculaire et de la perception de la profondeur, de la génèse des mouvements oculaires de vergence et de la fusion des hémichamps visuels.

Les études de Myers (1955, 1956) ont utilisé des chats chiasmatomisés afin de mettre en évidence le rôle du CC dans le transfert interhémisphérique d'apprentissage discriminatif (TIAD). Dans une tâche de TIAD, l'animal doit effectuer une discrimination monoculaire entre deux stimuli visuels. L'obstruction d'un oeil et la chiasmatomie permettent de restreindre l'information visuelle thalamo-corticale directe à l'hémisphère ipsilatéral par l'oeil non-obstrué. L'autre hémisphère ne peut recevoir l'information visuelle en provenance de l'oeil controlatéral que par l'entremise des liens commissuraux, notamment le CC. Lorsqu'il atteint un critère élevé de réussite, l'animal est testé avec l'oeil non-entraîné afin de vérifier la capacité de TIAD visuel. Les résultats de Myers (1955, 1956) montrent que les chats chiasmatomisés peuvent réussir la tâche initiale de discrimination ainsi que la tâche de transfert. Cependant, si les chats sont chiasmatomisés et callosotomisés, le TIAD visuel est rendu impossible (Myers, 1956). Ceci met en évidence l'importance du CC dans ce type de tâche visuelle.

Les études comportementales de Berlucchi et al. (1978, 1979) ont mis en évidence les effets de lésions corticales sur la capacité de TIAD chez les chats chiasmatomisés. Leurs résultats montrent que la capacité de TIAD des animaux chiasmatomisés et lésés des aires 17, 18 et 19 ne diffère pas de celle des animaux chiasmatomisés sans lésions corticales (Berlucchi et al., 1978). Cependant, si des lésions corticales sont effectuées au niveau des aires 7, 19, 21 et suprasylviennes, les animaux chiasmatomisés montrent un déficit important de TIAD (Berlucchi et al., 1979). Ces résultats suggèrent que les aires extrastriées sont davantage importantes pour réussir une tâche de TIAD que les aires primaires. Cependant, le rôle de l'aire 19 dans ce type de tâche demeure imprécis car une partie importante de cette aire est lésée chez les deux groupes d'animaux.

Une deuxième fonction visuelle à laquelle semble participer le CC est la fusion binoculaire et la perception de la profondeur. Un indice binoculaire important pour percevoir la profondeur réside dans la disparité spatiale créée par un stimulus situé devant ou derrière le point de fixation. Cet indice de disparité pourrait être encodé par des neurones binoculaires corticaux sensibles à la disparité qui reçoivent des inputs convergents des hémirétines nasales et temporales (Barlow et al., 1967; LeVay et Voigt, 1988; Lepore et al. 1992; Guillemot et al., 1993). Cependant, si un stimulus est situé au niveau du méridien vertical (MV), il atteint les deux hémirétines temporales dans le cas où il se trouve derrière le point de fixation et il y a disparité convergente. De même, si le stimulus est situé devant le point de fixation au niveau du MV, il atteint les deux hémirétines nasales et il y a disparité divergente. Dans ces cas échéants, l'information en provenance des deux yeux peut être dirigée vers le même hémisphère grâce au

chevauchement des fibres ganglionnaires nasales et temporales, à condition que la disparité spatiale n'excède pas un degré (Stone, 1966; Kingston et al., 1969; Sanderson et Sherman, 1971). Cependant, si la disparité spatiale horizontale excède un degré, l'information en provenance des deux yeux sera représentée bilatéralement au niveau des hémisphères cérébraux, ce qui nécessite vraisemblablement une communication interhémisphérique. Les CR des fibres calleuses présentent un recouvrement dans l'hémichamp ipsilatéral plus important que le chevauchement naso-temporal des cellules ganglionnaires de la rétine (Berlucchi et Rizzolatti, 1972; Richer, 1989). Il est donc possible que, dans une situation ou les stimuli sont présentés bilatéralement avec une disparité supérieure à un degré, le CC assure une vision non-diplopique (Westeimer et Mitchell, 1969).

Afin de mettre en évidence l'importance du CC dans la perception de la profondeur, Lepore et al. (1986) ainsi que Ptito et al. (1986) ont étudié l'effet d'une chiasmatomie et/ou d'une callosotomie sur la capacité à discriminer la profondeur à partir des stéréogrammes de Julesz. Leurs résultats montrent que le chat callosotomisé peut apprendre à discriminer une forme tridimensionnelle à partir d'indices purement binoculaires. Par contre, l'animal chiasmatomisé ne peut atteindre le critère de réussite bien qu'il montre une performance au-dessus du niveau de hasard (68%). Si l'animal est à la fois chiasmatomisé et callosotomisé, la perception de la profondeur à partir d'indices binoculaires de disparité spatiale est abolie. Ceci suggère d'une part que le CC à lui seul ne permet pas de discriminer la profondeur à partir d'indices binoculaires puisque les chats chiasmatomisés n'atteignent pas le critère de réussite. Cependant, puisque ces animaux montrent une certaine forme d'apprentissage à ce type de tâche contrairement à ceux qui subissent la chiasmatomie et la callosotomie, il est possible

d'avancer que la binocularité calleuse contribue d'une certaine façon à la perception stéréoscopique. Ceci est confirmé par les travaux de Blakemore (1970) et de Mitchell et Blakemore (1970) qui utilisent des sujets humains callosotomisé et chiasmatomisé. Un sujet humain ayant subi une chiasmatomie accidentelle peut évaluer la profondeur d'un objet placé au niveau du MV et en avant du point de fixation. De cette façon, le stimulus est analysé par les hémirétines temporales et subséquemment par chaque hémisphère. Dans cette situation, le CC pourrait permettre la communication interhémisphérique nécessaire à cette tâche (Blakemore, 1970). Finalement, un humain callosotomisé peut évaluer la distance d'un stimulus situé dans l'hémichamp gauche ou droit puisque l'information binoculaire est dirigée vers le même hémisphère. Cependant, si le stimulus est situé devant ou derrière le point de fixation au niveau du MV, le sujet callosotomisé ne peut évaluer correctement la distance (Mitchell et Blakemore, 1970).

Troisièmement, il semble que le CC joue un rôle dans la génèse des mouvements oculaires de vergence dans l'axe médian. Westeimer et Mitchell (1969) ont étudié les mouvements oculaires de vergence chez l'humain callosotomisé. La tâche consiste à fixer un point lumineux et à déplacer le regard vers un nouveau point lumineux qui apparaît à un autre endroit dans le champ visuel. Leurs résultats montrent que, si le nouveau stimulus apparaît plus près du sujet et se situe sur l'axe médian, les sujet humains callosotomisés sont incapables de converger leurs yeux vers cette nouvelle cible. Cependant, ils réussissent bien cette tâche si le nouveau stimulus apparaît à gauche ou à droite du point de fixation initial. Ces résultats suggèrent que le CC joue un rôle important dans la réalisation des mouvements de vergence des yeux au niveau du champ visuel central.

Finalement, une autre fonction du CC est d'assurer la fusion des hémichamps visuels. Tel que nous l'avons mentionné précédemment, le recouvrement naso-temporal des cellules ganglionnaires est limité à environ un degré du MV. Au-delà d'un degré, la fusion des hémichamps visuels est possible grâce aux neurones calleux visuels situés aux sites de représentation du MV (Berlucchi et Rizzolatti 1968; Innocenti 1980; Cynader et al. 1981; Lepore et Guillemot 1982). Ces neurones dirigent leurs projections dirigées vers des régions homotopiques et hétérotopiques de l'hémisphère opposé, là où est représenté le MV (Segraves et Rosenquist, 1982a, b). Les CR des neurones calleux touchent ou chevauchent le MV et peuvent s'étendre davantage vers la périphérie, ce qui explique la fusion des hémichamps visuels au-delà d'un degré.

Aires visuelles et projections calleuses

En plus des liens intrahémisphériques présents dans le cortex visuel, les différentes aires visuelles possèdent un grand nombre de liens interhémisphériques homotopiques et hétérotopiques. Les projections interhémisphériques homotopiques relient des aires visuelles homologues alors que les projections calleuses hétérotopiques relient des aires visuelles différentes. Les études anatomiques montrent que les liens calleux relient les régions limitrophes des aires 17/18 de façon homotopique (Innocenti, 1980). Cette région limitrophe des aires 17/18 consiste en une représentation du MV. Les neurones situés dans cette région envoient également des projections calleuses hétérotopiques aux aires 19 et PMLS dans la zone de représentation du MV (Wilson, 1968; Squatrito et al., 1981; Payne, 1986; Lepore et al., 1992).

Plusieurs études démontrent que l'abondance des liens calleux est plus importante au niveau des aires extrastriées comparativement à l'aire primaire 17. En utilisant la technique anatomique de Nauta, Ebner et Myers (1965) notent que la section du CC et de la commissure antérieure du chat ne provoque pas une dégénérescence importante au niveau de l'aire primaire 17. Par contre, ils ont observé une dégénérescence très dense au niveau de l'aire 18. D'autres études montrent que la section du CC chez le chat entraîne une dégénérescence marquée au niveau des aires 19 et PMLS (Garey et al., 1968; Wilson, 1968). Les études anatomiques plus récentes confirment que l'abondance des liens calleux est plus prononcée au niveau de l'aire PMLS (Innocenti et al. 1980; Dreher, 1986). La portion du champ visuel représentée dans les zones calleuses est également de plus en plus développée dans les aires extrastriées. Segraves et Rosenquist (1982a, b) estiment que l'étendue des CR visuels situés à la bordure des aires 17/18 ne dépasse guère plus de 10 degrés tandis qu'au niveau de l'aire PMLS, les CR calleux s'étendent au-delà de 60 degrés du MV.

Propriétés des fibres visuelles calleuses

Les études électrophysiologiques réalisées directement au niveau des fibres calleuses chez le chat normal sont peu nombreuses (Berlucchi et al., 1967; Hubel et Wiesel, 1967; Lepore et al, 1992; Richer, 1989, Schatz, 1977). Les résultats de Berlucchi (1967) montrent que la plupart des CR des fibres calleuses se trouvent à proximité de l'AC. Les études de Hubel et Wiesel (1967) indiquent que les CR des fibres calleuses touchent le MV ou sont à moins de quatre degrés de ce dernier. De plus, les CR de certaines fibres calleuses ont une organisation comparable à celle des cellules corticales S, C ou Ch. Une étude de Richer (1989) montre que les propriétés des CR des

fibres calleuses sont semblables à celles des cellules corticales. Les CR des fibres calleuses sont relativement bien définis et peuvent être sélectifs à l'orientation et/ou à la direction du stimulus. Aussi, les CR calleux sont généralement assez étendus, à l'instar de ceux des cellules des aires suprasylviennes qui possèdent de nombreux liens calleux.

Propriétés des cellules visuelles des zones calleuses

Une autre façon d'étudier les propriétés des CR visuels des fibres calleuses est l'utilisation d'un animal ayant subi la chiasmatomie. Chez ces sujets, les cellules corticales qui peuvent être activées par l'oeil controlatéral reçoivent nécessairement un input calleux étant donné la section sagittale médiane du chiasma optique. Les résultats obtenus avec ce type de préparation chirurgicale montrent que les neurones corticaux conservent les propriétés typiques des neurones enregistrés chez le chat normal (Hubel et Wiesel, 1965; Berlucchi et Rizzolatti, 1968; Lepore et Guillemot, 1982). Cependant, la chiasmatomie provoque une baisse importante des cellules binoculaires du cortex. Il semble toutefois qu'environ le tiers des cellules enregistrées dans la région limitrophe des aires 17/18 ainsi que dans l'aire PMLS demeurent binoculaires après la chiasmatomie (Lepore et Guillemot, 1982; Antonini et al., 1983; Lepore et al., 1992).

Antonini et al. (1983) ont étudié les CR des cellules enregistrées dans l'aire PMLS chez le chat chiasmatomisé. Les résultats montrent que les CR de l'aire PMLS sont très étendus comparativement aux aires 17 et 18 et peuvent être sélectifs à la direction du stimulus. Les CR binoculaires peuvent être situés dans l'hémichamp controlatéral ou ipsilatéral à proximité du MV ou chevaucher ce dernier, contrairement aux CR monoculaires qui sont seulement localisés dans l'hémichamp controlatéral. Ces

résultats soutiennent l'hypothèse que le CC pourrait assurer la fusion entre les hémichamps visuels.

Le corps calleux: un filtre spatio-temporel

En 1966, Enroth-Cugell et Robson ont utilisé des réseaux de bandes sinusoïdales afin de déterminer certaines propriétés spatio-temporelles telles la résolution spatiale et la sensibilité au contraste d'un CR visuel. Depuis, plusieurs études ont utilisé ce type de stimulation afin de décrire les propriétés visuelles des cellules de la rétine (Enroth-Cugell et Robson, 1966), du CGL (Cleland et al. 1971; Hoffmann et al., 1972; So et Shapley, 1981), du collicule supérieur (Bisti et Sireteanu, 1976) ainsi que celles des aires corticales 17/18 (Movshon et al. 1978a, b, c; Tolhurst et Thompson, 1981), 19 (Pollen et al., 1978; Tanaka et al., 1987), PMLS et PLLS (Morrone et al. 1986; Zumbroich et Blakemore, 1987). Ces études montrent que les neurones corticaux peuvent être sélectifs à une étendue très limitée de FS et de FT. De plus, ils présentent des seuils de contraste qui varient d'une cellule à une autre. Ces propriétés filtrantes observées au niveau de neurones individuels peuvent-elles être généralisées à un ensemble de fibres? Certains auteurs considèrent en effet qu'un groupe de fibres tel le CC puisse révéler de telles propriétés.

Maffei et al. (1986) ainsi que Berardi et al. (1987) ont étudié les propriétés spatio-temporelles des CR des cellules binoculaires de la zone calleuse des aires 17/18 chez le chat chiasmatomisé. Ils rapportent que 52% des cellules de l'aire 17 sont binoculaires alors que 73% le sont au niveau de l'aire 18. Berardi et al (1987) ont comparé les propriétés visuelles de cellules corticales binoculaires telles qu'obtenues par

la voie directe (géniculo-corticale) et par la voie calleuse. Les résultats montrent que les cellules corticales ont une résolution spatiale et temporelle plus basse lorsqu'elles sont stimulées par la voie calleuse plutôt que par la voie géniculo-corticale directe. De plus, la sensibilité au contraste est plus faible pour l'input calleux que pour l'input provenant de la voie directe. Cette hypothèse selon laquelle le CC agirait tel un filtre spatio-temporel a été soutenue par des enregistrements de potentiels évoqués visuels effectués directement dans le CC. En effet, ces enregistrements révèlent que les fibres calleuses ont des résolutions spatiales et temporelles beaucoup plus basses comparativement aux cellules des autres structures visuelles du chat.

Par contre, cette hypothèse semble moins évidente au niveau de l'aire 18 du chat chiasmatomisé. Berardi et al. (1987) notent que dans l'aire 18, seulement la moitié des cellules binoculaires montrent une différence de résolution spatiale et temporelle entre l'input calleux et l'input direct. De plus, seulement le tiers des cellules binoculaires ont une plus haute sensibilité au contraste lorsqu'elles sont stimulées par l'input direct plutôt que par l'input calleux.

Finalement, mentionnons que certaines études comportementales montrent également que la capacité de transfert d'information visuelle est plus limitée chez le chat chiasmatomisé que chez le chat normal. En effet, les chats normaux réussissent une tâche de transfert entre des réseaux de FS élevées, moyennes ou basses à des contrastes relativement bas (10-15%) et d'orientations différentes. Par contre, le chat chiasmatomisé à l'âge adulte est incapable de réussir une tâche de TIAD lorsque la FS est supérieure à 1,1 cycles/degré (c/deg). Le TIAD visuel est cependant possible pour une basse FS (0,6 c/d) avec un taux de contraste moyen (17%) (Berardi et al., 1988).

Les auteurs concluent que ces résultats confirment l'hypothèse selon laquelle le CC agit comme un filtre qui ne transmet que des basses FS et des hauts contrastes.

Nous avons des raisons de croire que cette dernière hypothèse mérite d'être vérifiée par des études supplémentaires. D'abord, les études électrophysiologiques de Berardi et al. (1987) à la base de cette hypothèse ont été effectuées sur un nombre très limité de cellules visuelles situées à la bordure des aires 17 et 18. Aussi, la dominance oculaire de ces cellules révèle que l'input direct est presque toujours dominant, en ce sens qu'il procure un taux de décharge plus élevé que l'input calleux. Or, nous savons que les propriétés des cellules visuelles binoculaires peuvent présenter des différences interoculaires et que certaines de ces différences peuvent être reliées à la dominance oculaire (Rose et Blakemore, 1974; Skottun et Freeman, 1984; Hammond et Fothergill, 1994). Il est donc difficile de savoir si les différences qui ont été observées par Berardi et al. (1987) révèlent des propriétés spécifiques du CC où si elles sont dues à d'autres paramètres tel que la dominance oculaire. Finalement, puisque les études comportementales de Berlucchi et al. (1978, 1979) suggèrent que les aires extrastriées sont déterminantes pour le TIAD, nous croyons pertinent de vérifier si les résultats de Berardi et al. (1987) s'appliquent aux cellules des aires extrastriées, lesquelles possèdent davantage de liens calleux.

CHAPITRE II

Article #1

Spatial and temporal frequency tuning and contrast sensitivity of single neurons in the area 21a of the cat

SPATIAL AND TEMPORAL FREQUENCY TUNING AND CONTRAST SENSITIVITY OF SINGLE NEURONS IN AREA 21A OF THE CAT.

Eric Tardif1-2, André Bergeron1-2, Franco Lepore1-2 and Jean-Paul Guillemot1-3

1 Groupe de Recherche en Neuropsychologie Expérimentale
2 Département de Psychologie, Université de Montréal, C. P. 6128, Succ. Centre-Ville, Montréal, Québec, H3C 3J7.
3 Département de Kinanthropologie, Université du Québec, C. P. 8888, Montréal, Québec, H3C 3P8.

Publié dans: **Brain Research** (1996), 716, 219-223

Send correspondence to:

Dr. Franco Lepore
Département de Psychologie
Université de Montréal
C.P. 6128 Succ. centre-ville
Montréal, Québec
Canada, H3C 3J7

Telephone: (514) 343-6503
Telefax: (514) 343-5787

Key Words: Area 21a, spatial frequency, temporal frequency, contrast sensitivity, extrastriate cortex, vision, cat.

Short Title: Spatial and temporal frequency selectivities in area 21a.

The spatial and temporal selectivities of single neurons in area 21a of the adult cat were investigated using sinusoidal gratings. Optimal spatial frequencies and visual acuity (high cut-off frequency) were fairly low and spatial bandwidth was mainly narrow. Contrast threshold was generally low but a substantial number of cells were only excited by high contrast stimuli. The temporal selectivity suggests that cells responded to a wide range of temporal frequencies.

Area 21 is one of several regions making up the suprasylvian gyrus of the cat visual cortex [10]. Based on the distribution of the receptive fields (RFs), it was further subdivided into two distinct regions (areas 21a and 21b) which occupy different positions within the cortical mantle [18].

RF properties of single neurons in the area 21a have been established using light or dark bars or edges, either flashed or drifted across the RFs [6, 11, 19]. So far, few attempts [7, 17] have been made to describe the RF properties of area 21a cells in terms of more precise parameters such as spatial and temporal frequency tuning, and contrast sensitivity. These properties have been described for cortical areas 17 [12, 13], 18 [1, 3, 14], 19 [8, 16] and PMLS [20] and have been instrumental in helping define the roles of these areas in vision.

The experiments reported here examine the spatial and temporal properties of single units in area 21a. The principal objective was to extend the findings obtained for the various visual areas to this extrastriate area which remains less well-known. The secondary objective was to determine to which primary source the RFs were most comparable.

The methods used for animal preparation, anesthesia, surgery, optical preparation and recording have been described in details in a previous paper [9]. Briefly, 15 acute experiments were carried out using adult cats initially intubated and anesthetized with a mixture of N2O : O2 (70 : 30) and Halothane (2 - 3% of total gaseous mixture). After the

surgery, the animal was paralyzed with gallamine triethiodide (Flaxedil 200 mg) and d-tubocurarine (Tubarine 20 mg) dissolved in 30 ml of lactated ringer solution with dextrose (5%), continuously infused (5.6 ml/h) through the saphenous vein cannula to maintain paralysis of extraocular muscles. During the induction of paralysis, the general anesthesia was maintained between 2 and 3 %. Then, it was gradually lowered and maintained at 0.5% for the duration of the experiment.

To prevent eye dehydratation and to improve image resolution, a neutral contact lens with a 3mm artificial pupil was placed on each eye. The optic quality of the eyes was routinely checked during the recording session and the image on the retina was focused on the display monitor by the use of additional appropriate dioptric lenses.

Drifting sine wave gratings (adjusted, where necessary, for length) were presented on a display monitor located 57 cm in front of the animal, as in [20]. The cell's discharge rate was recorded using the best direction and temporal frequency (as determined by ear) and the contrast was kept constant at 50%. For each cell tested at the various spatial frequencies, each data point of the tuning function corresponds to the response (in spikes/s) of the cell from which was subtracted the discharge rate recorded during blank presentations.

Temporal frequency tuning was assessed by using sine wave gratings having the best spatial frequency and drifting in the optimal direction at various temporal frequencies. The contrast was kept constant at 50% and the drift frequency varied from 0.5 to 24 Hz. The procedures for stimulus presentations and recording were the same as those used for evaluating spatial frequency tuning.

For the dominant eye of each cell, a response vs contrast curve was established using the optimal spatial and temporal frequencies drifting in the best direction. Contrast values varied from 0.5% to 50% and each were presented pseudo-randomly 10 times. Contrast

threshold was then determinated by linear interpolation of the data point and corresponds to the contrast value which elicited a response in 70% of the trials.

A total of 125 neurons were isolated in area 21a of the cat's cortex. Of these, 113 responded to visual stimulation; no cell was found which responded to the other modalities tested superficially (auditory, somatosensory). Most RFs centers (94%) were located within 10° eccentricity. The majority of cells were binocularly driven (80%) and orientation selective (93%). Most cells (87/108) had complex RF areas and a minority were either end-stopped (14/108) or simple (7/108). RFs covered a wide range of sizes (from 1.0 to 82.7 deg2), but most were relatively small, more than half being less than 10 deg2.

Spatial frequency tuning curves were derived for 108 cells. Example of a binocular complex cell is illustrated in Fig. 1A. The bandwidth can be measured, in octaves, and is generally considered to be an indicator of the spatial frequency filtering qualities of the unit. Visual acuity was defined as the spatial frequency where the tuning curve intersects the baseline (i.e., the high cut-off spatial frequency). Fig. 1B shows the percentage of cells with respect to this measure of visual acuity for the dominant eye. For 58 binocular cells, spatial frequency tuning curves were determined for both eyes in order to assess the matching between the two eyes. As expected, a significant relation ($r = 0.64$, $p < 0.001$) exists between the high cut-off spatial frequencies of the ipsilateral and contralateral eyes. An ocular dominance index (ODI) was calculated using the formula: $ODI = [(I / (I + C)]100$, where I represents the response to stimulation of the ipsilateral eye and C, the response of the contralateral eye. As illustrated in fig. 1C, acuity was usually higher for the dominant eye. There is a significant relation ($r = 0.63$, $p < 0.001$) between the ODI and the difference between the acuities derived for each eye (Fig.1C). For most cells with an ODI close to 50, the difference in resolution between the eyes is very low, whereas for the others the difference generally favors the dominant eye.

Fig 1D show the distribution of optimal spatial frequencies for the dominant eye. These are generally low and range from 0.07 to 1.29 c/deg, with a mean value of 0.36 ± 0.3 c/deg. Bandwidth ranged from 0.42 to 4.7 octaves (mean = 1.6 ± 0.9 octaves) and the majority of cells act as relatively narrow spatial frequency filters. For both variables, a highly significant relationship between the two eyes (optimal spatial frequency: $r = 0.91$, $p < 0.001$; spatial bandwidth: $r = 0.70$, $p < 0.001$) is found. Moreover, the small differences which sometimes existed were independent of ocular dominance.

The responses of 28 neurons were assessed to different temporal frequencies using drifting sine wave gratings at optimal spatial frequency and 50% contrast. This assessment was only carried out for the dominant eye and six representative units are shown in Fig. 2A. All units showed band-pass characteristics, which means that a cell's response generally increased as temporal frequency increased and dropped thereafter. Fig. 2B illustrates the distribution of cells with respect to optimal temporal frequencies. The cells responded vigorously to the different temporal frequencies with a mean optimal temporal frequency of 7.0 ± 4.0 c/s. Mean temporal bandwidth of the dominant eye was 2.9 ± 1.2 octaves. Thus, it seems that area 21a neurons respond to a wide range of temporal frequencies that are relatively higher than those of primary visual cortex.

For 81 cells, their responses to different contrasts were evaluated using their optimal spatial and temporal frequencies. Contrast thresholds varied from 2% to 30% (mean = 10.45 ± 9.6 %). Figure 2C shows the response at different contrasts of the dominant eye for three cells. Figure 2D shows the distribution of contrast thresholds measured in all cells. Although some cells required a relatively low amount of contrast for a response to be elicited (see unit 1 in Fig. 2C), others were found which could only be excited with high contrasts (see unit 3 in Fig. 2C). The contrast threshold was measured for each eye in 40 binocular cells. There is a significant relation ($r = 0.73$, $p < 0.001$) between the

relative thresholds of both eyes. When differences are found, these are independent of ocular dominance.

The purpose of these experiments was to investigate area 21a neurons to determine their spatial and temporal properties using sinusoidal gratings. It is of particular interest to compare these results with those obtained in other visual areas. The average visual acuity in area 17 is 2 c/deg and the maximum is 7 c/deg [14]. This is considerably higher than the values found in area 21a (mean = 0.96 c/deg, maximum = 2.22 c/deg.). Maximum visual acuity is, however, comparable with results reported for cells in areas 18 [1, 14], 19 [8,16], PMLS [20], superior colliculus [2] and the LPl region [4]. It is clear, therefore, that even though area 21a receives substantial inputs from area 17, the recipient cells no longer manifest the high spatial resolution of the cells of origin.

As far as temporal frequency tuning is concerned, all cells responded as band-pass units to defined but wide ranges of frequencies. The distribution of the mean optimal temporal frequencies (7.0 ± 4.0 c/s) shows that cells responded to fairly high temporal frequencies. On the other hand, the mean bandwidth is rather broad, suggesting that neurons in 21a are not very selective to the dynamic aspects of a stimulus.

Contrast threshold measurements showed that some cells required very low contrast to respond to the gratings. Others, on the other hand, required as much as 10 % contrast to be excited. This is probably another manifestation that cells in this region receive a variety of inputs.

Anatomical studies [5] have suggested that area 21a likely receives inputs from all three retinal channels (X, Y, W). It would thus be expected that neurons manifest different properties typical of these pathways. The X system (essentially coming from area 17) is probably reflected by the strong orientation selectivity and by the high spatial acuity found in some neurons. On the other hand, many cells also respond to low spatial frequencies and high temporal frequencies, as well as low contrast, suggesting that the Y

input (possibly relayed by areas 17 and 18) also contributes to the RF properties of some neurons. This hypothesis is consistent with the results of Dreher et al. [6] which show that selective pressure-blocking of Y inputs in one eye leads to modifications in the RF properties of neurons activated through this eye. Although it is difficult to relate W input to any particular RF property, it is quite likely that this system also contributes, via area 19, to the activation of cells in 21a.

One of the corollary aims of this study was to determine whether the spatial and temporal properties of cells in 21a resemble those of area 17, which constitutes its main source of inputs, or those of extrastriate areas, such as 18, 19 and PMLS. In general, there are substantial similarities in responses between cells present in 21a and those situated in these other extrastriate areas, as well as those in LPl, which shares reciprocal connections with these structures. In both extrastriate areas and LPl, the majority of cells are binocularly driven, with complex rather than simple RF and respond to lower frequencies compared to cells in area 17. On the other hand, results from our study and from others show that most cells in area 21a are not direction selective [6, 11, 19] as in area PMLS [15] a finding which points to a definitive distinction between the RF properties of cells in these two areas. Also, even though the cells in area 21a respond to lower frequencies, their spatial bandwidth is roughly comparable to that found in area 17 while spatial frequency tuning curves in both PMLS and the LPl seems to be slightly broader. In this respect, the input from the LPl is reflected more in area PMLS than in area 21a, in which spatial tuning is narrower. Neurons in area 21a also respond to a wide range of temporal frequencies, corresponding more to the characteristics of areas 18 and PMLS than to those of the primary area. Thus, in conclusion, a substantial proportion of neurons in area 21a demonstrate spatial selectivities more typical of the X system wheras the temporal properties are more similar to the Y system.

This study was supported by a grant from the Natural Science and Engineering Research Council of Canada (NSERC) and the Fonds pour la Formation de Chercheurs et l'Aide à la Recherche (FCAR) awarded to Franco Lepore and Jean-Paul Guillemot. A special thanks to Stephan Quessy for technical assistance.

[1] Berardi, N., Bisti, S., Cattaneo, A., Fiorentini, A. and Maffei, L., Correlation between the preferred orientation and spatial frequency of neurones in visual areas 17 and 18 of the cat, J. Physiol., 323 (1982) 603-618.

[2] Bisti, S. and Sireteanu, R., Sensitivity to spatial frequency and contrast of visual cells in the cat superior colliculus, Vision Res., 16 (1976) 247-251.

[3] Bisti, S., Carmignoto, G., Galli, L. and Maffei, L., Spatial frequency characteristics of neurones of area 18 in the cat: Dependence on the velocity of the visual stimulus, J. Physiol., 359 (1985) 259-268.

[4] Casanova C., Freeman R.D. and Nordmann J.P., Monocular and binocular response properties of cells in the striate-recipient zone of the cat's lateral posterior-pulvinar complex. J. Neurophysiol., 62 (1989) 544-557.

[5] Dreher, B., Thalamocortical and corticocortical interconnections in the cat visual system: relation to mechanism of information processing. In J.D. Pettigrew, K.J. Sanderson, and W.R. Levick (Eds.), Visual neuroscience, Cambridge University Press, Cambridge, 1986, pp. 290-314.

[6] Dreher, B., Michalski, A., Ho, H.T., Lee, C.W.F. and Burke, W., Processing of form and motion in area 21a of cat visual cortex, Visual Neurosci., 10 (1993) 93-115.

[7] Gabibov, I.M., Hemispheric interaction during the processing of spatial information, Usp. Fiziol. Nauk., 24 (4), (1993), 3-11.

[8] Guillemot, J.-P., Bergeron, A., Tardif, E., Richer, L., Ptito, M. and Lepore, F., Visual resolution of single cells in area 19 of split-chiasm cats, Soc.Neurosci. Abstr., 315.2 (1993).

[9] Guillemot, J.P., Paradis, M.C., Samson, A., Ptito, M., Richer, L. and Lepore, F., Binocular interaction and disparity coding in area 19 of visual cortex in normal and split-chiasm cats, Exp. Brain Res. 94 (1993) 405-17.

[10] Heath, C.J. and Jones, E.G., The anatomical organisation of the suprasylvian gyrus of the cat, Ergebnisse der Anat. 45 (1971) 1-61.

[11] Mizobe, K., Itoi, M. Kaihara, T. and Toyama, K., Neuronal responsiveness in area 21a of the cat, Brain Res., 438 (1988) 181-194.

[12] Movshon, J.A., Thompson, I.D. and Tolhurst, D.J., Spatial summation in the receptive fields of simple cells in the cat's striate cortex, J. Physiol., 283 (1978a) 53-77.

[13] Movshon, J.A., Thompson, I.D. and Tolhurst, D.J., Receptive field organisation of complex cells in the cat's striate cortex, J. Physiol., 283 (1978b) 79-99.

[14] Movshon, J.A., Thompson, I.D. and Tolhurst, D.J., Spatial and temporal contrast sensitivies in areas 17 and 18 and the cat's visual cortex, J. Physiol., 283 (1978c) 101-120.

[15] Rauschecker, J.P., von Grünau, M.W. and Poulin, C., Centrifugal organization of direction preferences in the cat's lateral suprasylvian visual cortex and its relation to flow field processing, J. Neurosci. ,7, (1987), 943-958.

[16] Tanaka, K., Ohzawa, I., Ramoa, A.S. and Freeman, R.D., Receptive field properties of cells in area 19 of the cat, Exp. Brain Res., 65 (1987), 549-558.

[17] Toyama, K., Mizobe, K., Akasa, E. and Kaihara, T., Neuronal responsiveness in areas 19 and 21a, and the posteromedial lateral suprasylvian cortex of the cat, Exp. Brain. Res., 99, (1994), 289-301.

[18] Tusa, R.J., and Palmer, L.A., Retinotopic organisation of areas 20 and 21 in the cat, J. Comp. Neurol., 193 (1980) 147-164.

[19] Wimborne, B.M. and Henry, G.H., Response characteristics of the cells of cortical area 21a of the cat with special reference to orientation specificity, J. Physiol., 449 (1992) 457-478.

[20] Zumbroïch, T.J. and Blakemore, C., Spatial and temporal selectivity in the suprasylvian visual cortex of the cat, J. Neurosci., 7(2) (1987) 482-500.

Figure Legends

Fig. 1 A. Spatial frequency tuning curves of a binocular cell recorded in area 21a. Filled and open circles correspond to the response of the contralateral and ipsilateral eye, respectively. The stimulus was a sinusoidal grating drifting at optimal direction and temporal frequency with a contrast of 50%. B. Distribution of the high cut-off spatial frequency (visual acuity) of the dominant eye for 108 cells recorded in area 21a. C. Difference between the high cut-off spatial frequencies (visual acuity) of the ipsilateral and contralateral eyes (n = 58 cells) plotted against the ocular dominance index (ODI). Negative values on the y axis are arbitrarily assigned to cells showing a higher visual acuity through the contralateral eye and positive values correspond to cells having higher acuities for the ipsilateral eye. Cells located in the lower left and the upper right quadrants indicate that resolution is higher for the dominant eye. With few exceptions, cells with an ODI close to 50 (balanced dominance) have comparable visual acuities. D. Distribution of the optimal spatial frequencies obtained for the dominant eye of 58 cells.

Fig. 2 A. Representative temporal frequency tuning curves for the dominant eye of 6 cells recorded in area 21a. The stimulus was a sinusoidal grating drifting at optimal direction and spatial frequency with a contrast of 50%. B. Distribution of the optimal temporal frequencies for the dominant eye of 28 cells recorded in area 21a. C. Examples of response vs contrast curves for 3 cells recorded in area 21a. Arrows indicates the contrast threshold (open triangles, threshold=3%; open circles, threshold=6%; filled circles, threshold=12%). D. Distribution of the contrast thresholds measured for the dominant eye of 81 cells.

Figure 1

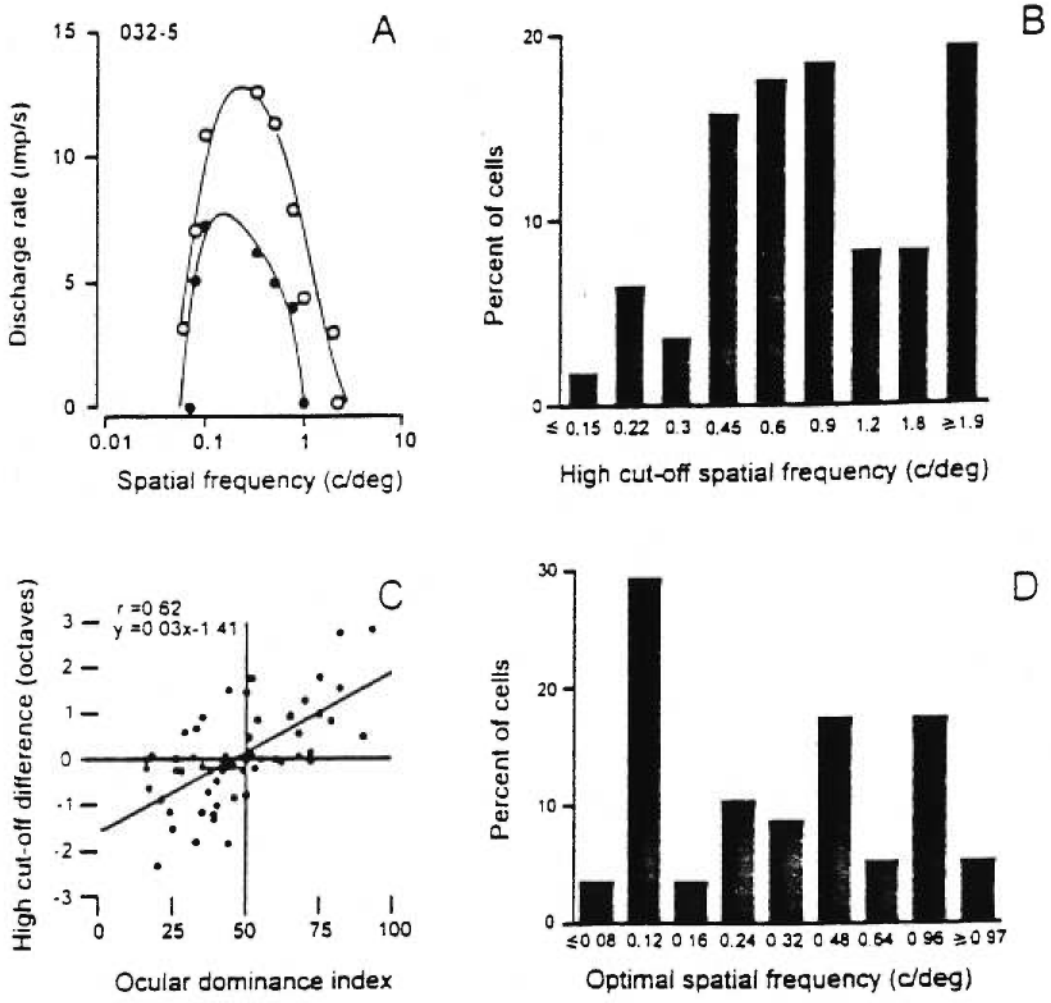
A
032-5
Discharge rate (imp/s)
15
10
5
0
0.01
0.1
1
10
Spatial frequency (c/deg)
B
Percent of cells
20
10
0
≤ 0.15
0.22
0.3
0.45
0.6
0.9
1.2
1.8
≥1.9
High cut-off spatial frequency (c/deg)
C
r =0 62
y =0 03x-1 41
High cut-off difference (octaves)
3
2
1
0
-1
-2
-3
0
25
50
75
100
Ocular dominance index
D
Percent of cells
30
20
10
0
≤0 08
0.12
0 16
0.24
0 32
0 48
0 64
0 96
≥0 97
Optimal spatial frequency (c/deg)

Figure 2

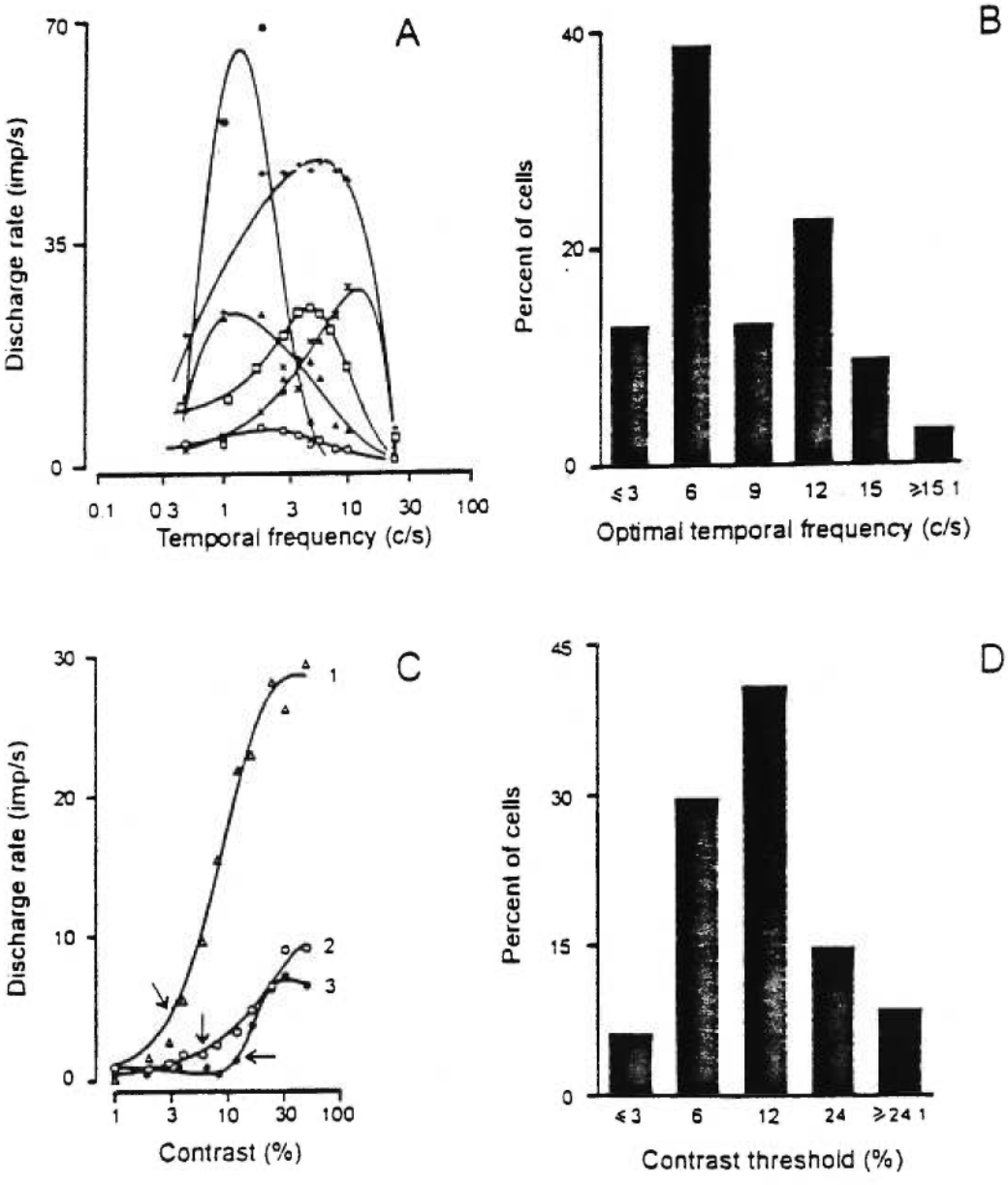
A
Discharge rate (imp/s)
70
35
0
0.1
0.3
1
3
10
30
100
Temporal frequency (c/s)
B
Percent of cells
40
20
0
≤3
6
9
12
15
≥15
Optimal temporal frequency (c/s)
C
Discharge rate (imp/s)
30
20
10
0
1
2
3
1
3
10
30
100
Contrast (%)
D
Percent of cells
45
30
15
0
≤3
6
12
24
≥24
Contrast threshold (%)

CHAPITRE III

Article #2

Spatial and temporal matching of receptive field properties of binocular neurons in area 19 of the cat

SPATIAL AND TEMPORAL MATCHING OF RECEPTIVE FIELD PROPERTIES OF BINOCULAR CELLS IN AREA 19 OF THE CAT

A. Bergeron [1], E. Tardif [1], F. Lepore [1-2] and J.-P. Guillemot [1-3].

[1-] Groupe de Recherche en Neuropsychologie Expérimentale
[2-] Département de Psychologie, Université de Montréal, C. P. 6128, Succ. Centre-Ville, Montréal, Québec, H3C 3J7.
[3-] Département de Kinanthropologie, Université du Québec à Montréal, C. P. 8888, Succ. Centre-Ville, Montréal, Québec, H3C 3P8.

Send correspondence to: Jean-Paul Guillemot
Département de Kinanthropologie,
Université du Québec à Montréal
C. P. 8888 Succ. Centre-Ville, H3C 3P8
Montréal, Québec, Canada

Telephone: (514) 987-3606
Telefax: (514) 343-5787
Email: r10475@nobel.si.uqam.ca

Running Title: Spatio-temporal matching in area 19 of the cat

Abbreviations:

σ: standard deviation

C: complex

cd/m^2: candela per square meter

Ch: complex end-stopped

c/deg: cycle per degree

deg: degree

deg/s: degree per second

ECG: electrocardiogram

EEG: electroencephalogram

Hz: Hertz

L_{max}: maximum luminance

L_{min}: minimum luminance

MΩ: mega Ohm

ODI: ocular dominance index

RF: receptive field

S: simple

Sh: simple end-stopped

Abstract - The spatial and temporal properties of single neurons were investigated in area 19 of the cat. We evaluated the matching of binocular receptive fields properties with regard to the respective strength of the ipsilateral and contralateral inputs. Results indicate that most cells in area 19 are well tuned to spatial and temporal frequencies and exhibit relatively low contrast threshold (mean = 6.8%) when assessed using optimal parameters and tested through the dominant eye. Spatial resolution (mean = 0.75 c/deg), optimal spatial frequencies (mean = 0.16 c/deg) were relatively low and spatial bandwidths (mean = 2.1 octaves) broader as compared to those of cells in area 17 but comparable to those of cells in other extrastriate areas. On the other hand temporal resolution (mean = 10.7 Hz), optimal temporal frequency (mean = 4.5 Hz) and temporal bandwidths (mean = 2.9 octaves) were higher and broader than in primary visual cortex. A significant relationship exists between most of the cell's properties assessed through either eye. For some parameters, such as spatial and temporal resolution, ocular dominance was shown to be significantly related to the extent of matching between the two eyes. For these parameters, binocular cells that exhibited a balanced ocular dominance were generally well matched with regard to the receptive field properties of each eye whereas the largest mismatches were found in cells that were more strongly dominated by one eye. These results suggest that visual input contributes to the activation of cells in area 19 in a redundant manner, possibly attesting to the multiplicity of parallel pathways to this area in the cat.

Key Words: Spatial frequency, temporal frequency, contrast sensitivity, extrastriate cortex.

Binocular vision requires that two retinal images be integrated by the visual system. Such integration is presumed to be achieved by binocular cells in the visual cortex, allowing the perception of a single image. For three-dimensional objects, the convergence of inputs on these cells can also lead to stereoscopic vision. As demonstrated in visual areas 17/18 [3, 34, 35], 19 [24, 43] and 21a [57] of the cat, a large proportion of binocular cells are sensitive to positional disparities or phase disparities [23], which could enable to perceive the inherent solidity of objects and to appreciate their position in three dimensional space with respect to the fixation point. Moreover, cells in the visual cortex may be sensitive to velocity differences, which could provide information about the direction of a stimulus moving in depth [7, 12]. In such studies, it was generally assumed that the two receptive fields (RF) of binocular cells had similar properties on the basis of early reports [29, 30]. Consequently, the visual stimuli used (either a bar or gratings) were always the same for the two eyes, as only the spatial position, phase or velocity varied between the two stimuli. However, recordings of binocular cells in areas 17/18 [5, 25, 33, 46, 49], 19 [2, 24, 43] and 21a [17, 55] have shown that, although there is a significant interocular matching between RFs properties such as position, size, spatial and temporal frequency tuning, orientation tuning and contrast sensitivities, these properties are not perfectly matched between the two eyes. One crucial characteristic of binocular cells relates to the relative strength of the cellular response to stimulation of the ipsilateral and contralateral eye [29]. These differences in ocular dominance may be related to the specificities of their binocular RFs properties. For example, several studies in the primary visual cortex of both cat [21, 22, 35] and monkey [44] suggest that binocular cells coding for crossed or uncrossed positional disparities exhibit stronger responses to stimulation of one eye while cells coding for stimuli on the fixation plane are more balanced in ocular dominance.

As the RFs properties of binocular cells may differ slightly between the two eyes, it implies that these cells can integrate two visual inputs with a certain degree of mismatch. However, grossly dissimilar monocular inputs lead to binocular rivalry and to alternating perception or suppression of the monocular images. If the non-correspondence between the two inputs is due to early misalignment of the eyes (strabismus), there is a drastic reduction of binocular cells in the visual cortex [11, 27, 40]. Perceptual studies suggest that the capacity to see a single image by the fusion of two monocular inputs depends on the geometrical arrangement of each monocular stimulus rather than on the positional disparities between them [9]. This suggests that there are at least two types of binocular interactions in the visual system: one is concerned with single vision and the other with stereoscopic perception.

These binocular interactions are processed in the visual cortex where the two inputs coming from each eye are integrated. In addition to the numerous intracortical and interhemispheric connections among the multiple visual areas, the latter also receive distinct inputs directly from subcortical structures. Direct projections of X fibers from the dorsal lateral geniculate nucleus are mainly restricted to area 17 [15, 16, 53]. This system, which allows for high spatial resolution, possibly accounts for the excellent interocular matching of RFs properties in areas 17/18 [49] as well as for the presence of cells finely tuned to positional disparities [34, 35]. In area 19, direct projections come mainly from either the C-laminae of the dorsal lateral geniculate nucleus, or the extrageniculate structures such as the medial part of the lateral posterior complex or from the medial interlaminar nucleus [6, 28]. As these subcortical regions receive both Y and W inputs from the retina, area 19 is likely to be innervated by these two kinds of input. However, anatomical studies suggest that the subcortical input to area 19 is mostly derived from W cells [15, 16, 31.52]. This direct input to area 19 (as well as to the lateral suprasylvian areas) possibly accounts for the residual vision present after lesion of areas 17/18 [51].

In area 19 of the normal cat, most cells have relatively small binocular RFs [1, 30] of either the complex or end-stopped types [18, 19, 30, 47, 54] that are tuned to orientation [18, 19] and spatial frequencies [54]. Despite the rather low spatial resolution provided by its W afferents, about one-third of the binocular cells are sensitive to positional disparity [24, 43], although their tuning curve has a relatively large bandwidth when compared to cells in areas 17/18. These properties probably depend in part, therefore, on afferents from area 17.

The RFs of binocular cells in area 19 are distinct from their counterpart in area 17 both with respect to their properties and the nature of their inputs. Therefore, this leads to the question of whether the extent of matching that occurs between the RFs properties of each eye is as excellent in area 19 as it is in area 17. The present study aims at answering this question by assessing the spatial and temporal characteristics of binocular cells in area 19 and comparing the degree of interocular matching for these properties.

EXPERIMENTAL PROCEDURES

Subjects

The experiment was carried out on 17 adult cats of either sex weighing between 2 and 4 kg each. The animals came from a Université de Montréal approved supplier. They were all in good health and had no apparent malformations or pathologies. All manipulations were carried out in accordance with the guidelines proposed by the Canadian Council on Animal Care and with those of the National Institute of Health concerning the preparation and maintenance of higher animals during neuroscience experiments. Moreover, the experimental protocols were approved by the University animal care committee. In accordance with these guidelines, all attempts were made to minimize suffering and reduce the number of animals used.

Surgery

On the day of recording, the cat received an i.m. injection of Atropine (Atro-Sol, 0.2 mg/kg) to reduce bronchial secretions. It was then anesthetized with a gaseous mixture of Nitrous Oxide: Oxygen (N_2O: O_2, 70:30) and halothane (2%), intubated with an endotracheal tube which was connected to a respiratory pump. The animal was placed in a modified stereotaxic apparatus (David Kopf). The saphenous vein was cannulated and a solution of 5% dextrose in lactated Ringer was continuously infused to maintain blood pressure and hydration. Respiratory rate and volume were controlled so as to maintain a constant level of expired CO_2 (4% ± 0.5%). Body temperature was kept constant at 38° C with the help of a thermostatically controlled heating waterpad. Heart rate was also monitored throughout the experiment. During all surgical procedures, general anesthesia was maintained between 1% and 2% of halothane. The scalp was shaved, the skull exposed and a small bone flap overlying area 19 (AP: 5 to -5; L: 4 to 9) was removed. A small incision was made in the dura overlying the cortex representing the center of visual field according to the maps of Tusa et al. [56]. The cortex

was covered with 4% agar in physiological saline to reduce pulsation and to prevent its dehydration. All pressure points and wounds were routinely infiltrated with local anesthetic (Xylocaine or Lidocaine). At the end of the surgery the halothane level was progressively reduced (0.5% / 15 min.) and maintained at 0.5% for the duration of the experiment. Stable heart rate and the absence of reflexes ensured that the anesthesia level was sufficient. Then, the animal was paralyzed with gallamine triethiodide (Flaxedil: 200 mg) and d-tubocurarine (Tubarine: 20 mg) dissolved in 30 ml of lactated Ringer solution with dextrose (5%). The mixture was continuously infused (5.6 ml/h) through the saphenous vein to maintain paralysis of extraocular muscles. ECG was constantly monitored and EEG, monitored intermittently yet regularly, showed slow-wave activity throughout the recording session. It must be noted that following the induction of paralysis, recording was delayed for at least four hours to insure physiological functions stabilization.

Optical preparation and recording procedure

In order to determine the relative positions of the areae centrales, retinal landmarks (optic discs and blood vessels) were projected on a tangent screen located 57 cm in front of the animal [20]. The relative position of the area centralis was considered to be situated 16 deg medially and 7.5 deg below the iso-elevation line of the center of each optic disk [8]. Pupils were routinely dilated by i.m. injections of atropine sulfate 1% (Atro-Sol, 0.2 mg/kg) and the nictitating membranes of the eyes were retracted with topical applications of phenylephrine hydrochloride (Neo-synephrine, 0.1%). A neutral contact lens having a 3 mm artificial pupil was placed on each eye to prevent dehydration and to improve image resolution. The images of the display monitor were focused on the retinae by the use of additional dioptric lenses, as dictated by direct retinoscopy. The optic quality of the eyes was routinely checked during the recording session.

Recordings were carried out with glass micropipettes filled with 2M NaCl having an impedance of 2-5 MΩ (measured at 1000 Hz). The micropipette was lowered perpendicularly to the cortical surface. Action potentials were conventionally amplified, displayed on an oscilloscope, filtered through a time/amplitude discriminator and transferred to an audio monitor and to a computer.

Visual stimulation and data collection

For each cell recorded, the position of the RF (minimal response field[3]) of each eye was mapped and explored manually using light or dark bars. The best stimulus parameters for direction, velocity, orientation, width and length were estimated based on the output of the audio monitor. Each RF was classified in terms of simple (S), complex (C) or end-stopped categories [26 29 30]. The principal inclusion criteria for the latter class was that the cell preferred an oriented grating of optimal length, whereby extending the stimulus out of the boundaries of the RF caused an important decrease in response (end-stopping). This category therefore included both simple (Sh) and complex (Ch) RFs, provided that they had the additional property of end-stopping. The criteria of DeValois et al. [13] and Skottun et al. [50] were also used to definitively classify the RF organization. The S- and Sh-type cells showed a modulated response waveform at the first harmonic (as revealed by a Fourier analysis) of the drifting grating at the optimal spatial frequency. The C and Ch-type cells showed an overall increase in their response component (mean firing rate) at the first harmonic of the drifting grating at the optimal spatial frequency. In binocular cells, the relative strength of the cellular response to stimulation of the ipsilateral and contralateral eye was assessed by calculating an ocular dominance index (ODI) using the following formula: ODI = (ipsilateral / ipsilateral + contralateral) x 100, where ipsilateral represent the response to monocular stimulation of the ipsilateral eye and contralateral represent the response to monocular stimulation of the contralateral eye.

To study the spatial and temporal selectivity of the cells, drifting sinusoidal gratings were generated with a Picasso image generator (Innisfree: Picasso model Rev. 8) and presented on a display monitor (Hewlett Packard, model 1321a; P31 phosphor) located 57 cm in front of the animal. The stimulation screen subtended 25 deg x 25 deg of visual angle and had a mean luminance of 5 cd/m^2 (measured with a spotmeter). However, for the end-stopped RFs (Sh and Ch) the size of the stimulus was varied systematically, and the size yielding the optimal response from the cell was used for quantitative tests. For the assessment of spatial frequency selectivity, the cell's discharge was recorded using the best stimulus direction at a temporal frequency of 2 Hz. The contrast was kept constant and it was increased gradually, over a period of 500 ms, until it reached 50%. The gradual increase was carried out to avoid evoking a transient response from the cell. The presentation of the drifting gratings lasted 3 s and an intertrial interval of 18 s was introduced to minimize cell adaptation [41]. The contrast was defined as follows: $(L_{max.}-L_{min.})/(L_{max.}+L_{min.}) \times 100$, where $L_{max.}$ is the maximum luminance and $L_{min.}$ is the minimum luminance of the spatial sinusoid. Each spatial frequency (0.04 to 2.4 c/deg per step of half-octave) was presented pseudo-randomly 10 times for 3 s, and a blank trial of the same duration and of the same mean luminance (5 cd/m^2) as the test grating was presented prior to the presentation of each drifting grating.

For the cells responding with a modulated pattern of activity (S and Sh), each data point of the tuning function corresponds to the modulation amplitude (in spikes/s) of the cell. For cells responding with a non-modulated pattern of activity (C and Ch), each data point corresponds to the mean response (in spikes/s) of the cell from which was subtracted the mean discharge rate recorded during the blank presentations. Each tuning curve was fitted using a curve fit software (Table curve: version 1; Jandel Scientific,

San Rafael, CA). The best fit curve thereby obtained had a high correlation ($r \geq 0.9$) with the data points and was used to evaluate the optimal spatial frequency and bandwidth.

Temporal frequency selectivity was assessed with the presentation of gratings having the best spatial frequency and drifting in the optimal direction at various temporal frequencies. The contrast was kept constant at 50% and the drift frequency varied from 0.5 to 24 Hz (per step of half-octave). The procedures for stimulus presentations, recordings and data analysis were identical to those used for the evaluation of the spatial frequency selectivity.

The contrast tuning of the cell was assessed by using gratings having the best spatial and temporal frequencies and drifting in the optimal direction. For the assessment of response vs contrast curves, the contrast of the gratings varied between 0.5 to 50% and each level was presented pseudo-randomly (ten trials for each contrast level) per step of half-octave. The contrast threshold was then fixed to the contrast level that elicited a response in 70% of the trials. The stimulus presentations, recordings and data analysis were carried out in the same manner as for assessing the spatial frequency tuning function.

Histology

At the end of the experiment, the cat was deeply anesthetized with 5% halothane, then perfused through the heart with an isotonic saline solution followed by formalin (4%). The brain was removed, placed in formalin and later prepared for histology. The block containing the electrolytic lesions was cut in coronal sections 40 μm thick. Every second section was kept and colored using the cresyl violet method. Electrodes penetrations were all within area 19, identified according to the maps of Otsuka and Hassler [42], Hubel and Wiesel [30] and Tusa et al. [56].

RESULTS

Receptive fields properties

More than 300 neurons were recorded in area 19 of the cat, but only cells (n = 204) which gave robust response to the stimuli were submitted to the quantitative protocol. Cells with bursting reponses or "hard to drive" were not tested. These kind of responses were usually encountered with cells having their RFs in the peripheral visual field; thus, only central vision was examined. Most of the cells recorded in area 19 gave stable and robust responses to dark bars; maximum response for all cells was from sinusoidal or square wave gratings presented during a short period of time (~3s). No clustering of unresponsive cells was found in the central representation of the visual field of area 19. All cells tested had the RF center of their dominant eye located within 5 deg of the vertical meridian and within 10 deg of the azimuth. The RFs were classified into four categories (C, Ch, S and Sh) using the criteria of Henry [26], De Valois et al. [13] and Skottun et al. [50]. Of all the cells recorded, 5% had their RFs classified as S and 5% as Sh. A typical spatial frequency tuning of a Sh cell is shown in Fig. 1A. The approach used for data analysis was, first, to derive series of 3 s peristimulus time histograms during the null condition (uniform field at the mean luminance of the gratings) and during the presentation of each drifting grating. As a rule, S and Sh cells showed a modulated response (see Fig. 1A). Each data point of the tuning function was then plotted according to the modulation amplitude of the response (Fourier fundamental response component) from which the response during the null condition was subtracted. As can be seen in Fig. 1A, this representative Sh cell shows a modulated response to all spatial frequencies. This is most evident at a spatial frequency of 0.16 c/deg The tuning curve of this cell reflects band-pass characteristics, from which the spatial bandwidth at

half-height can be estimated. This value is considered to reflect the cell's selectivity to spatial frequencies.

The majority of the cells recorded (56%) were classified as C while the remaining 34% were classified as Ch. A typical spatial frequency tuning curve of a C cell is shown in Fig. 1B. The peristimulus time histograms show no modulation of the response (as confirmed by Fourier analysis) at any spatial frequency but rather an overall increase of the discharge rate. Each data point of the tuning function in Fig. 1B corresponds to the mean firing rate (in spikes/s) of the cell from which the mean discharge rate recorded during the null presentations was subtracted. The tuning function of this C cell shows band-pass characteristics. Other examples of band-pass spatial frequency tunings are shown in Fig. 2 for five units. By these, four cells were Ch (cells A, B, C and E) and one was S (cell D). Although the spatial frequency tuning of most cells (74%) showed band-pass characteristics, some cells (26%) did not show attenuation of their response in the lowest spatial frequencies tested and were thus considered to be low-pass units. This distinction between low-pass and band-pass units should not be understood in absolute terms as it may result from the limited capacities of our stimulus presentation system to generate spatial frequencies in the lower range. Low-pass units were therefore not included in the computations of the optimal spatial frequencies and spatial bandwidths.

---

insert figure 1 approx. here

Spatial resolution

The spatial resolution of a cell was estimated to be the high cut-off spatial frequency which corresponds to the point on the tuning curve which intersects the baseline. The spatial resolution of the Sh cell in Fig. 1A is estimated to be 0.76 c/deg while that of the

C cell in Fig. 1B is 1.28 c/deg. Spatial frequency tunings curves presented in Fig. 2 shown that the spatial resolution of typical area 19 cells was around 1 c/deg. The distribution of the spatial resolution estimated for the dominant eye of 195 cells is shown in Fig. 3A. This distribution shows that cells in area 19 vary widely with respect to spatial resolution. The highest spatial resolution observed was 2.22 c/deg and the lowest was 0.12 c/deg (mean = 0.75 c/deg; σ = 0.51 c/deg).

For 78 binocular cells, spatial frequency tuning curves were obtained for both the ipsilateral and contralateral eye, in an attempt to assess the matching of the responses. A significant correlation ($r = 0.63$, $p < 0.001$) exists between the high cut-off spatial frequencies of the ipsilateral and contralateral eyes (Fig. 3B).

---

insert figure 2 and 3 approx. here

Despite the high degree of matching between the two eyes, it is clear from Fig. 3B that some interocular differences are present. For some cells, the high cut-off spatial frequency is higher for the ipsilateral eye whereas for others, it is higher for the contralateral eye. Generally, the interocular differences were smaller than 1 octave (mean = 0.6 octaves; σ = 0.68 octaves). However, a few cells showed more pronounced interocular differences in spatial resolution, some being as large as 3 octaves. As binocular cells presented different degrees of ocular dominance, the relationship between this parameter and the interocular differences in spatial resolution was examined. In Fig. 4, interocular differences in spatial resolution were plotted against the ODI. Negative values in the ordinate are arbitrarily assigned to a higher spatial resolution for the contralateral eye and positive values to a higher spatial resolution for the ipsilateral eye. Most cells exhibiting a balanced ocular dominance showed a relatively good interocular matching whereas cells dominated by either the ipsilateral

(ODI > 50) or contralateral eye (ODI < 50) generally showed higher spatial resolutions for the dominant eye. The relationship between differences in spatial resolution and ocular dominance was significant ($r = 0.55$ $p < 0.001$).

---

insert figure 4 and 5 approx. here

Optimal spatial frequency and spatial bandwidth

For 145 band-pass cells, the spatial frequency which elicited the strongest response (optimal spatial frequency) was derived from the spatial frequency tuning curve. For example, the optimal spatial frequency of the Sh cell presented in Fig. 1A was estimated to be 0.16 c/deg and that of the C cell in Fig. 1B was estimated to be 0.32 c/deg. Optimal spatial frequencies estimated from spatial frequency tuning curves shown in Fig. 2 aretypical of the cells in area 19 (cell A: 0.15 c/deg, cell B: 0.17 c/deg, cell C: 0.17 c/deg, cell D: 0.31 c/deg and cell E: 0.1 c/deg). The distribution of optimal spatial frequencies for the dominant eye is shown in Fig. 5A. Optimal frequencies are mostly low, ranging from 0.05 to 0.58 c/deg (mean = 0.16 c/deg; $\sigma = 0.09$ c/deg). The matching of the optimal frequencies between the ipsilateral and contralateral eyes was examined for 61 binocular cells. Figure 5B shows the relationship between the optimal frequencies of both eyes. A significant correlation ($r = 0.87$, $p < 0.001$) was found between the two eyes. The interocular differences were small (mean = 0.3 octaves; $\sigma =$ 0.29 octaves), the largest interocular difference being 1.1 octaves. These interocular differences in optimal spatial frequencies were not related to the ocular dominance.

---

insert figure 6 approx. here

The spatial bandwidth was measured at the half-height of the spatial frequency tuning curve and is considered to be an indicator of the spatial selectivity of the cell. For example, the spatial bandwidth of the Sh cell shown in Fig. 1A was estimated to be 1.2 octaves whereas that of the C cell in Fig. 1B was broader, namely 2.8 octaves. Spatial frequency tunings shown in Fig. 2 have different values of spatial bandwidth (cell A: 1.5 octaves, cell B: 2.9 octaves, cell C: 2.7 octaves, cell D: 2.4 octaves and cell E: 3.5 octaves). The distribution of the spatial bandwidths for the dominant eye of 145 cells is shown in Fig. 6A. Bandwidths ranged from 0.48 to 3.6 octaves (mean = 2.1 octaves; σ = 0.64 octaves) and the majority of cells seemed to act as relatively broad spatial frequency analyzers. For 61 cells, the spatial bandwidth was calculated for both eyes. Figure 6B shows the relationship between the spatial bandwidths of the ipsilateral and contralateral eye. Spatial bandwidths are well matched between the two eyes ($r = 0.62$, $p < 0.001$), although the relationship is weaker than it was for optimal spatial frequencies. The interocular differences were usually about half an octave (mean = 0.4 octaves; σ = 0.38 octaves) and the maximal difference was 1.5 octaves. The differences between the spatial bandwidths estimated for the two eyes were not related to ocular dominance.

---

insert figures 7 and 8 approx. here

Temporal resolution

The response to different temporal frequencies of 88 cells was assessed using sinusoidal gratings at 50% contrast, having optimal spatial frequency and swept in the optimal direction. All cells showed temporal frequency tuning curves with band-pass characteristics that suggest their selectivities to the dynamic aspect of a stimulus. The temporal tuning curves of five typical units are shown in Fig. 7. Although the response

was attenuated for temporal frequencies that differed from the optimal, many cells still responded to the highest temporal frequencies which could be presented with our stimulation system (24 Hz). Since many temporal frequency tuning curves did not intersect the base line, the high temporal frequency cut-off at half-amplitude was used as an estimate of the temporal resolution. The latter varied greatly from cell to cell, as illustrated in Fig. 7 (cell A: 9.3 Hz, cell B: 5.8 Hz, cell C: 5.6 Hz, cell D: 5.5 Hz and cell E: 19.1 Hz. The distribution of temporal cut-off frequencies estimated for the dominant eye of 88 cells is shown in Fig. 8A. The lowest temporal resolution found was 1.3 Hz and the highest was 22.6 Hz (mean = 10.7 Hz; σ = 5.7 Hz). The distribution indicates that the temporal resolution varied greatly and that many cells showed a relatively high temporal resolution. The temporal resolution of 52 cells was determined for both eyes in order to assess the temporal matching between the two eyes. The relationship between the temporal resolution of the contralateral and ipsilateral eyes is illustrated in Fig. 8B. A significant relationship ($r = 0.62$, $p < 0.001$) was found between the temporal cut-off for both eyes. The maximal interocular difference found in temporal resolution was 2.2 octaves (mean = 0.5 octaves; σ = 0.5 octaves). The influence of ocular dominance on temporal resolution is illustrated in Fig. 9, where interocular differences in temporal resolution are plotted against the ODI. The significant relationship ($r = 0.25$, $p < 0.05$) suggests that although the temporal resolution difference between the eyes is smaller for cells with a balanced ocular dominance, for the cells dominated by one eye there is a tendency for the dominant eye to show a higher temporal resolution.

---

insert figures 9 and 10 approx. here

Optimal temporal frequency and temporal bandwidth

In Fig. 7, it can be seen that cells vary with respect to their optimal temporal frequencies (cells A and B: 4 and 3 Hz respectively; cells C and D: 2 Hz; cell E: 8 Hz). The distribution of optimal temporal frequencies for the dominant eye is shown in Fig. 10A. The highest optimal temporal frequency was 13.4 Hz and the lowest was 0.7 Hz (mean value = 4.5 Hz; σ = 2.8 Hz). The matching of the optimal temporal frequencies was examined for 52 binocular cells. A significant relationship ($r = 0.57$, $p < 0.001$) was found between the optimal temporal frequencies estimated for both eyes, as can be seen in Fig. 10B. Although the maximal interocular difference was 2.2 octaves, differences were generally small (mean = 0.6 octaves; σ = 0.5 octaves). The differences between optimal temporal frequencies of both eyes are independent of the ocular dominance, as were optimal spatial frequencies.

---

insert figures 11 and 12 approx. here

Temporal frequency tuning curves in Fig. 7, which are representative of the majority of those found in the present study, show closely similar temporal bandwidths (A: 2.3 octaves; B: 2.7 octaves; C: 3 octaves; D: 3.1 octaves and E: 2.8 octaves). The distribution of temporal bandwidths estimated for the dominant eye of 88 cells is shown in Fig. 11A. Temporal bandwidths ranged from 0.9 to 5.3 octaves (mean = 2.8 octaves; σ = 1.1 octaves). All cells assessed for temporal selectivity exhibited band-pass characteristics although some cells were finely tuned to temporal frequencies while several others were more broadly tuned. Indeed, more than 40% of the cells had a large temporal bandwidth (> 3 octaves) while less than 20% had a temporal bandwidth below

two octaves. The temporal bandwidth was estimated for each of the two eyes in 52 cells. A significant relationship ($r = 0.45$, $p < 0.001$) was found between the temporal bandwidths measured for the ipsilateral and contralateral eyes (Fig. 11B). When differences between the temporal bandwidths of the two eyes were found, they were generally small (mean = 0.5 octaves; $\sigma = 0.5$ octaves), although a maximal difference of 2.2 octaves was found. The interocular differences in temporal bandwidth were independent of ocular dominance.

---

insert figure 13 approx. here

Contrast

Cells of area 19, like those in other visual areas, respond more strongly as contrast is increased and present a saturation of the response to very high contrasts. Figure 12 shows four typical responses vs contrast curves of area 19 cells, each obtained through stimulation with drifting sinusoidal gratings at optimal direction, spatial frequency and temporal frequency. The contrast threshold of most cells was relatively low (see Fig. 12; cell A: 2.5%, cell B: 1.5%) whereas other cells responded at higher contrasts (see Fig. 12; cell C: 10%; cell D: 15%). Generally, the response saturated at contrast values around 30% and no cells were found which were strongly inhibited by high contrasts, although some showed this tendency (Fig. 12; cell C).

---

insert figure 14 approx. here

For 153 cells, the contrast threshold was evaluated for the dominant eye. Threshold values ranged from 1% to 30% (mean = 6.8%; $\sigma = 5.5\%$). Figure 13A shows the distribution of the contrast thresholds estimated for the dominant eye. Most cells

showed a relatively low contrast threshold (lower than 6%) yet some cells responded only to high contrasts (greater than 15%). The contrast threshold was estimated for both eyes in 60 binocular cells. As illustrated in Fig. 13B, there was a significant relationship ($r = 0.87$, $p < 0.001$) between the contrast thresholds estimated for both eyes. Small interocular differences (mean = 0.3 octaves; $\sigma = 0.38$ octaves) were observed in some cells, the largest being 1.4 octaves. The relationship between ocular dominance and interocular threshold differences was evaluated and it was found that the dominant eye had a tendency to possess lower contrast threshold (Fig. 14). Indeed, there was a weak but significant relationship ($r = 0.21$, $p < 0.05$) between the interocular threshold difference and the ODI.

DISCUSSION

The aim of this study was to investigate the extent of interocular matching between the RFs properties of binocular cells in area 19 of the cat. More specifically, the spatial and temporal frequency tuning curves as well as contrast thresholds were assessed for both eyes with respect to a number of parameters, namely, spatial and temporal resolutions, optimal frequencies and bandwidths. For some of these parameters, the degree of similarity in ocular dominance was related to the extent of interocular matching.

Spatio-temporal properties of area 19 cells

The majority of cells recorded in area 19 had binocular RFs with complex organization and several cells showed end-stopping properties. Only a few cells had simple RFs, and half of these also exhibited end-stopping. In general, cells gave robust responses when stimulated with sinewave drifting gratings and exhibited spatial and temporal band-pass characteristics.

Most cells responded optimally to spatial frequencies between 0.08 c/deg and 0.24 c/deg and had relatively broad spatial bandwidths (> 1.8 octaves). It must be noted that Tanaka et al. [54] reported that cells in area 19 responded optimally to generally higher spatial frequencies than those in the present study. Although this discrepancy might be due to sampling biases, one other possibility is that it is due to differences in the stimuli used. In the study of Tanaka et al. [54], the mean luminance of the grating was rather high (80 cd/m^2); while in the present study it was much lower (5 cd/m^2). It is well known that the peak contrast sensitivity is shifted toward low frequencies when luminance is reduced [14], a phenomena which may account for the lower optimal spatial frequencies found in the present study. Despite these differences, results from both studies showed that optimal spatial frequencies of area 19 cells are lower than those of cells in area 17

[37, 38, 39], but comparable to those of cells in other extrastriate areas such as areas 18 [4, 39], 21a [55] and postero-medio-lateral suprasylvian area [36, 58]. Previous studies in areas 19 [54], 21a [55] and postero-medio-lateral suprasylvian area [58] also found that many cells had broad spatial bandwidths, which suggests that extrastriate areas contain cells that are not as finely tuned to spatial frequency as those in area 17 [37, 38, 39, 45]. Similarly, high cut-off spatial frequency, which is used as an estimate of spatial resolution, was also found to be considerably lower than in area 17 [37, 38, 39] but comparable with that found in areas 18 [4, 39], 21a [55] and postero-medio-lateral suprasylvian area [36, 58]. These results converge toward a common conclusion, namely, that the high spatial resolution of area 17 cells, probably attributable to the strong X input from the dorsal lateral geniculate nucleus, is not preserved in area 19 even though this area may receive this type of input from area 17. Cells in area 19 only respond to relatively low spatial frequencies possibly because their principal direct inputs are of the Y and W types that carry mainly low frequency signals. It is also possible that the various thalamocortical and intracortical converging inputs to cells in this area, though essential for form processing, no longer treat fine spatial details.

Temporal tunings were all band-pass and most cells responded optimally to drifting frequencies between 2 and 6 Hz. Temporal frequency tunings were broad, as revealed by temporal bandwidths above 3 octaves for more than 40% of the cells. An estimate of the temporal resolution was assessed by the temporal frequency high cut-off taken at half-amplitude of the temporal frequency tuning function. Most cells showed moderate temporal resolutions (> 6 Hz). Taking into account that temporal frequency tuning was assessed using the optimal spatial frequency (which was usually low; mean = 0.16 c/deg), it follows that many area 19 cells preferred high velocities. For instance, the cell illustrated (tuning curve E) in Fig. 7 responded best to a grating of 0.12 c/deg drifting at 8 Hz (corresponding to a velocity of 66.6 deg/s), and still responded strongly at a

temporal frequency of 10 Hz (which corresponds to a velocity of 83.3 deg/s). Optimal temporal frequencies estimated in area 19 cells (mean = 4.5 Hz) are slightly higher than in area 17 [48] (mean optimal temporal frequency = 2.9 Hz). Considering that temporal tuning functions are typically assessed by using the optimal spatial frequencies and that the latter are generally higher in area 17, one can conclude that area 19 cells respond to much higher velocities than those in area 17. These findings are surprising when compared with the results of Duysens et al. [18, 19] which showed that area 19 cells only respond to low velocities. However, it must be noted that the stimuli used in the latter experiments consist of light or dark bars whereas the present study used sinewave gratings. These two stimuli differ in a number of important characteristics. Bars have much broader spatial frequency spectrum (which actually includes high frequencies) and should therefore be considered as complex stimuli. The reduction of perceived velocity when high frequencies are presented [10] may reflect the low velocity preference found when cells are stimulated with bars. Moreover, gratings are periodical whereas bars are not. A drifting grating of, say, 10 Hz produces many luminance fluctuations in the RF (which are likely to elevate the neuronal discharge rate).

Interocular matching of receptive fields properties

A significant interocular correlation exists for spatial and temporal properties, as well as for contrast sensitivities of single cells in area 19. Although the degree of matching between optimal spatial and temporal frequencies of the two eyes is rather high, some differences are observed in a certain number of cells. As a general rule, interocular differences in all parameters measured were relatively small (about half an octave) but extended to more than one octave in a few cells. This suggests that cells in general play an important role in single vision by integrating two monocular inputs that have relatively similar RFs properties. When compared with studies of RFs matching in the striate cortex [49], these results suggest that, although binocular cells in areas 17 and 19

may differ in many aspects of their RFs properties (RFs size, orientation tuning, end-stopping and spatial frequency properties), interocular matching is comparable for both areas, at least for the parameters assessed here (optimal spatial frequencies, spatial bandwidths and contrast thresholds). Moreover, it suggests that important differences in intracortical activation and the type of direct input to these areas (the former receiving a strong X input while the latter mostly receiving Y and W inputs) do not affect the nature of interocular matching of RFs properties.

Relationships between interocular matching and ocular dominance

The cell's ocular dominance was related to the extent of matching between both eyes for some of the parameters tested. For example, cells with equally balanced ocular dominance had the same spatial resolution for each eye while those responding more strongly to stimulation through one eye had higher spatial resolution for this eye. The matching of temporal resolution and contrast sensitivity (both estimated using optimal spatial frequency) were related in the same manner to ocular dominance. Thus, cells exhibited higher temporal resolution and contrast sensitivity when tested through the dominant eye than through non-dominant eye. For some other parameters (optimal spatial frequencies, spatial bandwidths, optimal temporal frequencies and temporal bandwidths) the degree of ocular dominance was not shown to be related to the extent of interocular matching. Some of these parameters, such as bandwidths, might have been expected to differ interocularly according to ocular dominance because of possible differences in the shape of the two monocular tuning curves. However, it seems that it is not the case, either in area 19 (the present study) or in area 17 [49].

Similarly, contrast thresholds of cells in area 19 were well matched between the two eyes, as they were in area 17 [49]. However, some cells in both areas 17 and 19 showed interocular differences in their contrast threshold. Moreover, these differences were weakly but significantly related to ocular dominance. Do these differences render

the cell less apt to perform binocular processes such as single vision or disparity coding? Although psychophysical studies have shown that the presentation of two identical stimuli with different contrast levels in each eye leads to a diminution of stereoacuity in human subjects, it is important to note that, even with great contrast differences, single vision and stereopsis were still possible [32]. This is perhaps due to a contrast gain mechanism which is thought to originate in the cerebral cortex [41]. Therefore, although interocular matching is both predominant and probably essential to ensure single vision, the visual system can accommodate some discrepancies either through compensatory mechanisms or by ignoring them.

Acknowledgments - The authors wish to thank E. Massicotte and S. Montfort for their excellent technical assistance. This study was supported by grants from the Natural Science and Engineering Research Council of Canada (NSERC) and from the Fonds pour la Formation de Chercheurs et l' Aide à la Recherche (FCAR) awarded to J.- P. Guillemot and F. Lepore.

REFERENCES

1. Albus K. and Beckmann R. (1980) Second and third visual areas of the cat: interindividual variability in retinotopic arrangement and cortical location. *J. Physiol. (London)* **299**, 247-276.
2. Antonini A., Di Stefano M., Minciacchi D. and Tassinari G. (1985) Interhemispheric influences on area 19 of the cat. *Exp. Brain Res.* **59**, 171-184.
3. Barlow H. B. D., Blakemore C. and Pettigrew J. D. (1967) The neural mechanisms of binocular depth discrimination. *J. Physiol. (London)* **193**, 327-342.
4. Berardi N., Bisti S., Cattaneo A., Fiorentini A. and Maffei L. (1982) Correlation between the preferred orientation and spatial frequency of neurones in visual areas 17 and 18. *J. Physiol. (London)* **323**, 603-618.
5. Berardi N., Bisti S. and Maffei L. (1987) The transfer of visual information across the corpus callosum: spatial and temporal properties in the cat. *J. Physiol. (London)* **384**, 619-632.
6. Berson D. M. and Graybiel A. M. (1978) Parallel thalamic zones in the LP-pulvinar complex of the cat identified by their afferent and efferent connections. *Brain Res.* **147**, 139-148.
7. Beverley K. I. and Regan D. (1973) Evidence for the existence of neural mechanisms selectively sensitive to the direction of movement in space. *J. Physiol. (London)* **235**, 17-29.
8. Bishop P. O., Kozak W. and Vakkur G. J. (1962) Some quantitative aspects of the cat's eye: axis and plane of reference of visual field coordinates and optics. *J. Physiol. (London)* **163**, 466-502.
9. Braddick O. J. (1979) Binocular single vision and perceptual processing. *Proc. R. Soc. Lond.* **204**, 503-512.

10. Campbell F. W. and Maffei L. (1981) The influence of spatial frequency and contrast on the perception of moving patterns. *Vision Res.* **21**, 713-721.

11. Crawford M. L. J. and von Noorden G. K. (1980). Optically induced concomitant strabismus in monkeys. *Invest. Ophthalmol. Visual Sci.* **19**, 1105-1111.

12. Cynader M. and Regan D. (1978) Neurons in cat parastriate cortex sensitive to the direction of motion in three-dimensional space. *J. Physiol. (London)* **274**, 549-569.

13. De Valois R. L., Albrecht D. G. and Thorell L. G. (1982) Spatial frequency selectivity of cells in macaque visual cortex. *Vision Res.* **22**, 545-560.

14. De Valois R. L., Morgan H., Polson, M. C., Mead, W. R. and Hull E. M. (1974) Psychophysical studies of monkey vision. 1. Macaque luminosity and color vision tests. *Vision Res.* **14**, 53-67.

15. Dreher B. (1986) Thalamocortical and corticocortical interconnections in the cat visual system: relation to mechanisms of information processing. In *Visual Neuroscience* (eds Pettigrew J. D., Sanderson K. J., Levick W. R.), pp 290-314. Cambridge University Press, Cambridge.

16. Dreher B., Leventhal A. G. and Hale P. T. (1980) Geniculate input to cat visual cortex: a comparison of area 19 with areas 17 and 18. *J. Neurophysiol.* **44**, 804-826.

17. Dreher B., Michalski A., Ho H. T., Lee C. W. F. and Burke W. (1993) Processing of form and motion in area 21a of the cat visual cortex. *Visual Neurosci.* **10**, 93-115

18. Duysens J., Orban G. A., Van Der Glass H. W. and Maes H. (1982) Receptive field structure of area 19 as compared to area 17 of the cat. *Brain Res.* **231**, 293-308.

19. Duysens J., Orban G. A., Van Der Glass H. W. and Zegher F. E. (1982) Functional properties of area 19 as compared to area 17 of the cat. *Brain Res.* **231**, 279-291.

20. Fernald R. and Chase R. (1971) An improved method for plotting retinal landmarks and focusing the eyes. *Vision Res.* **11**, 95-96.

21. Ferster D. (1981) A comparison of binocular depth mechanisms in areas 17 and 18 of the cat visual cortex. *J. Physiol. (London)* **311**, 623-655.

22. Fisher B. and Kruger J. (1979) Disparity tuning and binocularity of single neurons in the cat visual cortex. *Exp. Brain Res.* **35**, 1-8.

23. Freeman R. D. and Ozhawa I. (1990) On the neurophysiological organization of binocular vision. *Vision Res.* **30**, 1661-1676.

24. Guillemot J.-P., Paradis M. C., Samson A., Ptito M., Richer L. and Lepore F. (1993) Binocular interaction and disparity coding in area 19 of visual cortex in normal and split-chiasm cats. *Exp. Brain Res.* **94**, 405-417.

25. Hammond P. and Pomfrett C. J. D. (1991) Interocular mismatch in spatial frequency and directionality characteristics of striate cortical neurones. *Exp. Brain Res.* **85**, 631-640.

26. Henry G. H. (1977) Receptive field classes of cells in the striate cortex of the cat. *Brain Res.* **133**, 1-28.

27. Hoffmann K. P. and Shoppmann A. (1984) Shortage of binocular cells in area 17 of visual cortex in cats with congenital strabismus. *Exp. Brain Res.* **55**, 470-482.

28. Holländer H. and Vanegas H. (1977) The projection from the lateral geniculate nucleus onto the visual cortex in the cat: A quantitative study with horseradish peroxidase. *J. Comp. Neurol.* **173**, 519-536.

29. Hubel D. H. and Wiesel T. N. (1962) Receptive fields, binocular interaction and functional architecture in the cat's visual cortex. *J. Physiol. (London)* **160**, 106-154.

30. Hubel D. H. and Wiesel T. N. (1965) Receptive fields and functional architecture in two nonstriate visual areas (18 and 19) of the cat. *J. Neurophysiol.* **28**, 229-289.

31. Kimura M., Shiida T., Tanaka K. and Toyama K. (1980) Three classes of area 19 cells of the cat classified by their neuronal connectivity and photic responsiveness. *Vision Res.* **20**, 69-77.

32. Legge G. E. and Gu, Y. (1989). Stereopsis and contrast. *Vision Res.* **29**, 989-1004.

33. Lepore F. and Guillemot J.-P. (1982) Visual receptive field properties of cells innervated through the corpus callosum in the cat. *Exp. Brain Res.* **46**, 413-424.

34. Lepore F., Samson A., Paradis M. C., Ptito M. and Guillemot J.-P. (1992). Binocular interaction and disparity coding at the 17-18 border: contribution of the corpus callosum. *Exp. Brain Res.* **90**, 129-140.

35. LeVay S. and Voigt T. (1988) Ocular dominance and disparity coding in cat visual cortex. *Visual Neurosci.* **1**, 395-414.

36. Morrone M., Di Stefano M. and Burr D. C. (1986) Spatial and temporal properties of neurons of the lateral suprasylvian cortex of the cat. *J. Neurophysiol.* **56**, 969-986.

37. Movshon J. A., Thompson I. D. and Tolhurst D. J. (1978) Spatial summation in the receptive fields of simple cells in the cat's striate cortex. *J. Physiol. (London)* **283**, 53-77.

38. Movshon J. A., Thompson I. D. and Tolhurst D. J. (1978) Receptive field organization of complex cells in the cat's striate cortex. *J. Physiol. (London)* **283**, 79-99.

39. Movshon J. A., Thompson I. D. and Tolhurst D. J. (1978). Spatial and temporal contrast sensitivity of neurones in areas 17 and 18 of the cat's visual cortex. *J Physiol (London)* **283**, 101-120.

40. Mower, G. D., Burchfiel, J. L. and Duffy, F. H. (1982) Animal models of strabismic amblyopia: physiological studies of visual cortex and the lateral geniculate nucleus. *Brain Res.* **281**, 311-327.

41. Ohzawa I., Sclar G. and Freeman R. D. (1985) Contrast gain control in the cat's visual cortex. *J. Neurophysiol.* **54**, 651-667.

42. Otsuka R. and Hassler R. (1962) Über Aufbau und Gliederung der corticalen Sehphäre bei der Katze. *Arch. Psychiatr. Nervenkr.* **203**, 212-234.

43. Pettigrew J. D. and Dreher B. (1987) Parallel processing of binocular disparity in the cat's retinogeniculocortical pathways. *Proc. R. Soc. Lond.* **B232**, 297-321.

44. Poggio G. F. and Fisher B. (1977) Binocular interaction and depth sensitivity of striate and prestriate cortical neurons of the behaving rhesus monkey. *J. Neurophysiol.* **40**, 1392-1405.

45. Robson J. G., Tolhurst D. J., Freeman R. D. and Ohzawa I. (1988) Simple cells in the visual cortex of the cat can be narrowly tuned for spatial frequency. *Visual Neurosci.* **1**, 415-419.

46. Rose D. and Blakemore C. (1974) An analysis of orientation selectivity in the cat's visual cortex. *Exp. Brain Res.* **20**, 1-17.

47. Saito H., Tanaka K., Fukada Y. and Oyamada H. (1988) Analysis of discontinuity in visual contours in area 19 of the cat. *J. Neurosci.* **8**, 1131-1143.

48. Saul A. B. and Humphrey A. L. (1992) Temporal-frequency tuning of direction selectivity in cat visual cortex. *Visual Neurosci.* **8**, 365-372.

49. Skottun B. C. and Freeman R. D. (1984) Stimulus specificity of binocular cells in the cat's visual cortex: ocular dominance and the matching of left and right eyes. *Exp. Brain Res.* **56**, 206-216.

50. Skottun B. C., De Valois R. L., Grosoe D. H., Movshon J. A., Albrecht D. G. and Bonds A. B. (1991) Classifying simple and complex cells on the basis of response modulation. *Vision Res.* **31**, 1079-1086.

51. Sprague J. M., Levy J., DiBerardino A. and Berlucchi G. (1977) Visual cortical areas mediating form discrimination in the cat. *J. Comp. Neurol.* **172**, 441-448.

52. Stone J. (1983) Parallel processing in the visual system. Plenum Press, New-York.

53. Stone J. and Dreher B. (1973) Projection of X- and Y- cells of the cat's lateral geniculate nucleus to areas 17 and 18 of visual cortex. *J. Neurophysiol.* **36**, 551-567.

54. Tanaka K., Ohzawa I., Ramoa A. S. and Freeman R. D. (1987) Receptive field properties of cell in area 19 of the cat. *Exp. Brain Res.* **65**, 549-558.

55. Tardif E., Bergeron A., Lepore F. and Guillemot J.-P. (1996) Spatial and temporal frequency tuning and contrast sensitivity of single neurons in area 21a of the cat. *Brain Res.* **716**, 219-223.

56. Tusa R. J., Rosenquist A. C. and Palmer L. A. (1979) Retinotopic organization of areas 18 and 19 in the cat. *J. Comp. Neurol.* **185**, 657-678.

57. Wang C. and Dreher B. (1996) Binocular interactions and disparity coding in area 21a of cat extrastriate visual cortex. *Exp. Brain Res.* **108**, 257-272.

58. Zumbroich T. J. and Blakemore C. (1987) Spatial and temporal selectivity in the suprasylvian visual cortex of the cat. *J. Neurosci.* **7**, 482-500.

FIGURE LEGENDS

Fig. 1. Tuning curve profiles and peri-stimulus time histograms (PSTH) of two cells in area 19 . The stimuli were sinusoidal gratings drifting (2 Hz) at optimal direction with a contrast of 50%. The PSTHs (duration: 3 s) for spatial frequencies tested are shown at left and the tuning curves profiles are shown at right. A) PSTHs and spatial frequency tuning curve for a Sh cell.. B) PSTHs and spatial frequency tuning curve for a C cell.

Fig. 2. Representative examples of spatial frequency tuning functions of five cells recorded in area 19. The stimulus was a sinusoidal grating of 50 % contrast drifting in the optimal direction at a constant temporal frequency (2 Hz). These units had clear optimal spatial frequencies and a spatial resolution of about 1 c/deg.

Fig. 3. Distribution of the high cut-off spatial frequency for the dominant eye of 195 cells recorded in area 19 (A). Matching of the high cut-off spatial frequencies of the ipsilateral and contralateral eyes of 78 cells (B). A significant relationship is present between the cut-off of both eyes. Note that the scattering indicates some difference between the high cut-off spatial frequency of the two eyes.

Fig. 4. Difference between the high cut-off spatial frequencies of the ipsilateral and contralateral eyes (n = 78 cells) plotted against the ocular dominance index. Negative values on the y axis are arbitrary assigned to cells showing a higher spatial resolution through the contralateral eye and positive values correspond to cells having higher spatial resolution for the ipsilateral eye. Cells located in the lower left and the upper right quadrants indicate that spatial resolution is higher for the dominant eye. With few exceptions, cells with an ocular dominance index close to 50 (balanced dominance)

have comparable spatial resolution. A significant relationship is found between the high cut-off difference and the ocular dominance.

Fig. 5. Distribution of the optimal spatial frequency for the dominant eye of 145 cells recorded in area 19 (A). Only the cells showing band-pass characteristics have been retained. Most cells respond best at relatively low optimal spatial frequencies. Matching of the optimal spatial frequencies of the ipsilateral and contralateral eyes of 61 cells (B). A significant relationship is present between the optimal spatial frequency of both eyes.

Fig. 6. Distribution of the spatial bandwidth in octaves for the dominant eye of 145 band-pass cells recorded in area 19 (A). The spatial bandwidth is evaluated at half the amplitude of the tuning curve. Most cells have a spatial bandwidth around 2 octaves. Matching of the spatial bandwidth of the ipsilateral and contralateral eyes of 61 cells (B). A significant relationship is present between the spatial bandwidth of both eyes.

Fig. 7. Typical temporal frequency tuning curves for the dominant eye of five cells recorded in area 19. For each cell the stimulus was a sinusoidal grating drifting at optimal direction and spatial frequency with a contrast of 50%. Note that these cells show band-pass characteristics and the temporal selectivity varied from cell to cell.

Fig. 8. Distribution of the high cut-off temporal frequency for the dominant eye of 88 cells recorded in area 19 (A). The distribution shows that the temporal selectivity of area 19 cells varied within a wide range of temporal frequencies. Matching of the high cut-off temporal frequencies of the ipsilateral and contralateral eyes of 52 cells (B). A significant relationship is present between the temporal high cut-off of both eyes. Note

that the scattering indicates some difference between the high cut-off temporal frequency of the two eyes.

Fig. 9. Difference between the high cut-off temporal frequencies of the ipsilateral and contralateral eyes (n = 52 cells) plotted against the ocular dominance index. The cells with an ocular dominance index close to 50 (balanced dominance) have comparable temporal high cut-off and cells with a high or low ocular dominance index have a much higher difference generally in favour of the dominant eye. A significant relationship is found between the temporal high cut-off difference and the ocular dominance.

Fig. 10. Distribution of the optimal temporal frequency for the dominant eye of 88 cells recorded in area 19 (A). The optimum response of cells in area 19 ranged at relatively low temporal frequencies. Matching of the optimal temporal frequencies of the ipsilateral and contralateral eyes of 52 cells (B). A significant relationship is found between the optimal temporal frequency of both eyes.

Fig. 11. Distribution of the temporal bandwidth in octaves for the dominant eye of 88 cells recorded in area 19 (A). Most cells have a spatial bandwidth around 2 to 4 octaves. Matching of the spatial bandwidth of the ipsilateral and contralateral eyes of 52 cells (B). A significant relationship is present between the temporal bandwidth of both eyes.

Fig. 12. Representative contrast curves for the dominant eye of four cells recorded in area 19. The stimulus was a sinusoidal grating drifting at optimal direction, spatial and temporal frequencies. Note that these cells present saturation at different level of contrast.

Fig. 13. Distribution of the contrast threshold evaluated for 153 cells in area 19 (A). The contrast threshold is established using the optimal spatial frequency and a temporal frequency of 2 Hz. Most cells began to respond at low contrast. Matching of the contrast threshold of the ipsilateral and contralateral eyes of 60 cells (B). A significant relationship is present between the contrast threshold of both eyes but some differences between the contrast threshold of both eyes is indicated by the scattering.

Fig. 14. Difference between the contrast threshold of the ipsilateral and contralateral eyes (n = 62 cells) plotted against the ocular dominance index. Cells with an ocular dominance index close to 50 (balanced dominance) have comparable contrast threshold. A negative significant relationship is found between the contrast threshold difference and the ocular dominance.

FIGURE 1

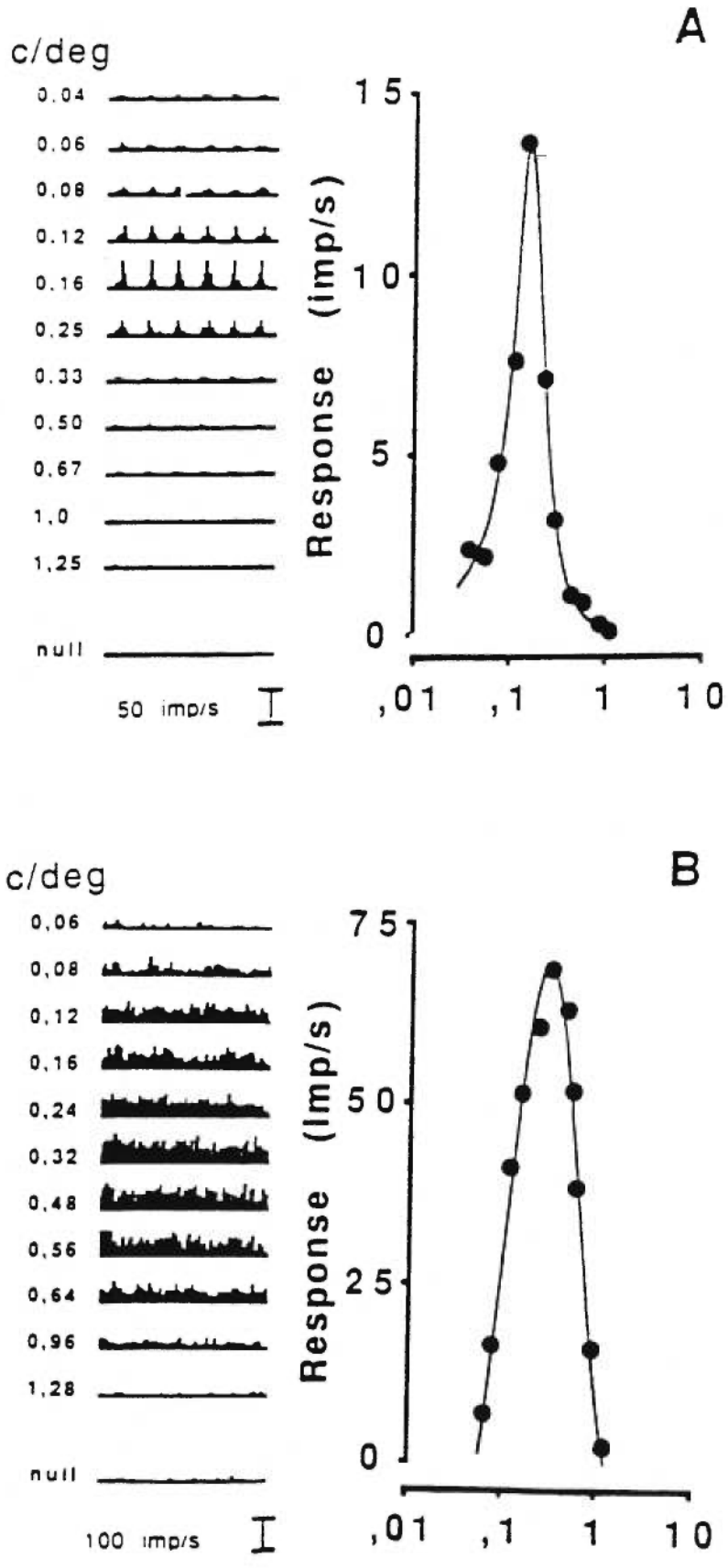
A
c/deg
0.04
0.06
0.08
0.12
0.16
0.25
0.33
0.50
0.67
1.0
1.25
null
50 imp/s
Response (imp/s)
15
10
5
0
,01
,1
1
10
B
c/deg
0,06
0,08
0,12
0,16
0,24
0,32
0,48
0,56
0,64
0,96
1,28
null
100 imp/s
Response (Imp/s)
75
50
25
0
,01
,1
1
10

FIGURE 2

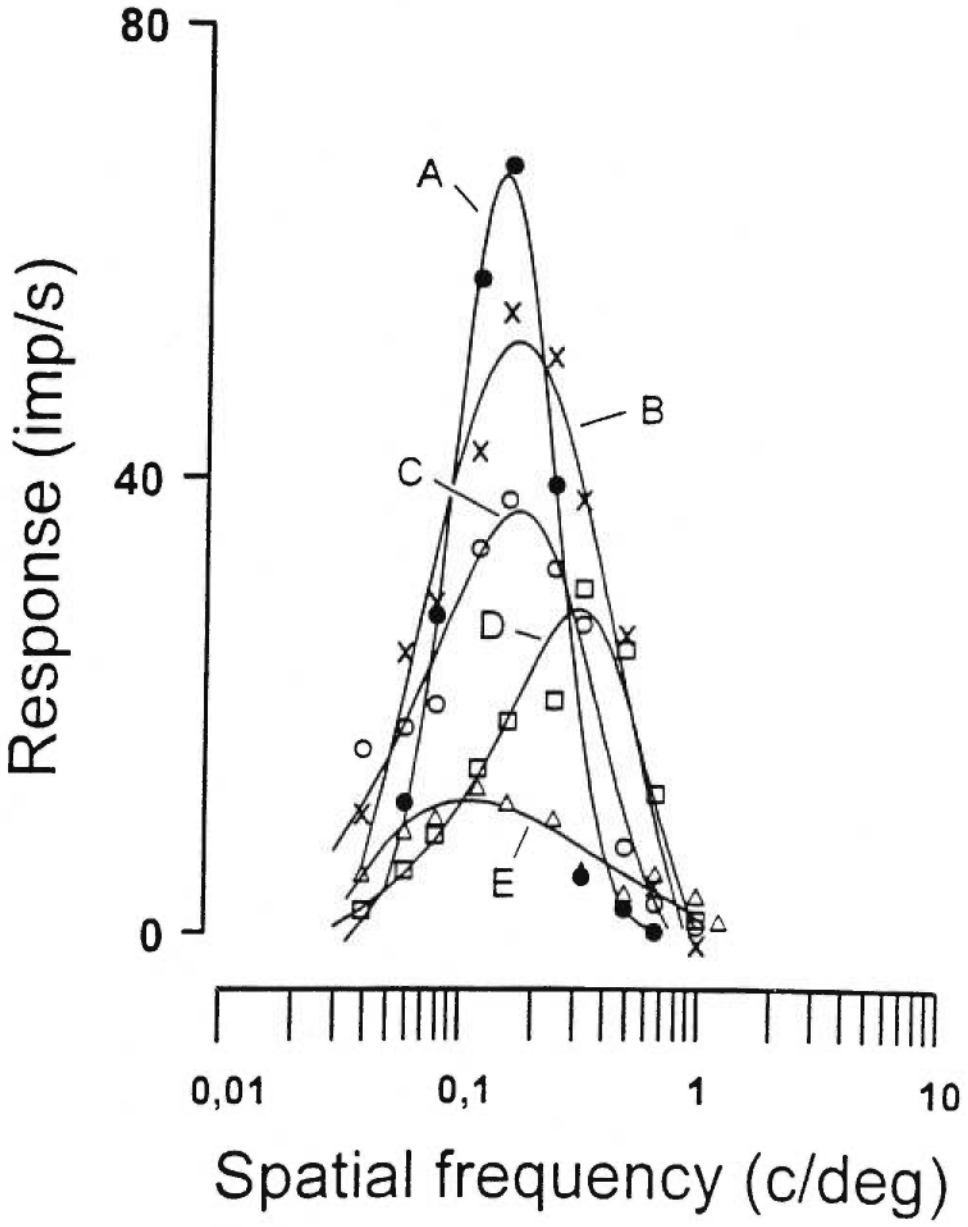
80
40
0
Response (imp/s)
A
B
C
D
E
0,01
0,1
1
10
Spatial frequency (c/deg)

FIGURE 3

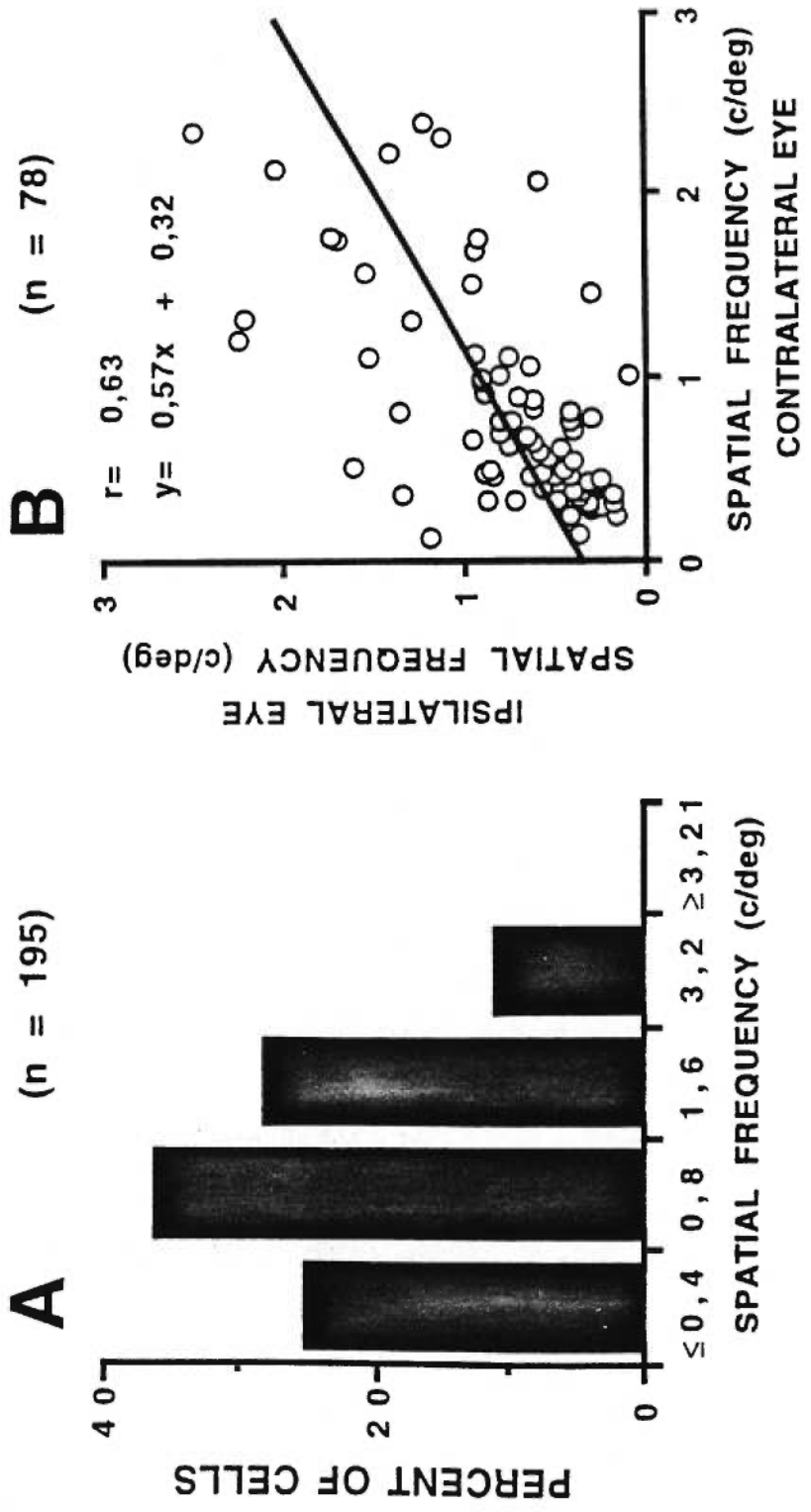
A
(n = 195)
PERCENT OF CELLS
40
20
0
≤0,4
0,8
1,6
3,2
≥3,21
SPATIAL FREQUENCY (c/deg)
B
(n = 78)
r= 0,63
y= 0,57x + 0,32
IPSILATERAL EYE
SPATIAL FREQUENCY (c/deg)
3
2
1
0
0
1
2
3
SPATIAL FREQUENCY (c/deg)
CONTRALATERAL EYE

FIGURE 4

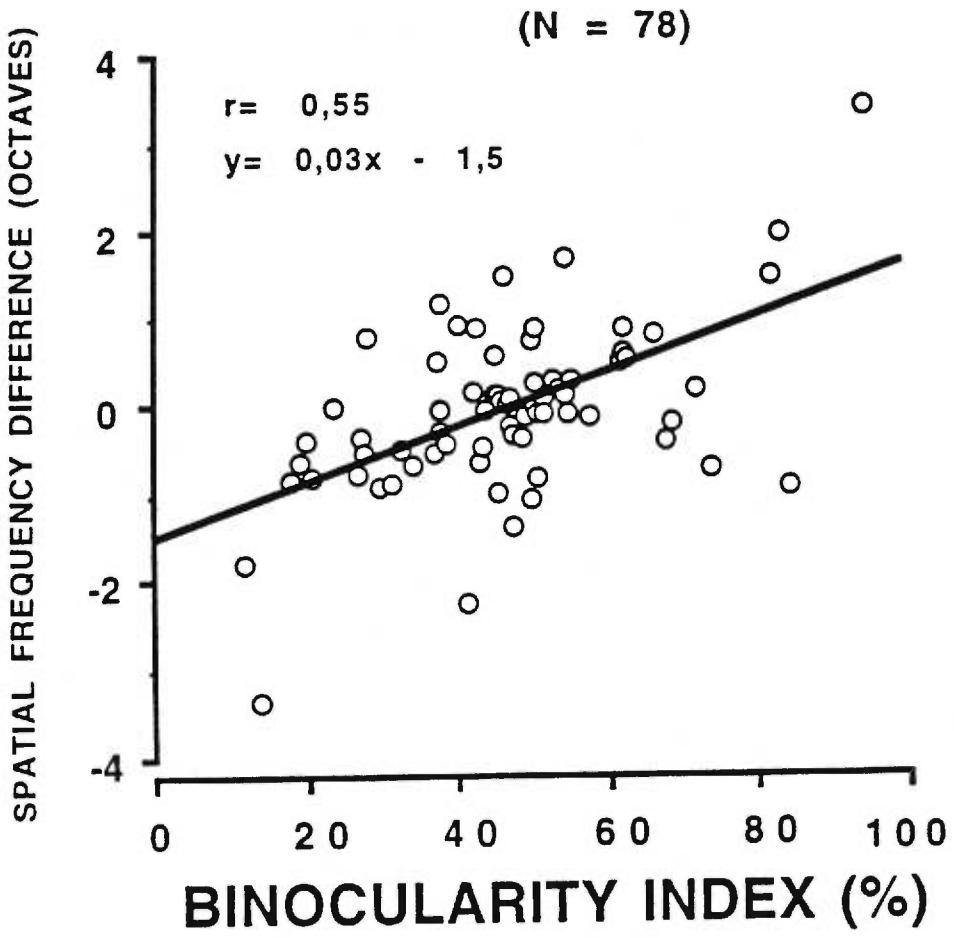
(N = 78)
r= 0,55
y= 0,03x - 1,5
SPATIAL FREQUENCY DIFFERENCE (OCTAVES)
4
2
0
-2
-4
0
20
40
60
80
100
BINOCULARITY INDEX (%)

FIGURE 5

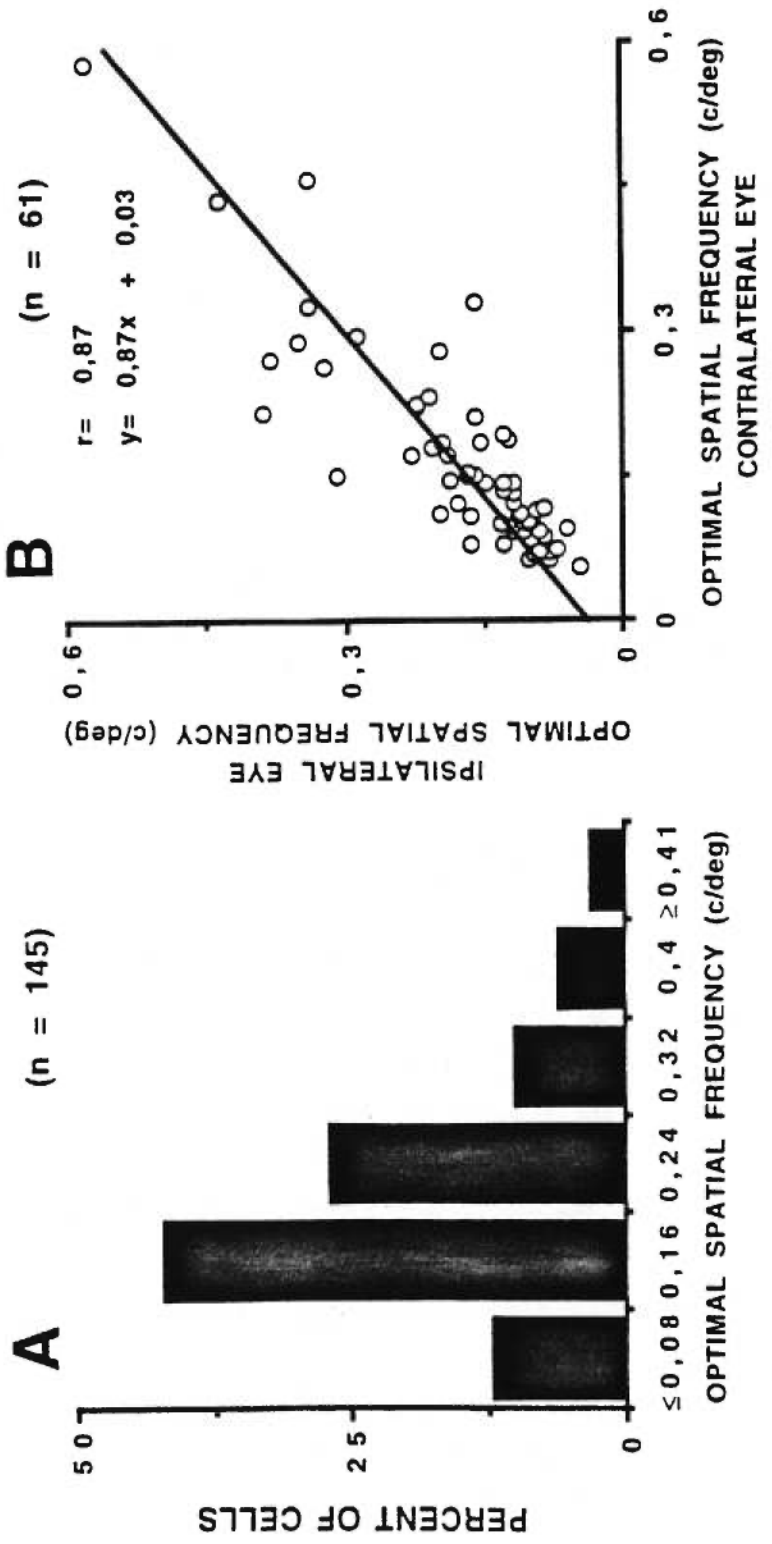
A
(n = 145)
PERCENT OF CELLS
50
25
0
≤0,08 0,16 0,24 0,32 0,4 ≥0,41
OPTIMAL SPATIAL FREQUENCY (c/deg)
B
(n = 61)
r= 0,87
y= 0,87x + 0,03
IPSILATERAL EYE
OPTIMAL SPATIAL FREQUENCY (c/deg)
0,6
0,3
0
0
0,3
0,6
OPTIMAL SPATIAL FREQUENCY (c/deg)
CONTRALATERAL EYE

FIGURE 6

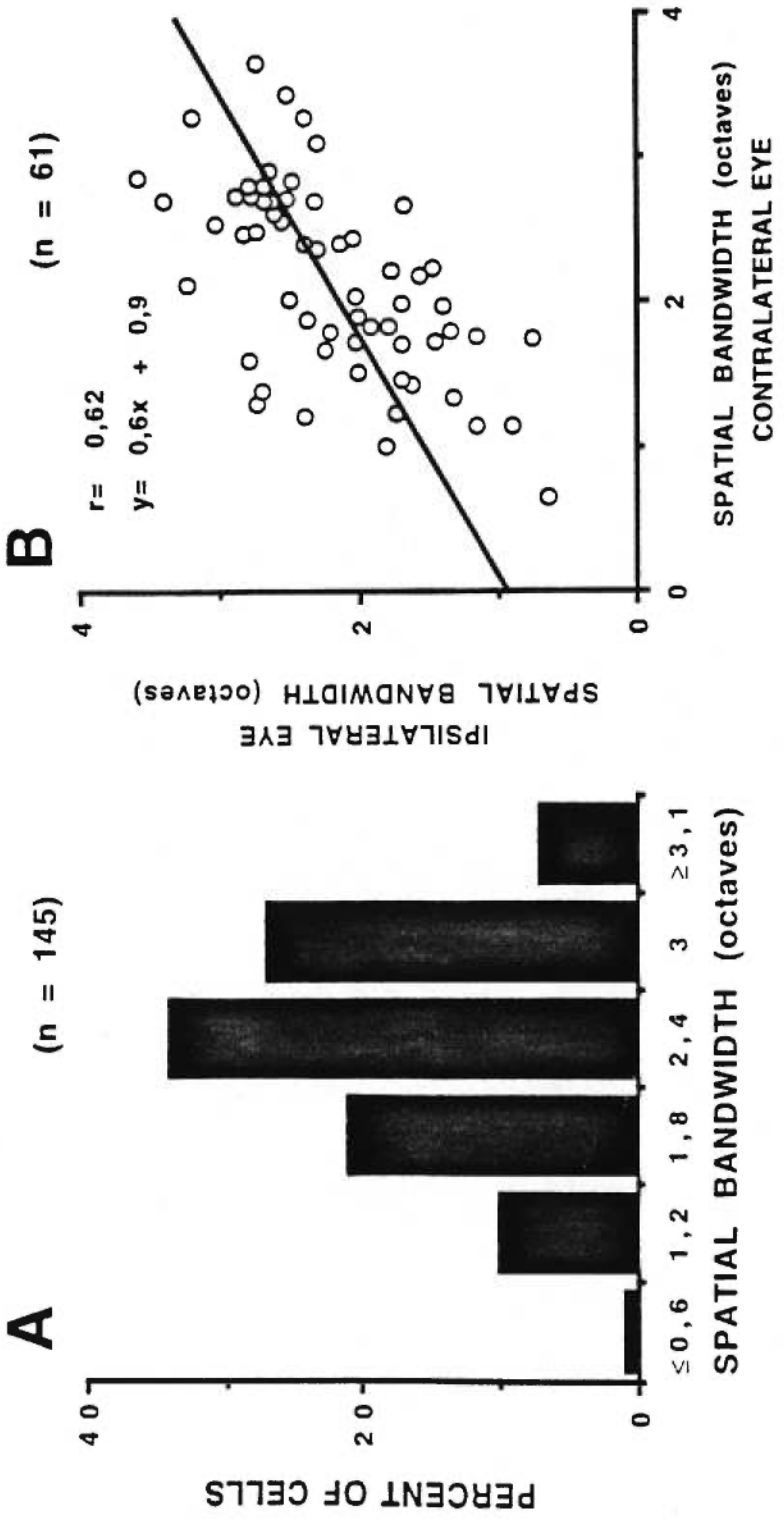
A
(n = 145)
PERCENT OF CELLS
40
20
0
≤0,6
1,2
1,8
2,4
3
≥3,1
SPATIAL BANDWIDTH (octaves)
B
(n = 61)
r= 0,62
y= 0,6x + 0,9
IPSILATERAL EYE
SPATIAL BANDWIDTH (octaves)
4
2
0
0
2
4
SPATIAL BANDWIDTH (octaves)
CONTRALATERAL EYE

FIGURE 7

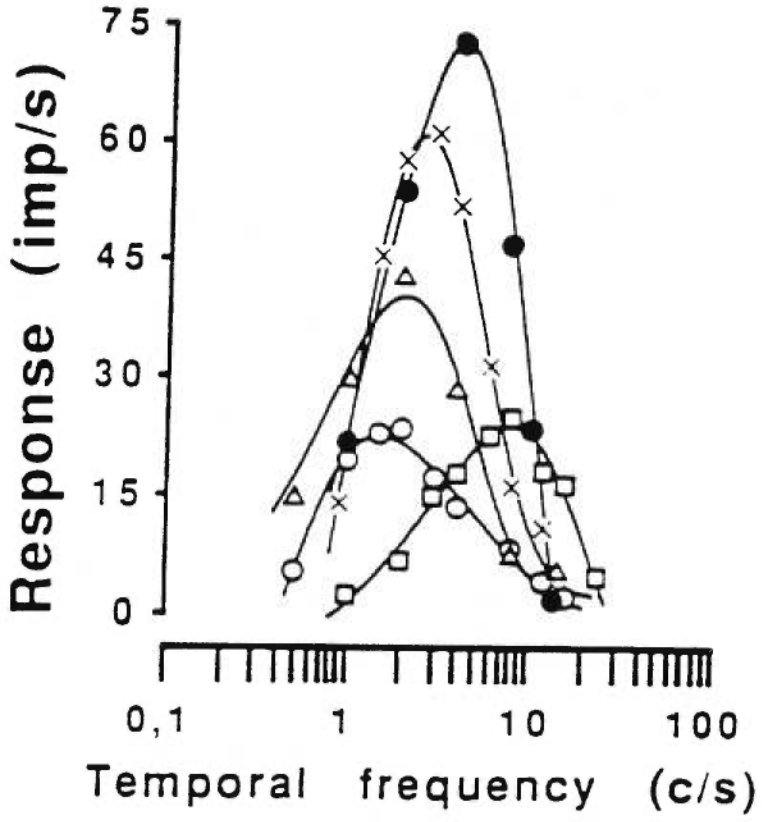
75
60
45
30
15
0
Response (imp/s)
0,1
1
10
100
Temporal frequency (c/s)

FIGURE 8

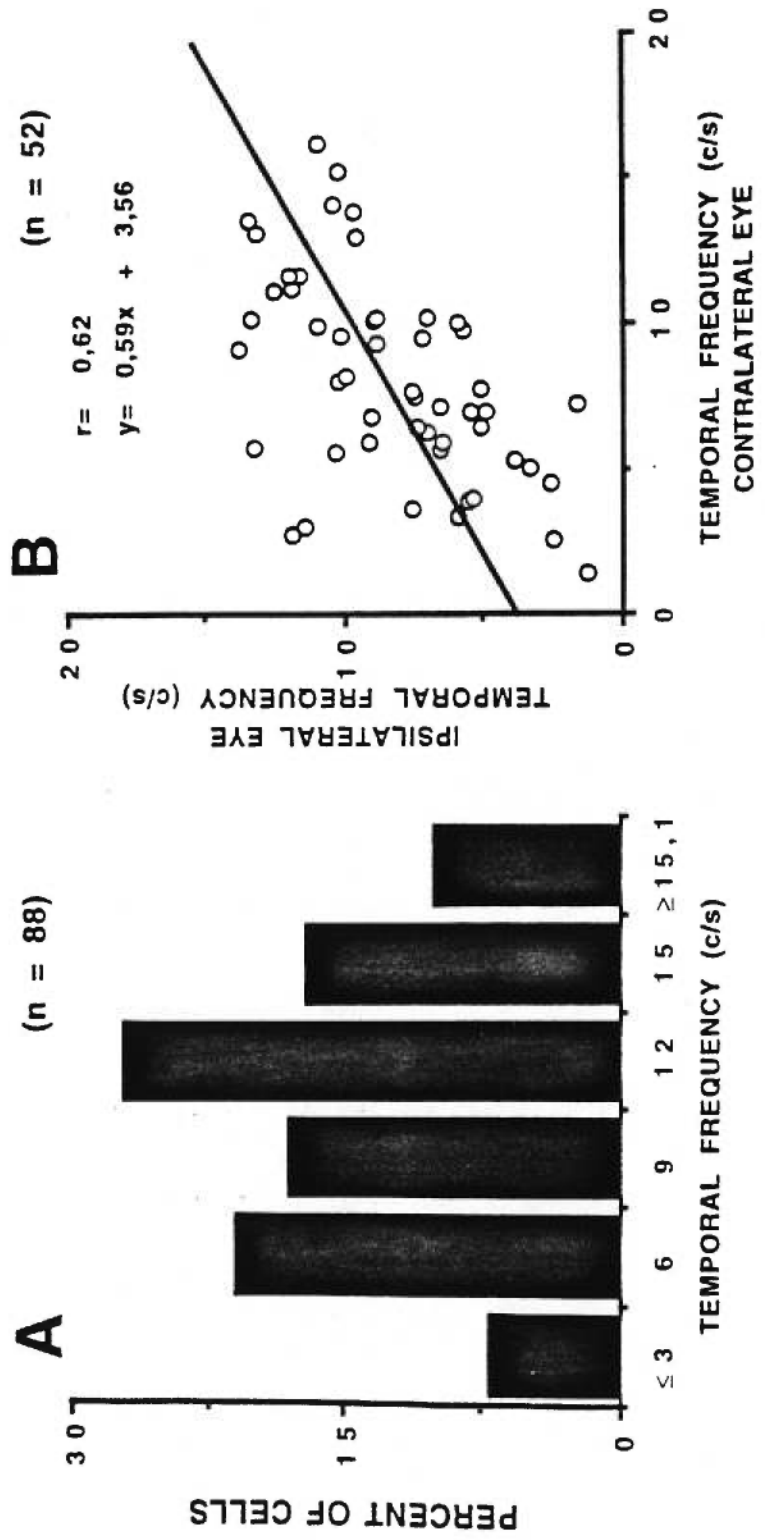
A
(n = 88)
PERCENT OF CELLS
30
15
0
≤3
6
9
12
15
≥15,1
TEMPORAL FREQUENCY (c/s)
B
(n = 52)
r= 0,62
y= 0,59x + 3,56
IPSILATERAL EYE
TEMPORAL FREQUENCY (c/s)
20
10
0
0
10
20
TEMPORAL FREQUENCY (c/s)
CONTRALATERAL EYE

FIGURE 9

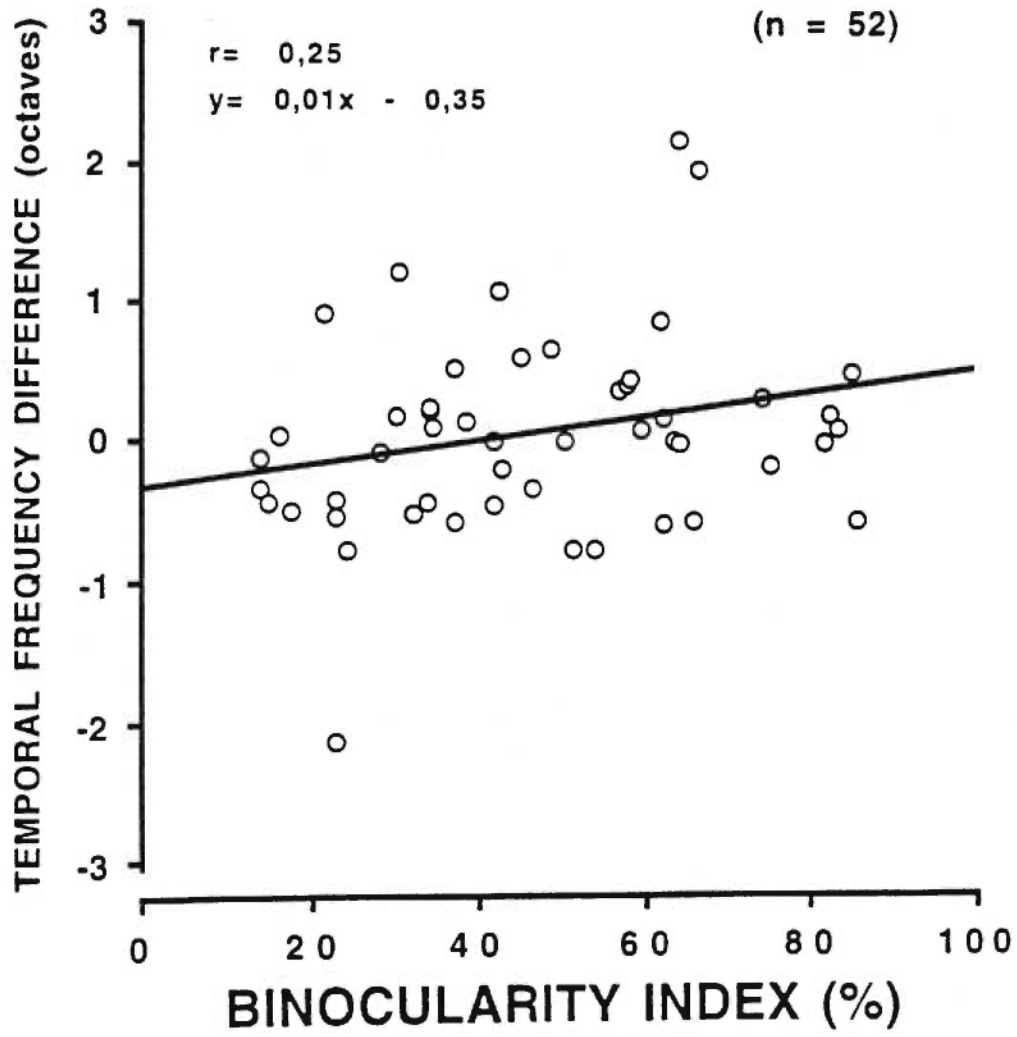
(n = 52)
r= 0,25
y= 0,01x - 0,35
TEMPORAL FREQUENCY DIFFERENCE (octaves)
3
2
1
0
-1
-2
-3
0
20
40
60
80
100
BINOCULARITY INDEX (%)

FIGURE 10

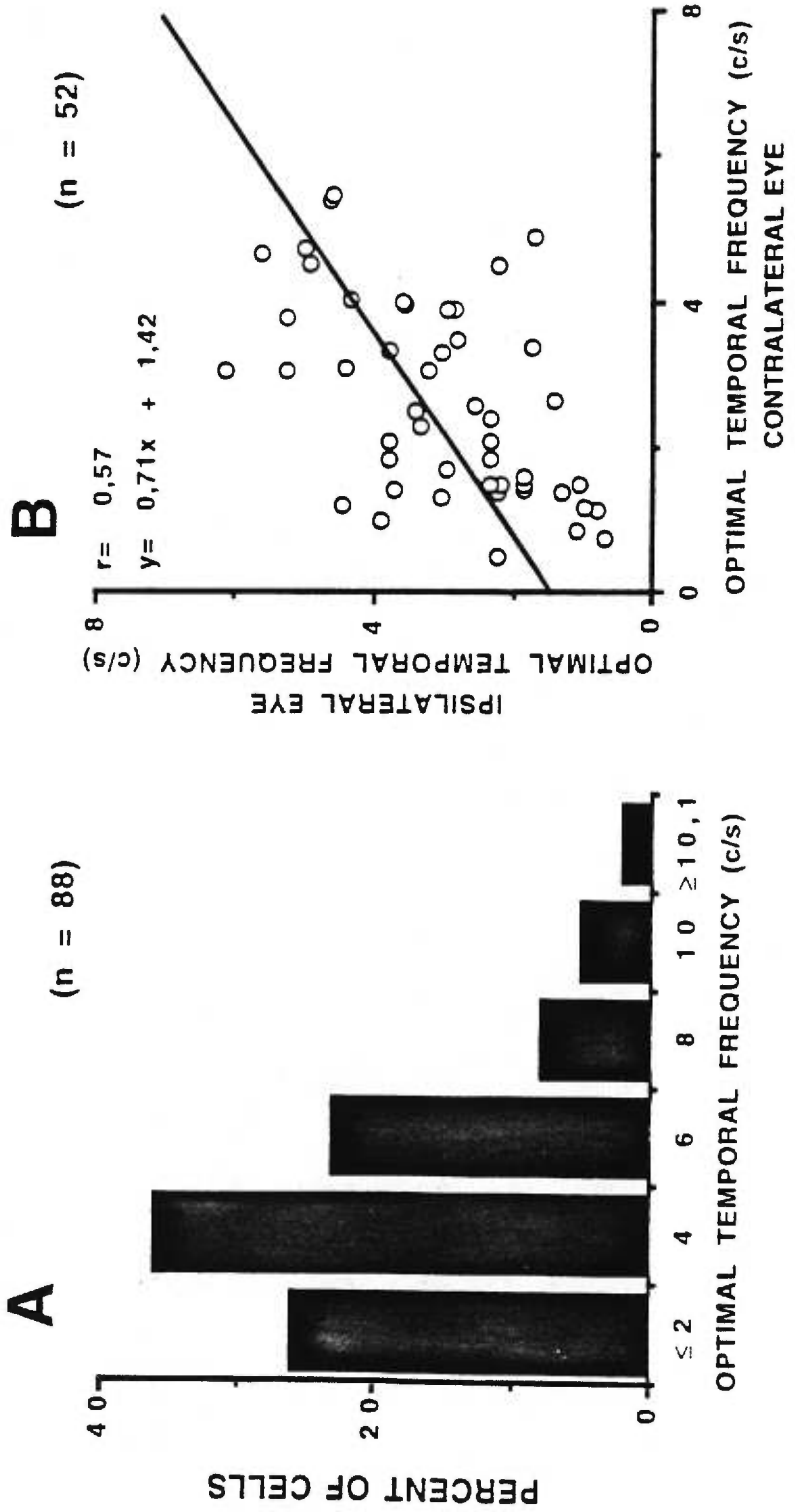
A
(n = 88)
PERCENT OF CELLS
40
20
0
≤ 2
4
6
8
10
≥10,1
OPTIMAL TEMPORAL FREQUENCY (c/s)
B
(n = 52)
r= 0,57
y= 0,71x + 1,42
OPTIMAL TEMPORAL FREQUENCY (c/s)
IPSILATERAL EYE
8
4
0
0
4
8
OPTIMAL TEMPORAL FREQUENCY (c/s)
CONTRALATERAL EYE

FIGURE 11

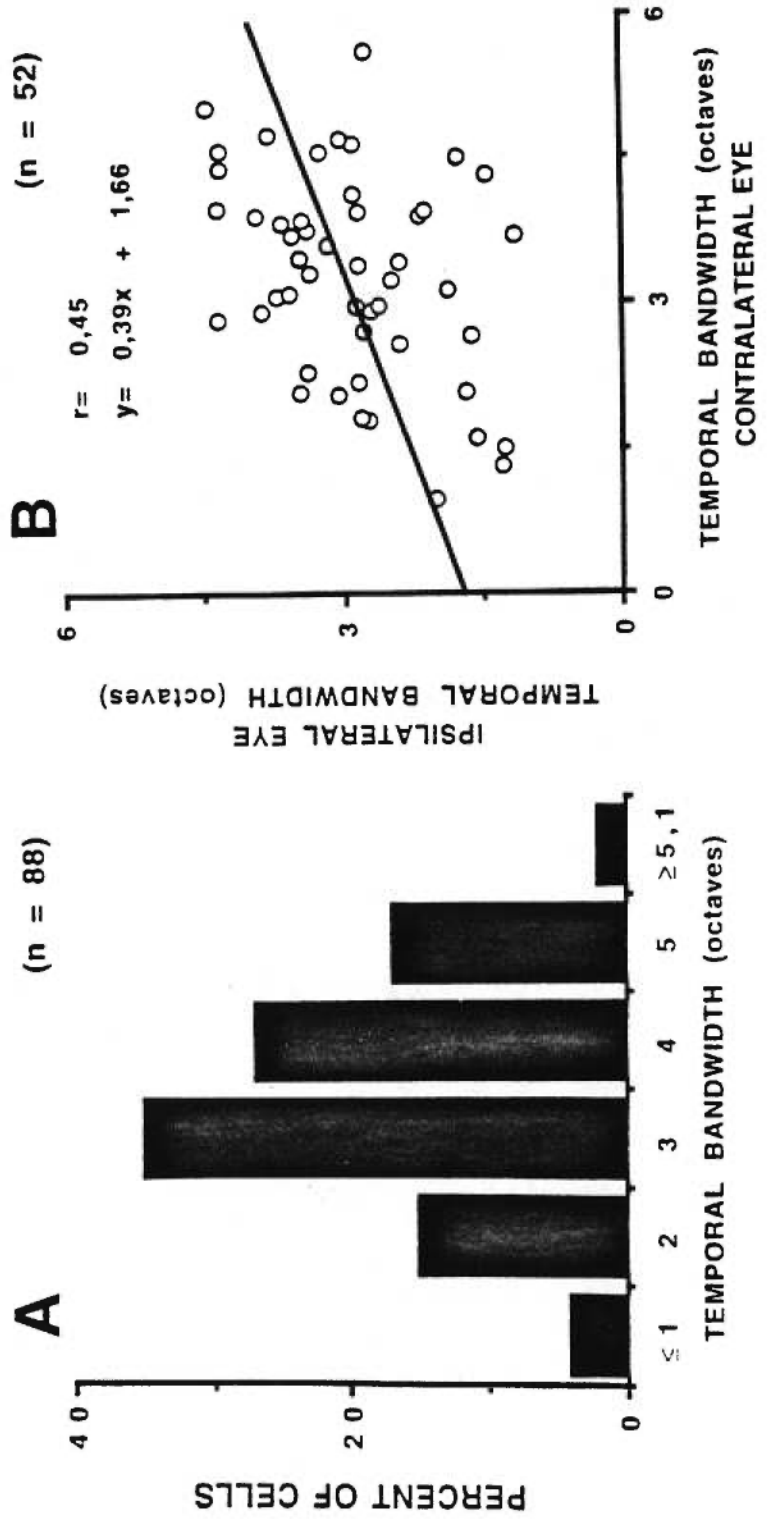
A
(n = 88)
PERCENT OF CELLS
40
20
0
≤1
2
3
4
5
≥5,1
TEMPORAL BANDWIDTH (octaves)
B
(n = 52)
r= 0,45
y= 0,39x + 1,66
IPSILATERAL EYE
TEMPORAL BANDWIDTH (octaves)
6
3
0
0
3
6
TEMPORAL BANDWIDTH (octaves)
CONTRALATERAL EYE

FIGURE 12

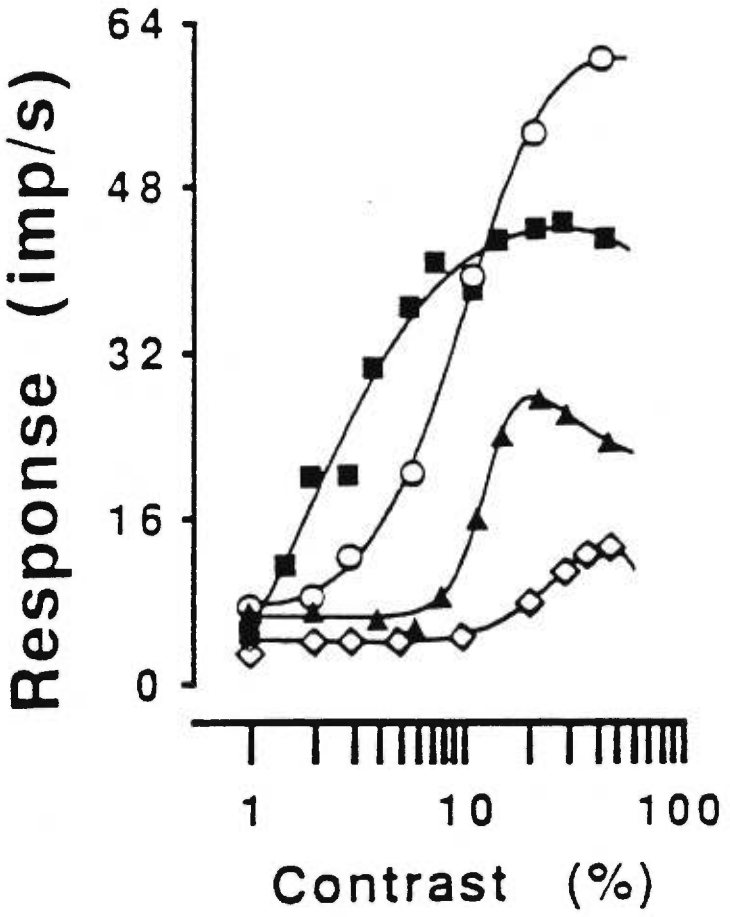

FIGURE 13

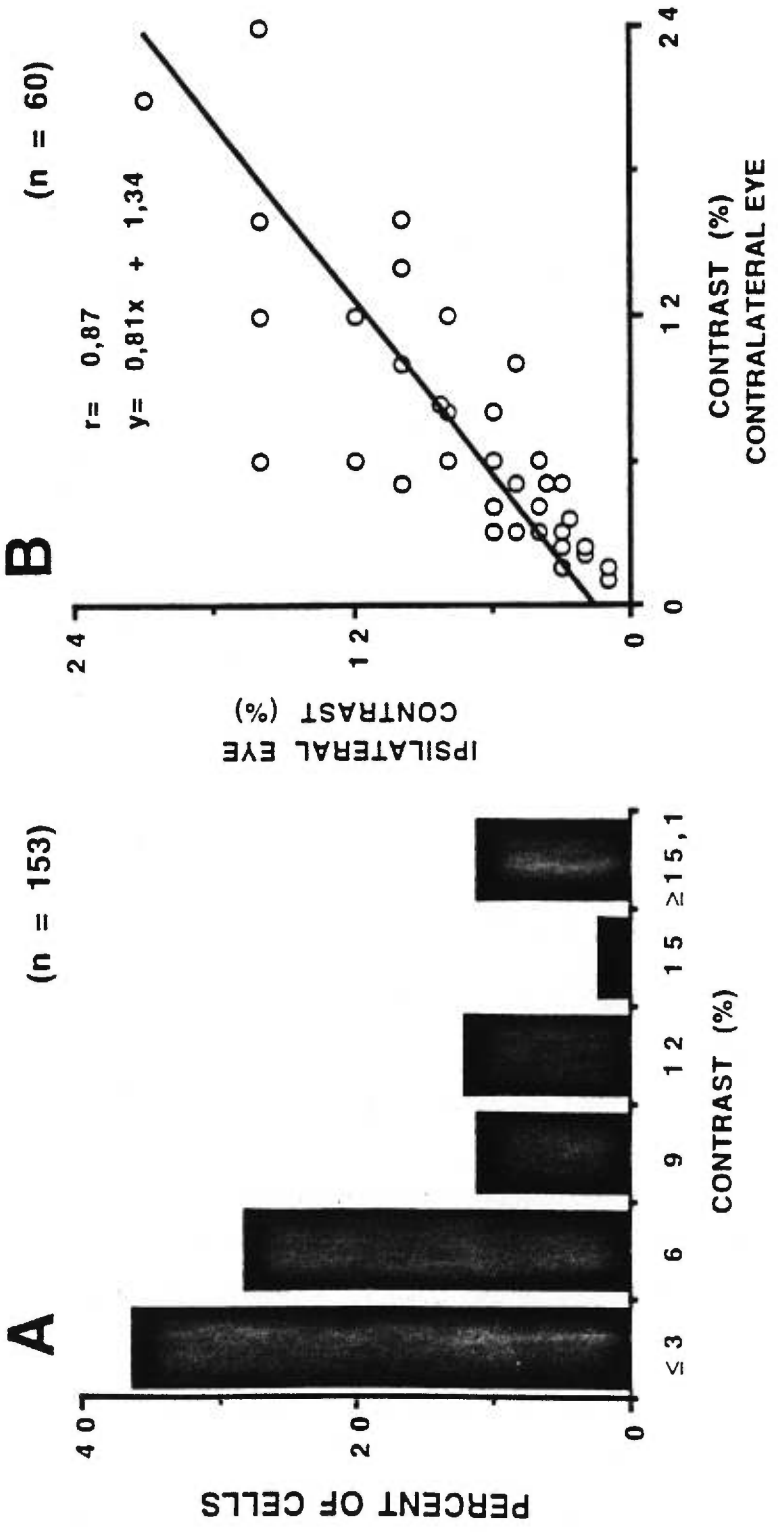
A
(n = 153)
PERCENT OF CELLS
40
20
0
≤ 3
6
9
12
15
≥15,1
CONTRAST (%)
B
(n = 60)
r= 0,87
y= 0,81x + 1,34
IPSILATERAL EYE
CONTRAST (%)
24
12
0
CONTRALATERAL EYE
CONTRAST (%)

FIGURE 14

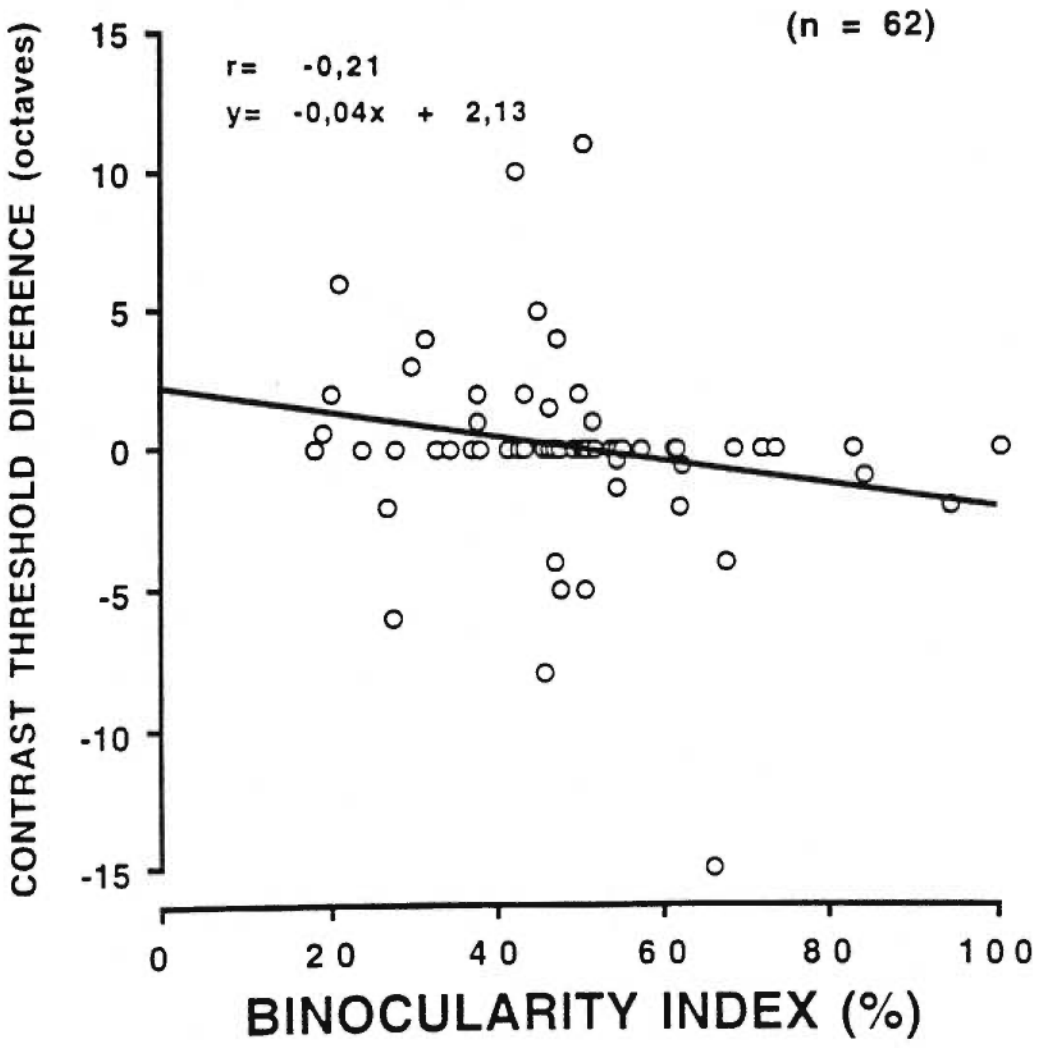
(n = 62)
r= -0,21
y= -0,04x + 2,13
CONTRAST THRESHOLD DIFFERENCE (octaves)
15
10
5
0
-5
-10
-15
0
20
40
60
80
100
BINOCULARITY INDEX (%)

CHAPITRE IV

Article #3

Spatial resolution and contrast sensitivity of single neurons in area 19 of split-chiasm cats: a comparaison with primary visual cortex

SPATIAL RESOLUTION AND CONTRAST SENSITIVITY OF SINGLE NEURONS IN AREA 19 OF SPLIT-CHIASM CATS: A COMPARISON WITH PRIMARY VISUAL CORTEX

Eric Tardif[1], Louis Richer[2], André Bergeron[1], Franco Lepore[1] and Jean-Paul Guillemot[1,3].

[1]Groupe de Recherche en Neuropsychologie Expérimentale, Département de Psychologie, Université de Montréal, C. P. 6128, Succ. Centre-Ville, Montréal, H3C 3J7, Canada.

[2]Université du Québec à Chicoutimi, Département de Psychologie, 555 Blvd de l'Université, Chicoutimi, G7H 2B1, Canada.

[3]Université du Québec à Montréal, Département de Kinanthropologie, C. P. 8888, Succ. Centre-Ville, Montréal, H3C 3P8, Canada.

Publié dans:

European Journal of Neuroscience (1997), 9, 1929-1939

Correspondence and reprints request should be addressed to:

J.-P. Guillemot, Département de Kinanthropologie, Université du Québec à Montréal, C.P. 8888, Succ. Centre-Ville, Montréal, H3C 3P8, Canada

Running title: Spatial sensitivity of visual neurons in split-chiasm cats

34 pages, 13 figures.

Key words: Corpus callosum, spatial frequency, contrast threshold, area 19, areas 17/18.

Abstract

Electrophysiological recordings were carried out in the callosal recipient zone of area 19 in both normal and split-chiasm cats and, for comparison purposes, at the border of areas 17/18 of split-chiasm cats. The influences of retino-thalamic and callosal inputs on a single cortical neurons were thereby evaluated. Extracellular recordings of single cells were made in the anesthetized and paralyzed cat in the zone representing central visual field. Receptive field properties were assessed using sine wave gratings drifting in optimal directions. Results showed that in area 19 as well as in areas 17/18 one-third of the cells are binocularly driven after the section of the optic chiasm. In area 19, the spatial resolution and contrast sensitivity of cells driven via the dominant eye are similar in the normal and split-chiasm groups. In areas 17/18 as well as in area 19 of split-chiasm cats, binocular cells show a significant interocular matching of their receptive field properties (spatial resolution and contrast threshold) although small differences are observed. These small interocular differences are related to the cell's ocular dominance rather than to the signal transmission route (thalamic or callosal).

Introduction

Behavioral experiments in cats have shown that the corpus callosum can mediate interhemispheric transfer of pattern discrimination when information is restricted to one hemisphere by a saggital section of the optic chiasm (Myers, 1955; 1956). Since these original studies were carried out, many anatomical and physiological experiments have been conducted to specify the possible roles of the corpus callosum in vision (for a review, see Berlucchi, 1990). Anatomical studies in the cat indicate that cortical callosal inputs form a complex organization and are particularly abundant at the 17/18 border (Innocenti, 1986). Callosal neurons at the 17/18 border have receptive fields (RF) located within five degrees of eccentricity (Payne, 1991; Payne *et al.*, 1991). In areas 19 and postero-medio-lateral suprasylvian sulcus, the callosal-recipient zone is more important both in terms of the density of callosal input and in the amount of visual field represented. In fact, the RFs of cells receiving a callosal input extend up to 20 degrees in area 19 (Antonini *et al.*, 1985) and 60 degrees in postero-medio-lateral suprasylvian sulcus (Segraves and Rosenquist, 1982a, b). Few studies (Berlucchi *et al.*, 1967; Hubel and Wiesel, 1967; Shatz, 1977; Lepore *et al.*, 1988) have described the visual properties of callosal fibers in the cat using single unit recordings carried out directly in the corpus callosum. These show that callosal fibers have RFs usually located near the area centralis and that their medial borders touch or straddle the vertical meridian. Taken together with anatomical studies, this suggests that the corpus callosum assures the midline fusion of the two visual hemifields. The implication of the corpus callosum in midline function was also demonstrated for the motor system (Spidalieri *et al.*, 1986) and for the somatosensory system of the cat (Guillemot *et al.*, 1988; Manzoni *et al.*, 1989), monkey (Guillemot *et al.*, 1987) and raccoon (Guillemot *et al.*, 1992).

The influence of callosal inputs on a cortical cell can most easily be investigated with the use of split-chiasm animals. With this preparation, it is possible to compare the contributions of both direct and callosal inputs on the visual RF properties of a cortical neuron. In binocular cells, the input from the contralateral eye is presumed to be transmitted from the opposite hemisphere via the callosum and that from the ipsilateral eye via the ipsilateral thalamus. The first electrophysiological study using this approach revealed that about 13% the cells at the 17/18 border remained binocular after a section of the optic chiasm (Berlucchi and Rizzolatti, 1968). Later studies in adult (Lepore and Guillemot, 1982; Antonini *et al.*, 1985; Lepore *et al.*, 1992; Milleret, 1994) and new-born split-chiasm cats (Milleret, 1994), reported a higher percentage of binocular cells at the 17/18 border and in area 19 (30% to 54% in the adult cat). In split-chiasm animals, binocular cells recorded in several cortical areas (17/18 border, 19 and postero-medio-lateral suprasylvian sulcus) showed a number of characteristics, such as orientation and directional tuning, spatial frequency selectivity and disparity sensitivity, which suggest that they are probably involved in form and depth perception (Berlucchi and Rizzolatti, 1968; Lepore and Guillemot, 1982; Antonini *et al.*, 1983, 1985; Berardi *et al.*, 1987; Lepore *et al.*, 1992; Guillemot *et al.*, 1993), as well as in the interocular transfer of adaptation aftereffect (Maffei *et al.*, 1986).

Although most studies show that there is an apparent similarity in RF properties evoked via the contralateral and ipsilateral pathways in split-chiasm cats, one set of experiments by Berardi and collaborators indicates that RFs may in fact differ with respect to some stimulus features. Berardi *et al.* (1987) showed that the contrast sensitivity of a cell was higher for the ipsilateral eye (i.e., the thalamic input) than for the contralateral eye (the transcallosal input). Moreover, the spatial and temporal resolutions derived through each eye were higher for the former than for the latter. It was thereby hypothesized that the corpus callosum acts as a spatio-temporal filter transmitting signals dominated by low

spatial and temporal frequencies with high contrasts. This hypothesis was supported by the recording of visual evoked potentials in the corpus callosum, which demonstrate lower values of spatial and temporal resolutions and contrast sensitivity than those typically found in visual cortical areas (Berardi *et al.*, 1987). Also, behavioral studies showed that interhemispheric transfer was imperfect in split-chiasm cats (Berardi and Fiorentini, 1988): in the normal cat, interocular transfer of oriented gratings having spatial frequencies of up to 3.2 c/deg was achieved whereas only spatial frequencies below 1.1 c/deg transferred interhemispherically in the chiasmatomized animal..

The hypothesis that the corpus callosum acts as a spatio-temporal filter is derived from the electrophysiological analysis of a restricted number of cells made at the 17/18 border of split-chiasm cats (Berardi *et al.*, 1987). In fact, recordings made in these same animals in area 18 indicate that only one third of the binocular cells had lower contrast thresholds for the ipsilateral thalamic signals than for the contralateral callosal signals. The purpose of the present study, therefore, was to investigate how these signals affect binocular cells in area 19 of split-chiasm cats and to compare the results to our own data collected from areas 17/18.

MATERIALS AND METHODS

Animals

Experiments were carried on 21 adult cats of either sex weighing from 2-4 kg. Although the animals came from a Université de Montréal approved supplier and were subjected to the usual quarantine upon arrival at the central animal quarters, they were also kept in the laboratory animal facility for at least 48 hours to give them the opportunity to adapt to local conditions. They were in good health and had no apparent malformations or pathological disorders. All surgical interventions, manipulations and husbandry were carried out within the guidelines proposed by the Canadian Council on Animal Care and those of NIH concerning the preparation and maintenance of higher animals during neuroscience experiments. Moreover, the experimental protocols were approved by the University animal care committee.

Surgery

For 14 animals, the optic chiasm was first sectioned under general anesthesia using the methods described by Myers (1955). They were then allowed to recuperate for a minimum of six to nine months. On the day of recording, a cat first received an i.m. injection of atropine (Atro-sol, 0.2 mg/kg) to limit bronchial secretions after which it was anesthetized with a gaseous mixture of nitrous oxide : oxygen (N_2O : O_2, 70:30) and halothane (5%). The animal was then intubated so that it could be artificially ventilated through a respiratory pump. The saphenous vein was cannulated in order to administer 5% dextrose in lactated Ringer solution to maintain blood pressure and hydration. During all surgical procedures, general anesthesia was maintained with 1-2% halothane. The

animal was placed in a modified stereotaxic apparatus (David Kopf). The trepanation was performed over area 19 (A-P: 5 to -5, L: 4 to 9) and/or areas 17/18 (A-P: 0-4; L:1-3). A small opening was made in the dura overlying the central visual field representation of area 17/18 and/or 19 (as defined by Tusa *et al.*, 1978; 1979) which was then covered with 4% agar in physiological saline. Once the brain has been exposed all pressure points and wounds were routinely infiltrated with local anesthetic (Xylocaine or lidocaine). At the end of the surgery the fluothane level was progressively reduced (0.5% / 15 min.) and maintained at 0.5% for the duration of the experiment. Stable heart rate and the absence of ear reflexes insured that the anesthesia level was sufficient. Then, the animal was paralyzed with gallamine triethiodide (Flaxedil, 200 mg) and d-tubocurarine (Tubarine, 15 mg) dissolved in 30 ml of lactated ringer solution with dextrose (5%). The mixture was continuously infused (5.6 ml/h) through the saphenous vein to maintain paralysis of extraocular muscles. Respiratory rate and volume were controlled so as to maintain a constant level of expired CO_2 (~4%). Body temperature was also kept constant (38° C) with the help of a thermostatically controlled heating waterpad. ECG was constantly monitored and EEG, monitored intermittently yet regularly, showed slow-wave activity throughout the recording session.

Optical preparation

In order to determine the relative positions of the areae centrales, retinal landmarks (optic discs and blood vessels) were projected on a tangent screen (Fernald and Chase, 1971) which was located 57 cm in front of the animal. The area centralis was considered to be situated 16° medially and 7.5° below the iso-elevation line of the center of each optic disk (Bishop *et al.*, 1962). Pupils were routinely dilated by i.m. injections of atropine sulfate 1% (Atro-sol, 0.2 mg/kg) and the nictitating membranes were retracted with topical

applications of phenylephrine hydrochloride (Neo-synephrine: 0.1%). To prevent eye dehydration and to improve image resolution, a neutral contact lens with a 3 mm artificial pupil was placed on each eye. Each area centralis were focused on the display monitor and corrected by the use of additional dioptric lenses as dictated by direct ophtalmoscopy. The optic quality of the eyes was routinely checked during the recording session.

Recording and stimulation procedures

Recording was carried out with glass micropipettes filled with 2M NaCl and having an impedance of 2-5 MΩ (measured at 1000 Hz). The location of area 19 was delimited by its position relative to the lateral sulci as proposed by Tusa *et al.* (1979). The micropipette was lowered perpendicularly to the cortical surface. Spikes were conventionally amplified, displayed on an oscilloscope, filtered through a time/amplitude discriminator and transferred to an audio monitor and computer. Upon isolating a cell, a stimulation procedure adapted from Henry *et al.*, (1967) was used. The positions of the RFs were determined and the spatial organization of each RF was mapped and explored using light and dark bars. The best stimulus parameters for direction, velocity, orientation, width and length was estimated based on the output of the audio monitor. The RFs were classified in terms of simple (S), complex (C), end-stopped simple (Sh) or end-stopped complex (Ch) categories using the criteria of Hubel and Wiesel (1962, 1965) and Henry *et al.* (1967). However, for the end-stopped cells (Sh and Ch) the size of the stimulus was varied systematically, and the size yielding the optimal response from the cell was used for quantitative tests.

For quantitative analysis, a display monitor (Hewlett Packard, model 1321a, with P31 phosphor) was placed 57 cm in front of the animal. The stimulation screen subtended 25° of visual angle and had a mean luminance of 5 cd/m^2 (measured with a spotmeter).

Sinusoidal gratings were produced with an image generator (Innisfree: Picasso model Rev. 8) controlled by computer. The spatial frequency, temporal frequency, direction, size and contrast of the gratings could thus be varied. To determine the spatial frequency tuning function, RFs were stimulated sequentially with sinusoidal gratings of different frequencies. The interval between successive spatial frequencies tested (0.06 to 2.4 c/deg) was usually half an octave. Each frequency was presented 10 times and the order of testing of the various spatial frequencies was pseudo-random. The cell's discharge rate was recorded at the best direction and at a temporal frequency of 2 Hz. The contrast was kept constant at 50% and was defined using the Mendelson formula: $(L_{max}-L_{min}/L_{max}+L_{min}) \times 100$, where L_{max} is the maximum luminance and L_{min} is the minimum luminance of the spatial sinusoid. Between each presentation, the RF was continuously stimulated with a uniform blank stimulus having the same mean luminance (5 cd/m^2) as the test grating. To generate the gratings, the contrast was increased gradually, over a period of 500 ms, until it reached 50%. This was done to avoid evoking a transient response from the cell. The presentation of the drifting gratings lasted 3 s and an intertrial interval of 18 s was introduced to minimize cell adaptation (Ohzawa *et al.*, 1985).

For every cell, the RF in each eye was explored individually with drifting sinusoidal gratings and the ocular dominance was evaluated quantitatively using the drifting optimal spatial frequency. The criteria of Skottun *et al.* (1991) was used to definitively classify the RF organization. Briefly, S- and Sh-type cells showed a modulated response waveform at the first harmonic (as revealed by a Fourier analysis) of the drifting grating at the optimal spatial frequency. The C- and Ch-type cells showed an overall DC increase in their response component (mean firing rate) at the first harmonic of the drifting grating at the optimal spatial frequency.

Data processing

Experiments were carried out and data was gathered and processed by a generic PC-486. The primary data analysis tool was the construction of 3 s peristimulus time histograms (500 bins) during the blank condition (uniform field at the mean luminance of the gratings) which immediately preceeded each presentation of the drifting grating. Another peristimulus time histograms (500 bins, duration: 3 s) was constructed during the presentation of the drifting grating. As a rule, response amplitude was specified by the DC response for the cells that showed an unmodulated pattern of discharge (C and Ch) during the optimal spatial frequency presentation, each data point of the tuning function corresponding to the mean firing rate (in spikes/s) of the cell from which was subtracted the mean discharge rate recorded during the blank presentations. For cells that showed a modulated response (S and Sh) during the optimal spatial frequency presentation, each data point of the tuning function was plotted according to the modulation amplitude of the response (Fourier fundamental response component) from which was subtracted the response during the blank presentations. The tuning curves were fitted by eye with a curve fit software (Table Curve: version 1; Jandel Scientific, San Rafael, CA). The optimal curve thereby derived had a high correlation ($r > 0.9$) with the data points and was used to evaluate the optimal spatial frequency and bandwidth.

Contrast sensitivity was evaluated using the optimal spatial frequency, as determined above, and drifting in the best direction at a temporal frequency of 2 Hz. A number of pre-determined contrast levels (range: 0.5% to 50%) was chosen, and each of these was presented pseudo-randomly 10 times. A response vs contrast curve was then established. Contrast threshold was determined by linear interpolation of the data points and corresponded psychophysically to the contrast value which elicited a response in 70%

of the trials. The stimulus presentations and recordings were carried out in the same manner as for assessing the spatial frequency tuning function.

Histology

At the end of the recording session, the cat was deeply anesthetized with 6% halothane, after which it was perfused through the heart with 0.9% saline followed by formalin (4%). The brain was removed, placed in formalin (4%) and later prepared for histology. In order to verify the completeness of the chiasma section, the block containing this structure was cut in coronal sections 40 μm thick. Every second section was kept and stained using the Kluver-Barrera method (Kluver and Barrera, 1953).

Electrodes penetrations were located at the border of areas 17/18 and/or in area 19, identified according to the Otsuka and Hassler (1962), Hubel and Wiesel (1965) and Tusa *et al.* (1978; 1979) maps. For animals which also had been subjected to a chiasmatomy, only the results of those animals which showed complete chiasma transection are presented in this report.

Results

Receptive fields properties of thalamo-cortical and callosally activated neurons in area 19

A total of 310 cells were recorded in area 19. Of these, 179 were recorded from split-chiasm cats and 131 from normal cats. All penetrations were made in the callosal recipient zone of area 19 according to the retinotopic maps of Otsuka and Hassler (1962), Hubel and Wiesel (1965) and Tusa *et al.* (1979) and all units had their RF centers located within five degrees of the midline. In the split-chiasm animals, all the binocular cells had RFs that touched or straddled the vertical meridian. Each cell had its RF classified as S, C, Sh or Ch. In both groups, most RFs were C or Ch but a few S and Sh cells were also found. In normal cats, 6% of the RFs were S, 56% were C and 38% were end-stopped, of which 6% were classified as Sh and 32% as Ch. In chiasmatomized cats, 9% of the RFs were classified as S, 74% as C and 17% were end-stopped (Sh = 2%; Ch = 15%). In normal cats, S cells were either binocular or monocular whereas in split-chiasm cats, all S cells were monocular.

Insert figure 1

Ocular dominance

For each cell, ocular dominance was assessed quantitatively on a scale from 1 (driven exclusively through the contralateral eye) to 7 (driven exclusively through the ipsilateral eye) (Hubel and Wiesel, 1962) using the optimal spatial frequency and stimulation parameters. In order to classify the binocular cells among the five intermediate categories, an ocular dominance index was calculated using the formula: (I/(I + C)) x 100, where I represents the response to stimulation of the ipsilateral eye and C, the response of the

contralateral eye. The ocular dominance index thereby obtained allowed for the classification using the following criteria: class 2: 1 - 20%; class 3: 21 - 40%; class 4: 41 - 60%; class 5: 61 - 80%; class 6: 81 - 99%. The resulting distribution is illustrated for both groups in figure 1. In normal cats, the majority of cells were binocularly driven with a preponderance of class 4 and a small bias for the contralateral eye. In split-chiasm cats, about one-third of the cells were binocular while the others could only be driven through the ipsilateral eye. The binocular cells found in these animals were also distributed in the five intermediate classes of ocular dominance, cells of class 4 being the most numerous.

Insert figures 2 and 3

Spatial frequency tuning curves

The spatial frequency selectivity was assessed with drifting sinusoidal gratings of 50% contrast. Each spatial frequency selected was presented for 10 trials of 3 s each at a drift frequency of 2 Hz. Examples of spatial frequency tuning curves are shown for normal cats (figure 2) and for split-chiasm cats (figure 3). The tuning curves of approximately two-thirds of the cells (normal = 90/131; split-chiasm = 111/179) were band-pass, which means that a cell had a clear optimal spatial frequency and that the response was attenuated for frequencies higher and lower than the optimal. Those cells (normal = 41/131; split-chiasm = 68/179) which did not show attenuation at the lowest spatial frequencies tested (e.g., cell CHI 66-3 in figure 3), were labeled low-pass and their bandwidth could not be measured. However, this distinction should not be understood in absolute terms as it may depend on the value of the lowest spatial frequency tested. The example illustrated in figure 2 (cell N 74-3) shows that this cell, classified as low-pass, manifested some

attenuation in the lowest spatial frequency tested, namely, 0.06 c/deg However, the attenuation did not reach half-height, making it impossible to estimate its bandwidth.

Insert figure 4

Spatial resolution

Spatial resolution was estimated for 310 cells (131 in the normal cat; 179 in the split-chiasm cat) by the high cut-off spatial frequency, which corresponds to the point on the tuning curve which intersects the baseline. The mean spatial resolution of the dominant eye was 0.94 c/deg (σ = 0.61 c/deg) for normal cats and 1.04 c/deg (σ = 0.66 c/deg) for split-chiasm cats. The distributions of the high cut-off spatial frequencies of the dominant eye are shown for both groups in figure 4. There is no significant difference between the two distributions.

For numerous binocular cells, the visual resolution was estimated for both eyes. In normal cats, this was done to assess the matching of the responses of the two eyes. In split-chiasm cats, the response to the stimulation of the ipsilateral eye can be directly compared to that evoked, through the callosum, to that of the contralateral eye. Results indicate (figure 5) that, in both groups, a significant relationship (normal, $r = 0.53$, $p < 0.001$; split-chiasm, $r = 0.42$, $p < 0.001$) exists between the high cut-off spatial frequencies measured through either eye. However, some differences do exist between the high cut-off spatial frequencies estimated for each eye, as shown in figures 2 and 3 (see cells N 22-2, N 74-3, N24-5, N 93-6, CHI 49-2, CHI 66-3, CHI 95-5 and CHI 159-6). In fact, for binocular cells with balanced ocular dominance (class 4), the spatial resolution is the same for both eyes (figures 2 and 3, see cells N 16-4 and CHI 72-4). The differences observed in the spatial resolution of the ipsilateral and contralateral eyes

are rather observed for cells belonging to the other classes of ocular dominance (classes 2, 3, 5 and 6). For these cells, the resolution is generally higher for the dominant eye (figures 2 and 3, see cells N 22-2, N 74-3, N24-5, N 93-6, CHI 49-2, CHI 66-3, CHI 95-5 and CHI 159-6). This is shown in figure 6, which plots the mean difference between the spatial resolution of each eye (in octaves) against ocular dominance. Positive values indicate that the high cut-off is higher for the ipsilateral eye and negative values, that it is higher for the contralateral eye. When ocular dominance is balanced (class 4), there is no differences in the high cut-off spatial frequencies of the two eyes. The differences between the high cut-off of the ipsilateral and contralateral eyes are most important when the cell is strongly dominated by one eye (classes 2 and 6) and smaller, though still present, for classes 3 and 5. These differences between the eyes are nonetheless marginal since, when all binocular cells are considered, there is no significant differences between the spatial resolution of the ipsilateral and contralateral eye, either in the normal or split-chiasm cats. The results also suggest that, in both normal and split-chiasm cats, when differences do exist, they are not determined by the nature of the input (thalamo-cortical or callosal), but rather by the ocular dominance. Similar results have also been observed in area 21a of the normal cat using the same experimental procedure (Tardif *et al.*, 1996).

Insert figures 5 and 6

Optimal spatial frequency and bandwidth

The optimal spatial frequency and bandwidth were estimated for 201 cells (90 in the normal and 111 in the split-chiasm cat). For each cell, these parameters were derived from the tuning curves fitted to the data points. The distributions of the optimal spatial

frequencies measured for the dominant eye are shown for both groups in figure 7. The mean optimal spatial frequency is 0.17 c/deg (σ = 0.11 c/deg) for the normal cat and 0.2 c/deg (σ = 0.13 c/deg) for the split-chiasm cat. Most cells had an optimal frequency between 0.09 c/deg and 0.32 c/deg and there was no significant difference between the two distributions. In 90 binocular cells (55 in the normal, 35 in the split-chiasm cat), the optimal spatial frequency was estimated for both eyes. Figure 8 shows that, for both groups, there is a very strong significant relationship (normal, $r = 0.84$, $p < 0.001$; split-chiasm, $r = 0.93$, $p < 0.001$) between the optimal spatial frequency estimated for the ipsilateral and contralateral eye. Moreover, in both groups, the differences found between the optimal spatial frequencies of the two eyes are relatively small and independent of ocular dominance.

Insert figures 7 and 8

The spatial bandwidth was estimated in 201 cells (90 in the normal; 111 in the split-chiasm cat) and was calculated at the half-height of the spatial frequency tuning function. The distributions of the spatial bandwidths estimated for the dominant eye are shown for both groups in figure 9. The mean spatial bandwidth is 2.13 octaves (σ = 0.65 octaves) for the normal cat and 2.20 octaves (σ = 0.69 octaves) for the split-chiasm cat. It is obvious from the distributions presented in this figure that there are no statistical differences between the two groups. For 90 binocular cells (55 in the normal and 35 in the split-chiasm cat), the spatial bandwidth was measured for the two eyes. Figure 10 shows that, for both groups, there is a significant relationship (normal, $r = 0.58$, $p < 0.001$; split-chiasm, $r = 0.56$, $p < 0.001$) between the spatial bandwidths estimated for the two eyes. As with the optimal spatial frequency, the small differences found between

the spatial bandwidths of the ipsilateral and contralateral eye are independent of ocular dominance.

Insert figures 9 and 10

Contrast threshold

For 225 cells (87 in the normal, 138 in the split-chiasm cat), the contrast threshold was estimated using a sinusoidal grating of optimal spatial frequency drifting at 2 Hz in the optimal direction. The mean contrast threshold for the dominant eye of cells in the normal cats is 5.2% (σ = 2.73%) and 4.83% (σ = 3.09%) for cells in the split-chiasm cats. The distributions of contrast thresholds of the dominant eye are shown for both groups in figure 11. The two distributions do not differ significantly and most cells had relatively low contrast thresholds (< 6% of contrast), although higher thresholds (> 9.1%) were also found. In 87 binocular cells (48 in the normal, 39 in the split-chiasm cat), the contrast thresholds were evaluated for both eyes. Figure 12 show that there is a significant relationship (normal, $r = 0.76$, $p < 0.001$; split-chiasm, $r = 0.61$, $p < 0.001$) between the contrast thresholds of the ipsilateral and contralateral eye. Although some important differences were found between the contrast thresholds of the two eyes (particularly in split-chiasm cats), these are independent of the inputs (thalamo-cortical or callosal) and of ocular dominance.

Insert figures 11 and 12

Receptive field properties of cells recorded at the 17/18 border of split-chiasm cats

The results described so far indicate that cells in area 19 have similar receptive field properties irrespective of their sources of input, namely, thalamo-cortical or callosal. At most, when differences are found, they correlate with ocular dominance and not with the origin of the inputs. They therefore do not support the main findings and conclusions of Berardi et al (1987) obtained in cells recorded at the 17-18 border, claiming that the callosum acts as a low spatial frequency-high contrast filter for the information that it transmits. These are important differences, which may stem from a number of factors, such as areal specificities, experimental approaches or sampling biases. In order to definitively resolve the problem of the nature of callosal transfer, we decided to extend our study to examine the receptive field properties of cells at the 17-18 border of split-chiasm cats. A brief description of the results is therefore given below.

Insert figure 13

A total of 139 cells were recorded at the 17/18 border of split-chiasm cats. The ocular dominance distribution of these cells is shown in Fig 13A. This distribution is similar to that found for area 19 of split-chiasm cats (see Fig 1). Most cells (67%) were monocular and could only be activated by the ipsilateral eye while the remaining cells (33%) were binocular. One significant finding is that binocular cells belonging to all ocular dominance classes were present in the sample. The distribution of these binocular cells shows that more cells had balanced ocular dominance (class 4) and that a comparable number of cells were dominated by either the ipsilateral (classes 5 and 6) or contralateral eye (classes 2

and 3). Two main parameters were examined for these binocular cells, namely, the high cut-off spatial frequency (spatial resolution) and the contrast tuning curve. The binocular cells recorded at the 17/18 border showed relatively high spatial resolutions for the dominant eye (mean = 1.73 c/deg; σ = 0.6 c/deg) as well as low contrast thresholds (mean = 2.13 %; σ = 1.3 %). A certain degree of interocular matching was found for these parameters. These findings are illustrated for contrast threshold in Fig. 13B and for spatial resolution in Fig. 13C. A significant relationship exists between the eyes for each of these two parameters, but it is lower for spatial resolution ($r = 0.36$; $p < 0.01$) than for contrast threshold ($r = 0.53$; $p < 0.001$). As was the case for area 19 of split-chiasm cats (see Fig 6), interocular differences in spatial resolution are not related to the sources of the inputs, i.e. thalamic or callosal, but rather to the cell's ocular dominance (Fig.13D). Indeed, these interocular differences in spatial resolution are significantly related to the ocular dominance index ($r = 0.8$; $p < 0{,}001$) and the dominant eye usually manifests a higher spatial resolution. Similarly, there is a significant but lower relationship ($r = 0{,}29$; $p < 0{,}05$) between the contrast threshold differences of the two eyes and the ocular dominance index. For areas 17/18, as for area 19 of split-chiasm cats, results confirm that when interocular differences exist in RF properties, they are not dependent on whether the input originates from the other hemisphere and is transmitted through the corpus callosum or whether it comes via the direct geniculo-cortical pathway, but rather on its efficacy in driving the recipient cell, i.e. the post-synaptic cell's ocular dominance. These results and consequent conclusion do not therefore support those of Berardi *et al.*, (1987). It would thus appear that the discrepency arises mainly because of sample differences with respect to ocular dominance distributions. In their study, no cell was found which could be driven more strongly through the contralateral eye whereas our distribution contains an important proportion (13/45 cells) of binocular cells that gave a stronger response to activation through the callosal pathway.

DISCUSSION

This study was carried out for a number of reasons: 1°- to assess how the RF properties of cells in area 19 of split-chiasm cats differ from those of normal cats, 2°- to compare the characteristics of the RF's generated via the ipsilateral thalamic versus the contralateral callosal pathway in split-chiasm cats and 3°- to contrast the results obtained in area 19 to those found at the 17/18 border of similarly prepared animals. No major differences in spatial frequency tuning or other RF properties were identified between the split-chiasm and normal cats. However, as expected, the profile of the ocular dominance distribution was greatly modified. Instead of the usual strong binocular activation, only a fraction of the neurons was activated by both eyes in split-chiasm cats. The remainder were only driven by stimulation of the ipsilateral eye. All binocular cells had RFs which touched or overlapped each other and touched or straddled the vertical meridian. These observations are compatible with the postulated role of the corpus callosum in the fusion of the two hemifields (Choudhury *et al.*, 1965; Whitteridge, 1965; Hubel and Wiesel, 1967; Berlucchi and Rizzolatti, 1968 ; Gazzaniga, 1970; Antonini *et al.*, 1985; Lepore and Guillemot, 1982; Berlucchi, 1990). It is, however, important to note that to assure midline fusion, this process probably acts in conjunction with the naso-temporal overlap that is already present in the retina (Stone, 1966; Sanderson and Sherman, 1971).

Spatial frequency characteristics

The spatial frequency tuning functions of cells were evaluated, allowing for their classification into band-pass and low-pass categories. As mentioned earlier, the latter classification is not absolute because it may be limited by the range of spatial frequencies tested in the lower portion of the scale. However, one notable observation is that the

chiasmatomy does not alter the proportion of cells having band-pass or low-pass properties. In other words, the overall spatial frequency selectivity is about the same for cells in normal and split-chiasm cats and, in the latter, it is identical for transcallosal and thalamic inputs. Moreover, there was no significant difference between the optimal spatial frequencies or spatial bandwidths of cells in the two groups. This suggests that although some neuronal properties may be altered by the chiasmatomy, for example, ocular dominance, spatial frequency tuning remains quite unchanged. In area 19, the mean optimal spatial frequency of band-pass cells is 0.17 c/deg for the normal cat and 0.2 c/deg for the split-chiasm cat and the respective mean values of spatial bandwidth is 2.13 and 2.20 octaves. These values are comparable with those obtained in other studies for neurons in areas 18 (Movshon *et al.*, 1978c; Berardi *et al.*, 1982), 19 (Tanaka *et al.*, 1987), 21a (Tardif *et al.*, 1996) and postero-medio-lateral suprasylvian sulcus (Morrone *et al.*, 1986; Zumbroïch and Blakemore, 1987) of the normal cat. However, our results and those obtained in these extrastriate areas differ from those reported in area 17, where optimal spatial frequencies are usually higher and spatial bandwidth sharper (Movshon *et al.*, 1978a, b).

Spatial resolution

One other important parameter that was estimated from the spatial frequency tuning functions is spatial resolution, which is defined as the high cut-off spatial frequency. In this study, the mean spatial resolution of cells in area 19 is 0.94 c/deg for normal cats and 1.04 c/deg for split-chiasm cats. Corresponding values obtained at the 17-18 border for split-chiasm cats are 1.73 c/deg. Again, the former are roughly comparable with results obtained in studies carried out in other extrastriate regions such as 18 (Movshon *et al.*, 1978c; Berardi *et al.*, 1982), 21a (Tardif *et al.*, 1996) and postero-

medio-lateral suprasylvian sulcus (Di Stefano *et al.*, 1985; Morrone *et al.*, 1986; Zumbroïch and Blakemore, 1987). Comparison of the spatial resolution of a cell driven by the ipsilateral eye (thalamic input) to that evoked through the contralateral (callosal input) eye indicates that signals transmitted along the two routes are closely matched. However, small differences occasionally emerged but they were not linked to the pathways but rather to the relative strengths of the responses evoked by the stimulation of the ipsilateral and contralateral eyes. The results showed that for the class 4 ocular dominance neurons, there were no differences between the spatial resolutions of the two eyes. When the strengths of inputs were unequal, however, (ocular dominance 2, 3, 5, 6) spatial resolution was always higher for the dominant eye. Thus, the resolution is based on the efficacy of the input in driving the recipient cell rather than whether it reaches the cortex via the thalamic or callosal pathway. This conclusion also appears to apply for neurons recorded at the 17/18 border. However, it contrasts with the one proposed by Berardi *et al.* (1987) from their studies of neurons in area 17. They showed that cells with higher spatial resolutions were activated by the ipsilateral eye and concluded that higher spatial frequencies are filtered out by the transcallosal pathway. We feel that these differences can best be explained by the fact that their sample was limited to 8 neurons, a number which was probably too small to lead to a firm conclusion.

Contrast threshold

For contrast thresholds, a significant relationship exists between the two pathways for binocular cells in areas 17/18 and 19. When small differences between the eyes were found, they were independent of both ocular dominance and signal transmission route, a result in partial agreement with that obtained in the study of Berardi *et al.* (1987) in area

18, where nine cells out of fourteen had similar contrast thresholds for the thalamic and the callosal inputs.

Functional implications

It is very clear from these results that the spatial properties of cells in area 19 derived through the callosal pathway are similar to those evoked via thalamo-cortical inputs. This conclusion is comparable to conclusions reached in similar studies on areas 17-18 (Berlucchi and Rizzolatti, 1968; Lepore and Guillemot, 1982; Lepore *et al.*, 1992; Milleret, 1994), 19 (Antonini *et al.*, 1985; Guillemot *et al.*, 1993) and suprasylvian regions (Antonini *et al.*, 1983), attesting to the apparent similarity of RF properties for gross spatial features (RF size, orientation and directional selectivities, position, etc.) derived from these two routes of activation. The only relevant studies examining more specific stimulus parameters (Berardi *et al.*, 1987) have come to the conclusion that the callosum only transmits low frequency and high contrast information to cells situated in area 17. The difference between these results and those reported in the present document can be explained in one of three ways. First, it is possible that some unexplained methodological factor is responsible for the lack of concordance of the results. We are, however, at a loss to identify what it is since the studies from the two laboratories use essentially similar methodologies. Another possibility, which is maybe more likely, is that results of both studies differ because of sample biases. In the study of Berardi *et al.* (1987) the relatively small number of cells recorded responded with a higher firing rate when stimulated via the ipsilateral eye (direct input), that is, all units were dominated by the direct input and none by the callosal one. We have shown that for both areas 17-18 and 19, what determines interocular differences is the relative strength of the responses obtained via each eye (or ocular dominance). Seen in this fashion, our results can even be

reconciled with those of Berardi *et al.* (1987) since they also showed that the dominant eye (which was always the ipsilateral one) manifested a higher spatial resolution and lower contrast threshold. However, as our sample also contained cells with equal ocular dominance and cells dominated by the contralateral eye, we found that, in the former case, the cells had the same properties for the two eyes and, in the latter, they had higher resolution and lower contrast thresholds when assessed via the contralateral (callosal) eye.

A final possibility is that the differences are true reflections of areal variations in the treatment of callosal information. It must be remembered that even in the original Berardi *et al.* (1987) experiment, results derived from areas 17 and 18 differed, in the sense that only a fraction of the cells in the latter area had lower resolutions when activated through the callosum. One would also have to assume when arguing along these lines that a significant proportion of the cells which we recorded at the 17/18 border of split-chiasm cats actually belonged to area 18. Although we attempted to sample equally both areas, our histological analyses did not permit us to asses with certainty that we had actually done so. If one accepts that the cells were in fact situated in area 18, it would then be possible to propose that there are important differences in the mode of activation of cells through the callosum for areas 18 and 19 with respect to area 17. These differences would derive from the nature of their respective inputs. One striking difference between the former areas and area 17 concerns their inputs from subcortical structures. Geniculate input to area 18 is essentially of the Y-type. Direct inputs to area 19 mainly comes from the C-laminae of the dorsal lateral geniculate, from the medial interlaminar nucleus and from the lateral posterior-pulvinar complex (Rodieck and Brening, 1983; Stone, 1983; Rosenquist, 1985; Dreher, 1986), structures which relay information that originate from both Y and W cells. Thus, the C-laminae of the dorsal lateral geniculate contain almost only W cells (Cleland *et al.*, 1976; Wilson *et al.*, 1976) while the medial interlaminar nucleus is characterized by a high proportion of Y cells (Kratz *et al.*, 1978; Dreher and

Sefton, 1979). Electrophysiological studies show that cells in extrastriate areas such as 19, 21a and postero-medio-lateral suprasylvian sulcus have relatively low contrast thresholds, low spatial resolutions and are broadly tuned to low spatial frequencies (Tanaka *et al.*, 1987; Zumbroïch and Blakemore, 1987; Tardif *et al.*, 1996). Cells in area 17, on the other hand, respond to higher frequencies and show sharp spatial frequency tuning (Movshon *et al.*, 1978a, b). This is probably a reflection of the fine spatial analysis performed by X cells that massively project to this area. Although in both normal and chiasmatomized cats, area 19 (and probably 18) cells are capable of spatial frequency analysis, their tuning is broader than in area 17. This suggests that the Y and W inputs do transfer unaltered across the callosum. As for area 17, the results of Berardi *et al.* (1987) would lead to the conclusion that cortical cells that are the recipients of X type input (high spatial resolution) probably do not send axons to the contralateral hemisphere (implying that all callosal neurons essentially reflect the properties of Y inputs) or, alternatively, that they do cross but that their properties are somewhat degraded as they do so, either at the pre-synaptic (callosal projecting neurons) or post-synaptic (callosal recipient neurons) level.

In chiasmatomized cats, W input to the cortex are greatly reduced, not only by the loss of crossed projections of the nasal hemiretina but also by the loss of crossed projections of the temporal hemiretina (Illing and Wässle, 1981). The spatial analysis that is observed at the cellular level in our cats is also probably attributable to remaining Y cells that come either directly to this extrastriate areas from subcortical structures or from lower order cortical areas such as 17.

In conclusion, our study shows that, in adult cats, a chiasmatomy does not induce great differences in the spatial frequency properties of single units in area 19 of the visual cortex. Among all the parameters tested, no significant differences were shown to exist between normal and operated cats. In binocular cells found at the 17/18 border and in area

19 of split-chiasm cats, small differences in visual resolution were explained in terms of ocular dominance rather than by the nature of the input. Taken together with the results of Berardi *et al.* (1987) obtained in area 18, the present study suggest that, in areas 17/18 and 19, callosal inputs to cortical cells give rise to cell properties comparable to those determined by direct thalamo-cortical inputs. With the remote exception of the X subsystem, the results do not support the hypothesis which suggests that the corpus callosum acts as a spatio-temporal filter for information originating in the contralateral hemisphere. Its effects appear to be more related to the efficacy of this input in driving the post-synaptic cell than to the quality of what is actually being transmitted. The latter can in fact only be evaluated through direct recordings of callosal fibers. This is precisely what we are presently examining in our laboratories .

ACKNOWLEDGMENTS

This study was supported by grants from the Natural Sciences and Engineering Research Council of Canada (NSERC) and the Fonds pour la Formation de Chercheurs et l'Aide à la Recherche (FCAR) awarded to Jean-Paul Guillemot and Franco Lepore. The authors are grateful to Eric Massicotte and Stéphane Montfort for technical assistance.

ABBREVIATIONS

C	complex
Ch	end-stopped complex
RF	receptive field
S	simple
Sh	end-stopped simple

REFERENCES

Antonini, A., Berlucchi, G. and Lepore, F. (1983) Physiological organization of callosal connections of a visual lateral suprasylvian cortical area in the cat. *J. Neurophysiol..*, **49**, 902-921.

Antonini, A., Di Stefano M., Minciacchi, D. and Tassinari, G. (1985) Interhemispheric influences on area 19 of the cat. *Exp. Brain Res.*, **59**, 171-184.

Berardi, N., Bisti, S., Cattaneo, A., Fiorentini, A. and Maffei, L. (1982) Correlation between the preferred orientation and spatial frequency of neurones in visual areas 17 and 18 of the cat. *J. Physiol . (London),* **323**, 603-618.

Berardi, N., Bisti, S. and Maffei, L. (1987) The transfer of visual information across the corpus callosum: spatial and temporal properties in the cat. *J. Physiol.. (London),* **384**, 619-632.

Berardi, N. and Fiorentini, A. (1988) Lateralization and orientational bias in the discrimination of mirror-symmetric complex gratings. *Perception*, **17**, 364.

Berlucchi, G. (1990) Commissurotomy studies in animals. In Boller, F. and Grafman, J. (eds), *Handbook of Neuropsychology*, Vol. 4, pp. 9-47.

Berlucchi, G. and Rizzolatti, G. (1968) Binocularly driven neurons in visual cortex of split-chiasm cats. *Science*, **159**, 308-310.

Berlucchi, G., Gazzaniga, M.S. and Rizzolatti, G. (1967) Microelectrode analysis of transfer of visual information by the corpus callosum. *Arch. Ital. Biol.*, **105**, 583-310.

Bishop, P.O., Kozak, W., and Vakkur, G. J. (1962) Some quantitative aspects of the cat's eye : axis and plane of reference of visual field coordinates and optics. *J. Physiol. (London),* **163**, 466-502.

Choudhury, B.P., Whitteridge, D. and Wilson, M.E. (1965) The function of the callosal connections of the visual cortex. *Quart. J. Exp. Physiol.*, **50**, 214-219.

Cleland, B.G., Levick, W.R., Morstyn, R. and Wagner, H.G. (1976) Lateral geniculate relay of slowly conducting retinal afferences to cat visual cortex. *J. Physiol. (London),* **255**, 299-320.

Di Stefano, M., Morrone, M.C. and Burr, D.C. (1985) Visual acuity of neurones in the cat lateral suprasylvian cortex. *Brain Res.*, **331**, 382-385.

Dreher, B. and Sefton, A.J. (1979) Properties of neurons in cat's dorsal lateral geniculate nucleus: a comparison between medial interlaminar and laminated parts of the nucleus. *J. Comp. Neurol.*, **183**, 47-63.

Dreher, B. (1986) Thalamocortical and corticocortical interconnections in the cat visual system: relation to mechanisms of information processing. In Pettigrew JD, Sanderson KJ, Levick WR (eds) *Visual neuroscience.* Cambridge University Press, Cambridge, pp. 290-314.

Fernald, R. and Chase R. (1971) An improved method for plotting retinal landmarks and focusing eyes. *Vision Res..*, **11**, 95-96.

Gazzaniga, M.S. (1970) *The bisected brain.* New-York: Appleton-Century Crofts.

Guillemot, J.-P., Lepore F., Prévost, L. Richer, L., Guilbert, M. (1988). Somatosensory receptive fields of fibres in the rostral corpus callosum of the cat. *Brain Res.*, **441**, 221-232.

Guillemot, J.-P., Paradis, M.-C., Samson, A., Ptito, M. and Lepore, F. (1993) Binocular interaction and disparity coding in area 19 of visual cortex in normal and split-chiasm cats. *Exp. Brain Res.*, **94**, 405-417.

Guillemot, J.-P., Richer, L., Ptito, M. and Lepore, F. (1992) Somatosensory receptive field properties of corpus callosum fibres in the raccoon. *J. Comp. Neurol.*, **321**, 124-132.

Guillemot, J.-P., Richer, L., Prévost, L., Ptito, M. and Lepore, F. (1987) Receptive field properties of somatosensory callosal fibers in the monkey. *Brain Res.*, **402**, 293-302.

Henry G.H., Bishop P.O. and Coombs J.S. (1967) Inhibitory and subliminal excitatory receptive fields of units in cat striate cortex. *Vision Res.*, **9**, 1289-1296.

Hubel, D.H. and Wiesel, T.N. (1962) Receptive fields, binocular interaction, and functional architecture in the cat's visual cortex. *J. Physiol. (London)*, **160**, 106-154.

Hubel, D.H. and Wiesel, T.N. (1965) Receptive fields and functional architecture in the two nonstriate visual areas (18 and 19) of the cat. *J. Neurophysiol.*, **28**, 229-289.

Hubel, D.H. and Wiesel, T.N. (1967) Cortical and callosal connections concerned with the vertical meridian of visual fields in the cat. *J. Neurophysiol.*, **30**, 1561-1573.

Illing, R.B. and Wässle, H. (1981) The retinal projection to the thalamus in the cat: a quantitative investigation and a comparison with the retinotectal pathway. *J. Comp. Neurol.*, **202**, 265-286.

Innocenti, G.M. (1986) General organization of callosal connections in the cerebral cortex. In Jones, E.G. and Peters, A. (eds), *Cerebral Cortex*, Vol. 5. Plenum Press, New-York, pp. 291-353.

Kluver, H. and Barrera, E. (1953) A method for combined staining of cells and fibres in the nervous system. *J. Neuropath. Exp. Neurol.*, **12**, 400-403.

Kratz, K.E., Webb, S.V. and Sherman, S.M. (1978) Studies of the cat's medial interlaminar nucleus: a subdivision of the dorsal lateral geniculate nucleus. *J. Comp. Neurol.*, **181**, 601-614.

Lepore, F., Ptito, M., Richer L. and Guillemot, J.-P. (1988) Cortico-cortical callosal connectivity: evidence derived from electrophysiological studies. *Prog. Brain Res.*, **75**, 187-195.

Lepore, F. and Guillemot, J.-P. (1982) Visual receptive field properties of cells innervated through the corpus callosum in the cat. *Exp. Brain Res.*, **46**, 413-424.

Lepore, F., Samson, A., Paradis, M.-C., Ptito, M. and Guillemot, J.-P. (1992) Binocular interaction and disparity coding at the 17/18 border: contribution of the corpus callosum. *Exp. Brain Res.*, **90**, 129-140.

Maffei, L., Berardi, N. and Bisti, S. (1986) Interocular transfer of adaptation after-effects in neurons of areas 17 and 18 of split-chiasm cats. *J. Neurophysiol.*, **55**, 966-976.

Manzoni, T., Barbaresi, P., Conti, F., Fabri, M. (1989) The callosal connections of the primary somatosensory cortex and the neural basis of midline fusion. *Exp. Brain Res.* **76**, 251-266.

Milleret, C., Houzel, J.C. and Buser, P. (1994) Pattern of development of the callosal transfer of visual information to cortical areas 17 and 18 in the cat. *J. European Neurosci.*, **6**, 193-202.

Morrone, M.C., Di Stefano, M. and Burr, D.C. (1986) Spatial and temporal properties of neurons of the lateral suprasylvian cortex of the cat. *J. Neurophysiol.*, **56**, 969-986.

Movshon, J.A., Thompson, I.D. and Tolhurst, D.J. (1978a) Spatial summation in the receptive fields of simple cells in the cat's striate cortex. *J. Physiol. (London),* **283**, 53-77.

Movshon, J.A., Thompson, I.D. and Tolhurst, D.J. (1978b) Receptive field organization of complex cells in the cat's striate cortex. *J. Physiol. (London)*, **283**, 79-99.

Movshon, J.A., Thompson, I.D. and Tolhurst, D.J. (1978c) Spatial and temporal contrast sensitivities in areas 17 and 18 in the cat's visual cortex. *J. Physiol. (London),* **283**, 101-120.

Myers, R.E. (1955) Interocular transfer of pattern discrimination in cats following section of crossed optic fibers. *J. Comp. Physiol. Psychol.,* **48**, 470-473.

Myers, R.E. (1956) Function of the corpus callosum in interocular transfer. *Brain*, **79**, 358-363.

Otsuka, R. and Hassler, R. (1962) Uber aufbau gliederung der corticalen sehsphare bei der katze. *Arch. Psychiat. Zeit. Neurol.*, **80**, 298-303.

Ohzawa, I., Sclar, G., Freeman, R.D. (1985) Contrast gain control in the cat's visual cortex. *J. Neurophysiol.*, **54**, 651-667.

Payne, B.R. (1991) Visual-field map in the callosal recipient zone at the border between areas 17 and 18 in the cat. *Visual Neurosci.*, **7**, 221-236.

Payne, B.R., Siwek, D.F. and Lomber, S.G. (1991) Complex transcallosal interactions in visual cortex. *Visual Neurosci.*, **6**, 283-289.

Rodieck, R.W. and Brening, R.K. (1983) Retinal ganglion cells: properties, types, general pathways and trans-species comparisons. *Brain. Behav. Evol* ., **23**,121-164.

Rosenquist, A. (1985) Connections of visual cortical areas in the cat. In Peters A, Jones EG (eds) *Cerebral cortex*. Plenum, New York, vol 3 pp. 81-117.

Sanderson, K.J. and Sherman, S.M. (1971) Nasotemporal overlap in visual field projected to lateral geniculate nucleus in the cat. *J. Neurophysiol.*, **34**, 453-466.

Segraves, M.A. and Rosenquist, A.C. (1982a) The distribution of the cells of origin of callosal projections in the cat visual cortex. *J. Neurosci.*, **2**, 1079-1089.

Segraves, M.A. and Rosenquist, A.C. (1982b) The afferent and efferent callosal connections of retinotopically defined areas in cat cortex. *J. Neurosci.*, **2**, 1090-1107.

Shatz, C. (1977). Abnormal interhemispheric connections in the visual system of Boston Siamese cats: a physiological study. *J. Comp. Neurol.*, **171**, 229-246.

Skottun, B.C., De Valois, R.L., Grosse, D.H., Movshon, J.A., Albrecht, D.G. and Bonds, A.B. (1991) Classifying simple and complex cells on the basis of response modulation. *Vision Res.*, **31**, 1079-1086.

Skottun, B.C. and Freeman, R.D. (1984) Stimulus specificity of binocular cells in the cat's visual cortex: ocular dominance and the matching of left and right eyes. *Exp. Brain Res.*, 56, 206-216.

Spidalieri, G., Guandalini, P. and Franchi, G. (1986) Motor responses mediated by orthodromic and antidromic activation of the rostral portion of the cat corpus callosum. *Exp. Brain Res.*, **64**, 133-142.

Stone, J. (1966) The naso-temporal division of the cat's retina. *J. Comp. Neurol.*, **126**, 585-599.

Stone, J. (1983) Parallel processing in the visual system. *The classification of retinal ganglion cells and its impact on the neurobiology of vision.* Plenum, New York.

Tardif, E., Bergeron, A., Lepore, F. and Guillemot, J.-P. (1996) Spatial and temporal frequency tuning and contrast sensitivity of single neurons in area 21a of the cat. *Brain Res.*, 716, 219-223.

Tanaka, K., Ohzawa, I., Ramoa, A.S. and Freeman, R.D. (1987) Receptive field properties of cells in area 19 of the cat. *Exp. Brain Res.*, **65**, 549-558.

Tusa, R.J., Rosenquist, A.C. and Palmer, L.A. (1978) Retinotopic organization of area 17 (striate cortex) in the cat. *J. Comp. Neurol.*, **177**, 213-236.

Tusa, R.J., Rosenquist, A.C. and Palmer, L.A. (1979) Retinotopic organization of areas 18 and 19 in the cat. *J. Comp. Neurol.*, **185**, 657-678.

Whitteridge D. (1965) Area 18 and the vertical meridian of the visual field. In Ettlinger, E.G. (ed.), *Functions of the corpus callosum.* J. and A. Churchill, London, pp. 115-120.

Wilson, P.D., Rowe, M.H. and Stone, J. (1976) Properties of relay cells in the cat's lateral geniculate nucleus: a comparison of W-cells with X- and Y-cells. *J. Neurophysiol.*, **39**, 1193-1209.

Zumbroïch, T.J. and Blakemore, C. (1987) Spatial and temporal selectivity in the suprasylvian visual cortex of the cat. *J. Neurosci.*, **7**, 482-500.

FIGURE LEGENDS

Fig.1: Distribution of ocular dominance for 310 cells recorded in area 19. In normal cats (dark bars), the majority of cells are binocular, with the exception of a few monocular cells which respond only to the contralateral eye (class 1) or the ipsilateral eye (class 7). In split-chiasm cats (open bars) the distribution contains many monocular units that respond only to the ipsilateral eye but about one-third of the cells are binocular. For both groups, binocular cells activated in equal strength by the two eyes (class 4) are predominant but cells in the others classes of ocular dominance are also found. More cells are found with moderate ocular dominance (class 3 and 5) and a few show strong ocular dominance (class 2 and 6).

Fig.2: Spatial frequency tuning functions of one monocular cell and five binocular cells recorded in area 19 of normal cats. The response of the cell to each spatial frequency tested is shown for the ipsilateral eye (open circles) and contralateral eye (filled circles). The stimulus was a sinusoidal grating drifting (2 Hz) at optimal direction with a contrast of 50%. The letter N indicates that the cell was registered in a normal cat. Digits above each tuning curve indicate the cell's number and its ocular dominance (last number). Most cells present a band-pass tuning curve but a few cells like N 74-3 were classified as low-pass because they do not shown clear evidence of attenuation in their responses at low spatial frequencies. The high cut-off of the dominant eye of the cells presented range from 0,3 c/deg (cell N 71-1) to 2.2 c/deg (cell N 93-6). When the response strength to the optimal spatial frequency is similar (cell N 16-4) for both eyes, the high cut-off is the same for the ipsilateral and contralateral eye. On the other hand, for cells dominated by one eye (cells N 22-2, N 74-3, N 24-5, N 93-6) some differences are found between the high cut-off of the ipsilateral and contralateral eye and these differences are related to the cell's ocular dominance.

Fig 3: Spatial frequency tuning functions of one monocular cell and five binocular cells recorded in area 19 of split-chiasm cats. The response of the cell to each spatial frequency tested is shown for the ipsilateral eye (open circles) and the contralateral eye (filled circles). The stimulus was a sinusoidal grating drifting (2 Hz) at optimal direction with a contrast of 50%. CHI refers to the fact that the cell came from a chiasma sectioned animal. Digits above each tuning curve indicate the cell's number and its ocular dominance (last digit). As shown in the normal cats, most cells present a band-pass tuning curve but a few cells like CHI 66-3 were classified as low-pass because they do not shown any evidence of attenuation in their responses at the low spatial frequencies. The high cut-off of the dominant eye of cells presented range from 0,5 c/deg (cell CHI 72-4) to 2.2 c/deg (cell CHI 95-5). When the response strength to the optimal spatial frequency is similar (cell CHI 72-4) for both eyes, the high cut-off is the same for the ipsilateral and contralateral eye. On the other hand, for cells dominated by one eye (cells CHI 49-2, CHI 66-3, CHI 95-5, CHI 159-6) some differences are found between the high cut-off of the ipsilateral and contralateral eye and these differences are related to the cell's ocular dominance.

Fig. 4: Distribution of the high cut-off spatial frequency for the normal (dark bars) and split-chiasm (open bars) cats. For each cell, the high cut-off spatial frequency is derived from the spatial frequency tuning function of the dominant eye. There is no differences between the two distributions.

Fig. 5: Relationship between the high cut-off spatial frequency of the ipsilateral and contralateral eye in the normal (left) and split-chiasm (right) cats. In both groups, their is a significant relation between the high cut-off of the ipsilateral and contralateral eye although the two eye are not perfectly matched.

Fig. 6: Differences between the high cut-off spatial frequency of the ipsilateral and contralateral eye for binocular cells plotted against the ocular dominance. Negative values on the y axis are arbitrarily assigned to cells showing a higher cut-off through the

contralateral eye and positive values correspond to cells having a higher cut-off through the ipsilateral eye. In both the normal (dark bars) and split-chiasm (open bars) cats, cells having a similar response strength for both eyes (class 4) do not show any differences in the high cut-off of the two eyes. Cells dominated by the ipsilateral (class 5 and 6) or contralateral (class 2 and 3) eye have a higher cut-off through the dominant eye.

Fig. 7: Distribution of the optimal spatial frequency for band-pass cells recorded in the normal (dark bars) and split-chiasm (open bars) cats. For each cell, the optimal spatial frequency is taken from the spatial frequency tuning function of the dominant eye. There is no significant differences between the two distributions.

Fig. 8: Relationship between the optimal spatial frequency of the ipsilateral and contralateral eye in the normal (left) and split-chiasm (right) cats. In both groups, there is a strong significant relation between the optimal spatial frequency of the two eyes.

Fig. 9: Distributions of the spatial bandwidth for band-pass cells recorded in the normal (dark bars) and split-chiasm (open bars) cats. For each cell, spatial bandwidth is taken at half amplitude of the spatial frequency tuning function of the dominant eye. There is no differences between the two distributions.

Fig. 10: Relationship between the spatial bandwidth of the ipsilateral and contralateral eye in the normal (left) and split-chiasm (right) cats. In both groups, there is a significant relation between the optimal spatial frequency of the two eyes.

Fig. 11: Distribution of the contrast thresholds estimated for cells recorded in the normal (dark bars) and split-chiasm (open bars) cats. The stimulus used to assessed the contrast threshold was a sinusoidal grating of optimal spatial frequency drifting at optimal direction with a temporal frequency of 2 Hz. For most cells, thresholds are relatively low ($< 6\%$) and there are no significant differences between the two distributions.

Fig. 12: Relationship between the contrast threshold of the ipsilateral and contralateral eye in the normal (left) and split-chiasm (right) cats. In both groups, there is a significant relation between the contrast threshold of the two eyes.

Fig. 13: Results obtained for cells recorded at the 17/18 border of the split-chiasm cat. **A**. Distribution of ocular dominance for 139 cells. About one third of the cells are binocular while the remaining can only be activated with the ipsilateral eye. **B**. Relationship between the contrast thresholds of the ipsilateral and contralateral eye for binocular cells. This figure shows that a significant relationship exists between the contrast thresholds of the two eyes. **C**. Relationship between the high cut-off spatial frequency of the ipsilateral and contralateral eye for binocular cells. A significant relationship is found between the spatial resolution of both eyes. **D**. The interocular differences in spatial resolution are related to ocular dominance. Negative values on the y-axis are arbitrarily assigned to cells showing a higher cut-off through the contralateral eye (callosal pathway) and positive values correspond to cells having a higher cut-off through the ipsilateral eye (thalamic pathway). Cells having a similar response strength for both eyes (class 4) do not show any differences in the high cut-off of the two eyes. Cells dominated by the ipsilateral eye (classes 5 and 6) or by the contralateral eye (classes 2 and 3) have a higher cut-off through the dominant eye.

FIGURE 1

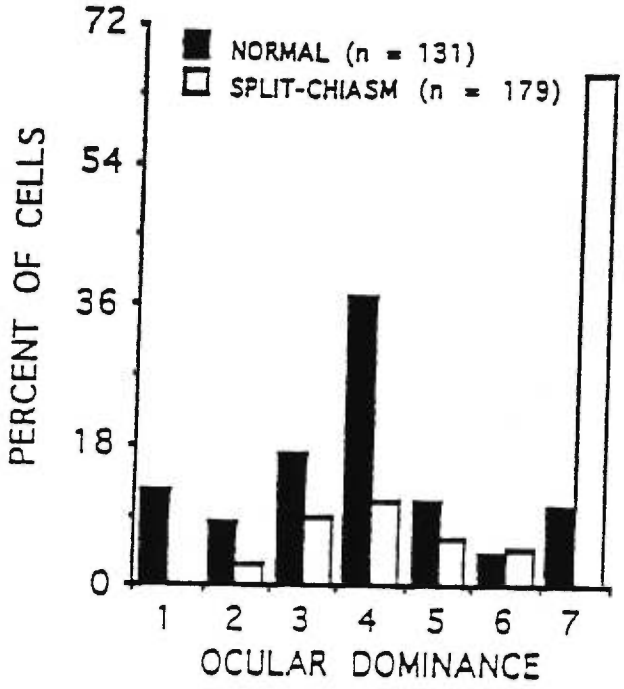
72
54
36
18
0
PERCENT OF CELLS
NORMAL (n = 131)
SPLIT-CHIASM (n = 179)
1 2 3 4 5 6 7
OCULAR DOMINANCE

FIGURE 2

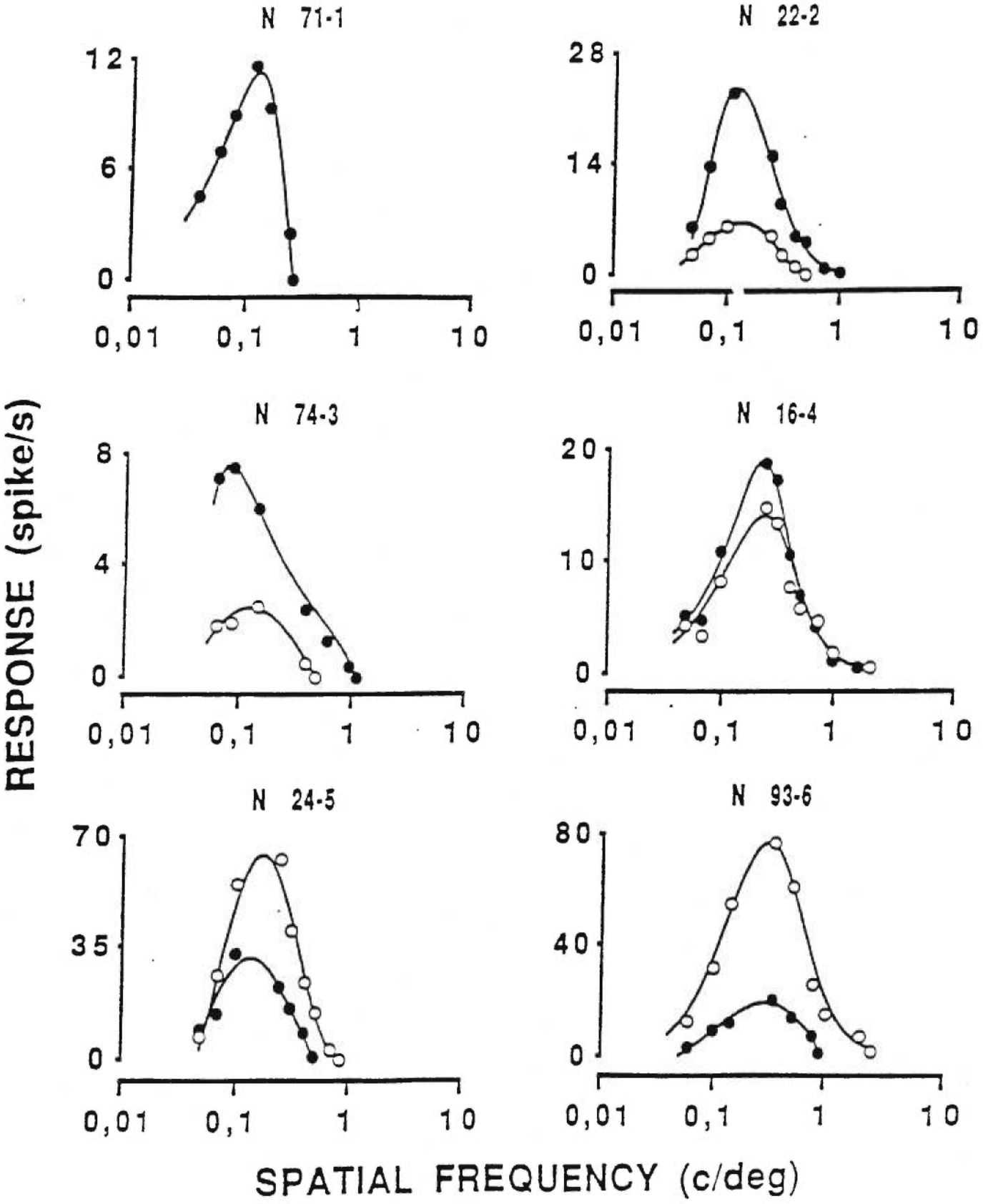
N 71-1
12
6
0
0,01
0,1
1
10
N 22-2
28
14
0
0,01
0,1
1
10
N 74-3
8
4
0
0,01
0,1
1
10
N 16-4
20
10
0
0,01
0,1
1
10
N 24-5
70
35
0
0,01
0,1
1
10
N 93-6
80
40
0
0,01
0,1
1
10
RESPONSE (spike/s)
SPATIAL FREQUENCY (c/deg)

FIGURE 3

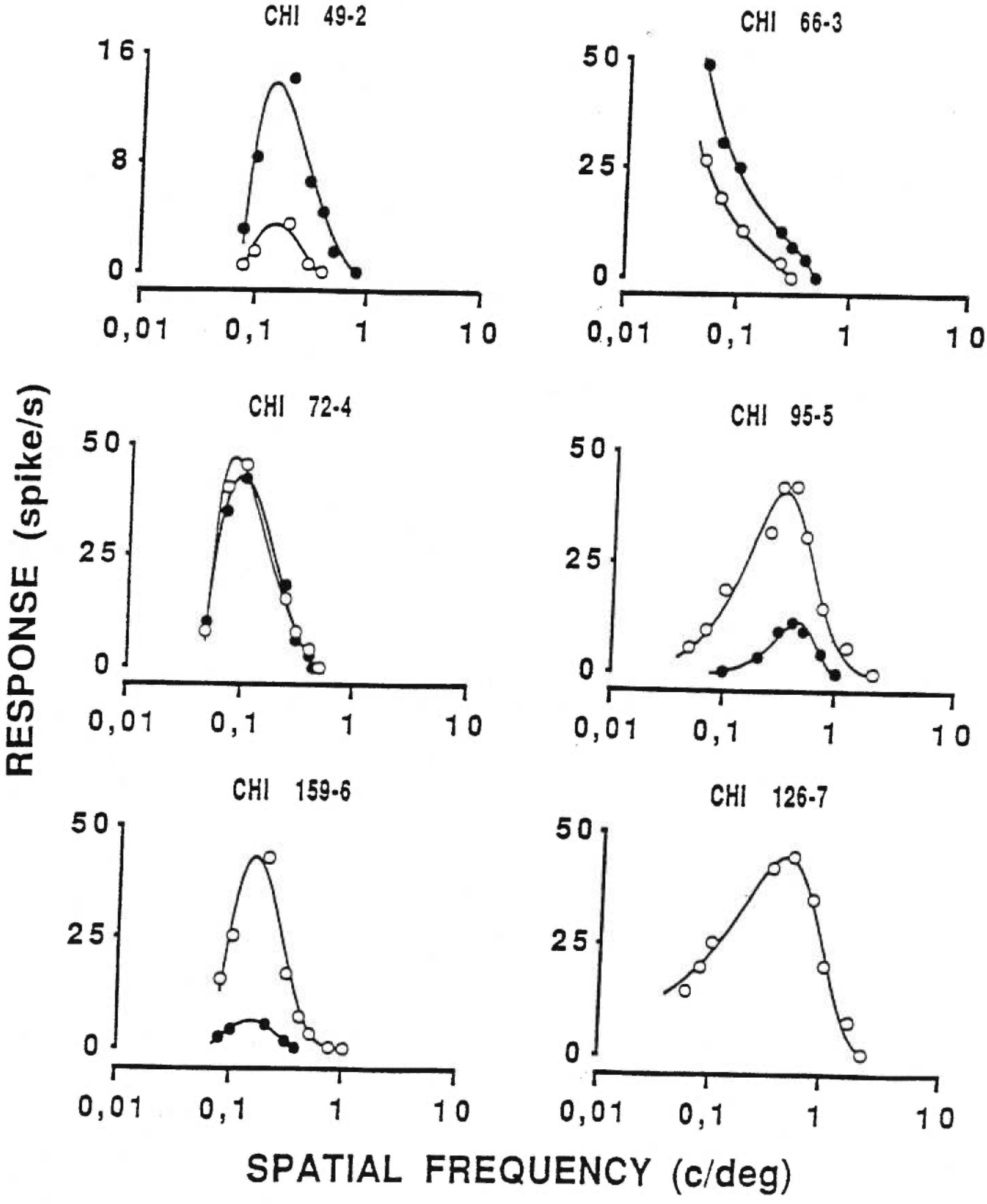
CHI 49-2
16
8
0
0,01
0,1
1
10
CHI 66-3
50
25
0
0,01
0,1
1
10
CHI 72-4
50
25
0
0,01
0,1
1
10
CHI 95-5
50
25
0
0,01
0,1
1
10
CHI 159-6
50
25
0
0,01
0,1
1
10
CHI 126-7
50
25
0
0,01
0,1
1
10
RESPONSE (spike/s)
SPATIAL FREQUENCY (c/deg)

FIGURE 4

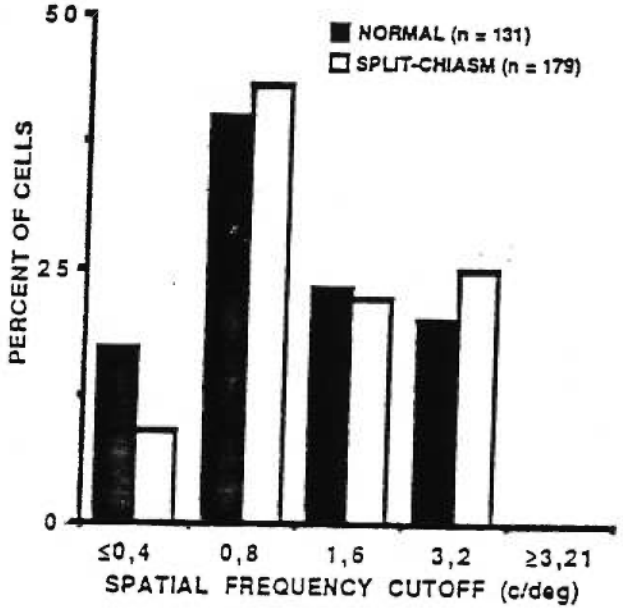
50
25
0
PERCENT OF CELLS
NORMAL (n = 131)
SPLIT-CHIASM (n = 179)
≤0,4
0,8
1,6
3,2
≥3,21
SPATIAL FREQUENCY CUTOFF (c/deg)

FIGURE 5

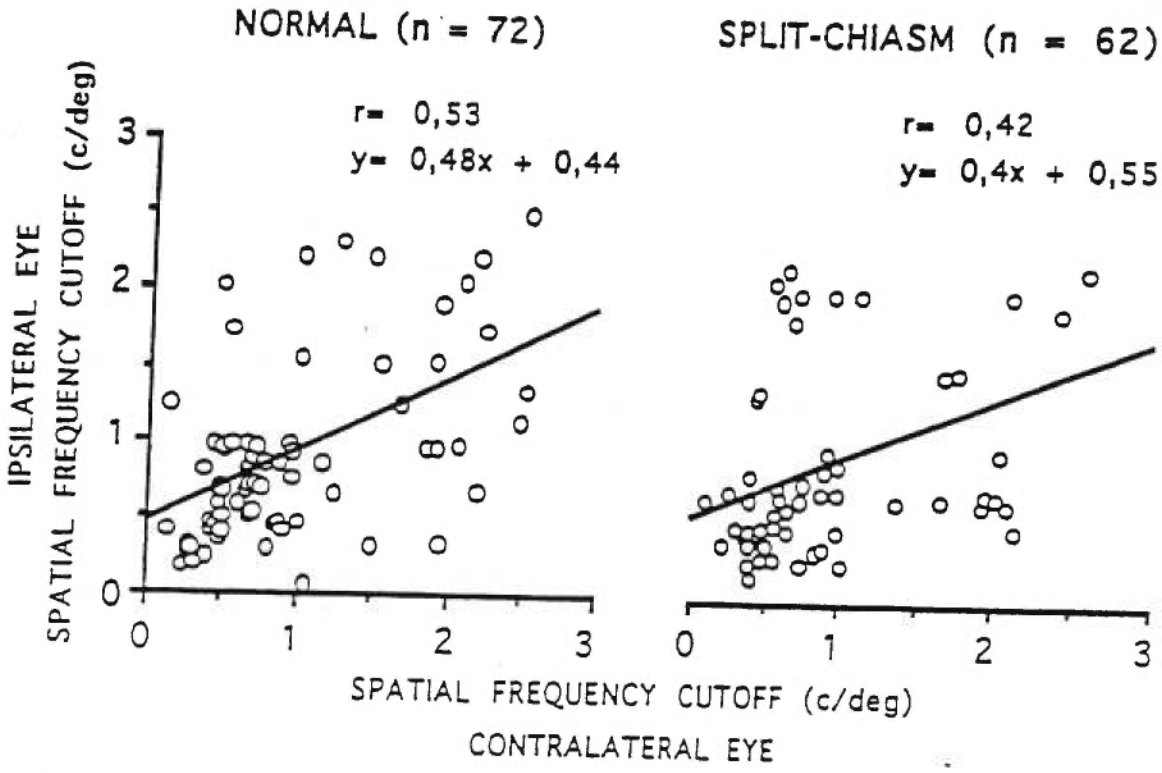
NORMAL (n = 72)
r= 0,53
y= 0,48x + 0,44
SPLIT-CHIASM (n = 62)
r= 0,42
y= 0,4x + 0,55
IPSILATERAL EYE
SPATIAL FREQUENCY CUTOFF (c/deg)
0
1
2
3
SPATIAL FREQUENCY CUTOFF (c/deg)
CONTRALATERAL EYE

FIGURE 6

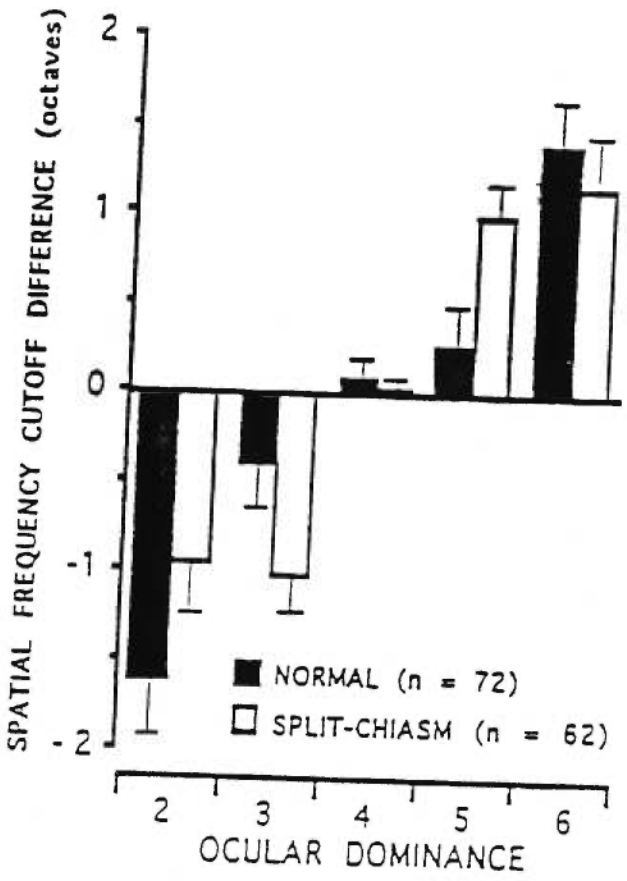
SPATIAL FREQUENCY CUTOFF DIFFERENCE (octaves)
2
1
0
-1
- 2
NORMAL (n = 72)
SPLIT-CHIASM (n = 62)
2
3
4
5
6
OCULAR DOMINANCE

FIGURE 7

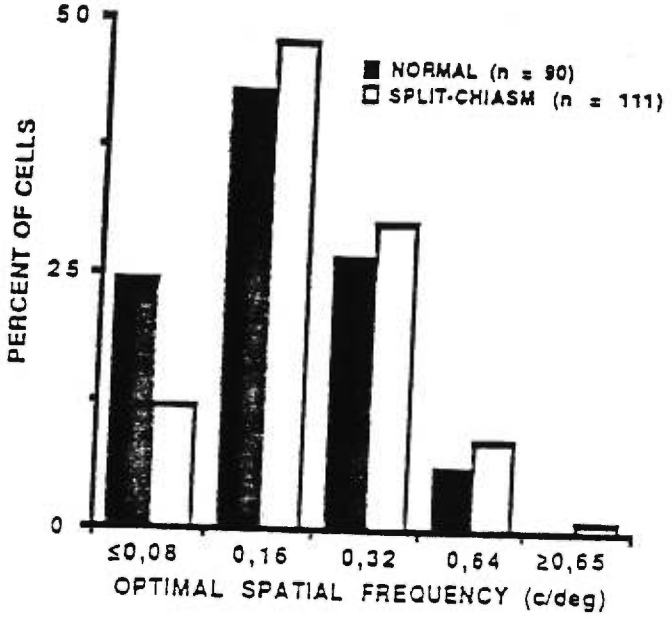
50
25
0
PERCENT OF CELLS
NORMAL (n = 90)
SPLIT-CHIASM (n = 111)
≤0,08
0,16
0,32
0,64
≥0,65
OPTIMAL SPATIAL FREQUENCY (c/deg)

FIGURE 8

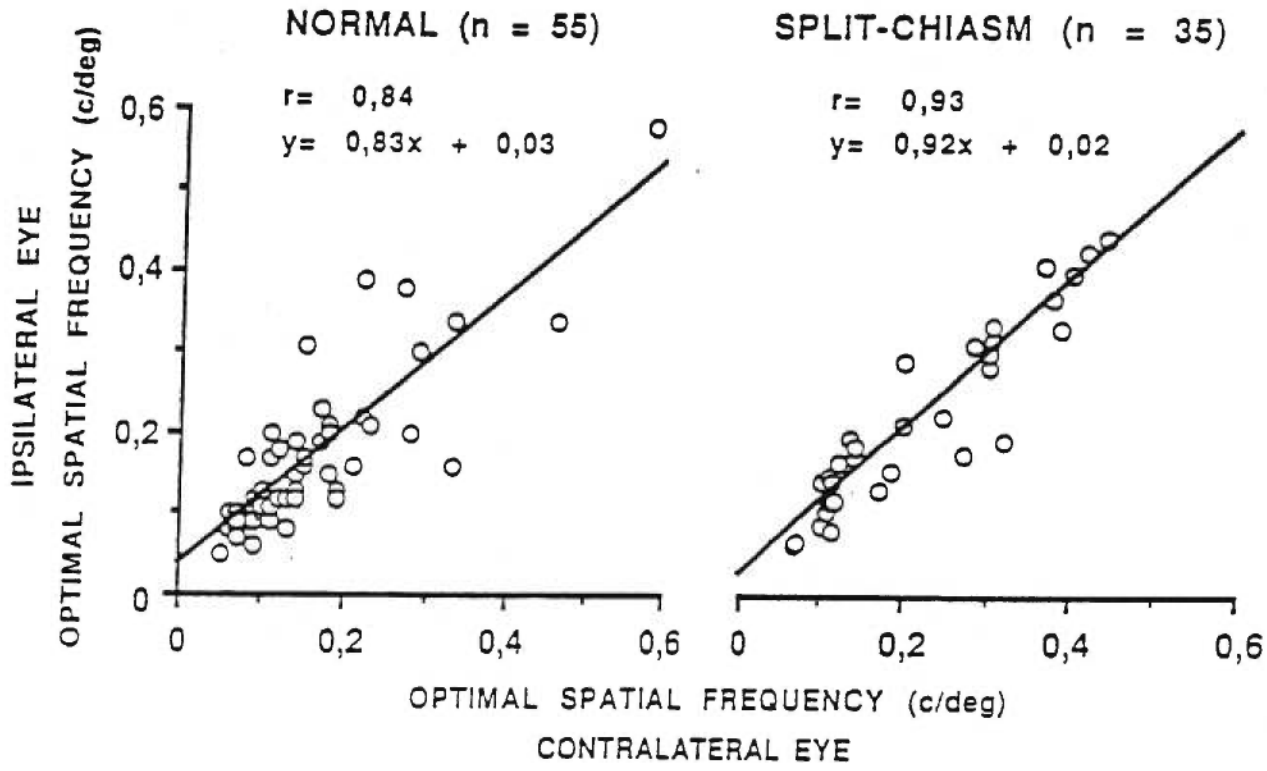
NORMAL (n = 55)
r= 0,84
y= 0,83x + 0,03
SPLIT-CHIASM (n = 35)
r= 0,93
y= 0,92x + 0,02
IPSILATERAL EYE
OPTIMAL SPATIAL FREQUENCY (c/deg)
0
0,2
0,4
0,6
OPTIMAL SPATIAL FREQUENCY (c/deg)
CONTRALATERAL EYE

FIGURE 9

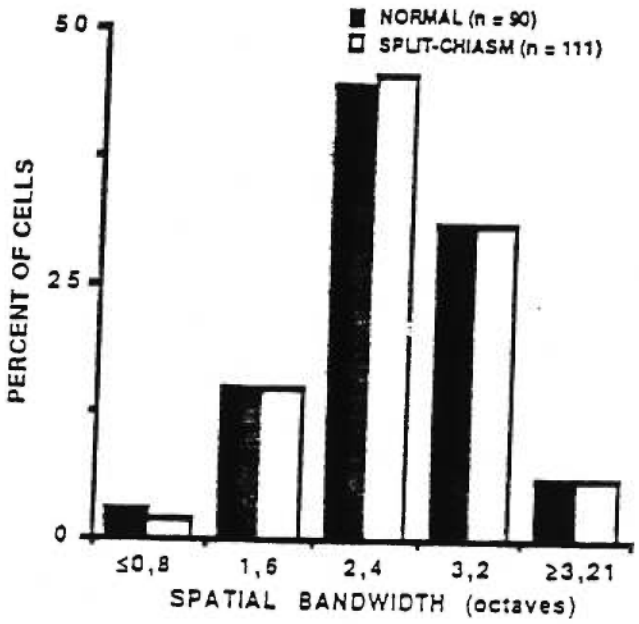
NORMAL (n = 90)
SPLIT-CHIASM (n = 111)
50
25
0
PERCENT OF CELLS
≤0,8
1,6
2,4
3,2
≥3,21
SPATIAL BANDWIDTH (octaves)

FIGURE 10

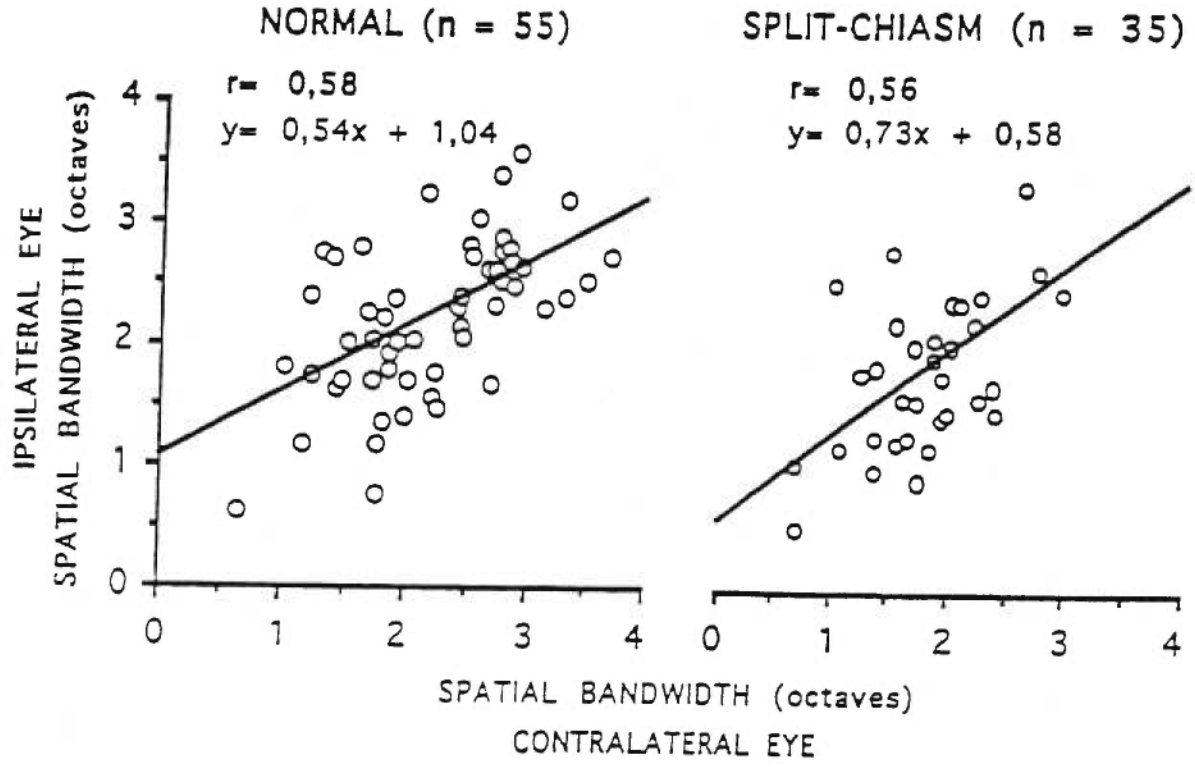
NORMAL (n = 55)
r= 0,58
y= 0,54x + 1,04
SPLIT-CHIASM (n = 35)
r= 0,56
y= 0,73x + 0,58
IPSILATERAL EYE
SPATIAL BANDWIDTH (octaves)
0
1
2
3
4
SPATIAL BANDWIDTH (octaves)
CONTRALATERAL EYE

FIGURE 11

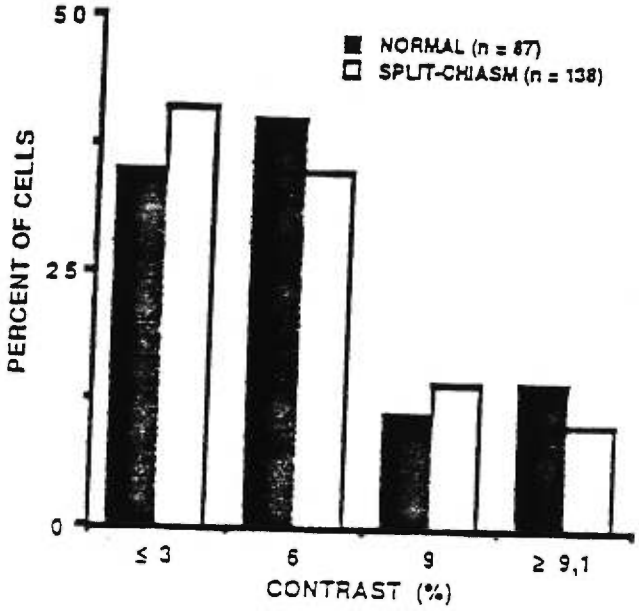
50
25
0
PERCENT OF CELLS
NORMAL (n = 87)
SPLIT-CHIASM (n = 138)
≤ 3
6
9
≥ 9,1
CONTRAST (%)

FIGURE 12

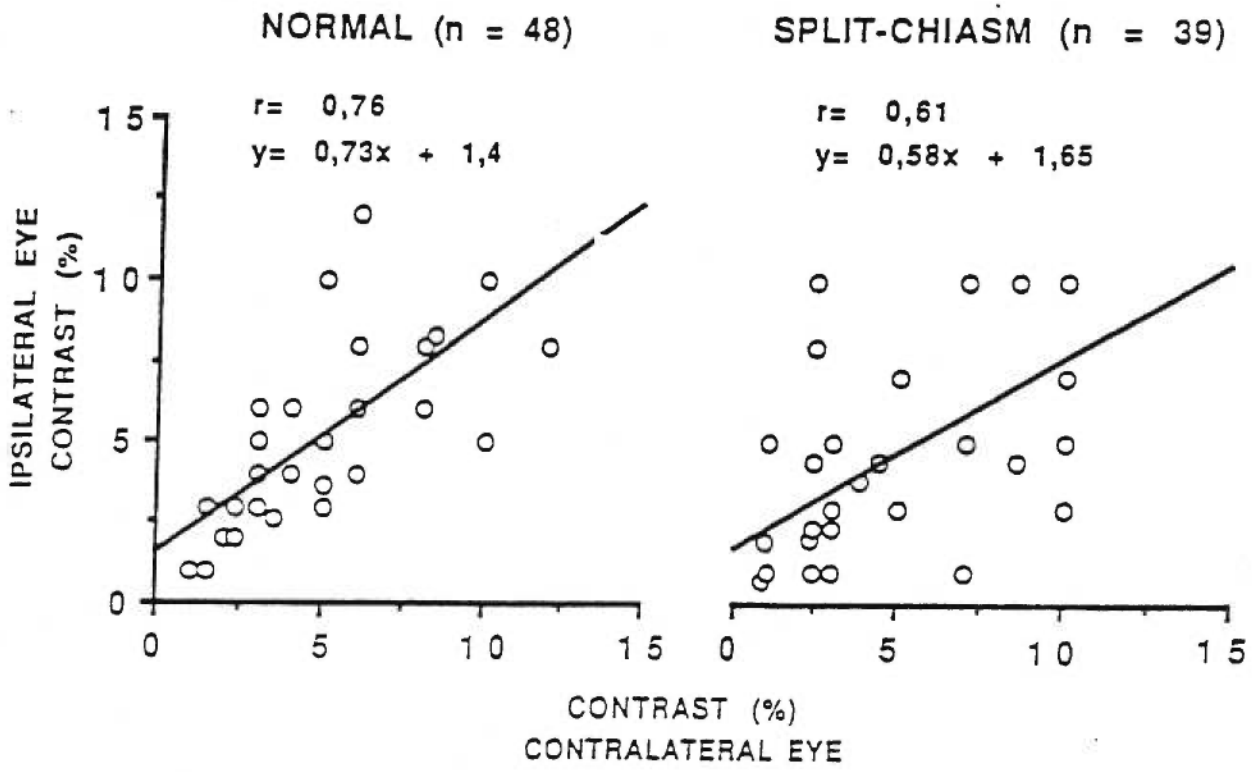
NORMAL (n = 48)
r= 0,76
y= 0,73x + 1,4
SPLIT-CHIASM (n = 39)
r= 0,61
y= 0,58x + 1,65
IPSILATERAL EYE CONTRAST (%)
CONTRAST (%) CONTRALATERAL EYE
0
5
10
15

FIGURE 13

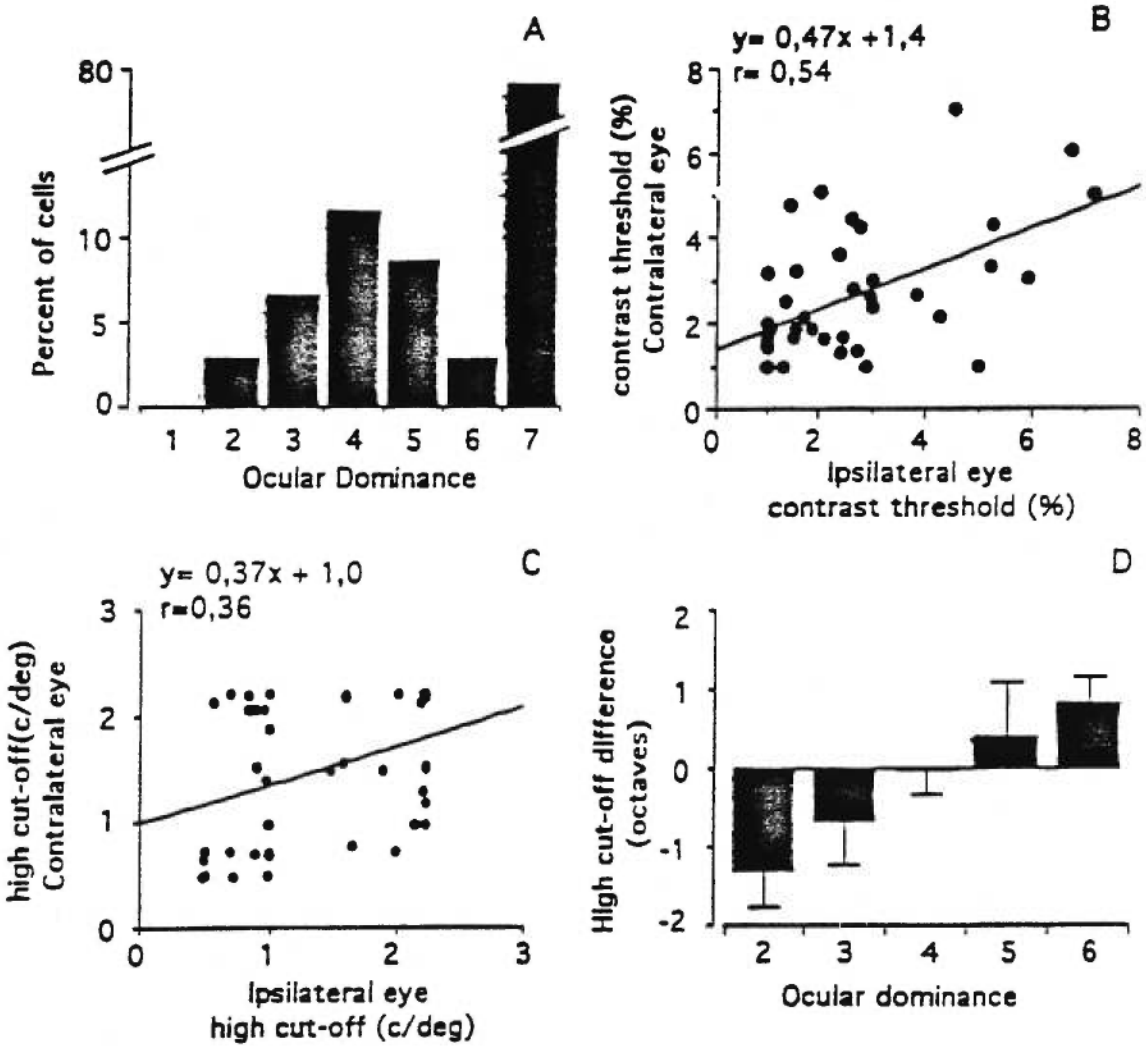
A
80
10
5
0
Percent of cells
1 2 3 4 5 6 7
Ocular Dominance
B
y= 0,47x +1,4
r= 0,54
8
6
4
2
0
contrast threshold (%)
Contralateral eye
0 2 4 6 8
Ipsilateral eye
contrast threshold (%)
C
y= 0,37x + 1,0
r=0,36
3
2
1
0
high cut-off(c/deg)
Contralateral eye
0 1 2 3
Ipsilateral eye
high cut-off (c/deg)
D
2
1
0
-1
-2
High cut-off difference
(octaves)
2 3 4 5 6
Ocular dominance

CHAPITRE V

Article #4

Direction selectivity and spatial frequency properties of single neurons in the area 21b of the cat

Spatial properties and direction selectivity of single neurons in area 21b of the cat.

Eric Tardif[1], André Bergeron[1], Franco Lepore[1-2], and Jean-Paul Guillemot[1-3].

[1] Groupe de Recherche en Neuropsychologie Expérimentale

[2] Département de Psychologie, Université de Montréal, C. P. 6128, Succ. Centre-Ville, Montréal, Québec, H3C 3J7.

[3] Département de Kinanthropologie, Université du Québec à Montréal, C. P. 8888, Succ. Centre-Ville, Montréal, Québec, H3C 3P8.

Running title: visual receptive fields in area 21b.

Key words: spatial frequency, temporal frequency, extrastriate, contrast sensitivity

Send correspondence to:
Jean-Paul Guillemot
Département de Kinanthropologie
Université du Québec à Montréal
C.P. 8888 Succ. Centre-Ville,
Montréal, Québec H3C 3P8
Canada

Telephone: (514) 987-3606
Telefax: (514) 987-6616
Email: r10475@nobel.si.uqam.ca

Abstract

The receptive field properties of single units were assessed in area 21b of the cat visual cortex. Visual cells in this area were binocular and showed relatively large receptive fields. Most cells were strongly sensitive to the direction drifting gratings. The mean value of the half-widths of the direction tuning curves (32 deg) suggests broader direction tunings than what is typically found in other visual areas. The spatial frequency tuning functions were either band-pass or low-pass. Cells responded optimally to low spatial frequencies (mean = 0.08 c/deg) and also showed low spatial resolution (mean = 0.29 c/deg). The estimated values of spatial bandwidths (mean = 2.2 octaves) suggest that area 21b cells act as relatively good spatial filters. Although some cells exhibited a low contrast threshold, most cells began to respond at intermediate or high contrast values (mean threshold = 15.5). Temporal frequency tuning functions were mostly band-pass and usually broad (mean temporal bandwidth = 3.3 octaves). Cells were found that responded optimally to various temporal frequencies (mean optimal temporal frequency = 3.2 Hz), although the majority preferred a temporal frequency below 4 Hz. These results suggest that, despite their low spatial resolution, cells in area 21b may contribute to the analysis of objects.

Introduction

The visual cortex of higher mammals is composed of many areas each containing a representation of visual space and each processing multiple aspects of vision. Behavioral studies in cats have shown that discrimination of simple components of perception, such as bar orientation, depends upon the integrity of visual areas 17/18 and of some suprasylvian areas (Vandenbussche *et al.*, 1991; Sprague *et al.*, 1996). However, the removal of areas 17/18 does not impair pattern discrimination, notwithstanding a reduction of visual resolution (Doty, 1971; Berkeley and Sprague, 1979). On the other hand, when lesions are performed in extrastriate areas (19, 20, 21, 7 and suprasylvian areas), pattern discrimination is severely affected (Sprague *et al.*, 1977). These suggests that although areas 17 and 18 are involved in the analysis of some simple components of the visual scene and in fine spatial resolution, pattern discrimination is more likely mediated by extrastriate areas. Recent studies in cats have shown that unilateral cooling of some suprasylvian areas induces a reversible hemineglect of the opposite hemifield (Payne *et al.*, 1996). Moreover, experiments using techniques of reversible cortical deactivation (Lomber *et al.*, 1996) suggest that a functional dissociation can be made between the middle and posterior parts of the suprasylvian visual cortex. The former is likely to be involved in visual orientation tasks as well as in the discrimination of direction while the latter contributes to the learning and recognition of patterns and objects.

Receptive fields (RFs) of cells in the various visual areas possess distinct spatial and temporal properties suggestive of the type of visual analysis that is achieved in a particular area. In the cat, although RFs properties of area 17 neurons have been extensively studied, they have been less so in extrastriate areas. Cells in area 17 have been shown to be selective to orientation (Hubel and Wiesel, 1962), spatial frequency

(Movshon *et al.*, 1978; Berardi *et al.*, 1982), temporal frequency (Saul and Humphrey, 1992) and positional disparities (Barlow *et al.*, 1967; Ferster, 1981; LeVay and Voigt, 1988; Lepore *et al.*, 1992). They are often finely tuned to spatial frequencies and exhibit high spatial resolution (Movshon *et al.*, 1978; Berardi *et al.*, 1982) which may be attributable to the strong X input that is mostly confined to this area.

Electrophysiological studies in extrastriate area have shown that the RF properties of cells may be related to the nature of the parallel input projecting to these areas. In area 18, cells have larger RFs and respond to higher velocities than cells in area 17 and 19, which reflect a strong Y input (Orban, 1984). Cells in area 19 have smaller RFs than those in area 18 and respond to lower velocities, which may be attributable to a predominant W input (Orban, 1984; Dreher *et al.*, 1986). Also, cells in both areas 18 and 19 are tuned to lower spatial frequencies and exhibit lower spatial resolution than cells in area 17 (Movshon *et al.*, 1978; Berardi *et al.*, 1982 Tanaka *et al.*, 1987). These latter properties suggest that the X signal carrying high spatial frequency information is poorly relayed to the majority of cells in extrastriate areas or undergoes important transformations within these areas.

Early studies of the cat's extrastriate cortex have described a large visual area surrounding the lateral suprasylvian sulcus, which was originally called the Clare-Bishop area or lateral suprasylvian area (Clare and Bishop, 1954; Hubel and Wiesel, 1969). Electrophysiological studies in this area have shown that neurons have large binocular RFs of the complex type which are particularly sensitive to moving stimuli and that many units are selective to stimulus direction (Hubel and Wiesel, 1969; Wright, 1969; Spear and Baumann, 1975; Turlejski, 1975; Camarda and Rizzolatti, 1976; Blakemore and Zumbroïch, 1987; Rauschecker *et al.*, 1987, von Grünau *et al.*, 1987; Gizzi *et al.*, 1990). The lateral suprasylvian area was further subdivided into several areas on the basis of retinotopic representations (Palmer *et al.*, 1978; Tusa *et*

al., 1980). Among these areas, the most investigated is the postero-medio-lateral suprasylvian (PMLS) area which is located in the posterior part of the lateral suprasylvian sulcus. Studies suggest that cells in PMLS process visual information concerning the relative direction of a moving stimulus (von Grünau and Frost, 1983) and optic flow-field (Rauschecker *et al.*, 1987; Sherk *et al.*, 1995; Kim *et al.*, 1997; Mulligan *et al.*, 1997).

Recently, a number of electrophysiological studies have focused on RF properties of cells in other extrastriate areas such as 21a (Mizobe *et al.* 1988; Dreher *et al.*, 1992; Wimborne *et al.*; 1992; Michalski *et al.*, 1994; Tardif *et al.*, 1996; Wang and Dreher, 1996). This area is located outside the suprasylvian sulcus but is in continuity with PMLS. Although both areas 21a and PMLS contain neurons with similar spatial frequency properties such as optimal frequency and resolution (Di Stefano *et al.*, 1985; Morrone *et al.*, 1986; Zumbroïch and Blakemore, 1987; Tardif *et al.*, 1996), they seem to differ on other parameters such as peak discharge rate, response to moving stimuli and to visual noise (Dreher *et al.*, 1996). For example, many neurons in PMLS are direction-selective (Spear and Baumann, 1975; von Grünau and Frost, 1983; Rausckecker *et al.*, 1987, Dreher *et al.*, 1996) while those in area 21a tend to be selective to orientation but not to direction (Wimborne and Henry, 1992; Dreher *et al.*, 1993; 1996).

Area 21b, lying in the posterior part of the suprasylvian sulcus, has not been much investigated, other than for its retinotopic organizations (Markuszka, 1978; Tusa *et al.*, 1980). This is probably in part because it is partially folded into the posterior suprasylvian sulcus (Tusa *et al.*, 1980). Its RFs appear to extend up to 60 deg of eccentricity and are mostly located in the upper contralateral field (Tusa *et al.*, 1980). Anatomical studies have shown that it has many connections with the lateral posterior nucleus (LP), more particularly, its "cortico-recipient zone" (LPl), but few with the

dorsal lateral geniculate nucleus (Symonds *et al.*, 1981; Raczkowski and Rosenquist, 1983; Updyke, 1983; Dreher, 1986). Areas 21b has reciprocal connections with 21a as well as with areas 17, 18 and 19, although the putative connections of the latter areas are less clear (Symonds and Rosenquist, 1984 a, b).

The present investigation has two objectives: first, to provide an insight on the selectivity of cells in area 21b to different properties of a visual stimulus (spatial frequency, temporal frequency, contrast and orientation/direction). Second, to compare these results with those typically found in other visual areas and in particular area 21a. The latter will help to determine whether area 21b is functionally distinct from adjoining area 21a in terms of the RF properties of their constituent neurons.

Materials and Methods

Subjects.

Experiments were carried out using adult cats of either sex weighing from 2-4 kg. They were in good health and had no apparent malformations or pathological disorders. All surgical interventions, manipulations and husbandry were carried out within the guidelines proposed by the Canadian Council on Animal Care and those of NIH concerning the preparation and maintenance of higher animal during neuroscience experiments. Moreover, the experimental protocols were approved by the Université de Montréal animal care committee.

Surgical procedures.

Each cat first received an i.m. injection of Atropine (Atro-sol, 0.2 mg/kg) to reduce bronchial secretions, after which it was anesthetized with a gaseous solution of Nitrous oxide: Oxygen (N_2O : O_2, 70 : 30) and Halothane (2%). The animal was then intubated, which allowed for artificial ventilation through a respiratory pump. The saphenous vein was cannulated in order to administer 5% dextrose in lactated Ringer solution to maintain blood pressure and hydration. During surgical procedures general anesthesia was maintained with Halothane (1% to 2% in the same gaseous mixture). The animal was placed in a modified stereotaxic apparatus (David Kopf) and trepanation was performed over area 21b as defined by Tusa and Palmer (1980) at Horsley-Clarke coordinates (A1 to P7, L10 to L16). A small opening was made in the dura overlying area 21b and the exposed cortex was further covered with 4% agar in physiological saline. After the surgery, halothane level was progressively reduced (0.5% /15 min.) and maintained at 0.5% for the duration of the experiment. Stable heart rate and the absence of reflexes ensured that the anesthesia level was sufficient. Then the animal was paralyzed with gallamine triethiodide (Flaxedil 200 mg) and d-

tubocurarine (Tubarine 15 mg) dissolved in 30 ml of lactated Ringer solution with dextrose (5%). The mixture was continuously infused (5.6 ml/h) through the saphenous vein to maintain paralysis of the extraocular muscles. Respiratory rate and volume were controlled so as to maintain a constant level of expired CO_2 (4% ± 0.5%). Body temperature was kept constant (38° C) with the help of a heating waterpad and heart rate was also continuously monitored. ECG was constantly monitored and the electroencephalogram (monitored intermittently yet regularly) showed slow-wave activity throughout the recording session.

Optical preparation.

In order to determine the relative position of the areae centrales, retinal landmarks (optic discs and blood vessels) were projected on the tangent screen (Fernald and Chase, 1971) which was located 57 cm in front of the animal. The area centralis was considered to be situated 16 deg medially and 7.5 deg below the isoelevation line of the center of each optic disk (Bishop *et al.*, 1962). Pupils were routinely dilated by i.m. injections of atropine sulfate 1% (Atro-sol, 0.2 mg/kg) and the nictitating membranes were retracted with topical applications of phenylephrine hydrochloride (Neo-synephrine: 0.1%). To prevent eye dehydration and to improve image resolution, a neutral contact lens with a 3 mm artificial pupil was placed on each eye. The optic quality of the eyes was routinely checked during the recording session and the images on the retinae were focused by the use of appropriate dioptric lenses, as dictated by direct ophtalmoscopy.

Recordings.

Recordings were carried out with glass micropipettes filled with 2M NaCl and having an impedance of 2-5 MΩ (measured at 1000 Hz). The location of area 21b was

assessed by its position relative to the middle and posterior sulci as proposed by Tusa and Palmer (1980). The micromanipulator was fixed to a rotating ball-joint so that the micropipette could be lowered perpendicularly to the cortical surface. Relatively long penetrations were made through the posterior bank of the posterior suprasylvian sulcus corresponding to area 21b. Action potentials were conventionally amplified, displayed on an oscilloscope, filtered through a time/amplitude discriminator and transferred to an audio monitor and to a computer. Upon isolating a cell, the stimulation procedure adapted from Henry *et al.* (1967) was used. The spatial position of the RFs were determined and the spatial organization of each RF was carefully explored and mapped using light and dark bars as well as edges and drifting sinusoidal gratings. The best stimulus parameters (directionality, velocity, orientation, width and length) as estimated from the output of the audio monitor, were determined for the dominant eye. RFs were first classified in terms of simple, complex, end-stopped simple and end-stopped complex categories using the criteria of Hubel and Wiesel (1962; 1965) and Henry *et al.* (1977).

Visual stimulation and data analysis.

For quantitative analyses, a display monitor (Hewlett Packard, model 1321a with P31 phosphor) was placed 57 cm in front of the animal. To study spatio-temporal selectivity of the cells, drifting sinusoidal gratings were used. The gratings were produced by an image generator (Innisfree: Picasso image synthesizer model Rev. 8) and controlled by a computer which allowed for the manipulation of spatial frequency, temporal frequency, orientation/direction, size and contrast of the sinusoidal grating. The stimulation screen subtended 25 deg × 25 deg and had a mean luminance of 5 cd/m^2 (measured with a spotmeter). However, to test the end-stopping of RFs the size of the stimulus was varied systematically, and the size yielding the maximal response

from the cell was used for quantitative protocols. For the determination of a spatial frequency tuning function, the RFs were monocularly stimulated with sinusoidal gratings. The interval between the spatial frequencies (0.025 c/deg to 2.4 c/deg) presented was usually a half-octave. The gratings were presented 10 times and the spatial frequencies were presented pseudo-randomly. The cell's discharge rate was recorded under the best direction and temporal frequency (2, 4 or 6 Hz) as evaluated by ear. Contrast was kept constant at 50% and was defined as: $L_{max.}$-$L_{min.}/L_{max.}+L_{min.}$, where $L_{max.}$ is the maximum luminance and $L_{min.}$ is the minimum luminance of the spatial sinusoid. Between each presentation, the RF was continuously stimulated with the illuminated blank screen (blank stimulus) having the same mean luminance (5 cd/m^2) as the grating. Each presentation was preceded by a period of 500 ms during which the contrast was increased from zero to 50%, but the cell's response was not recorded. This was done to prevent evoking a transient response from the cell. After each presentation, an inter-stimulus interval of at least 18 s was also introduced to minimize adaptation effects. During the blank stimulus presentation, the discharge rate was recorded for the 1 s preceding each grating presentation. The response to the drifting gratings was also recorded for a period of 1 s. A Fourier analysis was used to assess the modulation of the response at the first harmonic of the drifting grating. Then the criteria of Skottun *et al.* (1991) were used to definitely classify the RF organization. As a rule, response amplitude was specified by the DC response for the complex and end-stopped complex RFs that showed an unmodulated pattern of discharge at spatial frequencies higher than the optimum. Each data point of their tuning function corresponds to the mean firing rate (in spikes/s) from which was subtracted the mean discharge rate recorded during the blank presentations. For cells (simple and end-stopped simple) that showed a modulated response at spatial frequencies higher than the optimum, each data point of the tuning

function was plotted according to the modulation amplitude of the response (Fourier fundamental response component) from which was subtracted the response during the blank presentations. The tuning curves were fitted by eye with a commercial curve fit software (Jendel Scientific: Table Curve). The optimal chosen curve fit had a strong correlation ($r \geq 0.9$) with the data points and was used to evaluated the optimal frequency and bandwidth. Ocular dominance (Hubel and Wiesel, 1962) was evaluated for each cell on a scale from 1 (contralateral eye only) to 7 (ipsilateral eye only).

To evaluate the contrast threshold, the best spatial frequency, as tested previously and drifting in the same direction at the same temporal frequency, was used. This was assessed using 10 presentations of a given contrast (0.5% to 50%) selected pseudo-randomly. The contrast threshold was then determined as being the contrast value which elicited a response in 70% of the trials. The stimulus presentation and recording were executed in the same manner as for the assessment of spatial frequency tuning.

Some cells were examined to determine their temporal frequency selectivity. Different temporal frequencies were presented pseudo-randomly at a constant 50% contrast level. For the assessment of temporal frequency selectivity, the drift frequency varied from 0.5 to 24 Hz, usually by steps of half an octave. Stimulus presentation and recording procedures were similar to those used for the assessment of spatial frequency tuning.

Finally, some cells were also tested to evaluate their direction selectivity. This was achieved by using the best spatial frequency and by testing a total of 24 directions each 15 deg apart. The contrast was always kept constant at 50% and the presentations were pseudo-random. The drift direction was orthogonal to grating orientation. The details of stimulus presentation and recording were the same as for determining the spatial frequency tuning. The data thereby obtained were displayed on a polar plot in

which the response strength (from which was subtracted the cell's baseline) is illustrated by the vector length. In such representations, 0 deg corresponds to a grating drifting from right to left in front of the animal and 90 deg to a grating drifting from top to bottom. To estimate the extent of direction selectivity, a direction selectivity index (DI), similar to the one proposed by Dreher (1993), was calculated by using the formula: $DI = 100 \times (R_p - R_{np}) / R_p$, where R_p and R_{np} correspond respectively to the mean discharge rate (from which was subtracted the baseline level) to preferred and non-preferred directions.

Histology.

To confirm that the penetrations were located in area 21b, small electrolytic lesions (5 μA, 10 s) were made at 500-800 μm intervals while the electrodes were retracted during the experiment. At the end of the recording session, the animal was deeply anaesthetized with halothane (5%) and perfused through the heart with isotonic saline followed by 4% formalin. The brain was extracted from the skull, frozen and sectioned in the frontal plane. Sections 40 μm thick were taken and stained using the Nissl method. Histological analyses confirm that all cells were recorded from area 21b.

Results

Receptive fields and ocular dominance.

The activity of 110 visual neurons in area 21b was isolated. The RFs of all cells were mapped with the use of dark or light bars or edges. Most cells did not respond to narrow bars but were rather activated by large stimuli such as large dark bars or edges. Only 73 visual cells showed relatively well delimited RFs for the dominant eye. Even in these cases, RFs boundaries were not as precise as for cells in other visual areas such as the striate cortex. Other visual cells (n = 37) had very diffuse RFs with no clear boundaries and exhibited "sluggish" responses to visual stimulation. Because the RFs of the latter cells were almost impossible to map, they were not included in the analysis of RF sizes. Many other cells encountered during the penetrations gave no response to visual stimulation (gratings, bars or edges) and were not considered in the analysis of the data. The spatial organization of the RFs did not present adjacent ON/OFF regions typical of simple cells. Moreover, reducing the stimulus length or width did not increase the response, showing no apparent end-stopping zones. The latter characteristics are similar to those of complex cells found in areas 17/18 or 19.

All RFs mapped in area 21b are presented in Figure 1 by points which correspond to the center of the RF of the dominant eye. Although most RFs centers (89%) are located in the upper contralateral quadrant, some are also found in the inferior contralateral quadrant (6%) or in the ipsilateral superior quadrant (5%). RFs are distributed in central visual field, although some extend up to 60 deg in the contralateral hemifield. These results confirm those of Tusa and Palmer (1980) who first described the visual field representation of area 21b.

---

insert figure 1 approx. here

The distribution of RFs sizes is shown in Figure 2A. RFs were relatively large (mean = 357 deg^2; σ = 288 deg^2; range = 25 deg^2 to 1110 deg^2). Some RFs touched or straddled the vertical meridian (n = 18) and some extended up to 10 deg in the ipsilateral hemifield. Some RFs (n = 17) extended up to 24 deg below the horizontal meridian. The average size of RFs located at different azimuthal eccentricities is shown in Figure 2B. The RFs located within 5 deg (including those which had their center in the ipsilateral field) or 10 deg of azimuthal eccentricity had significatively smaller surfaces than the other RF (Kruskall Wallis one-way ANOVA, $\chi^2 = 14.3$; $p < 0.01$). Among the RFs which were located at more than 10 deg of eccentricity, there were no significant differences in sizes relative to location.

For all the visual cells recorded, ocular dominance was evaluated using the Hubel and Wiesel (1962) scale. The ocular dominance distribution is shown in Figure 2C. Most cells (93%) were binocular and the distribution shows a preponderance of class 4 with a bias for the contralateral eye. A few cells responded only to the ipsilateral (2%) or contralateral (6%) eye.

---

insert figure 2 approx. here

Spatial frequency tuning.

For 77 cells, the spatial frequency tuning was established using a temporal frequency of either 2, 4 or 6 Hz and a high contrast (50%). Generally, the presentation of sinewave drifting gratings produced a good cellular response. Narrow light or dark bars seemed to be less efficient but cells often responded well to manually presented edges or large dark bars which covered large parts of the visual field. When stimulated with drifting gratings at optimal direction, the response of cells showed an overall DC increase (mean firing rate) but no modulation with the stimulus drift frequency (as revealed by Fourier analysis) at optimal spatial frequency. Spatial frequency tuning curves were either band-pass (n = 46) or low pass (n = 31) and are illustrated by representative examples in Figure 3A-D. The band-pass cells in Figure 3A-C had clear optimal spatial frequencies above and below which the discharge rate was attenuated. The other cell (see Fig. 4D) had low-pass properties with no attenuation of the response in the low spatial frequencies. This distinction should however not be understood in absolute terms because the response of low-pass units might have decreased at very low spatial frequencies (i.e. below 0.025 c/deg); however, these could not be generated by our display apparatus.

---

insert figure 3 approx. here

Visual resolution.

The visual resolution of a cell was defined as the high cut-off spatial frequency derived from the spatial frequency tuning function. This corresponds to the point of the tuning curve that intersects the baseline. As shown in Figure 3A-D, cells in area

21b usually had a low spatial resolution (cell A: 0.24 c/deg; cell B: 0.4 c/deg; cell C: 0.29 c/deg; cell D: 0.14 c/deg) and no cell responded to drifting gratings of spatial frequencies greater than 1 c/deg. The distribution of high cut-off spatial frequencies measured through the dominant eye of 77 cells is shown in Figure 3E. The maximum value was 0.9 c/deg and the minimum was 0.04 c/deg (mean = 0.29 c/deg, $\sigma = 0.22$ c/deg). The distribution tends to be fairly unimodal, indicating that a rather homogeneous population of cells was recorded. Only two cells responded to spatial frequencies above 0.8 c/deg.

---

insert figure 4 approx. here

Optimal spatial frequency and spatial bandwidth.

For the 46 cells that had band-pass tuning functions, the optimal spatial frequencies and bandwidths were estimated from the spatial frequency tuning function. Most of these had a relatively low optimal spatial frequency (≤ 0.12 c/deg). For example, the cells illustrated in Figure 3A and 3C responded optimally to drifting gratings of 0.06 c/deg and 0.08 c/deg, respectively. Some units (11%) were optimally tuned to somewhat higher spatial frequencies (≥ 0.12 c/deg), such as the unit in Figure 3B which had an optimal spatial frequency estimated at 0.12 c/deg.

Although some cells were narrowly tuned to spatial frequencies, as revealed by their spatial bandwidths, (Fig. 3A: 1.4 octaves; 3B: 1.1 octaves), others responded to a wider range of spatial frequencies. An example of the latter case is shown in Figure 3C, where the cell has a spatial bandwidth of 2.1 octaves. The distribution of optimal

spatial frequencies and bandwidths established for the dominant eye are presented in Figures 3F and 3G respectively. Optimal spatial frequencies are low (mean = 0.08 c/deg; σ = 0.03 c/deg) and range from 0.03 c/deg to 0.14 c/deg while the spatial bandwidths were usually about 2 octaves (mean = 2.2 octaves; σ = 0.9 octaves) and ranged from 0.6 octaves to 4.4 octaves. This shows that cells in area 21b preferred low drifting spatial frequencies and had a generally broad tuning, although some (9%) had a very fine spatial frequency tuning (spatial bandwidths $\leq$ 1 octave).

---

insert figure 5 approx. here

Response vs contrast functions.

For 36 cells, we assessed the response to drifting gratings at different contrast levels. For this purpose, the optimal spatial and temporal frequencies were used, as well as optimal drift directions. In all cells recorded, the discharge rate increased when the contrast was elevated. Examples of response vs contrast functions are illustrated for three cells in Figure 4A. Cell 1 responded only to high contrasts and had a threshold estimated at 16%. This unit gave only a weak response when the contrast was set at 10% but the discharge rate increased drastically when higher contrasts ($\geq$ 20%) were tested. Cell 2 began to respond at intermediate contrast level and its threshold was estimated at 8% while cell 3 responded to very low contrast an had a threshold estimated at 2.5%. These two latter cells gradually increased their discharge rates with contrast level, although cell 2 responded more strongly. As can also be seen in these three representative units, although contrast thresholds differ from cell to cell,

the response of cells in area 21b tends to saturate when contrast levels reached 30%. The distribution of contrast thresholds is shown in Figure 4B. Thresholds range from 1% to 46% (mean = 15.5%, σ = 11.8%). The distribution illustrates that some cells were very sensitive to contrast but that many others (64%) only responded to contrasts higher than 8%.

---

insert figure 6 approx. here

Temporal frequency tuning functions.

The optimal spatial frequency and direction were used to evaluate the temporal frequency tuning of 57 neurons. A contrast of 50% was also used to maximize the cell's response. Most cells (n = 50) showed band-pass temporal frequency tuning functions, such as those illustrated in Figure 5A-B-D. These cells are characterized by a clear optimal temporal frequency and an important attenuation in the lower and higher temporal frequencies. A few cells (n = 7) showed no attenuation in the lowest temporal frequencies tested (0.5 Hz or 1 Hz) and were thus labeled as temporal low-pass units. An example of such a temporal low-pass function is shown in Figure 5C.

Only temporal band-pass units were considered to have an optimal temporal frequency and a temporal bandwidth. Figure 5A shows the temporal frequency tuning curve of a cell which had an optimal temporal frequency estimated at 4.7 Hz and was finely tuned to temporal frequencies, as estimated by its temporal bandwidth estimated at 1.5 octaves. The temporal frequency tuning shown in Figure 5B reveals that this unit had an optimal temporal frequency estimated at 1.4 Hz and was much more broadly tuned (temporal bandwidth = 4.1 octaves). The tuning function of the cell in Figure 5D was also very broad (temporal bandwidth = 5 octaves) and its optimal

temporal frequency was 2.2 Hz. This cell responded relatively well at temporal frequencies between 0.5 and 8 Hz but its discharge rate dropped dramatically at a temporal frequency of 16 Hz.

The distributions of the estimated optimal temporal frequencies and temporal bandwidths are shown in Figures 5E and 5F. Optimal temporal frequencies ranged from 0.7 Hz to 9.5 Hz (mean = 3.2 Hz, σ = 2.3 Hz) and temporal bandwidths ranged from 1.2 to 5.1 octaves (mean = 3.3 octaves, σ = 1 octave). Optimal temporal frequencies were widely distributed from low to high frequencies and although some cells preferred high temporal frequencies, most of them (74%) responded optimally to temporal frequencies lower than 4 Hz. On the other hand, given the fact that some cells responded better to low spatial frequencies and that these spatial frequencies were used to assess their temporal selectivity, it follows that they responded to rather high velocities. Although some cells (12%) had temporal bandwidths lower than 2 octaves, most temporal tuning functions were rather broad and covered more than 3 octaves.

Orientation and direction selectivity.

The preferred orientation or direction was determined for the dominant eye in 74 of the 110 cells recorded. The distribution of preferred orientations of these cells did not show any sign of anisotropy. More precise evaluations of orientation/direction tuning was assessed quantitatively for 30 of these cells. This was done using the optimal spatial and temporal frequencies as well as a high contrast (50%) to maximize the cell's response. The directional tunings thereby obtained showed that many cells responded better when the grating drifted in a particular direction and gave almost no response to stimulation in the opposite direction, although stimulus orientation remained unchanged. Representative examples of such direction-selective units are

illustrated by polar plots in Figure 6A-B. In these illustrations, the vector length corresponds to the mean firing rate from which was subtracted the cell's baseline. The cell in Figure 6A responded optimally to directions between 270 deg and 300 deg with an optimal direction of 285 deg. However, when the stimulus direction differed from the optimal by 30 deg, the response was greatly reduced and was almost null for opposite directions. The cell in Figure 6B responded better when the stimulus direction was 300 deg but also responded to a wider range of directions. A few other cells (10%) responded better when the stimulus had a particular orientation, but gave a similar response even for opposite drift directions. These cells were therefore considered as orientation-selective. An example of such a cell is illustrated in Figure 6C. This cell responded optimally to a grating drifting between 30 deg and 75 deg but responded almost equally well when the same grating drifted in the opposite directions (between 210 deg and 240 deg). On the other hand, this cell did not respond strongly when the grating orientation was orthogonal to these preferred orientations. Finally, other cells (20%) responded to several directions and showed an attenuation of their response to other directions. An example of such a unit is illustrated in Figure 6D. The polar plot of these cells shows that the directions eliciting strong responses tend to be quasi orthogonal to each other. Given the fact that the latter cells show an untypical pattern of response with no single tuning function from which can be derived the half-widths, they were not included in these analyses.

In order to estimate the extent of direction selectivity, a direction selectivity index (DI) was calculated. Results are shown in Figure 6E for 24 cells. It is clear that many cells are selective to a given direction (as illustrated in Figure 6A and 6B) and that their responses are greatly attenuated for the opposite direction, although grating orientation remains unchanged. Indeed, 70% of the cells showed a DI above 80% which means that these cells are clearly selective to grating direction. It is also

important to note that few cells showed a low DI (≤ 40%), which indicates that these cells are clearly orientation selective regardless of the grating direction. The remaining cells showed intermediate DI values, meaning that they responded better to a given direction although their response was mildly attenuated when the stimulus drifted in the opposite direction.

In order to estimated the sharpness of direction tunings, the half-width of the tuning curve at half-height of the maximal response was estimated. The direction half-widths ranged from 9.5 deg to 48 deg (mean = 32 deg; σ = 12 deg) The distribution of direction half-widths is shown in Figure 6F for 24 cells. Many cells (67%) were broadly tuned (half-width ≥ 31 deg) to direction while a few units present a fine tuning (half-width ≤ 20 deg; 17% of the cells). The remaining cells (16%) were moderately tuned (half-width ≥ 21 deg and ≤ 30 deg).

Discussion

The aim of this study was to describe the RF properties of cells in area 21b of the cat in order, first, to clarify its internal functional organization and, second, to attempt to deduce its possible implication in the processing of visual information. The spatial and temporal properties, contrast sensitivity and direction selectivity of single neurons were thus evaluated, given that the electrophysiological studies that originally described area 21b (Tusa *et al.*, 1980) were limited to its retinotopic representation. The discussion will therefore compare the present results with those observed in other visual areas, including areas 17, 18, 19, PMLS and, especially, adjoining 21a with the specific objective of functionally differentiating area 21b from this area. Based on this analysis of the RFs, an attempt will be made to examine the possible implications of area 21b in visual processing.

Comparison with other visual areas.

It is important to note that cells in area 21b were often difficult to drive with visual stimuli (dark or light bars) that are generally very effective in other visual areas such as 17, 18 and 19. Moreover, many RFs were difficult to map and did not present clear boundaries. Nonetheless, a number of cells responding relatively well to large stimuli such as edges and to low spatial frequencies were found. The RFs encountered in area 21b were very large compared to those in areas 17 (Hubel and Wiesel, 1962), 18 (Hubel and Wiesel, 1965), 19 (Hubel and Wiesel, 1965; Albus and Beckmann, 1980) and 21a (Wimborne and Henry, 1992; Dreher *et al.*, 1993) but were comparable to those found in PMLS and particularly PLLS areas (Rauschecker *et al.*, 1987; von Grünau *et al.*, 1987). Such units showing large RFs with imprecise limits have also been described in subcortical LPl (Chalupa and Abramson, 1988; Casanova *et al.*,

1989), which receives input from the striate cortex and sends numerous projections to extrastriate areas, including areas 21a and 21b (Symonds *et al.*, 1981; Raczkowski and Rosenquist, 1983; Updyke, 1983; Dreher, 1986). Based solely on RF sizes, the input from LPl seems to be strongly reflected in the properties of cells area 21b and less in area 21a.

The majority of cells in area 21b were selective to stimulus direction. Such direction-selective units are also common in both areas 17 and 18 but less in area 19 (Orban 1984). However, the direction half-widths are broader for cells in area 21b than for those of area 17, although there are some discrepancies across the studies investigating the latter area (Henry *et al.*, 1974; Rose and Blakemore, 1974; Hammond and Andrews, 1978). The RF properties of cells in area 21b are in fact more comparable in this regard to those of cells in PMLS and PLLS areas which also exhibit strong direction selectivity with broad direction half-widths (Blakemore and Zumbroïch, 1987). Moreover, cells in LPl also show direction selectivities which resemble those of areas PMLS and 21b. Comparing 21b to 21a, a number of differences stand out. First, Dreher *et al.* (1993) found that cells in area 21a are significantly less selective to direction than cells in areas 17 and 18 but are rather orientation-selective. Also, Wimborne and Henry (1992) noted that cells in area 21a were not often selective to stimulus direction and found no cell in which the response was totally suppressed in the non-preferred direction, a characteristic often encountered in area 21b.

Visual cells recorded in area 21b responded well to drifting spatial frequencies and clearly preferred low spatial frequencies. The spatial frequency tuning curves of cells in area 21b revealed both band-pass and low-pass properties. These two profiles of spatial frequency tuning curves were also found in cells of areas 17 (Ikeda and Wright, 1975), 18 (Movshon *et al.*, 1978), 19 (Tardif *et al.*, 1997), 21a (Tardif *et al.*,

1996) and PMLS (Zumbroïch and Blakemore, 1987). By comparing the optimal spatial frequencies of band-pass cells among different visual areas, it can be observed that they are similar in many extrastriate areas (18, 19, 21a and PMLS) but that they differ from those found in area 17. Indeed, the mean values of optimal spatial frequencies in these extrastriate areas are: area 18: 0.22 c/deg (Movshon *et al.*, 1978), area 19: from 0.17 c/deg (Tardif *et al.*, 1997) to about 0.4 c/deg (Tanaka *et al.*, 1987), area 21a: 0.36 c/deg (Tardif *et al.*, 1996), PMLS area: 0.16 c/deg., (Zumbroïch and Blakemore, 1987). All these values are considerably lower than those of cells in area 17 (mean optimal spatial frequencies = 0.86 c/deg and 0.93 c/deg for simple and complex cells respectively (Movshon *et al.*, 1978)). This is possibly due to a strong X signal from the geniculate nucleus to area 17 which carries high spatial frequency information. One of the most relevant point of the present study is that optimal spatial frequencies (mean = 0.08 c/deg) and visual resolution (mean = 0.29 c/deg) of cells in area 21b are considerably lower than those obtained in all visual areas mentioned above. The spatial bandwidths of cells in area 21b (mean = 2.2 octaves) are nonetheless similar to those of cells in area 19 in which the mean spatial bandwidth of cells varied from 1.9 octaves (Tanaka *et al.*, 1987) to 2.13 octaves (Tardif *et al.*, 1997) and to those in the PMLS area (mean spatial bandwidth = 2.2 octaves, Zumbroïch and Blakemore, 1987). On the other hand, spatial bandwidths of cells in areas 19, 21b and PMLS area seem to be slightly broader than those of cells in area 17, 18 and 21a, where the mean spatial bandwidths is estimated at 1.5 octaves, 1.49 octaves and 1.6 octaves respectively (areas 17 and 18: Movshon *et al.*, 1978; area 21a: Tardif *et al.*, 1996). These comparisons of spatial bandwidths suggest that the fine spatial frequency selectivity encountered in area 17 is only reflected in some extrastriate areas which possibly receive more direct afferences from this area.

The response vs contrast curves of cells in area 21b had shapes similar to those observed for cells in area 17 (Maffei and Fiorentini, 1973; Dean, 1981; Tolhurst *et al.*, 1981; Albrecht and Hamilton, 1982), 18 (Chino *et al.*, 1988), 19 (Tardif *et al.*, 1997), 21a (Tardif *et al.*, 1996) and PMLS (Zumbroïch and Blakemore, 1987). Although there are some variations in the shape of response vs contrast curves among cortical cells, the discharge rate of most cells in all visual areas increases as a function of contrast and tends to saturate at high contrast. Nonetheless, it appears that the contrast thresholds of cells in area 21b are similar to those of area 21a (Tardif *et al.*, 1996) but are generally much higher than those of cells in areas 17 (Dean, 1981; Tolhurst *et al.*, 1981), 18 (Chino *et al.*, 1988) and 19 (Tardif *et al.*, 1997). However, it should be remembered that the contrast thresholds are higher when low mean luminance is used (Hess and Lillywhite, 1980). Since we used a low mean luminance (5 cd/m^2) compared to Dean (1981), Tolhurst *et al.* (1981) and Chino *et al.* (1988) who used a mean luminance of 300 cd/m^2, 150 cd/m^2 and 27 cd/m^2, respectively, this may in part explain the higher contrast thresholds in area 21b. On the other hand, contrast thresholds of cells in area 19 estimated by using the same mean luminance have nonetheless shown much lower threshold values (mean contrast threshold = 5%; Tardif *et al.*, 1997).

The temporal frequency tuning functions of cells in area 21b are mainly band-pass and only a few cells showed a temporal low-pass function. This suggest that cells in this area are selective to the dynamic aspects of a stimulus. The mean optimal temporal frequency of cells in area 21b (3.2 Hz) is not very different from that of cells in areas 17 and 18 (17: 2.9 Hz, 18: 3.2 Hz; Saul and Humphrey, 1992). This value is also comparable to that obtained in area 19 (around 3 Hz; Tanaka, 1987) but lower than those obtained in areas PMLS (around 5 Hz; Morrone *et al.*, 1986) and 21a (7 Hz; Tardif *et al.*, 1996) areas. However, since some of these areas may differ with respect

to their optimal spatial frequencies, it follows that they may prefer different velocities despite their similar optimal temporal frequencies. For example, cells in area 21a have higher optimal temporal frequencies than cells in area 21b (by a factor of two) but they also differ in their optimal spatial frequencies: cells in area 21a are optimally tuned to higher spatial frequencies. If optimal velocities are estimated from the ratio of mean optimal spatial frequency and mean optimal temporal frequency observed in both areas, cells in area 21b prefer velocities near 40 deg/s whereas those in area 21a prefer velocities near 19 deg/s. This means that area 21b cells, despite being tuned to lower temporal frequencies, actually prefer velocities one octave higher than those in area 21a.

Areas 21a and 21b: are they functionally distinct areas?

One of the corollary aim of this study was to determine if areas 21a and 21b contain cells with similar RF properties or if they can be differentiated on the basis of these properties. A comparison between the results obtained in the present study with those of other studies in area 21a (Mizobe *et al.* 1988; Wimborne *et al.*; 1992; Dreher *et al.*, 1992; Michalski *et al.*, 1994; Tardif *et al.*, 1996; Wang and Dreher, 1996) clearly shows that these two areas can be clearly differentiated. Cells in area 21a have smaller RFs, respond to higher spatial frequencies and are orientation-selective while cells in areas 21b have larger RFs, respond to lower spatial frequencies and are direction-selective. Considering these differences, it can be suggested that these two visual areas process different kinds of visual information. Indeed, cells in area 21a are likely to be involved in spatial analysis since many of them are finely tuned to spatial frequencies (Tardif *et al.*, 1996) and to orientation (Wimborne and Henry, 1992; Dreher *et al.*, 1993). As such properties are also found in area 17, it is also possible that cells in area 21a process similar information. In this sense, it can be advanced that

the X signal, mostly confined to area 17 and carrying high spatial frequency information, is transmitted to area 21a. This would not be the case for area 21b. Indeed, the high spatial resolution and fine orientation selectivity of cells in area 17 is not observed in area 21b cells. Rather, the low spatial frequency and high velocity preference of cells in area 21b suggest that they possibly receive a strong Y signal from areas 17 and/or 18, either directly or via the LPl region of the thalamus.

Although areas 21a and 21b contain cells with different RF properties which suggest that they may process different attributes of the visual scene such as form and motion, these functions may not be mutually exclusive. Indeed, our results clearly show that most cells in area 21b have RFs which are centrally located and are also well tuned to low spatial frequencies. They are thus capable of a certain degree of spatial analysis. On the other hand, cells in area 21a are also tuned to temporal frequencies (Tardif *et al.*, 1996) or to the velocity of a moving bar (Dreher *et al.*, 1993) which suggests that they are capable of motion processing.

Acknowledgments

This study was supported by grants from the Natural Science and Engineering Research Council of Canada (NSERC) and the Fonds pour la Formation de Chercheurs et l'Aide à la Recherche (FCAR) awarded to Jean-Paul Guillemot and Franco Lepore. The authors are grateful to Eric Massicotte and Stéphane Montfort for technical assistance.

References

Albrecht DG., Hamilton DB (1982) Striate cortex of monkey and cat: contrast response functions. J. Neurophysiol 48: 217-237.

Albus K, Beckmann R (1980) Second and third visual areas of the cat: interindividual variability in retinotopic arrangement and cortical location. J Physiol (Lond) 299: 247-276.

Barlow HB, Blakemore C, Pettigrew JD (1967) The neural mechanism of depth discrimination. J Physiol (Lond) 193: 327-342.

Berkley MA, Sprague JM (1979) Striate cortex and visual acuity functions in the cat. J Comp Neurol 187: 679-702.

Berardi N, Bisti S, Cattaneo A, Fiorentini A, Maffei, L (1982) Correlation between the preferred orientation and spatial frequency of neurones in visual area 17 and 18 of the cat. J Physiol (Lond) 323: 603-618.

Bishop PO, Kozak W, Vakkur GJ (1962) Some quantitative aspects of the cat's eye: axis and plane of reference of visual field coordinates and optics. J Physiol (Lond) 163: 466-502.

Blakemore C, Zumbroïch TJ (1987) Stimulus selectivity and functional organization in the lateral suprasylvian visual cortex of the cat. J Physiol (Lond) 389: 569-603.

Casanova C, Freeman RD, Normann JP (1989) Monocular and binocular response properties of cells in the striate-recipient zone of the cat's lateral posterior-pulvinar. J Neurophysiol 62: 544-557.

Camarda RM, Rizzolatti G (1976) Visual receptive fields in the lateral suprasylvian area (Clare-Bishop area) of the cat. Brain Res 101: 427-443.

Chalupa LM, Abramson BP (1988) Receptive-field properties in the tecto- and striate-recipient zones of the cat's lateral posterior nucleus. In Progress in Brain Research (Hicks TP, Benedek G, eds), pp. 85-94. Amsterdam: Elsevier Science Publishers.

Chino YM, Ridder WH III, Czora EP (1988) Effects of convergent strabismus on spatio-temporal response properties of neurons in cat area 18. Exp Brain Res 72: 264-278.

Clare MH, Bishop GH (1954) Response from an association area secondarily activated from optic cortex. J Neurophysiol 17: 271-277.

Dean AF (1981) The relationship between response amplitude and contrast for cat striate cortical neurones. J Physiol (Lond) 318: 413-427.

Di Stefano M, Morrone MC, Burr DC (1985) Visual acuity of neurones in the cat lateral suprasylvian cortex. Brain Res 331: 382-385.

Doty RW (1971) Survival of pattern vision after removal of striate cortex in the adult cat. J Comp Neurol 143: 341-370.

Dreher B (1986) Thalamocortical and corticocortical interconnections in the cat visual system: relation to the mechanisms of information processing. In Visual Neuroscience (Pettigrew JD, Sanderson KJ , Levick WR, eds), pp. 290-314. Cambridge: Cambridge University Press.

Dreher B, Michalski A, Ho RHT, Lee CWF, Burke W (1993) Processing of form and motion in area 21a of the cat visual cortex. Vis Neurosci 10: 93-115.

Dreher B, Wang C, Turlejski KJ, Djavadian RL, Burke W (1996) Areas PMLS and 21a of the cat visual cortex: two functionnally distinct areas. Cereb Cortex 6: 585-599.

Fernald R, Chase R. (1971) An improved method for plotting retinal landmarks and focusing the eyes. Vision Res, 11: 95-96.

Ferster D (1981) A comparaison of binocular depth mechanisms in areas 17 and 18 of the cat visual cortex. J Physiol (Lond) 311: 623-655.

Gizzi MS, Katz E, Schumer RA, Movshon JA, (1990) Selectivity for orientation and direction of motion of single neurons in the cat striate and extrastriate visual cortex. J Neurophysiol 63: 1529-1543.

Hammond P, Andrews DP (1978) Orientation tuning of cells in areas 17 and 18 of the cat's visual cortex. Exp Brain Res 31: 341-351.

Henry G, Dreher B, Bishop PO (1974) Orientation specificity of cells in cat striate cortex. J Neurophysiol 37: 1394-1409.

Henry GH (1977) Receptive field classes of cells in the striate cortex of the cat. Brain Res 133: 1-28.

Hess RF, Lillywhite P. (1980) Effect of luminance on contrast coding in cat visual cortex. J Physiol (Lond), 300: 56-57.

Hubel DH, Wiesel TN (1962) Receptive fields, binocular interaction, and functional architecture in the cat's visual cortex. J Physiol (Lond) 160: 106-154.

Hubel DH, Wiesel TN (1965) Receptive fields and functionnal architecture in two nonstriate visual areas (18 and 19) of the cat. J Neurophysiol 28: 229-289.

Hubel DH, Wiesel TN (1969) Visual area of the lateral suprasylvian gyrus (Clare-Bishop area) of the cat. J Physiol (Lond) 202: 251-260.

Ikeda H, Wright MJ, (1975) Spatial and temporal properties of "sustained" and "transient" neurones in area 17 of the cat's visual cortex. J Physiol (Lond) 22: 363-383.

Kim JN, Mulligan K, Sherk H (1997) Stimulated optic flow and extrastriate cortex. 1. Optic flow versus texture. J Neurophysiol 77: 554-561.

LeVay S, Voigt T. (1988) Ocular dominance and disparity coding in cat visual cortex. Visual Neurosci 1: 395-414.

Lepore F, Samson A, Paradis M-C, Ptito M, Guillemot J-P (1992) Binocular interaction and disparity coding at the 17-18 border: contribution of the corpus callosum. Exp Brain Res 90: 129-140.

Lomber SG, Payne BR, Cornwell P, Long KD (1996) Perceptual and cognitive visual functions of parietal and temporal cortice in the cat. Cereb Cortex 6: 673-695.

Maffei L, Fiorentini A (1973) The visual cortex as a spatial frequency analyser. Vision Res 13: 1255-1267.

Markuszka J (1978) Visual properties of neurons in the posterior suprasylvian gyrus of the cat. Exp Neurol, 59: 146-161.

Michalski A, Wimborne BM, Henry GH (1994) The role of ipsilateral and contralateral inputs from primary visual cortex on the responses of area 21a neurons. J Physiol (Lond) 466: 133-156.

Mizobe K, Itoi M, Kaihara T, Toyama K (1988) Neuronal responsiveness in area 21a of the cat. Brain Res 438: 307-310.

Morrone MC, Di Stefano M, Burr DC (1986) Spatial and temporal properties of neurons of the lateral suprasylvian cortex of the cat. J Neurophysiol 56: 969-986.

Movshon JA, Tompson ID, Tolhurst DJ (1978) Spatial and temporal contrast sensitivies in areas 17 and 18 in the cat's visual cortex. J Physiol (Lond) 283: 101-120.

Mulligan K, Kim JN, Sherk H. (1997) Stimulated optic flow and extrastriate cortex. 2. Response to bar versus large-field stimuli. J Neurophysiol 77: 562-570.

Orban GA (1984) Neuronal operations in the visual cortex. In: Studies of Brain Function (Barlow HB, Bullock TH, Florey E, Grüsser O-J, Peters A, eds), vol 11. Berlin Heidelberg: Springer-Verlag.

Palmer LA, Rosenquist, AC, Tusa RJ (1978) The retinotopic organization of lateral suprasylvian visual areas in the cat. J Comp Neurol 177: 237-256.

Payne BR, Lomber SG, Geeraerts S, Vandergucht E, Vandenbussche E (1996) Reversible visual hemineglect. Proc Natl Acad Sci USA 93: 290-294.

Raczkowski D, Rosenquist AC (1983) Connections of the multiple visual cortical areas with the lateral posterior-pulvinar complex and adjacent thalamic nuclei in the cat. J Neurosci 3: 1912-1942.

Rauschecker JP, von Grünau MW, Poulin C (1987) Centrifugal organization of direction preferences in the cat's lateral suprasylvian visual cortex and its relation to flow field processing. J Neurosci 7: 943-958.

Rose D, Blakemore C (1974) An analysis of orientation selectivity in the cat's visual cortex. Exp Brain Res 20: 1-17.

Sanderson KJ, Sherman SM (1971) Nasotemporal overlap in visual field projected to lateral geniculate nucleus in the cat. J Neurophysiol 34: 453-466.

Saul AB, Humphrey LA (1992) Temporal-frequency tuning of direction selectivity in cat visual cortex. Visual Neurosci 8: 365-372.

Segraves M, Rosenquist AC (1982) The distribution of the cells of origin of callosal projections in cat visual cortex. J Neurosci 2: 1079-1089.

Sherk H, Kim JN, Mulligan K (1995) Are the prefered directions of neurons in cat extrastriate cortex related to optic flow? Visual Neurosci 12: 887-894.

Skottun BC, De Valois RL, Grosoe DH, Movshon JA, Albrecht DG, Bonds AB (1991) Classifying simple and complex cells on the basis of response modulation. Vision Res 31: 1079-1086.

Spear PD, Baumann TP (1975) Receptive-field characteristics of single neurons in lateral suprasylvian area of the cat. J Neurophysiol 38: 1403-1420.

Sprague JM, de Weerd P, Xiao, DK, Vandenbussche E, Orban GA (1996) Orientation discrimination in the cat - its cortical locus. 2. Extrastriate cortical areas. J Comp Neurol 364: 32-50.

Sprague JM, Levy J, Di Berardino A, Berlucchi G (1977) Visual cortical areas mediating form discrimination in the cat. J Comp Neurol 172: 441-488.

Stone J (1966) The naso-temporal division of the cat's retina. J Comp Neurol 126: 585-599.

Symonds LL, Rosenquist AC, Edwards SB, Palmer LA (1981) Projections of the pulvinar-lateral complex to visual cortical areas in the cat. Neurosci 6:1995-2020.

Symonds LL, Rosenquist AC (1984a) Corticocortical connections among visual areas in the cat. J Comp Neurol 229: 1-38.

Symonds LL, Rosenquist AC (1984b) Laminar origins of visual corticocortical connections in the cat. J Comp Neurol 229: 39-47.

Tanaka K, Ohzawa I, Ramoa AS, Freeman RD (1987) Receptive field properties of cells in area 19 of the cat. Exp Brain Res 65: 549-558

Tardif E, Bergeron A, Lepore F, Guillemot J-P (1996) Spatial and temporal frequency tuning and contrast sensitivity of single neurons in area 21a of the cat. Brain Res 716: 219-223.

Tardif E, Richer L, Bergeron A, Lepore F, Guillemot J-P (1997) Spatial resolution and contrast sensitivity of single neurons in area 19 of split-chiasm cats: a comparaison with primary visual cortex. Eur J Neurosci 9: 1929-1939.

Tolhurst DJ, Movshon JA, Thompson ID (1981) The dependance of response amplitude and variance of cat visual cortical neurones on stimulus contrast. Exp Brain Res 41: 414-419.

Tremblay F, Ptito M, Lepore F, Guillemot J-P (1987) The distribution of visual callosal projections in the Siamese cat: an HRP study. J Hirnfors 28: 491-503.

Turlejski K, (1975) Visual responses of neurons in the Clare-Bishop area of the cat. Act Neurobiol Exp 35: 189-208.

Tusa RJ, Palmer LA (1980) Retinotopic organization of areas 20 and 21 in the cat. J Comp Neurol 193: 147-164.

Updyke BV (1983) A reevaluation of the functional organization and cytoarchitecture of the feline lateral posterior complex, with observations on adjoining cell groups. J Comp Neurol 219: 143-181.

Vandenbussche E, Sprague JM, de Weerd P, Orban GA (1991) Orientation discrimination in the cat: its cortical locus. 1. Areas 17 and 18. J Comp Neurol 305: 632-658.

von Grünau MW, Frost BJ (1983) Double-opponent process mechanism underlying RF-structure of directionnally specific cells of the cat lateral suprasylvian area Exp Brain Res 49: 84-92.

von Grünau MW, Zumbroïch TJ, Poulin C (1987) Visual receptive field properties in the posterior suprasylvian cortex of the cat: a comparaison between the areas PMLS and PLLS. Vision Res 27: 343-356.

Wang C, Dreher B (1996) Binocular interactions and disparity coding in area 21a of cat extrastriate visual cortex. Exp Brain Res 108: 257-272.

Wimborne BM, Henry GH (1992) Response characteristics of the cells of cortical area 21a of the cat with special reference to orientation specificity. J Physiol (Lond) 449: 457-478.

Wright MJ (1969) Visual receptive fields of cells in a cortical area remote from the striate cortex in the cat. Nature 223: 973-975.

Zumbroïch TJ, Blakemore C (1987) Spatial and temporal selectivity in the suprasylvian visual cortex of the cat. J Neurosci 7: 482-500.

Figure legends

Fig. 1. Spatial distribution of receptive fields mapped in area 21b. Each point corresponds to the center of the receptive field of the dominant eye. Most receptive fields were located in the upper quadrant of the contralateral visual field but a few were nonetheless found in the lower contralateral visual field.

Fig. 2. Distribution of receptive field sizes (**A**) of area 21b cells. Distribution of receptive field sizes with respect to the eccentricity of their center (**B**). Receptive fields located within 5 deg and between 5 and 10 deg were significantly smaller. Ocular dominance distribution (**C**) of area 21b cells. Category 1 and 7 include monocular cells driven only through the contralateral and ipsilateral eye respectively. The intermediate categories include binocular cells and category 4 includes cells which responded equally well to stimulation of either of the eyes. Most cells were binocular, and a bias for the contralateral eye could be observed.

Fig. 3. Examples of typical spatial frequency tuning functions (**A-D**) established for the dominant eye. The stimulus was a high contrast (50%) sinewave grating drifting in the optimal direction. Each point corresponds to the mean firing rate (from which was substracted the cell's baseline) for a particular spatial frequency. Cells in **A** and **C** are band-pass while cell in **D** is low-pass. Distribution of high cut-off spatial frequencies (**E**), which are indicators of the spatial resolution of the cells, as assessed through the dominant eye. Only a few cells responded to spatial frequencies above 0.8 c/deg and no cells showed high spatial resolution ($\geq$ 1.6 c/deg.). Distribution of optimal spatial frequencies (**F**) estimated from the spatial frequency tuning functions. Almost all cells responded optimally to relatively low spatial frequencies. Distribution of spatial

bandwidths (full width at half-height), which are indicators of the range of spatial frequencies to which the neurons were selective (**G**). The distribution is approximately normal and is centered between 2 and 3 octaves.

Fig. 4. Examples of response vs contrast functions established for 3 cells (**A**). The stimulus was a sinewave grating of optimal spatial and temporal frequency drifting in the optimal direction. Arrows indicate the contrast threshold, which was defined as the contrast level eliciting a response in 70% of the presentations. Distribution of contrast thresholds (**B**). Some cells were very sensitive to contrast although others only responded to intermediate or even high contrasts.

Fig. 5. Examples of temporal frequency tuning functions assessed through the dominant eye (**A-D**). The stimulus was a high-contrast sinewave grating of optimal spatial frequency drifting in optimal direction. Cells in **A**, **B** and **D** had a temporal band-pass function while unit shown in **C** presented a temporal low-pass function. Distribution of optimal temporal frequencies (**E**) of band-pass cells estimated from the temporal frequency tuning functions. Distribution of temporal bandwidths (full width at half-height) estimated from the temporal frequency tuning functions of temporal band-pass cells (**F**). Most cells showed a relatively broad temporal tuning but a few cells were finely tuned to temporal frequencies.

Fig. 6. Polar plots of the orientation/direction selectivity of four cells (**A-D**), as assessed with sinewave gratings drifting in 24 different directions. The direction-selective cell illustrated in **A** was finely tuned (half-width = 20 deg) while the orientation-selective cell in **C** showed a much broader tuning (half-width = 48 deg). The direction-selective cell in **B** showed a half-width typical of area 21b cells (30.5 deg). Cell in **D** responded to multiple directions. Scale bars = 10 imp./s. Direction selectivity index (**E**) showing that most cells were strongly selective to stimulus direction. The half-width at half-height of direction tunings (**F**). This measure is used to estimate the

sharpness of direction selectivity. Most cells showed a relatively broad direction tuning and a few were finely tuned.

FIGURE 1

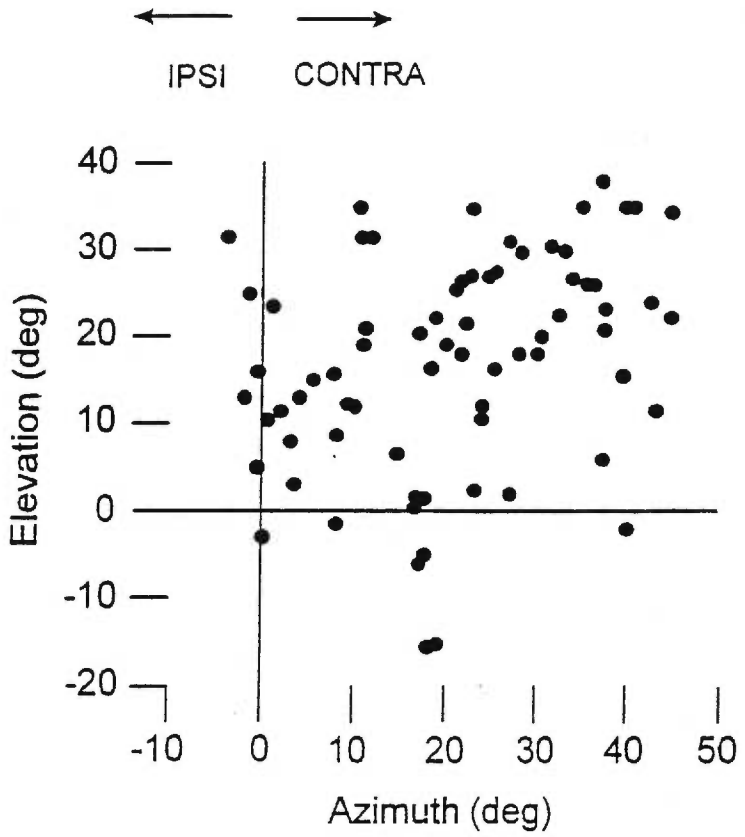
IPSI
CONTRA
40
30
20
10
0
-10
-20
Elevation (deg)
-10
0
10
20
30
40
50
Azimuth (deg)

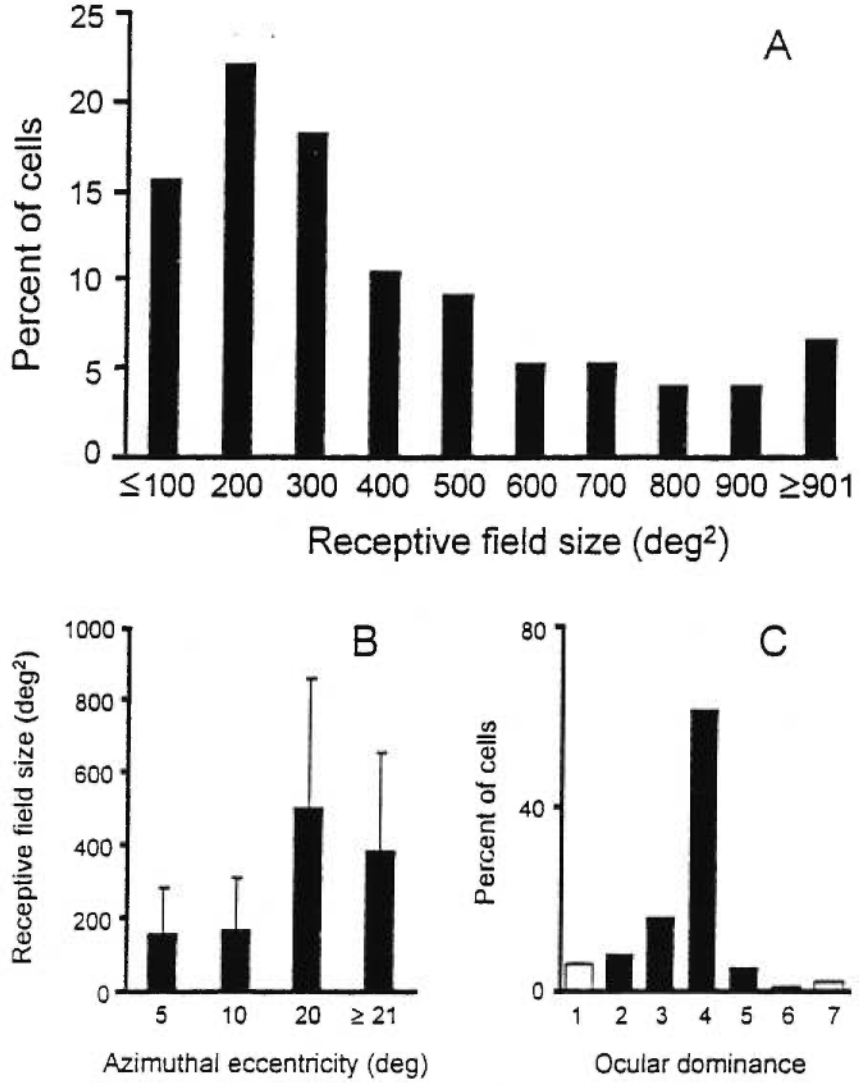
A
Percent of cells
25
20
15
10
5
0
≤100 200 300 400 500 600 700 800 900 ≥901
Receptive field size (deg²)
B
Receptive field size (deg²)
1000
800
600
400
200
0
5 10 20 ≥ 21
Azimuthal eccentricity (deg)
C
Percent of cells
80
40
0
1 2 3 4 5 6 7
Ocular dominance

FIGURE 3

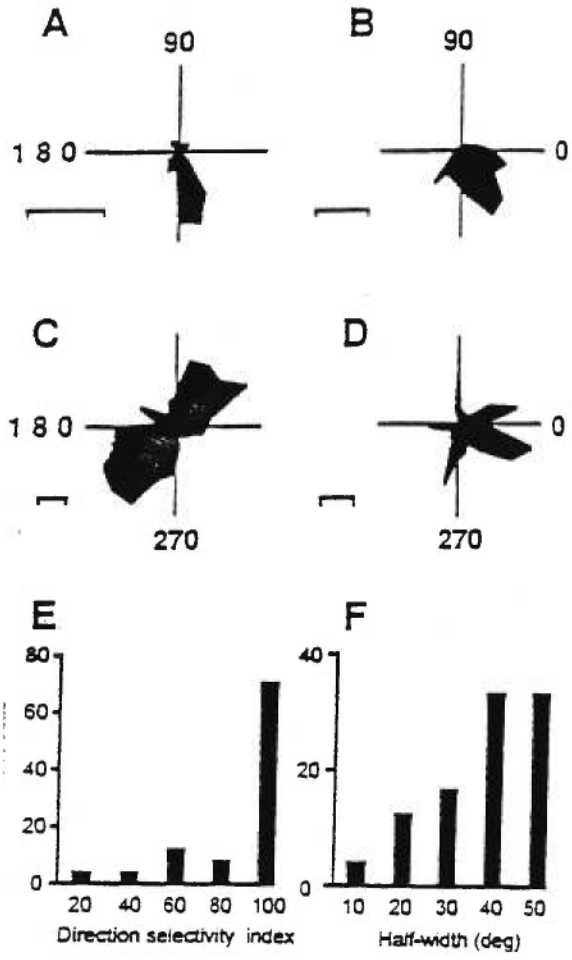
A
90
180
B
90
0
C
180
270
D
0
270
E
80
60
40
20
0
20 40 60 80 100
Direction selectivity index
F
40
20
0
10 20 30 40 50
Half-width (deg)

FIGURE 4

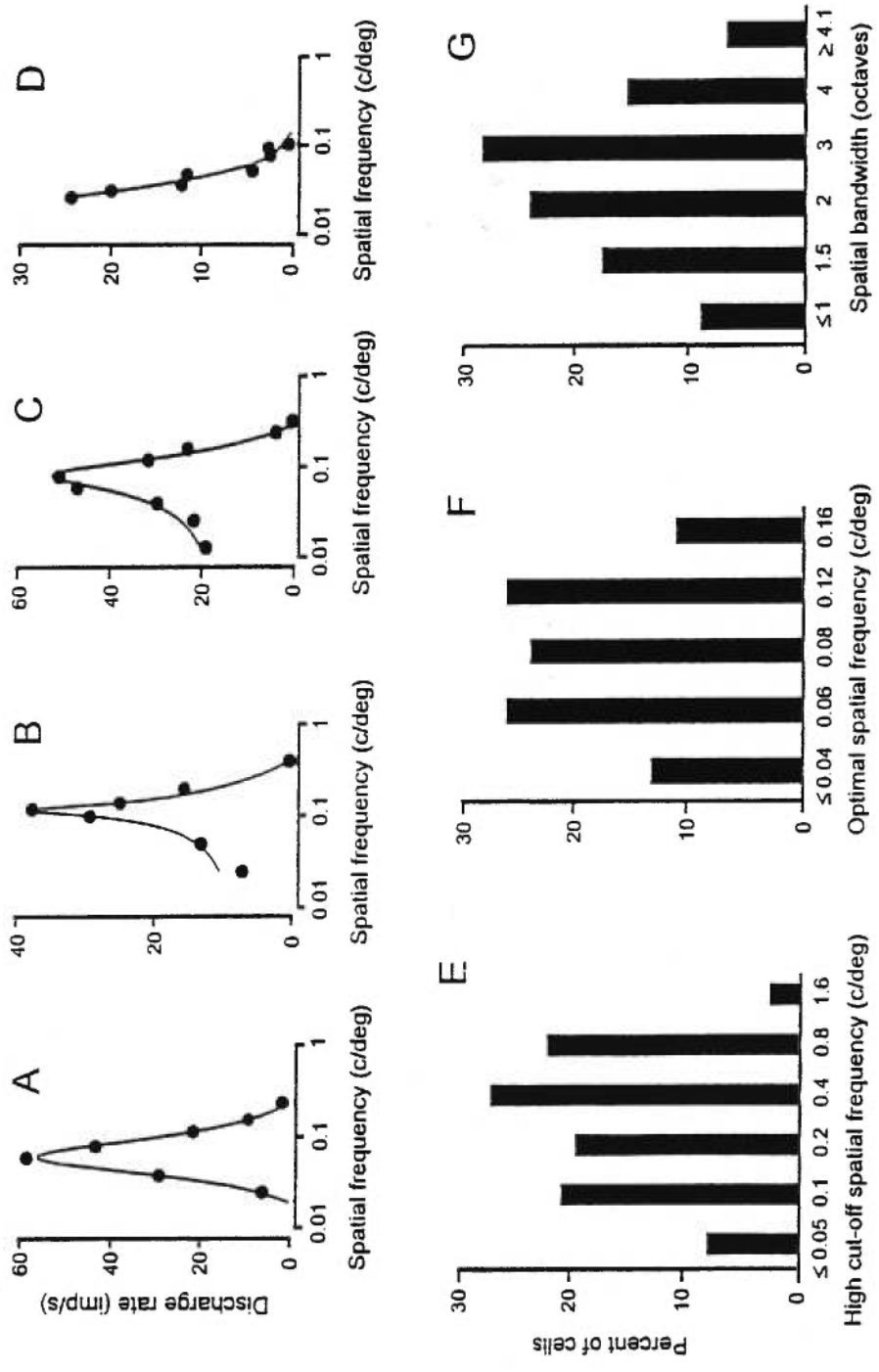
A
B
C
D
E
F
G
Discharge rate (imp/s)
Spatial frequency (c/deg)
Percent of cells
High cut-off spatial frequency (c/deg)
Optimal spatial frequency (c/deg)
Spatial bandwidth (octaves)

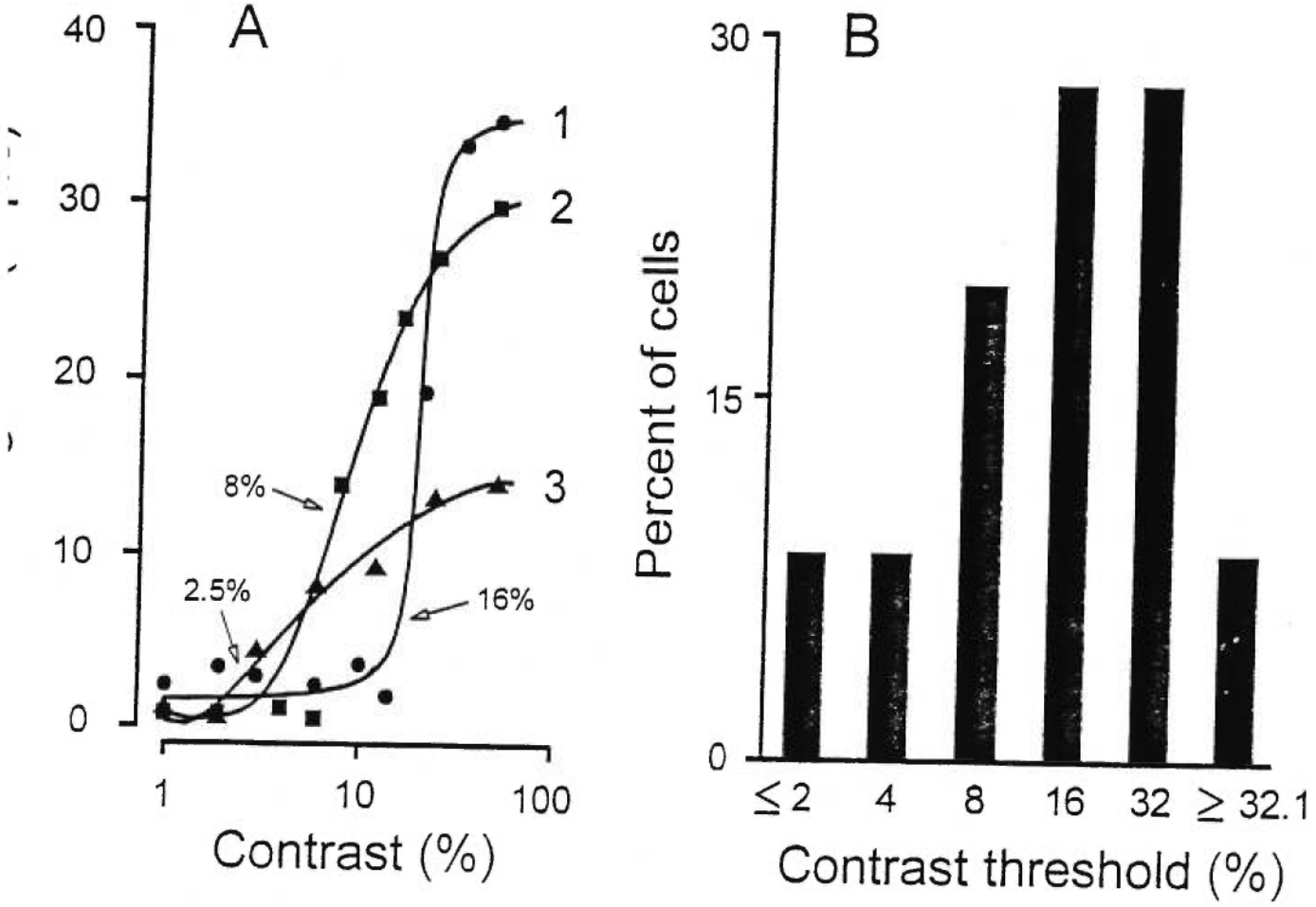
A
40
30
20
10
0
1
2
3
8%
2.5%
16%
1
10
100
Contrast (%)
B
30
15
0
Percent of cells
≤ 2
4
8
16
32
≥ 32.1
Contrast threshold (%)

FIGURE 6

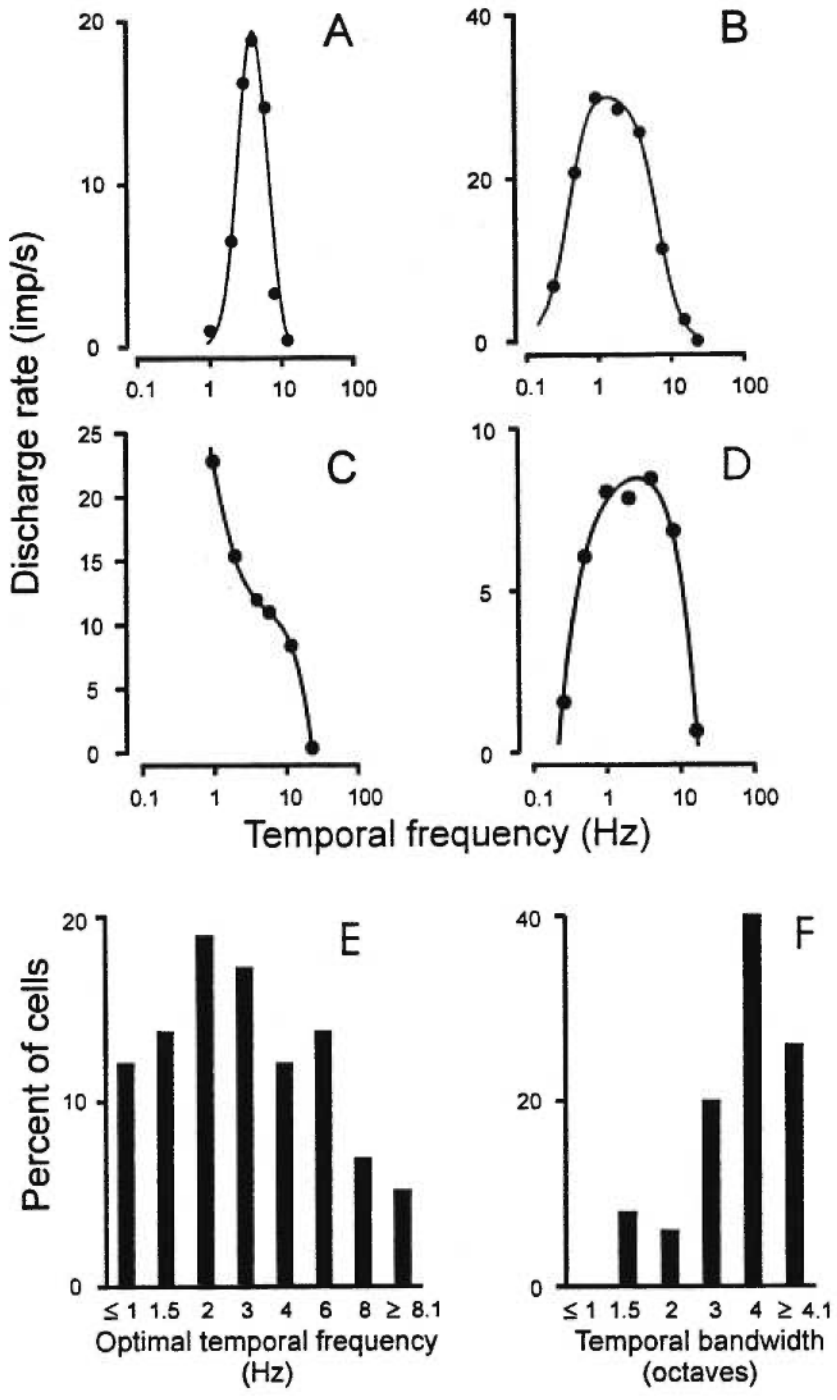
A
B
C
D
E
F
Discharge rate (imp/s)
Temporal frequency (Hz)
Percent of cells
Optimal temporal frequency (Hz)
Temporal bandwidth (octaves)
≤ 1 1.5 2 3 4 6 8 ≥ 8.1
≤ 1 1.5 2 3 4 ≥ 4.1

CHAPITRE VI

Discussion Générale

L'objectif général de nos études est de décrire les propriétés visuelles des cellules des aires extrastriées, à l'aide de réseaux de FS. Nous nous sommes intéressés plus particulièrement aux propriétés des aires extrastriées 19, 21a et 21b chez le chat normal. De plus, chez l'animal chiasmatomisé, nous avons comparé les propriétés des cellules visuelles qui ont été identifiées par stimulation indépendante de la voie géniculo-corticale et calleuse. Dans un premier temps, nous comparerons nos résultats avec ceux d'autres études effectuées chez le chat. Ensuite, nous aborderons le sujet des voies visuelles chez le chat et leur relation avec les aires visuelles. Finalement, nous discuterons du concept d'analyseur de fréquences spatiales.

Propriétés générales des cellules des aires visuelles extrastriées

Plusieurs études montrent que les différentes aires visuelles diffèrent entre elles par la taille des CR des cellules qu'elles contiennent. À ce sujet, nous avons remarqué que les CR des cellules de l'aire 19 sont plutôt petits comparativement à ceux des aires 21a et 21b. Les résultats d'études précédentes avaient déjà permis de conclure que les CR visuels étaient plus étendus au niveau de l'aire 21a par rapport à l'aire 19 (Hubel et Wiesel, 1965; Albus et Beckmann, 1980; Dreher, 1986, Dreher et al., 1993). Selon Dreher (1986) et Dreher et al. (1996), les aires visuelles se distinguent les unes des autres par la taille moyenne des CR visuels situés à différentes excentricités. Il serait possible de classer les aires visuelles suivant la taille moyenne de leurs CR visuels en ordre croissant. Une telle classification se présente comme suit: l'aire 17, l'aire 19, l'aire 18, l'aire 21a et finalement l'aire PMLS. En outre, nos résultats montrent que les CR des cellules de l'aire 21b sont très étendus, à l'instar de ceux des aires PMLS et PLLS (Rauschecker et al., 1987; von Grünau et al., 1987).

Nous avons procédé à une classification des CR selon leur organisation spatiale en termes de cellules S, C, Ch et Sh. Pour le faire, nous avons utilisé les critères de Hubel et Wiesel (1962, 1965), Henry (1977) ainsi que ceux de Skottun et al. (1991). Nos résultats montrent que la majorité des cellules des aires 19, 21a et 21b sont du type C. Cependant, il existe des différences entre ces aires visuelles quant aux proportions de cellules C, S, Ch et Sh qui y ont été identifiées. Ainsi, dans l'aire 19, nous avons identifié un nombre important de cellules du type Ch, alors que ce dernier type de cellule est plus rare dans l'aire 21a. Dans l'aire 21b, toutes les cellules que nous avons enregistrées sont du type C. Des cellules de types S et Sh sont présentes dans les aires 19 et 21a mais dans une faible proportion. La présence de cellules du type S au niveau des aires extrastriées va à l'encontre de l'hypothèse d'un traitement purement sériel. En effet, dans ces aires, les CR des cellules du type S sont probablement formés à partir des afférences directes qui proviennent de CGL dorsal, du NIM ou de l'aireron du corps genouillé. Ces afférences directes sont nombreuses au niveau de l'aire 17 mais plus limitées dans les aires extrastriées, ce qui pourrait expliquer la faible proportion de cellules du type S au niveau des aires 19 et 21a.

La majorité des cellules visuelles enregistrées au niveau des aires 19, 21a et 21b sont binoculaires. Aussi, elles montrent différents degrés de dominance oculaire, selon les critères de Hubel et Wiesel (1962). En outre, nous avons remarqué une prédominance de cellules activées de façon équivalente par chaque oeil, c'est-à-dire, les cellules de classe 4 et un nombre plus restreint de cellules de classes intermédiaires. Cette prédominance de cellules activées de façon équivalente par chaque oeil est particulièrement remarquable en ce qui à trait aux cellules de l'aire 21b. De plus, un

biais est généralement observé dans toutes les aires extrastriées en faveur de l'oeil controlatéral, ce qui pourrait être attribuable à une plus grande proportion de fibres qui croisent au niveau du chiasma optique chez le chat.

Nous avons observé l'existence d'une relation interoculaire significative entre les propriétés visuelles des cellules binoculaires corticales. En effet, une cellule visuelle binoculaire donnée tend à conserver des propriétés similaires pour chaque oeil. Cependant, cette relation n'est pas parfaite et de petites différences interoculaires sont observées, autant chez les animaux normaux que chiasmatomisés. Pour ces deux groupes d'animaux, nous avons montré que les différences interoculaires de résolution spatiale pouvaient s'expliquer par la dominance oculaire. En effet, les différences interoculaires de résolution spatiale sont surtout observées au niveau des cellules qui ont une dominance oculaire non-équivalente. Plus particulièrement, une cellule corticale donnée montre généralement une résolution spatiale supérieure pour l'oeil dominant, c'est-à-dire celui qui provoque un plus haut taux de potentiels d'action. Lorsque la dominance oculaire est équivalente (cellules de classe 4), les propriétés spatiales et temporelles sont relativement identiques pour les deux yeux. Chez l'animal chiasmatomisé, ces observations ont permis de conclure que les différences interoculaires entre les propriétés spatiales des cellules corticales ne sont pas reliées à la nature de l'input (direct ou calleux) mais plutôt à la dominance oculaire. Nous expliquons les dissemblances de nos résultats avec ceux de Berardi et al. (1987) par le fait que la plupart des cellules enregistrées par ces auteurs émettaient un taux de potentiels d'action supérieur lorsqu'elles étaient activées par l'oeil ipsilatéral (voie directe).

Le haut taux de correspondance interoculaire entre les propriétés visuelles des cellules binoculaires des aires extrastriées suggèrent qu'elles peuvent participer à des processus binoculaires tels la fusion binoculaire et la stéréopsie. De plus, des résultats similaires obtenus chez l'animal chiasmatomisé suggèrent que la convergence des inputs directs et calleux au niveau des cellules corticales peuvent aussi permettre de tels processus. En effet, certaines études montrent que les cellules des aires extrastriées peuvent être sélectives à la disparité spatiale et que cette propriété peut être observée chez les chats normaux (Guillemot et al., 1993, Wang et Dreher, 1996) ou chiasmatomisés (Guillemot et al., 1993). Donc, en dépit des différentes afférences qui aboutissent vers les aires 17 et 18 par rapport aux aires extrastriées, la correspondance interoculaire entre les propriétés des cellules visuelles est comparable entre ces mêmes aires.

Sélectivité à l'orientation et à la direction

La sélectivité à l'orientation et à la direction est une caractéristique importante des cellules visuelles corticales (Hubel et Wiesel, 1963), thalamiques (Thompson et al., 1994) et rétiniennes (Shou et al., 1995) chez le chat. Plus particulièrement, de nombreuses études ont porté sur la sélectivité à l'orientation et à la direction au niveau des différentes aires visuelles. La majorité des cellules corticales des aires 17, 18, 19 et 21a sont sélectives à l'orientation du stimulus (Hubel et Wiesel, 1963, 1965; Orban, 1984; Dreher, 1986; Wimborne et al., 1992; Dreher et al., 1993). Aussi, plusieurs cellules des aires 17, 18, 21a et PMLS sont sélectives à la direction du stimulus comparativement à l'aire 19 où moins de cellules sont directionnelles (Orban, 1984; Dreher, 1986).

Un des objectifs généraux de notre étude était de vérifier si les cellules visuelles de l'aire 21b sont sélectives à l'orientation et à la direction et de comparer nos résultats avec ceux qui ont été obtenus dans d'autres aires visuelles. Afin d'estimer la sélectivité à l'orientation et à la direction des cellules, nous avons utilisé des FS balayant le CR. Nos résultats montrent que la majorité des cellules visuelles de l'aire 21b sont sélectives à la direction du stimulus. Si nos résultats sont comparés à ceux de Dreher (1992), nous observons que la proportion de cellules qui présentent un indice de direction supérieur à 80 % est plus importante dans l'aire 21b que dans les aires 17, 18 et 21a; alors que les cellules de l'aire 21a sont davantage sélectives à l'orientation du stimulus. Par ailleurs, de nombreux auteurs ont remarqué que la majorité des cellules visuelles des aires PMLS et PLLS sont fortement sélectives à la direction (Hubel et Wiesel, 1969; Wright, 1969; Spear et Baumann, 1975; Turlejski, 1975; Camarda et Rizzolatti, 1976; Blakemore et Zumbroich, 1987; Rauschecker et al., 1987, von Grünau et al., 1987; Gizzi et al., 1990), ce qui se rapproche davantage des résultats que nous avons obtenus dans l'aire 21b.

En général, nous pouvons affirmer que les cellules des aires 21a et 21b se distinguent par leurs profils de réponses à différentes orientations et directions. La plupart des cellules de l'aire 21a sont sélectives à l'orientation et présentent des valeurs de demi-largeurs relativement peu élevées tandis que les cellules de l'aire 21b sont plutôt sélectives à la direction et ont des valeurs de demi-largeurs plus élevées. En ce sens, nous pouvons affirmer que les cellules de l'aire 21a sont davantage impliquées dans l'analyse de la forme tandis que celles de l'aire 21b, à l'instar de celles des aires PMLS et PLLS, peuvent encoder la direction du déplacement d'un stimulus.

Profils de réponses aux fréquences spatiales

Nos résultats montrent que la résolution spatiale moyenne des cellules de l'aire 19 est quelque peu inférieure à celle des cellules de l'aire 21a (Tardif et al., 1996, 1997). En effet, la résolution spatiale moyenne de l'oeil dominant des cellules de l'aire 19 est de 0,75 c/deg alors qu'elle est de 0,94 c/deg pour les cellules de l'aire 21a. Cette différence est principalement attribuable au nombre plus important de cellules de l'aire 21a qui répondent à des FS supérieures à 1 c/deg. D'autre part, nos résultats montrent que les cellules de l'aire 21b répondent à des FS beaucoup plus basses par rapport à celles des aires 19 et 21a. En effet, les cellules de l'aire 21b ont une résolution spatiale moyenne de 0,29 c/deg ainsi qu'une FS optimale moyenne de 0,08 c/deg, ce qui diffère nettement des résultats observés au niveau des aires 19 et 21a.

Une comparaison entre les résultats obtenus dans plusieurs aires visuelles permet de conclure que les cellules de l'aire 17 possèdent en moyenne une résolution spatiale et des FS optimales supérieures à celle des cellules des aires extrastriées (Maffei et Fiorentini, 1973; Movshon, 1978c; Tolhurst et Thompson, 1981). Ceci pourrait être attribuable aux nombreuses afférences du type X au niveau de cette aire. Aussi, les résultats de notre étude ainsi que ceux de Zumbroich et Blakemore (1987), Gizzi et al. (1990), Tanaka et al. (1987) et Movshon et al. (1978c) permettent de conclure ce qui suit: la résolution spatiale et les FS optimales des cellules visuelles des aires 18, 19, 21a et PMLS sont comparables. Ces mêmes propriétés spatiales sont, en outre, comparables à celles des cellules du LPl (Casanova et al., 1989), lesquelles constituent un input prédominant au niveau de plusieurs aires extrastriées. Cependant, nos résultats montrent que les cellules visuelles de l'aire 21b ont une résolution spatiale

nettement inférieure par rapport à celle qui est observée dans les autres aires visuelles. Ces comparaisons nous amènent à considérer que différents niveaux de traitement de l'information visuelle du type spatial pourraient exister entre les aires visuelles. Ainsi, l'aire 17 pourrait analyser les hautes FS; les aires 18, 19, 21a et PMLS seraient sélectives à des FS de valeurs intermédiaires alors que l'aire 21b (et peut-être d'autres aires visuelles) traiteraient les basses FS.

Sensibilité au contraste

Pour plusieurs cellules des aires 19, 21a et 21b, nous avons observé la réponse des cellules visuelles à différents niveaux de contraste. Nos résultats montrent que l'allure générale des courbes ainsi obtenues ressemble à celles qui ont été observées au niveau des cellules de l'aire 17 (Maffei et Fiorentini, 1973; Tolhurst et Movshon, 1975; Tolhurst et al., 1981; Albrecht et Hamilton, 1982). En effet, la réponse cellulaire augmente selon le niveau de contraste. De plus, la forme des courbes de réponses au contraste ainsi que le seuil de contraste indiquent une grande variation d'une cellule à une autre. D'autre part, nous avons remarqué, en règle générale, que la réponse des cellules tend à saturer losque le contraste atteint environ 30 %. Nous avons aussi observé que le seuil de contraste des cellules binoculaires est généralement comparable pour l'oeil ipsilatéral et controlatéral. Ceci est semblable à ce qui a été observé au niveau de l'aire 17 (Skottun et Freeman, 1984). Chez les animaux chiasmatomisés, nous avons observé que les différences interoculaires de sensibilité au contraste ne sont pas reliées à la nature de l'input (direct ou calleux). Ce résultat tend à infirmer l'hypothèse selon laquelle le CC agit comme un filtre sélectif aux hauts contrastes.

Profils de réponses aux fréquences temporelles

Nous avons observé que les courbes de syntonisation aux FT des cellules des aires 19, 21a et 21b sont presque exclusivement du type passe-bande. Aussi, nous avons remarqué que les cellules de ces aires visuelles peuvent répondre à une vaste étendue de FT. Néanmoins, certaines différences existent entre ces aires quant aux FT optimales des cellules visuelles qu'elles contiennent. Bien que les cellules de l'aire 19 et 21a montrent des FT optimales supérieures à celles de l'aire 21b, ceci pourrait être attribuable à la sélectivité particulière aux basses FS des cellules de l'aire 21b. En fait, nous avons remarqué que les neurones de l'aire 21b, de par leur sélectivité aux basses FS, pourraient encoder des vélocités plus élevées comparativement aux aires 19 et 21a.

Les résultats obtenus dans d'autres aires visuelles montrent que les cellules des aires 17, 18 et PMLS ne diffèrent pas de façon marquée quant à leurs profils de réponses aux FT (Movshon et al., 1978c, Zumbroich et Blakemore, 1987; Gizzi et al., 1990; Saul et Humphrey, 1991). En effet, les FT optimales des cellules de ces aires se situent généralement entre 2 et 4 Hz. Cependant, les cellules des aires 18 et PMLS répondent optimalement à de basses FS comparativement à celles de l'aire 17. Il est alors possible que les cellules des aires 18 et PMLS répondent à des vélocités plus élevées par rapport à celles de l'aire 17 principalement parce qu'elles sont sélectives à de plus basses FS.

Traitement parallèle et hiérarchique de l'information visuelle chez le chat

Un des objectifs de nos travaux était de vérifier dans quelle mesure l'organisation parallèle des voies visuelles chez le chat est préservée au niveau des aires extrastriées. Nous savons qu'il existe au moins trois voies visuelles distinctes au niveau de la rétine et du CGL, lesquelles sont formées des cellules de types X, Y et W. Cependant, les projections corticales de ces trois types de cellules sont complexes et les aires visuelles reçoivent généralement plus d'un type d'afférence. De plus, un riche réseau de connections intracorticales existe entre les aires visuelles. Au niveau des aires extrastriées, est-il possible d'affirmer qu'il existe toujours un traitement parallèle?

Un des postulats à l'origine de la théorie des systèmes parallèles est que différents aspects de la scène visuelle tels la forme et le mouvement sont traités séparément par des voies spécifiques. Chez le chat, la réponse soutenue des cellules X ainsi que leur forte concentration au niveau de l'AC suggèrent qu'elles pourraient être impliquées dans l'analyse de la forme. D'autre part, la réponse phasique des cellules Y ainsi que leur proportion plus importante en périphérie rétinienne laissent croire qu'elles auraient plutôt un rôle à jouer dans l'analyse du mouvement. Toutefois, il est possible que certaines propriétés des cellules comme la résolution spatiale et temporelle soient dépendantes de certaines caractéristiques du stimulus. Par exemple, les cellules X peuvent montrer une résolution temporelle supérieure aux cellules Y si le stimulus est formé de hautes FS. De leur côté, les cellules Y peuvent atteindre une résolution spatiale supérieure aux cellules X si des hautes FT sont utilisées ou si le stimulus subit des changements abrupts de contraste (So et Shapley, 1981; Sherman, 1985). Il n'est donc pas impossible qu'un type de cellule donné puisse analyser de multiples

composantes de la scène visuelle; cela pourrait en fait dépendre en partie des propriétés du stimulus à analyser. On ne peut donc pas associer de façon absolue l'analyse de la forme aux cellules X et l'analyse du mouvement aux cellules Y, du moins en ce qui à trait au système visuel du chat. Toutefois, on peut envisager que dans des circonstances naturelles, une haute résolution spatiale est surtout requise lorsque le stimulus se déplace de manière relativement lente et que les cellules X sont plus appropriées à résoudre une telle tâche. Inversement, la détection des stimuli qui se déplacent à de hautes vitesses ne requiert pas nécessairement une analyse spatiale détaillée ce qui reflète une situation dans laquelle les cellules Y seraient probablement impliquées.

Les expériences comportementales chez le chat suggèrent en fait que la capacité de discrimination entre des formes géométriques ne relève probablement pas de l'intégrité du système X. En effet, une lésion des aires 17 et 18 perturbe considérablement le système X mais n'empêche pas la discrimination de la forme (Doty, 1971). Cependant, cette lésion entraîne une baisse importante de la résolution spatiale (Berkeley et Sprague, 1982). Ces résultats nous poussent à établir une distinction importante entre l'analyse de la forme et celle des détails fins de la scène visuelle. En fait, la capacité à discriminer les formes chez le chat pourrait plutôt être tributaire des voies Y et W, lesquelles sont davantage dirigées vers les aires extrastriées. Cette affirmation est d'ailleurs appuyée par les études comportementales de Sprague et al. (1977) qui montrent que des lésions étendues des aires extrastriées affectent considérablement la capacité à discriminer les formes.

Ces observations comportementales montrent que les voies directes dirigées vers les aires extrastriées peuvent assurer une vision relativement bonne chez le chat.

Cependant, les lésions effectuées dans les aires extrastriées incluent presque invariablement un groupe d'aires visuelles. Par exemple, les lésions effectuées par Sprague et al. (1977) incluent les aires 7, 19, 21a, 21b et plusieurs aires suprasylviennes. Conséquemment, il demeure difficile d'établir si ces aires diffèrent entre elles quant au type de traitement visuel qu'elles effectuent et si les connections intracorticales peuvent rendre compte de certaines propriétés visuelles observées au niveau de ces aires. Nos enregistrements effectués dans différentes aires extrastriées montrent que les propriétés visuelles des cellules des ces aires ont certaines caractéristiques communes, dont la sélectivité aux FS. De plus, les profils de réponses aux FS des cellules des aires extrastriées pourraient rendre compte de la capacité à discriminer la forme. En effet, la plupart des cellules de ces aires sont du type passe-bande et répondent mieux à une étendue relativement limitée de FS. Puisque ces aires extrastriées ne reçoivent pas d'input direct du type X, ceci appuie l'hypothèse selon laquelle les systèmes Y et W peuvent jouer un rôle important dans l'analyse de la forme. Plus particulièrement, la présence de cellules sélectives aux FS et à la longueur d'un stimulus au niveau de l'aire 19 suggère que l'input direct du type W, particulièrement important dans cette aire, pourrait en fait participer à l'analyse de la forme.

Nos résultats laissent également supposer que le traitement parallèle est en partie conservé par l'entremise de certains liens intracorticaux. En effet, nous avons observé qu'une proportion substantielle de cellules de l'aire 21a ont une haute résolution spatiale en dépit de la taille relativement importante de leurs CR. Par contre, ce type de cellule est plutôt rare au niveau de l'aire 19 et absent dans l'aire 21b. Il est donc possible que le signal du type X soit transmis à partir de cellules de l'aire 17 possédant des CR relativement petits vers des aires extrastriées spécifiques, dont l'aire 21a. De plus, cette

idée est appuyée par la présence de cellules très sélectives à l'orientation, lesquelles peuvent répondre à des barres de dimensions inférieures à leurs CR (Dreher et al., 1993).

D'autre part, puisque la capacité à discriminer entre des formes géométriques ne semble pas dépendre de l'intégrité du système X, quel serait le rôle des cellules à haute résolution spatiale au niveau des aires extrastriées? Une interprétation possible est que ces cellules soient impliquées dans l'analyse de formes plus complexes, faisant appel à la capacité de résoudre les hautes FS. Par exemple, il semble que l'habileté à reconnaître les visages soit dépendante de l'intégrité de certaines régions visuelles associatives (Damasio, 1982). De plus, l'enregistrement de cellules sélectives à des visages au niveau du cortex inféro-temporal du primate supporte cette idée (Desimone et al., 1984). Une telle fonction sous-tend en partie l'analyse de hautes FS associées aux détails qui permettent de distinguer entre des visages différents. En fait, il semble que la distinction entre les visages nécessite davantage l'analyse de hautes FS que celle de basses FS (Fiorentini et al., 1981). Si les neurones à haute résolution spatiale que nous avons identifiés au niveau de l'aire 21a sont impliqués dans des tâches comparables chez le chat, nous serions en mesure d'affirmer que le système visuel de cet animal fonctionne à la fois de façon parallèle et sérielle. En ce sens, le traitement parallèle signifie que le système X à haute résolution est préservé dans une aire extrastriée spécifique tandis que le traitement sériel se reflète dans la dimension importante des CR qui pourraient traiter des stimuli très complexes dans une grande partie du champ visuel.

En ce qui concerne l'aire 21b, nous avons remarqué qu'une grande proportion de cellules de cette aire sont sélectives à la direction du stimulus. De plus, ces cellules sont

sélectives à de très basses FS et répondent à de hautes vélocités. La proportion de cellules fortement sélectives à la direction est également plus prononcée au niveau des aires 18 et PMLS comparativement aux aires visuelles 17, 19 et 21a (Orban, 1984; Dreher, 1986). Cependant, il est difficile d'établir l'origine exacte de la sélectivité à la direction des cellules des aires extrastriées. En effet, cette propriété pourrait provenir des aires primaires mais pourrait aussi être transmise par l'intermédiaire du noyau LPl, lequel reçoit des afférences du cortex visuel et possède également des cellules directionnelles à grands CR (Chalupa et Abramson, 1988; Casanova et al., 1989). Une autre possibilité est que la sélectivité à la direction soit créée à partir des afférences directes du CGL vers les aires extrastriées. Il semble cependant que la sélectivité à la direction des cellules des aires extrastriées soit en partie due à des afférences des aires primaires car la lésion des aires 17, 18 et 19 entraîne une diminution du nombre de cellules directionnelles de l'aire PMLS (Guido et al., 1990). Par ailleurs, une lésion ou désactivation de l'aire 17 n'entraîne pas de changements importants dans la proportion de cellules directionnelles au niveau de l'aire 18 (Dreher et Cottee, 1975; Sherk, 1978). Il est donc possible que cette propriété origine du cortex visuel primaire et qu'elle soit véhiculée vers des régions spécifiques telles les aires PMLS et 21b.

La sélectivité à la direction des cellules visuelles est vraisemblablement un élément déterminant pour assurer différentes fonctions dont la distinction entre la figure et le fond. Cette distinction implique que le sujet est capable de regrouper les propriétés communes d'un stimulus afin de le distinguer par rapport aux autres stimuli qui constituent la scène visuelle. Il semble que les neurones de l'aire PMLS du chat possèdent certaines propriétés qui pourraient rendre compte d'une telle habileté. En effet, des études électrophysiologiques ont montré que ces neurones possèdent des CR

dont l'organisation est antagoniste à la direction (von Grünau et Frost, 1983). Cette organisation suppose que le CR excitateur est entouré d'une vaste région modulatrice qui peut influencer la réponse du neurone selon sa direction relative par rapport au stimulus excitateur. Si le stimulus excitateur (par exemple, un point sombre ou lumineux) est superposé à un bruit visuel se déplaçant dans la même direction que le stimulus, il n'y a plus de mouvement relatif entre la figure et le fond. Dans cette situation, la réponse de la cellule subit une atténuation considérable. Inversement, si le stimulus et le bruit visuel sont dirigés dans des directions opposées, le mouvement relatif entre la figure et le fond est accentué et la réponse cellulaire est augmentée. Bien que nous n'ayons pas testé directement si ces propriétés existent au niveau des cellules directionnelles de l'aire 21b, il est possible d'envisager qu'elles puissent se comporter de façon similaire dans de telles circonstances. En effet, ces cellules partagent beaucoup de caractéristiques communes avec les cellules de l'aire PMLS dont des CR étendus et sélectifs à la direction. De plus, ces deux aires reçoivent de nombreuses afférences du noyau LPl et de l'aire 18, lesquelles régions contiennent une forte proportion de cellules sélectives à la direction (Raczkowski et Rosenquist, 1983; Symonds et Rosenquist, 1984). En effet, bien qu'il demeure difficile d'identifier les mécanismes responsables de telles propriétés, elles semblent être redevables à des interactions excitatrices et inhibitrices entre les différentes voies parallèles (von Grünau et Frost, 1983).

En résumé, nous pouvons affirmer que certaines différences existent entre les aires extrastriées du chat quant aux proportions de cellules qui présentent des caractéristiques particulières. Cependant, chaque aire visuelle contient aussi des cellules qui peuvent présenter des propriétés différentes, ce qui reflète probablement la diversité des afférences qui aboutissent dans une aire donnée. En effet, le système visuel du chat

semble posséder une organisation parallèle lui permettant de maintenir un haut niveau fonctionnel en l'absence des aires primaires. De plus, ces voies parallèles pourraient interagir entre elles pour donner lieu à des propriétés spécifiques au niveau des cellules visuelles. Toutefois, cela n'exclut pas l'existence d'un traitement hiérarchique qui pourrait assurer certaines fonctions supérieures.

Le cortex visuel est-il un analyseur de fréquences spatiales?

La plupart des études électrophysiologiques qui portent sur les cellules visuelles corticales mettent en évidence la spécificité de leur réponse à un paramètre donné. Idéalement, la spécificité d'une cellule visuelle à un paramètre est caractérisée par un taux de décharge maximal à une valeur donnée de ce paramètre et par une atténuation progressive de la réponse à des valeurs qui diffèrent de cette valeur optimale. Ainsi, les cellules corticales peuvent être considérés comme étant des filtres du type passe-bande qui ne répondent qu'à une étendue limitée de valeurs d'un paramètre. Parmi les nombreux paramètres qui peuvent être encodés par les cellules visuelles corticales, les FS ont suscité un intérêt particulier. En effet, certains auteurs (Pollen et al., 1971; Maffei et Fiorentini, 1973) ont suggéré que le cortex visuel pourrait fonctionner tel un analyseur de fréquences spatiales. Selon cette hypothèse, les cellules visuelles pourraient traiter séparément les composantes élémentaires qui forment un stimulus complexe, lequel serait par la suite reconstruit à partir de l'activité nerveuses de ces cellules. Cette hypothèse s'inspire essentiellement de l'analyse de Fourier permettant de décomposer tout stimulus visuel ou auditif complexe en ses différentes harmoniques sinusoïdales. Les données expérimentales à l'origine de cette conception du système visuel proviennent surtout du fait que les cellules de types S et Sh ont des CR

excitateurs formés de régions ON/OFF antagonistes et adjacents dont la sensibilité est modulée sinusoïdalement dans l'espace selon une longueur et/ou une orientation particulière. Lorsqu'elles sont stimulées par une FS sinusoïdale d'une valeur donnée et correctement orientée, ces cellules montrent un patron de décharge modulé à la FT du stimulus. De plus, cette modulation varie en amplitude selon la concordance entre la FS et le filtre, en l'occurrence le CR visuel. Ce type de cellule peut ainsi agir tel un filtre linéaire car la réponse (output) conserve les propriétés périodiques de la FS sinusoïdale (input). Ainsi, ces cellules pourraient encoder les FS d'un stimulus lumineux à partir de l'amplitude de modulation de leurs réponses.

D'autre part, les cellules de types C et Ch répondent de façon différente aux FS. Leur patron de décharge est uniforme et ne présente habituellement pas de modulation à la FT de stimulation, sauf pour un certain type de cellules appelées cellules complexes périodiques (Pollen et Ronner, 1975; Pollen et al., 1971). La réponse de ces dernières cellules aux FS est caractérisée par un certain degré de modulation qui se superpose à une élévation uniforme de leur taux de décharge. Mis à part ce type de cellules, les cellules de types C et Ch répondent aux ondes sinusoïdales par une élévation uniforme du taux de décharge, lequel ne contient pas de composante périodique particulière. Cependant, le taux de décharge de ces cellules, bien qu'il soit non-modulé, peut varier selon la valeur des FS qui sont présentées. En fait, la plupart des cellules C et Ch montrent une FS optimale et répondent à une étendue limitée de FS. Cette dernière propriété nous motive à considérer les cellules C comme étant des filtres non-linéaires qui pourraient, dans une certaine mesure, participer à l'analyse des FS. Les résultats que nous avons obtenus dans l'aire 19 (Tardif et al., 1997), 21a (Tardif et al., 1997) et 21b montrent que les cellules de ces aires extrastriées sont du type C. De plus, de

nombreuses cellules de l'aire 19 sont du type Ch. D'autre part, nous avons trouvé peu de cellules de types S ou Sh dans les aires 19 et 21a et aucune dans l'aire 21b. Ainsi, nous pouvons croire que la majorité des cellules des aires extrastriées 19, 21a et 21b peuvent agir en tant que filtres non-linéaires.

Puisque chaque aire visuelle est formé de millions de cellules, lesquelles répondent optimalement à différentes valeurs d'un paramètre donné, pouvons-nous considérer qu'une population de cellules peut aussi agir tel un filtre de FS et si oui, les multiples aires visuelles peuvent-elles former des filtres sélectifs à différentes valeurs de FS? Nos résultats suggèrent en effet que les aires extrastriées 19 (Tardif et al., 1997), 21a (Tardif et al., 1996) et 21b répondent à des étendus différentes de FS. En effet, les cellules de l'aire 21b sont activées par les basses FS tandis que celles des aires 19 et 21a répondent surtout à des FS de valeurs intermédiaires, bien qu'un nombre important de cellules de l'aire 21a répondent à de hautes FS. D'autre part, il semble clair que les cellules de l'aire 17 sont davantage sélectives aux hautes FS (Maffei et Fiorentini, 1973; Movshon et al., 1978 a, b, c; Tolhurst et Tompson, 1981; Berardi et al., 1982). Donc, nous pouvons affirmer que les différentes aires visuelles encodent des étendues différentes de FS, ce qui est appuyé par une comparaison entre les valeurs moyennes des FS optimales observées au niveau des différentes aires: l'aire 17: un c/deg (Tolhurst et Tompson, 1981); l'aire 21a: 0,36 c/deg (Tardif et al., 1996); l'aire 19: 0,17 c/deg (Tardif et al., 1997) et l'aire 21b: 0,08 c/deg.

À la lueur de ces résultats, nous pouvons nous demander si les propriétés filtrantes qui sont observées au niveau des aires visuelles peuvent s'appliquer à d'autres structures anatomiques véhiculant de l'information visuelle, notamment le CC. Nos

résultats (Tardif et al., 1997) montrent que les propriétés visuelles des cellules corticales de l'aire 19 obtenues par une stimulation des voies directe ou calleuse sont comparable. Aussi, bien que certaines différences interoculaires sont observées d'une cellule à une autre, les résultats montrent que ces différences ne sont pas redevables à la nature de l'input (direct ou calleux). Donc, si des propriétés filtrantes existent au niveau des fibres calleuses visuelles, l'intégration post-synaptique effectuée par les cellules corticales qui reçoivent un input de ces fibres donne lieu à des propriétés visuelles similaires à celles obtenues par un input direct. Nous pouvons donc envisager que l'information visuelle transmise par le CC soit comparable à celle véhiculée par la voie directe.

Une transformation importante qui s'opère au niveau du cortex visuel primaire par rapport aux structures inférieures telles le CGL est le rétrécissement de la largeur des courbes de syntonisation aux FS. En effet, les cellules du cortex visuel primaire ont des bande-passantes spatiales beaucoup plus étroites que celles du CGL et sont donc sélectives à une étendue plus réduite de FS. Puisque les stimuli complexes contiennent un spectre formé d'innombrables FS (incluant de très hautes FS), on pourrait présumer qu'un tel raffinement se poursuit au niveau des aires extrastriées. Cependant, les résultats obtenus au niveau des aires extrastriées 19 (Tardif et al., 1997), 21a (Tardif et al., 1996), 21b et PMLS (Zumbroich et Blakemore, 1977) montrent clairement que ceci n'est pas le cas; les cellules des aires extrastriées sont en général moins sélectives aux FS que celles de l'aire 17. Que signifie cette observation? Une interprétation possible est que les cellules des aires primaires soient davantage impliquées dans une analyse du type local, tandis que celles des aires extrastriées auraient la capacité d'effectuer une analyse globale. En effet, la petite taille des CR des cellules des aires primaires (plus particulièrement celle des cellules du type S) procure une analyse spatiale précise mais

limitée à une petite partie du champ visuel. Par contre, les grands CR observés au niveau des aires extrastriées pourraient intégrer différentes composantes de l'image visuelle. En fait, les expériences comportementales chez le chat suggèrent qu'une telle distinction fonctionnelle entre les aires primaires et extrastriées est plausible. Hughes et Sprague (1986) ont vérifié l'effet de lésions corticales des aires primaires ou extrastriées sur la capacité à effectuer des analyses de types local et global de la scène visuelle. Une analyse locale consiste à discriminer entre deux stimuli formés de nombreux petits traits possédant une orientation donnée. Chaque stimulus contient un certain nombre de traits disposés à la même orientation, laquelle est différente pour l'autre stimulus. En principe, l'animal peut réussir une telle tâche de discrimination en effectuant une analyse limitée à une petite partie de l'espace. Dans la tâche d'analyse globale, les deux stimuli sont formés de points espacés de façon à créer l'impression de rangées possédant une orientation donnée, laquelle diffère entre les deux stimuli. Cette impression est redevable au principe de groupement par proximité et est donc dépendante d'une analyse globale de la scène. Les résultats de Hughes et Sprague (1986) suggèrent qu'une lésion des aires 17 et 18 affecte davantage l'analyse locale de la scène visuelle tandis que des lésions des aires extrastriées provoquent des déficits plus importants au niveau de l'analyse du type global. Il est donc possible que les petits CR des aires 17 et 18 qui sont très sélectifs à l'orientation et aux hautes FS soient importants pour effectuer une analyse visuelle locale. D'autre part, une analyse visuelle globale semble plutôt être tributaire de l'activité des cellules à grands CR des aires extrastriées.

Selon Hughes et Sprague (1986), l'analyse du type global effectuée à partir des stimuli qu'ils ont employés nécessite essentiellement le traitement de basses FS. À ce sujet, nous avons remarqué que dans certaines aires extrastriées (surtout les aires 21a et

21b), de nombreuses cellules ont de grands CR qui s'étendent dans la partie centrale du champ visuel, une propriété qui n'est pas observée au niveau des aires primaires. Ceci nous porte à croire que la forme générale des grands objets situés dans la partie centrale du champ visuel est vraisemblablement analysée par les cellules des aires extrastriées. En effet, il semble que les cellules des aires primaires qui possèdent des CR centraux ne répondent pas optimalement à de basses FS (Maffei et Fiorentini, 1973; Movshon et al., 1978c) ni aux formes plus larges que leurs CR (Bishop et al. 1971). Toutefois, certains auteurs ont noté la présence de cellules du type passe-bas au niveau de l'aire 17 (Ikeda et Wright, 1975).

Il est donc possible de concevoir le système visuel sous la forme d'un analyseur de FS mais cette conception suppose l'existence de structures anatomiques rigoureusement organisées. Par exemple, on peut se demander comment un tel analyseur pourrait arriver à grouper des points à partir de leur proximité et d'en dégager une certaine orientation alors que l'analyse spectrale des points eux-mêmes contient d'innombrables FS à toutes les orientations. Face à une telle situation, un système d'analyseur de FS serait aux prises avec de nombreux paramètres à considérer. Afin de résoudre cette tâche de groupement perceptif, il semble que le système d'analyse de FS devrait montrer une organisation anatomique rigoureuse fonctionnant de pair avec celle qui à trait à l'analyse des orientations (Hubel et Wiesel, 1963). Il semble qu'une telle organisation puisse exister au niveau du cortex visuel primaire (Maffei et al., 1977; Tootell et al., 1981), mais elle n'a pas encore été mise en évidence dans les aires extrastriées du chat. Jusqu'à présent, il est donc possible d'envisager que le système visuel puisse initialement analyser les FS afin de transmettre un input organisé vers les

aires supérieures, un point de vue qui se rapproche considérablement d'une conception hiérarchique.

CONCLUSION GÉNÉRALE

Nos études se veulent une contribution à une meilleure compréhension du traitement visuel qui s'effectue au niveau des aires extrastriées du chat. Les enregistrements électrophysiologiques ont mis en évidence la sélectivité à différents paramètres des cellules visuelles situées dans certaines aires extrastriées. Chez l'animal chiasmatomisé, nous avons comparé la contribution respective des voies directes et calleuses au niveau des cellules corticales.

Nos résultats nous amènent à affirmer que les cellules visuelles des aires extrastriées peuvent accomplir un haut niveau de traitement de l'information visuelle. La majorité des cellules visuelles de ces aires sont sélectives aux FS et aux FT, ce qui nous pousse à croire qu'elles contribuent à l'analyse des composantes spatio-temporelles de la scène visuelle. De plus, les proportions de cellules qui possèdent des caractéristiques particulières diffèrent selon les aires visuelles. Ceci suggère qu'il pourrait exister un certain degré de spécialisation au niveau des différentes aires visuelles du chat. De plus, la description des voies anatomiques chez cet animal nous permet d'interpréter nos résultats sur une base plus détaillée.

Il semble évident que les systèmes de traitement parallèles dans le système visuel du chat soient déterminants pour assurer un haut niveau fonctionnel. Nos résultats suggèrent que ces voies peuvent en partie être préservées au niveau des aires extrastriées. Ainsi, nous pouvons envisager que le signal du type X puisse être transmis directement de l'aire 17 vers l'aire 21a et que certains neurones de cette aire aient la capacité de traiter de hautes FS à l'intérieur de grands CR. Par ailleurs, il est possible que le signal Y qui prédomine dans l'aire 18, soit dirigé vers les aires suprasylviennes et 21b, lesquelles pourraient analyser certaines composantes dynamiques de la scène

visuelle. De plus, il est aussi possible que le signal W qui constitue un input important vers l'aire 19 possède certaines capacités à traiter l'information spatiale. Aussi, les projections de l'aire 19 vers d'autres aires associatives contribueraient à un niveau d'analyse suffisant pour maintenir le niveau fonctionnel observé chez le chat dont les aires primaires sont lésées.

En conclusion, nous sommes en mesure d'affirmer que les aires extrastriées, bien qu'elles soient beaucoup moins connues que les aires primaires, jouent des rôles essentiels dans le système visuel du chat. Malgré que l'analyse visuelle réalisée par les cellules de ces aires semble en général moins précise par rapport à celles des aires primaires, elle pourrait être déterminante pour la survie de l'animal. De plus, cette forme d'analyse générale est probablement celle qui prévaut en cas de perturbations partielles du système visuel.

RÉFÉRENCES GÉNÉRALES

Albrecht, D.G. & Hamilton, D.B. (1982). Striate cortex of monkey and cat: contrast response function. Journal of Neurophysiology, 48, 217-237.

Albus, K. & Beckmann, R. (1980). Second and third visual areas in the cat: interindividual variability in retinotopic arrangement and cortical location. Journal of Physiology, 299, 247-276.

Antonini, A., Berlucchi, G. & Lepore, F. (1983). Physiological organization of callosal connections of a visual lateral suprasylvian cortical area in the cat. Journal of Comparative Neurology, 49, 902-921.

Barlow, H.B.D., Blakemore, C. & Pettigrew, J.D. (1967). The neural mechanisms of binocular depth discrimination. Journal of Physiology, 193, 327-342.

Benedek, G., Norita, M. & Creutzfeldt, O.D. (1983). Electrophysiological and anatomical demonstration of an overlapping striate and tectal projection to the lateral posterior-pulvinar complex of the cat. Experimental Brain Research, 52, 157-169.

Berardi, N., Bisti, S., Cattaneo, A., Fiorentini, A. & Maffei, L. (1982). Correlation between the preferred orientation and spatial frequency of neurons in visual areas 17 and 18 of the cat, Journal of Physiology, 323, 603-618.

Berardi, N., Bisti, S. & Maffei, L. (1987). The transfert of visual information across the corpus callosum: spatial and temporal properties in the cat. Journal of Physiology, 384, 619-632.

Berardi, N., Bisti, S., Fiorentini, A. & Maffei, L. (1988). The transfert of visual information across the corpus callosum in cats, monkeys and human: spatial and temporal properties. Progress in Brain Research, 75, 181-185.

Berkeley, M.A. & Sprague, J.M. (1982). Striate cortex and visual acuity functions in the cat. Journal of Comparative Neurology, 187, 679-702.

Berlucchi, G. & Rizzolatti, G. (1968). Binocularly driven neurons in visual cortex of split-chiasm cats. Science, 159, 308-310.

Berlucchi, G. & Rizzolatti, G. (1972). Physiological mechanism underlying interhemispheric transfert of visual information in the cat. Proceedings of the international colloquium on interhemispheric relationships, Slovenska Akademiaivied, Bratislava.

Berlucchi, G., Gazzaniga, M.S. & Rizzolatti, G. (1967). Microelectrode analysis of transfert of visual information by the corpus callosum. Archives Italiennes de Biologie, 105, 583-596.

Berlucchi, G., Sprague, J.M., Lepore, F. & Mascetti, G.G. (1978). Effects of lesions of areas 17, 18, and 19 on interocular transfert of pattern discriminations in split-chiasm cats. Experimental Brain Research, 31, 275-297.

Berlucchi, G., Sprague, J.M., Antonini, A. & Simoni, A. (1979). Learning and interhemispheric transfert of visual pattern discrimination following unilateral suprasylvian lesions in split-chiasm cats. Experimental Brain Research, 34, 551-574.

Berson, D.M. & Graybiel, A.M. (1978). Parallel thalamic zones in the LP-pulvinar complex of the cat identified by their afferent and efferent connections. Brain Research, 147, 139-148.

Bishop, G.H., Clare, M.H., & Landau, W.M. (1969). Further analysis of fibers groups in the optic track of the cat. Experimental Neurology, 24, 386-399.

Bishop, P.O., Coombs, J.S. & Henry, G.H. (1971). Responses to visual contours: spatio-temporal aspects of excitation in the receptive fields of simple striate neurons. Journal of Physiology, 219, 625-657.

Bisti, S. & Sireteanu, R.C. (1976). Selectivity to spatial frequency and contrast of visual cells in the cat superior colliculus. Vision Research, 16, 247-251.

Blakemore, C. (1970). Binocular depth perception and the optic chiasm. Vision Research, 10, 43-47.

Blakemore, C. & Zumbroich, T.J. (1987). Stimulus selectivity and functional organization in the lateral suprasylvian visual cortex of the cat. Journal of Physiology, 389, 569-603.

Boycott, B.B. & Wässel, H. (1974). The morphological types of ganglion cells of the domestic cat's retina. Journal of Physiology, 240, 397-419.

Cajal, S.R. (1893). La rétine des vertébrés. La cellule, 9, 17-257.

Camarda, R.M. & Rizzolatti, G. (1976). Visual receptive fields in the lateral suprasylvian area (Clare-Bishop area) of the cat. Brain Research, 101, 427-443.

Casanova, C., Freeman, R.D. & Normann, J.P. (1989). Monocular and binocular response properties of cells in the striate-recipient zone of the cat's lateral posterior-pulvinar. Journal of Neurophysiology, 62, 544-557.

Chalupa, L.M. & Abramson, B.P. (1988). Receptive-field properties in the tecto- and srtiate- recipient zones of the cat's lateral posterior nucleus. Dans T.P. Hicks, G. Benedek (éds), Progress in Brain Research (pp. 85-94). Amsterdam: Elsevier Science.

Cleland, B.G. & Levick, W.R. (1974). Properties of rarely encountered types of ganglion cells in the cat's retina and an overall classification. Journal of Physiology, 240, 457-492.

Cleland, B.G., Dubin, M.W. & Levick, W.R. (1971). Sustained and transient neurons in the cat's retina and lateral geniculate nucleus. Journal of Physiology, 217, 473-496.

Cleland, B.G., Levick, W.R. & Sanderson, K.J. (1973). Properties of sustained and transient ganglion cells in the cat's retina. Journal of Physiology, 228, 649-680.

Cynader, M., Lepore, F. & Guillemot, J.-P. (1981). Inter-hemispheric competition during postnatal developpement. Nature, 290, 139-140.

Damasio, A.R., Damasio, H. & Van Hoesen, G.W. (1982). Prosopagnosia: anatomical basis and behavioral mechanisms. Neurology, 32, 331-341.

Derrington, A.M. & Fuchs, A.F. (1979). Spatial and temporal properties of X and Y cells in the cat lateral geniculate nucleus. Journal of Physiology, 293, 347-364.

Desimone, R., Albright, T.D., Gross, C.G. & Bruce, C. (1984). Stimulus-selective properties of inferior temporal neurons in the macaque. Journal of Neuroscience, 4, 2051-2062.

Doty, R.W. (1971). Survival of pattern vision after removal of striate cortex in the adult cat. Journal of Comparative Neurology, 143, 341-370.

Dreher, B. (1986). Thalamocortical and corticocortical interconnections in the cat visual system: relation to the mechanism of information processing. Dans J.D. Pettigrew, K.J. Sanderson, W.R. Levick (éds), Visual Neuroscience (pp. 290-314). Cambridge: Cambridge University Press.

Dreher, B. (1996). Areas PMLS and 21a of cat visual cortex are not only functionally but also hodologically distinct. Dans M. Norita, T. Bando, B. Stein (éds), Progress in Brain Research, Vol. 112. Amsterdam: Elsevier Science.

Dreher, B. & Cottee, L. (1975). Visual receptive-field properties of cells in area 18 before and after acute lesions in area 17. Journal of Neurophysiology, 38, 735-750.

Dreher, B., Leventhal, A.G. & Hale, P.T. (1980). Geniculate input to cat visual cortex: a comparaison of area 19 with areas 17 and 18. Journal Neurophysiology, 44, 804-826.

Dreher, B., Michalski, A., Ho, R.H.T., Lee, C.W.F. & Burke, W. (1993). Processing of form and motion in area 21a of the cat visual cortex. Visual Neuroscience, 10, 93-115.

Duysens, J., Orban, G.A., van der Glas, H.W. & De Zegher, F.E. (1982a). Fonctional properties of area 19 as compared to area 17 of the cat. Brain Research, 231, 279-291.

Duysens, J., Orban, G.A., van der Glas, H.W. & Maes, H. (1982b). Receptive field structure of area 19 as compared to area 17 of the cat. Brain Research, 231, 293-308.

Ebner, F.B. & Myers, R.E. (1965). Distribution of corpus callosum and anterior commissure in the cat and raccoon. Journal of Comparative Neurology, 124, 353-375.

Enroth-Cugell, C. & Robson, J.G. (1966). The contrast sensitivity of retinal ganglion cells of the cat. Journal of Physiology, 187, 517-522.

Fiorentini, A., Maffei, L. & Sandini, G. (1983). The role of high spatial frequencies in face perception. Perception, 12, 195-201.

Ferster, D. & Le Vay, S. (1978). The axonal arborisation of lateral geniculate neurons in the striate cortex of the cat. Journal of Comparative Neurology, 182, 923-944.

Frishman, L.J., Schweitzer-Tong, D.E. & Goldstein, E.B. (1983). Velocity tuning of cells in dorsal lateral geniculate nucleus and retina of the cat. Journal of Neurophysiology, 50, 1393-1414.

Fukada, Y. (1971). Receptive fields properties of cat optic nerve fibres with special reference to conduction velocity. Vision Research, 11, 209-226.

Fukuda, Y. & Stone, J. (1974). Retinal distribution and central projections of Y-, X- and W- cells of the cat's retina. Journal of Neurophysiology, 37, 749-772.

Garey, L.J. & Blakemore, C. (1977). The effects of monocular deprivation on different neuronal classes in the lateral geniculate nucleus of the cat. Experimental Brain Research, 28, 259-278.

Garey, L.J. & Powell, T.P.S. (1967). The projections of the lateral geniculate nucleus upon the cortex in the cat. Proceedings of the Royal Society of London- Series B: Biological Sciences, 169, 107-126.

Garey, L.J., Jones, E.G. & Powell, T.P.S. (1968). Interrelationship of striate and extrastriate cortex with the primary relay sites of the visual pathway. Journal of Neurology, Neurosurgery and Neuropsychiatry, 31, 135-137.

Geisert, E.E. (1980). Cortical projections of the lateral geniculate nucleus in the cat. Journal of Comparative Neurology, 190, 793-812.

Gilbert, C.D. & Kelly, J.P. (1975). The projections of cells in differents layers of the cat's visual cortex. Journal of Comparative Neurology, 163, 81-107.

Gizzi, M.S., Katz, E. & Movshon, J.A. (1990). Spatial and temporal analysis by neurons in the representation of the central visual field in the cat's lateral suprasylvian visual cortex. Visual Neuroscience, 5, 463-468.

Gizzi, M.S., Katz, E., Schumer, R.A. & Movshon, J.A. (1990). Selectivity for orientation and direction of motion of single neurons in the cat striate and extrastriate visual cortex. Journal of Neurophysiology, 63, 1529-1543.

Guido W., Tong, L. & Spear, P.D. (1990). Afferent bases of spatial- and temporal-frequency processing by neurons in the cat's posteromedial lateral suprasylvian cortex: effects of removing areas 17, 18, and 19. Journal of Neurophysiology, 64, 1636-1651.

Guillemot, J.-P., Paradis, M.-C., Samson, A., Ptito, M. & Lepore, F. (1993). Binocular interaction and disparity coding in area 19 of visual cortex in normal and split-chiasm cats. Experimental Brain Research, 94, 405-417.

Guillery, R.W. (1966). A study of Golgi preparations from dorsal lateral geniculate nucleus of the cat. Journal of Comparative Neurology, 128, 21-50.

Guillery, R.W., Geisert, E.E., Polley, E.H. & Mason, C.A. (1980). An analysis of the retinal afferents to the cat's medial interlaminar nucleus and to its rostral thalamic extension, the "geniculate wing". Journal of Comparative Neurology, 194, 117-142.

Hammond, P. & Fothergill, L.K. (1994). Cat striate cortex: monocular and interocular comparaison of spatial-frequency selectivity. Anais Academia Brasileira de Ciencias, 66, 95-113.

Henry, G.H. (1977). Receptive fields classes of cells in the striate cortex of the cat. Brain Research, 133, 1-28.

Hickey, T.L. & Guillery, R.W. (1974). An autoradiographic study of retinogeniculate pathway in the cat and the fox. Journal of Comparative Neurology, 156, 239-254.

Hoffman, K.P. (1973). Conduction velocity pathways from retina to superior colliculus in the cat: a correlation with receptive field properties. Journal of Neurophysiology, 36, 409-424.

Hoffman, K.-P. & Stone, J. (1971). Conduction velocity of afferences to cat visual cortex: a correlation with cortical receptive fields properties. Brain Research, 32, 460-466.

Hoffman, K.-P., Stone, J. & Sherman, S.M. (1972). Relay of receptive fields properties in the dorsal lateral geniculate nucleus of the cat. Journal of Neurophysiology, 35, 518-531.

Höllander, H. & Vanegas, H. (1977). The projections from the lateral geniculate nucleus onto the visual cortex in the cat: a quantitative study with horesradish peroxidase. Journal of Comparative Neurology, 173, 519-536.

Hubel, D.H. & Wiesel, T.N. (1962). Receptive fields, binocular interaction and functional architecture in the cat's visual cortex. Journal of Physiology, 160, 106-154.

Hubel, D.H. & Wiesel, T.N. (1963). Shape and arrangement of columns in cat's striate cortex. Journal of Physiology, 165, 559-568.

Hubel, D.H. & Wiesel, T.N. (1965). Receptive fields and functional architecture in two nonstriate visual areas (18 and 19) of the cat. Journal of Neurophysiology, 28, 229-289.

Hubel, D.H. & Wiesel, T.N. (1967). Cortical and callosal connections concerned with the vertical meridian of visual fields in the cat. Journal of Neurophysiology, 30, 1561-1573.

Hubel, D.H. & Wiesel, T.N. (1969). Visual area of the lateral suprasylvian gyrus (Clare-Bishop area) of the cat. Journal of Physiology, 202, 251-260.

Hughes, H.C. & Sprague, J.M. (1986). Cortical mechanisms for local and global analysis of visual space in the cat. Experimental Brain Research, 61, 332-354.

Ikeda, H. & Wright, M.J. (1975). Spatial and temporal properties of "sustained" and "transient" neurones in area 17 of the cat's visual cortex. Journal of Physiology, 22, 363-383.

Illing, R.B. & Wässel, H. (1981). The retinal projection to the thalamus in the cat: a quantitative investigation and a comparaison with the retinotectal pathways. Journal of Comparative Neurology, 202, 265-285.

Innocenti, G.M. (1980). The primary visual pathway through the corpus callosum: morphological and functional aspects in the cat. Archives Italiennes de Biologie, 118, 124-188.

Itoh, K., Conley, M. & Diamond, I.T. (1981). Different distributions of large and small ganglions cells in the cat after HRP injections of single layers of the lateral geniculate body and the superior colliculus. Brain Research, 207, 147-152.

Kelly, J.P. & Gilbert, C.D. (1975). The projections of differents morphological types of ganglions cells in the cat retina. Journal of Comparative Neurology, 163, 65-80.

Kingston, W.J., Vadas, M.A. & Bishop, P.O. (1969). Multiple projections of the visual field to the medial portion of the dorsal lateral geniculate nucleus and the adjacent nuclei of the thalamus of the cat. Journal of Comparative Neurology, 136, 295-316.

Kuffler, S.W. (1953). Discharge patterns and functional organisation of the mammalian retina. Journal of Neurophysiology, 16, 37-38.

Lehmkuhle, S., Kratz, K.E., Mangel, S.C. & Sherman, S.M. (1980). Spatial and temporal sensitivity of X- and Y- cells in dorsal lateral geniculate nucleus of the cat. Journal of Neurophysiology, 43, 520-541.

Lepore, F. & Guillemot, J.-P. (1982). Visual receptive fields properties of cells innervated through the corpus callosum in the cat. Experimental Brain Research, 46, 413-424.

Lepore, F., Ptito, M. & Lassonde, M. (1986). Stereoperception in cats following section of the corpus callosum and/or optic chiasm. Experimental Brain Research, 61, 258-264.

Lepore, F., Ptito, M., Richer, L. & Guillemot, J.-P. (1988). Cortico-cortical callosal conncetivity: evidences derived from electrophysiological studies. Dans T.P. Hicks, G. Benedek, (éds), Vision within extrageniculo-striate systems (pp 187-195). Amsterdam: Elsevier Science.

Lepore, F., Samson, A., Paradis, M.-C., Ptito, M. & Guillemot, J.-P. (1992). Binocular interaction and disparity coding at the 17/18 border: contribution of the corpus callosum. Experimental Brain Research, 90, 129-140.

LeVay, S. & Ferster, D. (1977). Relay cell classes in the lateral geniculate nucleus of the cat and the effects of visual deprivation. Journal of Comparative Neurology, 172, 563-584.

LeVay, S. & Voigt, T. (1988). Ocular dominance and disparity coding in cat visual cortex. Visual Neuroscience, 1, 395-414.

Leventhal, A.G. (1979). Evidence that the different classes of relay cells of the cat's lateral geniculate nucleus terminate in different layers of the striate cortex. Experimental Brain Research, 37, 349-372.

Leventhal, A.G., Rodieck, R. & Dreher, B. (1985). Central projections of cat ganglion cells. Journal of Comparative Neurology, 237, 216-226.

Livingstone, M. S. & Hubel, D.H. (1988). Segregation of form, color, movement and depth: anatomy, physiology and perception. Science, 240, 740-749.

Maffei, L. & Fiorentini, A. (1973). The visual cortex as a spatial frequency analyser. Vision Research, 13, 1255-1267.

Maffei, L. & Fiorentini, A. (1977). Spatial frequency rows in the striate visual cortex. Vision Research, 17, 257-264.

Maffei, L., Berardi, N. & Bisti, S. (1986). Interocular transfert of adaptation after effect in neurons of area 17 and 18 of split-chiasm cats. Journal of Neurophysiology, 55, 966-976.

Maciewicz, R.J. (1975). Thalamic afferences to areas 17, 18 and 19 of cat cortex traced with horseradish peroxidase. Brain Research, 84, 308-312.

Mitchell, D.E. & Blakemore, C. (1970). Binocular depth perception and the corpus callosum. Vision Research, 10, 49-54.

Mizobe, K., Itoi, M., Kaihara, T. & Toyama, K. (1988). Neuronal responsiveness in area 21a of the cat. Brain Research, 438, 307-310.

Morrone, M.C., Di Stefano, M. & Burr, D.C. (1986). Spatial and temporal properties of neurons of the lateral suprasylvian cortex of the cat. Journal of Neurophysiology, 56, 969-986.

Movshon, J.A., Thompson, I.D. & Tolhurst, D.J. (1978a). Spatial summation in the receptive fields of simple cells in the cat's striate cortex. Journal of Physiology, 283, 53-77.

Movshon, J.A., Thompson, I.D. & Tolhurst, D.J. (1978b). Receptive field organisation of complex cells in the cat's striate cortex. Journal of Physiology, 283, 79-99.

Movshon, J.A., Thompson, I.D. & Tolhurst, D.J. (1978c). Spatial and temporal contrast sensitivity of neurons in areas 17 and 18 of the cat's visual cortex. Journal of Physiology, 283, 101-120.

Myers, R.E. (1955). Interocular transfert of pattern discrimination in cats following section of crossed optic fibers. Journal of Comparative Physiology and Psychology, 48, 470-473.

Myers, R.E. (1956). Function of corpus callosum in interocular transfert. Brain, 79, 358-363.

Orban, G.A. (1984). Neuronal operations in the visual cortex Dans H.B. Barlow, T.H. Bullock, E. Florey, O.-J. Grüsser & A. Peters (éds.), Studies of Brain Functions, Vol. 11, Berlin: Springer-Verlag.

Orban G.A., Kennedy, H. & Maes, H. (1981). Response to movement of neurons in areas 17 and 18 of the cat: velocity sensitivity. Journal of Neurophysiology, 45, 1043-1058.

Palmer, L.A., Rosenquist, A.C. & Tusa, R.J. (1978). The retinotopic organisation of lateral suprasylvian visual areas in the cat. Journal of Comparative Neurology, 177, 237-256.

Payne, B.R. (1986). Role of callosal cells in the functional organisation of cat striate cortex. Dans F. Lepore, M. Ptito, H.H. Jasper, (éds), Two hemispheres-one brain: functions of the corpus callosum (pp. 231-254). New-York: Alan Liss.

Pollen, D.A. & Ronner, S.F. (1975). Periodic excitability changes across the receptive fields of complex cells in the striate and parastriate cortex of the cat. Journal of Physiology, 245, 667-697.

Pollen D.A., Lee, J.R. & Taylor, J.H. (1971). How does the striate cortex begin the reconstruction of the visual world?. Science, 173, 74-77.

Pollen, D.A., Andrews, B.W. & Feldon, S.E. (1978). Periodic complex cells in cortical area 19 of the cat. Vision Research, 18, 347-350.

Ptito, M., Lepore, F. & Guillemot, J.-P. (1991). Stereopsis in the cat: behavioral demonstration and underlying mechanisms. Neuropsychologia, 6, 443-464.

Raczkowski, D. & Rosenquist, A.C. (1983). Connections of the multiple cortical areas with the lateral posterior-pulvinar complex and adjacent thalamic nuclei in the cat. Journal of Neuroscience, 3, 1912-1942.

Rauschecker, J.P., von Grünau, M.W. & Poulin, C. (1987). Centrifugal organization of direction preferences in the cat's lateral suprasylvian visual cortex and its relation to flow field processing. Journal of Neuroscience, 7, 943-958.

Richer, L. (1989). Caractéristiques fonctionnelles des fibres visuelles du corps calleux chez le chat. Thèse de Doctorat, Université de Montréal, Montr_al.

Rose, D. & Blakemore, C. (1974). An analysis of orientation selectivity in the cat's visual cortex. Experimental Brain Research, 20, 1-17.

Row, M.H. & Stone, J. (1976). Properties of ganglion cells in the visual streak of the cat's retina. Journal of Comparative Neurology, 167, 99-126.

Saul, A.B. & Humphrey, A.L. (1992). Temporal-frequency tuning of direction selectivity in cat visual cortex. Visual Neuroscience, 8, 365-372.

Sanderson, K.J. & Sherman, S.M. (1971). Nasotemporal overlap in visual field projected to the lateral geniculate nucleus in the cat. Journal of Neurophysiology, 34, 453-466.

Sherk, H. (1978). Area 18 cell responses in cat during reversible inactivation of area 17. Journal of Neurophysiology, 41, 204-215.

Shatz, C. (1977). Abnormal interhemispheric connections in the visual system of the Boston Siamese cats: a physiological study. Journal of Comparative Neurology, 171, 229-246.

Segraves, M.A. & Rosenquist, A.C. (1982a). The distribution of the cells of origin of callosal projections in cat visual cortex. Journal of Neuroscience, 2, 1079-1089.

Segraves, M.A. & Rosenquist, A.C. (1982b). The afferent and efferent callosal connections of retinotopically defined areas in cat cortex. Journal of Neuroscience, 2, 1090-1107.

Sherman, S.M. (1985). Functional organization of the W-, X-, and Y- cell pathways in the cat: a review and hypothesis. Dans J.M. Sprague, A.N. Epstein (éds), Progress in psychobiology and physiological psychology, Vol. 11 pp. 234-314. Orlando: Academic Press.

Shou, T., Leventhal, A.G., Thompson, K.G. & Zhou, Y. (1995). Direction biases of X and Y type retinal ganglion cells in the cat. Journal of Neurophysiology, 73, 1414-1421.

Skottun, B.C. & Freeman, R.D. (1984). Stimulus specificity of binocular cells in the cat's visual cortex: ocular dominance and the matching of left and right eyes. Experimental Brain Research, 56, 206-216.

Skottun, B.C., De Valois, R.L., Grosse, D.H., Movshon, J.A., Albrecht, D. & Bonds, A.D. (1991). Classifying simple and complex cells on the basis of response modulation. Vision Research, 31, 1079-1086.

So, Y.T. & Shapley, R. (1981). Spatial tuning of cells in and around lateral geniculate nucleus of the cat: X and Y relay cells and perigeniculate interneurons. Journal of Neurophysiology, 45, 107-120.

Spear, P.D. & Baumann, T.P. (1975). Receptive-field caracteristics of single neurons in lateral suprasylvian visual area of the cat. Journal of Neurophysiology, 38, 1403-1420.

Sprague, J.M., Levy, J., DiBerardino, A. & Berlucchi, G. (1977). Visual cortical areas mediating form discrimination in the cat. Journal of Comparative Neurology, 172, 441-488.

Squatrito, S., Galletti, C., Battaglini, P.P. & Sanseverino, E.R. (1981). An autoradiographic study of bilateral cortical projections from cat area 19 to lateral suprasylvian visual area. Archives Italiennes de Biologie, 119, 21-42.

Stone, J. (1966). The naso-temporal division of the cat's retina. Journal of Comparative Neurology, 126, 585-599.

Stone, J. (1978). The number and distribution of ganglion cells in the cat's retina. Journal of Comparative Neurology, 180, 753-772.

Stone, J. (1983). Parallel processing in the visual system. The classification of retinal ganglion cells and its impact on the neurobiology of vision, New-York: Plenum.

Stone, J. & Dreher, B. (1973). Projections of X- and Y- cells of the cat's lateral geniculate nucleus to areas 17 and 18 of visual cortex. Journal of Neurophysiology, 36, 551-567.

Stone, J. & Fukuda, Y. (1974). Properties of cat retinal ganglion cells: a comparaison of W-cells with X- and Y-cells. Journal of Neurophysiology, 37, 722-748.

Stone, J. & Hoffman, K.-P. (1972). Very slow conducting ganglion cells in the cat's retina. A major new functional type?. Brain Research, 43, 610-616.

Sur, M. & Sherman, S.M. (1982). Retinogeniculate terminations in cat: morphological differences between X and Y- cell axons. Science, 218, 389-391.

Sur, M. & Sherman, S.M. (1984). The position sensitivity of retinal X- and Y-cells in cats. Experimental Brain Research, 56, 497-501.

Symonds, L.L. & Rosenquist, A.C. (1984). Corticocortical connections among visual areas in the cat. Journal of Comparative Neurology, 229, 1-38.

Tanaka, K., Ohzawa, I., Ramoa, A.S. & Freeman, R.D. (1987). Receptive fields properties of cells in area 19 of the cat. Experimental Brain Research, 65, 549-558.

Tardif, E., Bergeron, A., Lepore, F. & Guillemot, J.-P. (1996). Spatial and temporal properties and contrast sensitivity of single neurons in area 21a of the cat. Brain Research, 716, 219-223.

Tardif, E., Richer, L., Bergeron, A., Lepore, F. & Guillemot, J.-P. (1997). Spatial resolution and contrast sensitivity of single neurons in area 19 of split-chiasm cats: a comparaison with primary visual cortex. European Journal of Neuroscience, 9, 1929-1939.

Thompson, K.G., Zhou, Y. & Leventhal., A.G. (1994). Direction sensitive X and Y cells within the A laminae of the cat's LGNd. Visual Neuroscience, 11, 927-938.

Tolhurst, D.J. & Movshon, J.A. (1975). Spatial and temporal contrast sensitivity of striate cortical neurones. Nature, 257, 674-675.

Tolhurst, D.J. & Thompson, I.D. (1981). On the variety of spatial frequency selectivities shown by neurons in area 17 of the cat. Proceedings of the Royal Society of London-Series B: Biological Sciences, 213, 183-199.

Tolhurst, D.J., Movshon, J.A. & Thompson, I.D. (1981). The dependence of response amplitude and variance of cat visual cortical neurones on stimulus contrast. Experimental Brain Research, 41, 414-419.

Tootell, R.B.H., Silverman, M.S. & De Valois, R.L. (1981). Spatial frequency columns in primary visual cortex. Science, 214, 813-815.

Turlejski, K. (1975). Visual responses of neurons in the Clare-Bishop area of the cat. Acta Neurobiologiae Experimentalis, 35, 189-208.

Tusa, R.J. & Palmer, L.A. (1980). Retinotopic organisation of areas 20 and 21 in the cat. Journal of Comparative Neurology, 193, 147-164.

Tusa, R.J., Palmer, L.A. & Rosenquist, A.C. (1978). The retinotopic organisation of area 17 (striate cortex) in the cat. Journal of Comparative Neurology, 177, 213-236.

Tusa, R.J., Rosenquist, A.C. & Palmer, L.A. (1979). Retinotopic organisation of area 18 and 19 in the cat. Journal of Comparative Neurology, 185, 657-678.

Updyke, B.V. (1977). Topographic organisations of the projections from cortical areas 17, 18 and 19 onto the thalamus, pretectum and superior colliculus in the cat. Journal of Comparative Neurology, 173, 81-111.

von Grünau, M. & Frost, B.J. (1983). Double-opponent-process mechanism underlying RF-structure of directionally specific cells of cat lateral suprasylvian visual area. Experimental Brain Research, 49, 84-92.

von Grünau, M., Zumbroich, T.J. & Poulin, C. (1987). Visual receptive field properties in the posterior suprasylvian cortex of the cat: a comparaison between the areas PMLS and PLLS. Vision Research, 27, 343-356.

Wang, C. & Dreher, B. (1996). Binocular interaction and disparity coding in area 21a of cat extrastriate cortex. Experimental Brain Research, 108, 257-272.

Wässel, H. & Illing, R.B. (1980). The retinal projection to the superior colliculus in the cat. A quantitative with HRP. Journal of Comparative Neurology, 190, 333-356.

Westheimer, G. & Mitchell, D.E. (1969). The sensory stimulus for disjonctive eye movements. Vision Research, 9, 749-755.

Wilson, M.E. (1968). Cortico-cortical connexions of the cat visual areas. Journal of Anatomy, 102, 375-386.

Wimborne, B.M. & Henry, G.H. (1992). Response caracteristics of the cells of cortical area 21a of the cat with special reference to orientation specificity. Journal of Physiology, 449, 457-478.

Wright, M.J. (1969). Visual receptive fields of cells in cortical area remote from the striate cortex in the cat. Nature, 223, 973-975.

Zumbroich, T.J. & Blakemore, C. (1987). Spatial and temporal selectivity in the suprasylvian visual cortex of the cat. Journal of Neuroscience, 7, 482-500.